Spring 2015

Using PCSWMM to simulate first flush and assess performance of extended dry detention ponds as structural stormwater BMPs in a large polluted urban watershed

Muhieddine Saadeddine Kabbani
University of Iowa

USING PCSWMM TO SIMULATE FIRST FLUSH AND ASSESS PERFORMANCE OF EXTENDED DRY DETENTION PONDS AS STRUCTURAL STORMWATER BMPS IN A LARGE POLLUTED URBAN WATERSHED

by

Muhieddine Saadeddine Kabbani

A thesis submitted in partial fulfillment of the
requirements for the Doctor of Philosophy degree in Civil
and Environmental Engineering in the Graduate College of
The University of Iowa

May 2015

Thesis Supervisor: Professor Jerald L. Schnoor

Graduate College
The University of Iowa
Iowa City, Iowa

CERTIFICATE OF APPROVAL

PH.D. THESIS

This is to certify that the Ph.D. thesis of

Muhieddine Saadeddine Kabbani

has been approved by the Examining Committee
for the thesis requirement for the Doctor of Philosophy degree in Civil and Environmental Engineering at the May 2015 graduation.

Thesis Committee:

Jerald L. Schnoor, Thesis Supervisor

William E. Eichinger

Craig L. Just

A. Jacob Odgaard

Mary Skopec

To my daughter Nairmeen Fariha, who is the light of my days

ACKNOWLEDGMENTS

I would like to thank my advisor Dr. Jerald Schnoor for his insight and guidance. I would also like to thank my committee members, Dr. William Eichinger, Dr. Craig Just, Dr. Jacob Odgaard and Dr. Mary Skopec for their insight and for serving on my committee.

I gratefully acknowledge funding from Computational Hydraulics International (CHI water), the Executive Council for Graduate and Professional Students (ECGPS) at the University of Iowa, and the Graduate College at the University of Iowa. I would like to sincerely thank Dr. Dale E. Wurster of the Graduate College for his support and encouragement, which were crucial to the progress of this thesis. I also thank the Capitol Region Watershed District for their cooperation in providing data necessary for the completion of this work.

Lastly, I would like to thank my family for all their love and encouragement. To my father, who did not live to see this work but whose guidance allowed me to fulfill my dreams. To my mother and brothers, without whose faithful support none of this would have been possible. And to my beloved wife for her incredible patience and constant help. My deepest thank you.

ABSTRACT

Urbanization and increase of impervious areas impact stormwater runoff and can pollute receiving waters. Total suspended solids (TSS) are of particular concern as they can act as a transport agent for other pollutants. Moreover, the existence of the first flush phenomenon (FF), whereby the first stage of storm runoff is the most concentrated, can also have profound ecological effects on receiving waters. Understanding the various types of pollutants in watershed stormwater, their correlation with rainfall parameters (precipitation depth and previous dry days) and with TSS, and the existence of FF is crucial to the design of the most suitable structural best management practice (BMP) that can mitigate their harm. Personal Computer Storm Water Management Model (PCSWMM) is a well-known computer model that can simulate urban runoff quantity and quality and model BMPs. The use of PCSWMM to simulate the first flush phenomenon and to evaluate the effectiveness of structural BMPs has not been previously investigated for a large urban watershed with seriously polluted stormwater runoff.

This research is concerned with the study of a framework for designing structural best management practices (BMPs) for stormwater management in a large watershed that is based on comprehensive analysis of pollutants of concern, rainfall parameters of influence, and the existence of FF. The framework was examined using the PCSWMM computer model in the St Anthony Park watershed, an urban watershed in St Paul, Minnesota with a large drainage area of 3,418 acres that discharges directly into the Mississippi River via a storm tunnel. A comprehensive study was undertaken to characterize the overall St. Anthony Park watershed stormwater quality trends for the period of record 2005-2013 for heavy metals, nutrients (ammonia and total phosphorus), sediment (TSS), and bacteria (*E. coli*). Stormwater was found

to be highly contaminated as measured by exceedance of the Minnesota Pollution Control Agency (MPCA) water quality standards and as compared to data obtained from the National Stormwater Quality Database (NSQD). None of the examined parameters significantly correlated with precipitation depth. Concentrations of most heavy metals, total phosphorus and TSS positively correlated with previous dry days, and most pollutants correlated positively with TSS, which provided a strong rationale for using TSS as a representative pollutant in PCSWMM and in examining BMP efficiency. Moreover, BMPs that targeted the particulate fraction in stormwater would be the most efficient in reducing stormwater pollution.

A PCSWMM model was built based on the existing drainage system of the watershed, which consisted of inlet structures, manholes, pipes and deep manholes that connect the network pipes to a deep drainage tunnel discharging directly into Mississippi River. The model was calibrated and validated using recorded storm and runoff data. FF was numerically investigated by simulating pollutant generation and washoff. Using three different numerical definitions of FF, the existence of FF could be simulated, and was subsequently reduced by simulating extended dry detention ponds in the watershed.

Extended dry detention ponds (EDDPs) are basins whose outlets are designed to detain stormwater runoff for a calculated time that allows particles and associated pollutants to settle. Extended dry detention ponds are a potential BMP option that could efficiently control both water quantity (by diverting initial volumes of stormwater, thus addressing FF) and quality (by reducing suspending pollutants, thus addressing TSS and co-contaminants). Moreover, they are the least-expensive stormwater treatment practice on a cost per treated unit area. Two location-based designs were examined. The first was an EDDP at the main outfall (OFmain), while the second was a set of seven smaller EDDPs within the vicinity of deeper manholes of the deep tunnel (distributed EDDPs).

Distributed EDDPs were similar to the OFmain EDDP at reducing peak stormwater flow (52-61%) but superior in reducing TSS loads (20-25% for small particles and 43-45% for larger particles based on the particle sedimentation rate removal constant k) and in reducing peak TSS loads (67-75%). These efficiencies were obtained using the dynamic and kinematic wave routing methods, indicating that they could be used interchangeably for this watershed. The steady state routing method produced unrealistic results and was subsequently excluded from FF analysis. Finally, distributed EDDPs were superior to OFmain EDDP at eliminating FF per the stringent fifth definition ($\Delta > 0.2$). This was true for small values of k. However, larger values of k and other FF tests (above the 45º no-flush line and FF coefficient $b < 1$) showed that BMP implementation overall failed to completely eliminate FF. This suggested that the extended time required by EDDPs to efficiently remove pollutants from stormwater via settling would compromise their ability to completely eliminate FF.

In conclusion, a comprehensive framework was applied so as to better design the most efficient BMPs by characterizing the overall St. Anthony Park watershed stormwater pollutants, their correlation with rainfall parameters and with TSS, and the magnitude of FF. A cost-effective, rapid, and accurate method to simulate FF and study the optimal BMP design was thus implemented for a large urban watershed through the PCSWMM model.

PUBLIC ABSTRACT

Urbanization impacts stormwater runoff and pollutes receiving waters. Total suspended solids (TSS) are of particular concern as they can act as a transport agent for other pollutants. Moreover, the existence of the first flush phenomenon (FF), whereby the first stage of storm runoff is the most polluted, can also have profound effects. This research is concerned with the study of a framework for designing structural best management practices (BMPs) that mitigate stormwater harm in a large watershed based on comprehensive analysis of pollutants, rainfall parameters of influence, and the existence of FF. The framework was examined in St Anthony Park watershed, a large urban watershed in St Paul, Minnesota that outlets directly into the Mississippi River via a storm tunnel. The use of the Personal Computer Storm Water Management Model (PCSWMM) to simulate FF and to evaluate the effectiveness of structural BMPs has not been previously investigated for an urban setting with seriously polluted stormwater runoff like St Anthony Park watershed.

St. Anthony Park watershed stormwater was found to be highly contaminated, and most pollutants correlated positively with TSS. Subsequently, TSS were used to represent pollutants in PCSWMM. The model was built based on the existing drainage system of the watershed, and was calibrated and validated using recorded storm and runoff data. FF was numerically examined using various numerical methods and was found to exist. Subsequently, extended dry detention ponds (EDDPs) were examined as a potential BMP option that could efficiently control both water quantity (by diverting initial volumes of stormwater, thus addressing FF) and quality (by reducing TSS). EDDPs are basins that detain stormwater runoff for a calculated time to allow particles and associated pollutants to settle. Two location-based designs were examined: either a central EDDP at

the main outfall on the Mississippi River, or a set of seven smaller EDDPs upstream. Distributed EDDPs were more efficient at reducing peak and total TSS loads. However, distributed EDDPs failed to completely eliminate FF, which was attributed to the long duration of time required for TSS to settle. Nonetheless, the high efficiencies seen when examining the other parameters indicate that distributed EDDPs were still successful at reducing stormwater pollution and should be considered for implementation. A cost-effective, rapid, and accurate method to simulate FF and study the optimal BMP design was thus implemented for a large urban watershed through the PCSWMM model. The results of the research study should better inform legislators and decision makers on optimal stormwater management at the St. Anthony Park watershed.

TABLE OF CONTENTS

LIST OF TABLES

LIST OF FIGURES

CHAPTER I:

INTRODUCTION

Perspective

Stormwater runoff in large volumes has adverse effects in urban settings if the drainage infrastructure is not adequate for receiving such volumes from impervious areas and streets and transporting it to water bodies. In addition, runoff has a major adverse effect which is attributed to its flow over impervious and pervious urban areas. Pollutants that build up over dry periods are washed off and transported by runoff to receiving water bodies, jeopardizing aquatic life, polluting plausible sources of fresh water, and adding costs to treating this water before pumping it to the community (Gromaire-Mertz, Garnaud et al. 1999, Wang, Wei et al. 2011). Of the different types of pollutants carried by stormwater runoff, total suspended solids (TSS) are of primary concern, since their transport from urban areas into streams can have detrimental effects. In addition to degrading aquatic ecosystems, TSS can act as a transport agent for toxic compounds such as heavy metals, pesticides, and biodegradable organic matter (Davis and McCuen 2005). Moreover, the existence of the first flush phenomenon (FF) in the watershed, whereby the first stage of storm runoff is the most polluted, can also have profound effects (Deletic 1998). Understanding the various types of pollutants in watershed stormwaters, their correlation with rainfall parameters and with TSS, and the existence of FF is crucial to the design of the most suitable structural best management practices (BMPs) that can mitigate their harm (Davis and McCuen 2005).

Among the various computer models developed for stormwater management, drainage infrastructural design, and planning, the Personal Computer Storm Water Management Model (PCSWMM) is unique in its dynamic hydraulic and hydrological modeling capabilities of simulating runoff quantity and quality in urban areas. In addition to its ability to model structural BMPs, PCSWMM can also model the reduction of pollution concentration through treatment in storage units or by natural processes in the drainage network (Environmental Protection Agency (EPA) , Rossman 2005, Poresky 2007). The use of PCSWMM to understand the dynamics of FF and to simulate the control and remediation of water quality violations by implementation of structural best management practices (BMPs) is a novel application of this powerful tool.

Problem statement

The Mississippi River has a variety of water quality problems at different scales, but nutrients (primarily nitrogen and phosphorus) and sediments are the two primary water quality problems at the scale of the entire river (Committee on the Mississippi River and the Clean Water Act: David A. Dzombak 2007). This river passes through many cities and lies in the vicinity of many others. Consequently, many stormwater outfalls spread over its banks carrying polluted runoff to its stream. Untreated stormwater runoff can be significantly contributing to its pollution, which underscores the importance of efficiently treating stormwater to reduce its impact.

The city of St. Paul in Minnesota is situated on the Mississippi River. Hydrologically, St. Paul could be divided into several urban watersheds that drain into the Mississippi River. One of these watersheds is the St. Anthony Park watershed, which has a stormwater drainage system consisting of inlets that receive water from impervious and pervious areas of the watershed and carry them through gravity pipes to deep shafts that connect to a deep drainage tunnel and eventually to an outfall over the Mississippi River.

This research is concerned with the study of a framework for designing structural BMPs for stormwater management that is based on comprehensive analysis of pollutants of concern, rainfall parameters of influence, and the existence of FF. The study aims at analyzing the St. Anthony Park watershed stormwater runoff, associated pollutants generated, and measures to reduce them before they are disposed in the Mississippi River. The main questions that are addressed are:

- Based on water quality parameters including heavy metals (cadmium, chromium, copper, lead, nickel and zinc), nutrients (ammonia and total phosphorus), sediment (TSS), and bacteria (*E. coli*), how polluted are the stormwaters of the St. Anthony Park watershed that are being directly discharged into the Mississippi River?
- Using Spearman's correlation test, how are rainfall parameters (precipitation depth and previous dry days) impacting pollutant levels?
- Using Spearman's correlation test, how are the various pollutants correlating to TSS?
- Using five different FF definitions, can PCSWMM numerically simulate the existence of FF in the absence of detailed temporal storm event data?
- What is the most efficient structural BMP design that can be used to reduce peak runoff flows by at least 40% and peak TSS loads by at least 60%? And what is their distribution/configuration with respect to the drainage system?

Research objectives

The ultimate objective of this research study is to generate a comprehensive understanding of nonpoint sources pollution in urban stormwater at St. Anthony Park watershed, their correlation with rainfall parameters, and the magnitude of the first flush phenomenon in order to better design5*5 efficient structural BMPs. This main objective requires the completion of the following specific objectives and validation of the associated hypotheses:

Specific-Objective #1: Characterize the overall St. Anthony Park watershed stormwater quality trends for the period of record 2005-2013 and assess the correlation of various pollutants with rainfall parameters (precipitation depth and previous dry days) and with suspended sediment concentrations (measured as Total Suspended Solids, TSS). This evaluation is necessary to assess stormwater pollution impact on the Mississippi River waters.

Hypothesis # 1: The concentrations of heavy metals (cadmium, chromium, copper, lead, nickel and zinc), nutrients (ammonia and total phosphorus), sediment (total suspended solids), and bacteria (*E. coli*) in stormwaters exceed surface water quality standards set by MPCA and median pollutant concentrations measured in stormwaters of other urbanized areas in the U.S.

Hypothesis # 2: The studied stormwater pollutants (from Hypothesis #1) correlate positively with the previous dry days but not with precipitation depth (total inches of rainfall per storm) of their corresponding storms.

Hypothesis # 3: The studied stormwater pollutants (from Hypothesis #1) correlate positively with total suspended solids (TSS); thus TSS can be subsequently used in the PCSWMM model as a representative pollutant.

To achieve specific-objective #1, the following tasks should be performed:

- Plot data for stormwater quality parameters for the period of record 2005-2013
- Analyze exceedances of the MPCA and NSQD standards for each parameter
- Correlate each stormwater quality parameter with rainfall precipitation depth and previous dry days
- Correlate the MPCA and NSQD exceedances of each stormwater quality parameter with rainfall parameters precipitation depth and previous dry days
- Correlate each stormwater quality parameter with TSS

Specific-Objective #2: Use the stormwater management model PCSWMM to numerically study the existence of the first flush (FF) phenomenon at the subwatershed and watershed outfalls of St. Anthony Park.

Hypothesis # 1: The FF phenomenon can be simulated with the PCSWMM model when using the exponential buildup and washoff function but not the Event Mean Concentration (EMC) washoff function.

Hypothesis # 2: Using five different definitions of FF, the FF phenomenon is numerically simulated at the outfall of the St. Anthony Park watershed.

To achieve specific-objective #2, the following tasks should be performed:

- Build, calibrate and verify the PCSWMM model hydrologically using field data
- Use dynamic wave, kinematic wave, and steady flow routing methods with either EMC washoff or exponential buildup and washoff
- Plot the hydrograph at the outfall of drainage system on Mississippi River
- Plot the pollutograph at the outfall of drainage system on Mississippi River
- Plot $M_{(t)}/M_{(total)}$ versus $V_{(t)}/V_{(total)}$ to calculate the magnitude of the FF phenomenon at the outfall on Mississippi River
- Examine the FF phenomenon using five different definitions

Specific-Objective #3: Use the built PCSWMM model to model extended dry detention ponds (EDDPs) as a structural BMP and examine different locations to reduce pollutant concentrations (represented by TSS) in stormwater runoff and to reduce the impact of FF.

Hypothesis # 1: EDDPs are efficient at reducing peak stormwater flow by at least 40%.

Hypothesis # 2: EDDPs are efficient at reducing total pollutant loads by at least 30% (as represented by TSS) in stormwater.

Hypothesis # 3: EDDPs are efficient at reducing peak pollutant loads by at least 60% (as represented by TSS) in stormwater.

Hypothesis # 4: EDDPs placed near the vicinity of deep manholes that received drainage water from the shallow network are more efficient at reducing pollutants in stormwater (as represented by TSS) than a single EDDP placed at the outfall of the watershed.

Hypothesis # 5: The dynamic and kinematic wave routing methods produce more accurate results than the steady state routing method as depicted by the hydrographs and pollutographs

Hypothesis # 6: Using three different definitions of FF, EDDPs are efficient at eliminating FF

To achieve specific-objective #3, the following tasks should be performed:

- Simulate St. Anthony Park watershed stormwater runoff using PCSWMM and three routing methods: dynamic wave, kinematic wave, and steady flow routing methods
- Model EDDPs using PCSWMM and examine the reduction of peak stormwater flow (cfs)
- Model EDDPs using PCSWMM and examine the reduction of TSS in total load (tons) and peak flow (kg/hr)
- Implement modeled structural BMPs at deep manholes and plot hydrographs and pollutographs at these locations (option 1)
- Implement modeled structural BMPs at the outfall of the drainage tunnel and plot hydrographs and pollutograph at the outfall (option 2)
- Plot $M_{(t)}/M_{(total)}$ versus $V_{(t)}/V_{(total)}$ and examine the change in the magnitude of the FF phenomenon at the outfall on the Mississippi River
- Examine the FF phenomenon using three different FF definitions

CHAPTER II:

LITERATURE REVIEW

Urbanization

Urbanization includes the addition of impervious layers such as asphalt pavements and concrete slabs on originally natural land surfaces. Fletcher *et al.* (Fletcher, Andrieu et al. 2013) mentioned the effects of urbanization and increase of impervious areas on increasing runoff volumes and rates, losses of infiltration and base-flow, and simplification of the drainage network. This ultimately causes faster response of runoff to rainfall and leads to reduced recession times and shorter times of concentration. These processes affect hydrology in the primary area and impact the water quality of its runoff. Runoff movement in urban areas is intercepted by gullies on the streets that draw volumes of running water into a stormwater system. In the absence of stormwater systems and/or in the case of their limited capacity or their poor management, runoff flows over streets in streams.

Surface water flow in urban areas collects pollutants that are produced by human activities in urbanized areas and transports them with it to wherever its destiny is. Transported or picked pollutants range from toxic materials that are remnants of transportation systems to trash on sidewalks and pesticides from agricultural lands. A case study by Hopkinson & Day (Hopkinson and Day 1980) at an upland near Louisiana swamp forest showed that the projected increase of 321% of urban land at the expense of agricultural lands would cause runoff rate to be higher by 4.2 times and the nutrient runoff of nitrogen would increase by 28% and that of phosphorous by 16%. Usually, polluted runoff eventually ends in a certain body of water which can be a lake, reservoir, or the sea or percolates into groundwater at locations where physical properties of soil permit. Tong and Chen (Tong and Chen 2002) found a significant statistical relationship between land use and in-stream water quality mainly for phosphorous, nitrogen, and fecal coliform. From here rises the concern for the quality of water that is produced by urban runoffs. Wang *et al.* (Wang, Wei et al. 2011) mentions that urban storm runoff can result in important water quality problems, which include direct pollution of receiving waters and impairment of water treatment processes due to changes in intake of raw water quality and reduction of sewer system efficiency. Generally, runoff drainage networks are insufficient at managing wet weather flows, which makes it important to intervene in the urban water cycle at all levels to reduce runoff pollution and volume (Gromaire-Mertz, Garnaud et al. 1999).

Urban hydrology

Fletcher *et al.* (Fletcher, Andrieu et al. 2013), in his paper "*Understanding, management and modeling of urban hydrology and its consequences for receiving waters: A state of the art*", considers urban hydrology as a "master variable driving ecological degradation". Moreover, the developments in this science aim at improving the management of urban storm water for the enhancement of sanitation and public health, protection of environment and livability of cities, and flood protection.

Zoppou (Zoppou 2001) states that predicting stormwater quality accurately depends on adequate modeling of flow. Therefore, the first inputs when modeling urban stormwater quality disposed in water bodies are urban hydrology elements. The movement and circulation processes of water in the urban hydrology context are controlled by physical processes designated as the hydrologic cycle. The hydrologic cycle in urban settings consists of the following stages (Chow 1964):

- Precipitation
- Interception

- Infiltration: in addition to being affected by perviousness of land surfaces, the capacity of soil infiltration is also affected by antecedent precipitation such as short-interval high intensity rains coming after dry periods. A minimal steady infiltration rate is approached after one to two hours
- Depression storage and detention: precipitation that is trapped in superficial depressions of different depths and sizes
- Overland flow
- Gutter storage: usually has a greater effect in reducing peak flows than detention surfaces
- Conduit storage: the volume detained in the conduit can lessen the hydrograph peak rate flow

Precipitation, which is described in hydrology science as water reaching the earth surface in either liquid or solid form (Linsley, Kohler et al. 1949), is the main input in the hydrologic cycle path. Exact estimation of rainfalls at urban catchments is a prerequisite for evaluating rainfall-runoff response (Fletcher, Andrieu et al. 2013). Precipitation can be in one of the following forms: snow, rain, hail, or their variations like sleet and drizzle. Factors affecting precipitation are: atmospheric moisture and pressure, temperature, and wind (Viessman, Lewis et al. 1989).

The main characteristics for precipitation are (Seybert 2006):

- Volume, with units of area x depth
- Duration or time period of rainfall event
- Intensity, with units of velocity
- Frequency or the return period of a certain storm

Cities or urban areas affect precipitation amounts. In urban areas, newly constructed surfaces, which have different thermal properties than the previously natural land, change the processes in boundary layers creating what is called urban heat islands (UHI). Often, their effect extends downwind of the urban areas (Shepherd, Pierce et al. 2002).

Interception is that amount of precipitation that is retained by vegetation stems, canopy, or any other form of surfaces. Interception decreases the amount available from the initial stages of the storm. An extreme consideration by Soil Conservation Service is that an initial abstraction must be fulfilled before the water is available to runoff. This initial abstraction is designated to be proportional to soil storage capacity (Kibler and American 1982). However, in urban areas, precipitation intercepted by vegetation is not as important as that held on building surfaces and roofs and evaporated from there (Ward 1975).

In urban watersheds, the enlarged area of impervious areas reduces infiltration and increases significantly the surface runoff volume (Fletcher, Andrieu et al. 2013). For the calculation of runoff volumes and rates in urban watersheds, several methods are available (Akan and Houghtalen 2003):

- Unit hydrograph methods such as: Espey Ten-Minute Unit Hydrograph, SCS Unit Hydrograph, and Time-Area Unit Hydrographs
- Soil conservation service methods: TR-55 Graphical Peak Discharge Method, and TR-55 Tabular Hydrograph Method
- Santa Barbara Unit Hydrograph Method
- USGS regression equations
- The Rational Method
- The Kinematic-Rational Method

Water quality parameters

Suspended solids: are the elementary pollutants in the water environment. They are particulates of silt, clay, dirt, small vegetation particles, and even bacteria. All of these are designated as the total suspended solids (TTS) and are measured in mg/L. Turbidity is an indicator of the presence of TSS in a water body. Generally, not all TSS are toxic; however, TSS washoff, suspension, and transport from impervious, developed, or open ground and their later settling in water columns of a water environment/body have negative effects. TSS sometimes deposit on the natural bottom of streams, making food unavailable for all of the organisms in it. In addition, it can block light penetration in water, affecting photosynthesis of aquatic plant growth which is the food source and shelter for high level organisms. Also, TSS can act as a transport agent for toxic compounds such as heavy metals, pesticides, and biodegradable organic matter (Davis and McCuen 2005).

Oxygen demanding substances: are organic substances found in water that are metabolized by bacteria while consuming oxygen in water according to the following reaction:

$$\text{Organic matter} + O_2 \xrightarrow{\textit{microbes}} CO_2 + H_2O + \text{Cells}$$

Usually their measurement is either BOD (Biochemical Oxygen Demand), COD (Chemical Oxygen Demand), or TOC (Total Organic Carbon) (Davis and McCuen 2005).

Nitrogen compounds: are the nutrients that simulate the growth of algae. Substantial amounts of oxygen are oxidized by nitrogen species. Nitrogen appears in water in several forms like: organic nitrogen, nitrite ion (NO_2^-), nitrate ion (NO_3^-), and ionized and non-ionized ammonia (NH_4^+ and NH_3) (Chin 2006).

Phosphorous: is needed for living things to grow. It is commonly found in water in three forms: the ortho-phosphorous ($H_2PO_4^-$, HPO_4^{-2}) form, various organic forms, or as polymer phosphate. Total phosphorous is the total of all these three forms. Phosphorous has a strong attractive force to particulates, sediments, and soils and is carried with them. It enters runoff from washoff of excess fertilizers, decayed vegetation, and animal wastes. High concentrations of phosphorous can lead to eutrophication (Davis and McCuen 2005).

Microbial pathogens: are disease-causing organisms that include bacteria, viruses, and protozoa. The main diseases caused by pathogens are: typhoid, cryptosporidiosis, and cholera (Davis and McCuen 2005).

Heavy metals: this group includes cadmium, chromium, lead, copper, mercury, zinc, and nickel. High concentrations of heavy metals are toxic to humans, flora, and fauna. They are commonly adsorbed to suspended solids. Their danger lies in the fact that they do not degrade in the environment (Davis and McCuen 2005).

Oils and grease: the adverse effects of oil and grease arise from the fact that they coat parts of aquatic animals such as fish, affecting the efficiency of oxygen transfer. In addition, when they degrade they impose an oxygen demand (Davis and McCuen 2005).

Toxic organic compounds: these include pesticides, polycyclic aromatic hydrocarbons, and solvents. The most dangerous are pesticides because they kill or change the growth or reproductive traits of animal species and plants (Davis and McCuen 2005).

Trash: is transported by sheet and gutter flow during storm events. Some of the trash is made up of plastic and coated papers which are slow in degradation (Davis and McCuen 2005).

Loss of water species: many aquatic insect species, such as benthic macroinvertebrates, are intolerant of pollutants and will not be found in polluted waters. Evaluating the diversity (richness) of these populations can thus be used as a determinant of the degree of water pollution. Biological metrics that evaluate the loss of water species include taxa richness and EPT taxa richness. Taxa richness is a measure of the number of different kinds of organisms (taxa) in a collection, which reflects the overall diversity of the biological community. EPT taxa richness is the total number of taxa within the pollution-sensitive orders Ephemeroptera (mayflies), Plecoptera (stoneflies), and Trichoptera (caddisflies). Both metrics decrease with decreasing water quality (Reif, Survey et al. 2002).

Drivers for water quality degradation

Streams draining urbanized catchments are ecologically degraded, as reflected by elevated concentrations of nutrients and contaminants and reduced biotic richness. The impacts of urban land use on stream water quality are mainly attributed to stormwater runoff, in turn driven primarily by impervious surfaces. Stormwater runoff is efficiently transported away from impervious surfaces by piped stormwater drainage systems, and studies have found that runoff volume increases in direct proportion to impervious surfaces. Since most urban catchments are impervious, a positive correlation has also been found between catchment urbanization and concentrations of some stream water pollutants (Center for Watershed Protection (CWP) 2003b, Walsh, Roy et al. 2005, Hvitved-Jacobsen, Vollertsen et al. 2010).

Another important driver of urban impacts on stream water quality is deforestation, particularly in the riparian zone. Riparian zones consist of vegetated areas along both sides of streams and have important ecological influence on water chemistry and organic matter input. Deforestation in the riparian zone effectively removes the vegetation that normally filters pollutants from stormwater runoff (Walsh, Roy et al. 2005).

Water quality in urban stormwater-runoff

Concerns about urban runoff quality are increasing due to the noticeable negative phenomena detected in receiving waters of runoff such as lakes, rivers, streams, etc. existing in the vicinity of cities, dwellings, or other urbanized areas. Researchers are contemplating that increased river bank erosion, damage of river ecosystems, rapid eutrophication, and deterioration of water bodies' water quality are due to flows from urban runoff (Taebi and Droste 2004). Subsequently, urban stormwater runoff is renowned to be the most important cause of environmental contaminants accumulating in receiving watercourses (Davis and Birch 2010).

Pollutants found in urban runoff that jeopardize the quality of water systems include nutrients, heavy metals, sediments, hydrocarbons and oils, and oxygen-demanding constituents (Zhao, Shan et al. 2007).

The United States Environmental Protection Agency (EPA) has added to the aforementioned contaminants that affect water quality the following:

- Pesticides used in lawns and gardens
- Bacteria ,viruses, and nutrients from pet wastes and deteriorating septic tanks
- Road salts
- Thermal pollution coming from dark impervious surfaces, for example roofs and roads

The sources of contaminants in urban storm water are categorized by the EPA (Environmental Protection Agency (EPA) 1999) as follows:

- Bacteria and viruses originating from roads, leaky sanitary sewer lines, sanitary pipe connections, lawns, streets, animal wastes, and septic tanks
- Nutrients, mainly nitrogen and phosphorous, coming from atmospheric deposition, cars exhausts, soil erosion, animal wastes, detergents, and agricultural fertilizers
- Oil and grease/hydrocarbons mainly from streets, driveways, parking areas, all types of vehicles maintenance areas, and gas stations
- Sediments and floatables coming from streets, roads, construction sites, lawns, driveways, atmospheric deposition, and erosion occurring in stormwater channels

- Metals sources such as vehicles, atmospheric deposition, bridges, industrial areas, soil erosion, decaying metal surfaces, and combustion procedures
- Organic materials from animal wastes, landscaped areas, and residential lawns and gardens
- Pesticides and herbicides from landscaped areas, soil wash-off, roadsides, utility right-of-ways, and residential lawns and gardens

On the other hand, storm water pollution is partly originating from polluted rainwater. Atmospheric deposition adds to urban rain contamination (Huston, Chan et al. 2009).

With all these pollution sources, the sustainability of water bodies that receive disposed urban stormwater has become an increasingly important issue towards the end of the last century.

Regulations and acts have been issued to control the quality of urban stormwater passed to lakes, rivers, estuaries, etc. in the locale of urban areas. The effects of pollutants of the diffusive type on water bodies' quality as mentioned by (Novotny 1995) are:

- The increase in the amount of production nutrients that cause eutrophication
- Diminution of oxygen due to degradation of organic matter in the receiving water
- Health problems caused by infective organisms like bacteria, viruses, and protozoa
- Alluvial deposits resulting from alluvial runoff
- The increase in lake acidity due to atmospheric deposition
- The increase in salt concentrations producing salinization
- The addition of toxic micro-pollutants including industrial chemicals, pesticides, heavy metals, and herbicides which consequently cause mortality and morbidity of aquatic microorganisms

Eutrophication is a serious jeopardy to the aquatic life in the water body. The phenomenon of eutrophication is a direct result of the flourish of phytoplankton in the course of water life. The cause of this flourish is the abundance of nutrition loads, causing massive production of algae. Nutrients that play a noticeable role in water quality modification are: nitrogen phosphorous, silica and carbon. The adverse effects of eutrophication on water systems include changing the water system chemistry with respect to concentrations of oxygen and carbon dioxide, which ultimately affect the existence of aquatic life and the pH of water, respectively. Another effect of eutrophication is the alteration of ecosystem composition, whereby the original biota is banished for the dominance of other species that can be causing taste and odor problems or may even be toxic (making water undrinkable). Finally, the increase in the quantity of some floating plants and other species of scum hinders the usage of the water system for navigation or as a dump body for treated effluent from treatment plants by clogging its filters (Chapra 1997).

As mentioned, the main cause of eutrophication is the nutrient high loading in a water system. Nutrients include several chemical elements (mainly phosphorous, nitrogen, carbon, and silicon) which provide the building blocks for life in aquatic systems. Nutrients that are needed in large quantities for cell production are called macronutrients, while others that are needed in small quantities are called micronutrients. Macronutrients include phosphorous, sulfur, carbon, oxygen, nitrogen, iron, and silica. On the other hand, micronutrients include manganese, zinc, and copper (Chapra 1997).

Alluvial deposits in water systems have a crucial influence on the hydraulic behavior of water systems; however, their role in carrying bacteria and viruses is yet another issue of paramount importance. Bacteria and viruses carried to a water body adsorb to sediment particles and eventually settle. Resultant contaminated particles, when suspended again, pollute water particles around them (Thomann and Mueller 1987).

Point and nonpoint pollution sources in urban areas

Human activities add constituents (pollution) to the natural water quality, which is termed *background pollution* and is caused by contact of water with rocks, undisturbed soils, geologic formations, etc. Pollutants can generally be categorized according to their origin (one of two sources): those created by man activities and those which are initiated by natural processes. Moreover, pollution sources can be classified as being either from nonpoint sources (diffusive pollution) or from point sources. Point source pollution is detected at discrete recognizable points and can be measured and assessed directly. In the urban settings, point source pollution can be disposal points from sewerage treatment plants. Human activities contribute widely to nonpoint sources such as: construction, transportation, and buildup of litter and dust on impervious urban lands (Novotny and Chesters 1981).

Sources of nonpoint pollution mentioned by Novotny (Novotny 2003) that may occur in urban areas are:

- Pollution deposition from atmosphere dry and wet deposition
- Pollution from land surfaces: impervious areas, pollutants attached to runoff-eroded soil particles from pervious areas, and pollutants that are elutriated from soils
- Pollution from subsurfaces: storage tanks and landfills leaking contaminants to groundwater, chemical elements transported horizontally by groundwater flow, chemical constituents applied to soil surface and carried through infiltration to groundwater zones, and infiltration of groundwater into storm and combined sewers
- Pollution from drainage system sources (stormwater drainage and runoff systems)

- Pollution accumulated in sewers: solids and slime
- Erosion from drainage channels, streambank, and channel bottom
- Chemical constituents released from polluted aquatic sediment

The main characteristics of nonpoint sources are (Novotny and Chesters 1981):

- Their diffusive discharge behavior occurs at alternating periods related to the occurrence of meteorological events (‘wet weather flows’)
- Sources of nonpoint pollution cannot be monitored at the point of origin since they are difficult to be determined and traced
- Pollution accumulates over a wide area of land and is transported overland before reaching surface waters
- Removal or control of pollutants should be done at specific sites
- The most effective and feasible control for nonpoint pollution source are land management measures and architectural control in urban areas and conservation measures in rural areas
- The range of nonpoint source pollution is partially related to geologic and geographic conditions, along with certain uncontrollable climatic events which differ from year to year and from place to other

In general, nonpoint source pollution in urban areas is carried by surface runoff from hydrologically active areas. Hydrologically active areas are areas where surface runoff originates. Subsequently, they are areas of nonpoint pollution needing control and management. In urban lands, hydrologically active areas are areas with high groundwater table and/or tight soils, surfaces with frozen soils during spring rains, and impervious areas (Novotny and Chesters 1981).

Estimation of nonpoint source pollutant loads in urban areas: surface loads

Pollutants carried by surface runoff include sediment inputs that are due to erosion from wash-off of accumulated solids on impervious surfaces (roofs, parking lots, streets, etc.) and soil surfaces. The eroded matter transports with it organic matter, metals, and other naturally occurring cations and anions in the dissolved phase, solid phase or both. There are several methods to estimate surface pollution loads (Novotny 2003).

Characterizing land-emitted pollutants and correlating loads to them is one of the methods. Another method is to multiply the pollutant concentration to runoff volume in case approximate concentrations in the runoff are known. Also, event mean concentrations of pollutants in runoff can be used to calculate loads. Event mean concentrations are estimated and characterized by statistical analysis for the most common land usage in the boundaries of a specific geographical area (Novotny 2003). Samples need to be taken frequently (hourly) from sensors or automatically as grab samples by ISCO samplers.

Urban water quality modeling

A model as defined in the Oxford dictionary is “a simplified mathematical description of a system or process used to assist calculations and predictions.” It defines the components of a system and the relationships among them, and identifies the processes in the system whether they are physical, chemical, or biological using mathematical expressions (Hvitved-Jacobsen, Vollertsen et al. 2010). Its broad aim is to mimic reality and reproduce the performance of a system.

When it comes to modeling of urban runoff pollution, constructing a model helps in predicting the pollution loads, dispersion extent, and their fate in receiving water systems. The purpose is to help describe pollutants in runoff, regions affected, water courses polluted, and the controls or best management practices (BMPs) to mitigate the impaired systems.

The deterministic approaches for modeling urban wet weather water quality have been presented by Huber (Huber 1986) and are as follows:

- Constant concentration
- Regression equations and loading functions
- Rating curves
- Buildup-washoff
- Land surface erosion, and scour and deposition in sewers
- Other miscellaneous sources

Constant concentration

This method is the simplest because it sets the concentration of each pollutant to a fixed value, and the runoff annual load is produced by multiplying this concentration by the annual runoff volume (Novotny 1995). However, this approach is most robust when accompanied with a refined hydraulic model for precise simulations of stormwater flows (Huber 1986).

The constant concentration that is used is either the Event Mean Concentration (EMC) or Loading Rates. EMC by definition is the mean concentration of a certain pollutant in runoff and is calculated by dividing the total mass load of a pollutant to the total runoff volume. On the other hand, loading rate (LR) takes into consideration that concentration rates are site-specific. However, this procedure is not feasible.

Wanielista (Wanielista, Kersten et al. 1997) presented the procedure for determining EMC and LR. For determining EMC, sampling of flows at regular intervals during a runoff event, and estimating flow rates all over the event are done. Concentrations of samples are calculated at the laboratory. Subsequently, the weighted average of these concentrations is calculated as follows:

$$EMC = \frac{\sum CiQi}{\sum Qi}$$

C_i: sample i concentration

Q_i: The flow rate of runoff at sampling time

As for calculating LR, sampling is done for many storm events at longer time intervals (years), and the equation for LR is:

$$LR = \frac{M}{A}$$

LR: has units of (kg/ha-yr) or (lb/acre-yr)

M: mass total of pollutant collected over interval time of sampling

A: the area of watershed from where the pollutant was sampled

Regression equations and loading functions

Strom water pollution measurements are regressed against different variables or factors that are deemed to affect the quality of storm water. Such variables can be hydrologic characteristics of urban watershed, constituents of road pavement, economic activities in the urban area, etc.

Rating curves

As noted by (Huber 1986), rating curves is a regression formulation where the pollutant load is the only variable regressed against runoff volume, whereas the mathematical function is of power form. Davis and Birch (Davis and Birch 2010) showed that the usefulness of this method is based on its ability to present problematic data in a meaningful routine as compared to the use of EMC (constant concentration approach).

Buildup/washoff

The buildup term stands for the accumulation of solids (with pollutants adsorbed to their surfaces) and other pollutants during dry weather, which are consequently washed off during a storm event (Novotny 1995). Wang *et al.* (Wang, Wei et al. 2011) discusses the buildup/washoff model and displays the main features and mathematical equations formulated in it. The two pivotal factors in the buildup/washoff model are the antecedent dry days and the total runoff volume. The processes that occur in the antecedent dry days are the continuous accumulation and elimination of pollutants.

The buildup of pollutants during dry weather on impervious surfaces comes from different sources, including atmospheric deposition, littering, earth erosions, car emissions and decays, snow amassing etc. On the other hand, the removal of these pollutants can be due to road cleaning, wind erosion, and minor flows of water (Huber 1986).

Some research work has been done to experiment the relationship among the following three factors: runoff volume, previous dry days, and pollutants carried in the washoff process. While some studies showed that there is no strong relation between solids accumulating on paved surfaces and previous dry days, others showed that their build up in that period should not be underestimated. On the other hand, a correlation exists between TSS carried by runoff and the total volume of runoff. Yet still there is research work to investigate whether previous dry days should be included as a variable for buildup/washoff models.

The buildup mathematical functions of Huber *et al.* (Huber 1986) relate the amounts of solids and pollutants accumulated to previous dry days. These can be of several types: linear, exponential, power, or Michaelis-Menton:

- *Linear:*

$$P = a.t$$

P= Mass of pollutant accumulated on surface

t = duration since last time of cleaning or storm runoff

a = rate parameter

- *Power:*

$$P = a.t^b$$

b = exponent

a = rate parameter

- *Exponential:*

$$P = P_L.(1-e^{-bt})$$

P_L= Maximum amount of pollutant mass that accumulate on surface

- *Michaelis-Menton:*

$$P = \frac{P_L.t}{b+t}$$

b = half saturation constant

The washoff formulation that is most commonly used is the exponential function, and the derivation as presented by Wang *et al.* (Wang, Wei et al. 2011) is developed as follows:

$$\frac{dM}{dt} = -KM$$

M: amount of pollutant per unit area of catchment (mg/m^2)

t: time in minutes

K: rate by which the pollutant is washed with units (1/min)

Integrating both sides of equation yields:

$$M = M_0 e^{(-KT)}$$

M_0: the initial pollution amount found on the surface of the catchment (mg/m^2)

T: the duration of the storm event

In this model K is assumed to vary linearly with average runoff rate, thus K = C$\bar{R}$, then:

$$M = M_0 e^{(-CR)}$$

C: pollutant washoff coefficient with units (1/mm)

R= $\bar{R}$ T: the total volume of runoff (mm)

$\bar{R}$: the average runoff rate (mm/min)

In conclusion, the amount of pollutant washed off per unit area W (mg/m^2) is:

$$W = M_0[1-e^{(-CR)}]$$

Statistical methods

Novotny (Novotny 1995) describes the main concept in this approach, which lies in the fact that EMC is not constant but exhibits a lognormal frequency distribution. When joined with the lognormal distribution of runoff volumes, it can produce the distribution of runoff pollution loads. The derived result can also be combined to runoff flows distribution to generate lognormal distribution of in-stream concentrations.

First flush

The first flush concept (FF) is based on the idea that the first stage of storm runoff is the most polluted runoff flow (Deletic 1998). Determining and measuring FF is important for efficient design of treatment practices (Davis and McCuen 2005). FF phenomenon occurring at urban wet weather is a controversial subject. Due to the absence of a clear definition of the phenomenon, some scientists do not believe in its reality and its effect on the sizing of treatment infrastructure (Saget, Chebbo et al. 1995). On the other hand, Lee et al. (Lee, Bang et al. 2002) defined FF as “the initial period of storm runoff during which the concentration of pollutants is substantially higher than during later stages”.

Deletic (Deletic 1998) mentioned that FF occurrence and characteristics are controversial because it is defined in different ways. FF is determined by plotting curves of cumulative fraction of total pollutant mass versus total cumulative volume of runoff. Researchers differed at this point: Geiger (Geiger 1987) suggested that FF occurs when these curves have an initial slope greater than 45^{o} and the point of maximum divergence from the 45^{o} slope measures FF. On the other hand, French researchers (Saget, Chebbo et al. 1995) defined the FF occurrence when 80% of the pollutant load is transported through the first 30% volume of runoff (Deletic 1998).

Studying the existence of the FF phenomenon in a watershed is imperative for decision-makers to design specific best management practices that can divert the initial portion of runoff with the highest pollutant load prior to its disposal in receiving waters. One way to analyze FF occurrence is to plot dimensionless cumulative runoff volume (F) vs dimensionless cumulative pollutant load (L) (Lee, Bang et al. 2002):

$$L = M_t/M$$

$$F = V_t/V$$

L: cumulative pollutant mass (load) fraction; dimensionless

M_t: total cumulative pollutant mass at time t

M: total pollutant mass

F: cumulative runoff volume fraction; dimensionless

V_t: total cumulative runoff volume at time t

V: total runoff volume

FF occurs at time (t) in case L is greater than F at all durations of storm events. Figure 1 is an example of a data plot to determine if FF occurred. The rule is if data lie on the 45° slope line then pollutants are uniformly distributed over the durations of storm events. When data lie below the 45° line slope, then dilution is considered to occur and FF does not exist. The last case is when data lie above 45° slope line then FF has occurred (Lee, Bang et al. 2002).

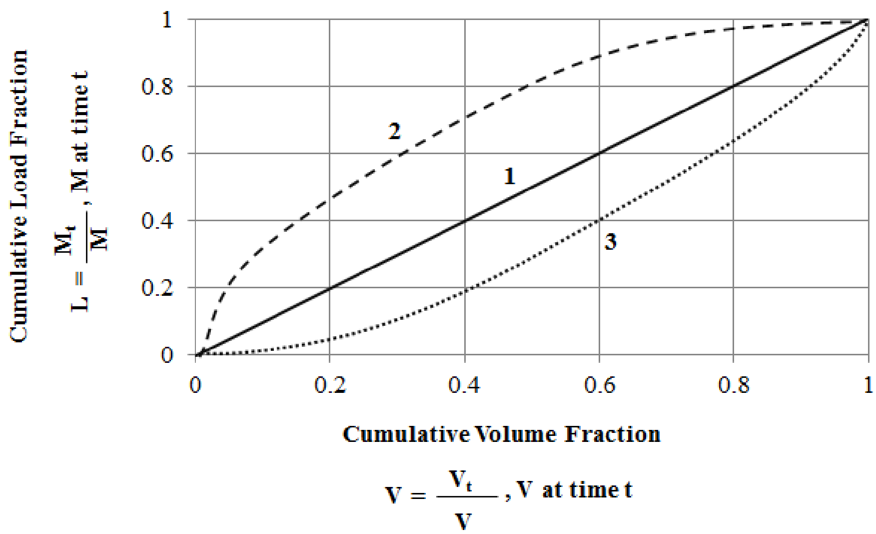

Figure 1. Plot of dimensionless cumulative flow rate versus dimensionless cumulative load. Line 1 is the 45° slope line. When data lie on Line 1, pollutants are uniformly distributed over the durations of storm events and FF does not exist. When data lie on Line 2 (above Line 1), FF has occurred. When data lie on Line 3 (below Line 1), dilution has occurred and FF does not exist – Modified from (Davis and McCuen 2005).

Best Management Practices (BMPs)

The physical systems that are used for the treatment of runoff are named Best Management Practices (BMPs) (Davis and McCuen 2005). EPA (Environmental Protection

Agency (EPA) 1999) mentions the goals of BMPs which are: flow control, pollutant removal, sedimentation, flotation, filtration, infiltration, and pollutant source reductions.

Low Impact Development (LID) practices are categorized under BMPs. The idea of LID emphasizes the balance of water and pollutant by integrating land development with environmental issues. LID focuses on management and land use which reduce environmental impacts. The main aim of LID is to reduce impervious areas as much as possible and to retain water runoff on site as long as possible with natural measures. For runoff drainage, vegetated swales and filter strips are preferred to gutter systems which rapidly transport runoff. The vegetated swales and filter strips slow the flow of runoff and increase the chance of infiltration into the ground, keeping fewer pollutants conveyed. Another LID measure is diverting roof rain into vegetated areas (Davis 2005).

Structural BMPs

Structural BMPs, which are engineered and constructed systems to control the quantity and quality of stormwater, are grouped into the following categories (Environmental Protection Agency (EPA) 1999):

- Infiltration systems: include infiltration basins, porous pavement systems, and infiltration trenches or wells, which capture a volume of runoff and infiltrate it into the ground. These systems provide control for both water quantity (by reducing the volume of discharged stormwater) and quality (by removing pollutants and particles during percolation).
- Detention systems: include detention basins and underground vaults, pipes and tanks, which capture a volume of runoff and temporarily retain it for gradual release. While

some settling of particulate matter may occur, a large portion gets resuspended by subsequent runoff events. As such, these systems mainly provide water quantity control.

- Retention systems: include wet ponds and underground pipes or tanks. Unlike detention systems, these systems maintain a significant permanent volume of water in between runoff events, and provide control of both water quality and quantity. Mechanisms of pollutant removal include sedimentation (which is less likely to be affected by subsequent runoff events in the permanent pool) and other mechanisms such as filtration of suspended solids by vegetation.
- Constructed wetland systems: include wetland basins and channels, which are similar to retention and detention systems except that a major portion of the surface area contains wetland vegetation. Constructed wetlands provide water quality control and are particularly appropriate where groundwater is close to the surface so as to provide the water necessary to sustain the wetland system.
- Filtration systems: include devices that employ granular filtration media such as sand, soil, or a membrane to remove particulate pollutants in the runoff.
- Biofilters (vegetated systems): include swales and filter strips, which mimic the functions of a natural forest ecosystem for treating storm water runoff. Treated water is subsequently allowed to infiltrate into the surrounding soil, or is collected and discharged.
- Miscellaneous and vendor supplied systems: include catch basin inserts, hydrodynamic devices, filtration devices, and other proprietary systems, incorporate some combination of filtration media, hydrodynamic sediment removal, oil and grease removal, and screening to remove pollutants.

Extended dry detention ponds

Dry detention ponds (also known as detention ponds or basins) are basins whose outlets have been designed to detain stormwater runoff for some minimum time (e.g., 24 hours) to allow particles and associated pollutants to settle. As such, they do not have a large permanent pool of water, but are often designed with small pools at the inlet and outlet of the basin (Environmental Protection Agency (EPA) 2014).

Traditionally, dry detention ponds are one of the most widely used stormwater structural BMPs. Due to the absence of a permanent pool, they are more effective at removing particulate pollutants (such as TSS) by way of settling than soluble pollutants. Typical removal rates can reach 61% for TSS and range 26-54% for metals (Schueler 1997, Environmental Protection Agency (EPA) 2014).

Extended dry detention ponds (EDDPs) have two stages, whereby runoff from small storms is detained in the bottom stage to allow pollutant settling, while the top stage remains dry except during large storms. The small volume is retained in the bottom stage long enough to achieve the targeted level of pollutant removal (Akan and Houghtalen 2003). When the bottom stage is naturalized with a vegetated surface, the dry extended detention pond's efficacy at removing pollutants is enhanced. The vegetated surface lends the properties of vegetated swales to the ponds by providing additional pollutant removal through vegetative filtering, biological uptake, and infiltration into the underlying soil media (Maryland Department of the Environment 2000). EDDPs have enhanced pollutant removal capabilities that are very similar to those of wet detention ponds (80-90% TSS removal) (Chin 2006). Moreover, they can remove bacteria (including fecal streptococci, fecal coliform, *E.coli*, and total coliform) at 78% efficiency (Debo and Reese 2002). EDDPs (Figure 2) are the least-expensive stormwater treatment practice on a cost per treated unit area, and their maintenance is estimated to be 3-5% of the construction cost annually (Debo and Reese 2002).

Figure 2. An example of an extended dry detention pond – Modified from http://www.vwrrc.vt.edu/swc/NonPBMPSpecsMarch11/VASWMBMPSpec15EDPOND.html.

Stormwater management models

Over the years, numerous computer models have been developed for stormwater management, drainage infrastructural design, and planning. Table 1 summarizes the features of some of the most commonly used models.

Among the different models, PCSWMM was chosen to address the objectives of this research study. Its features, capabilities and advantages over other models are discussed in the following section.

<u>PCSWWM model</u>

PCSWMM, from Computational Hydraulics International – CHI- (http://www.chiwater.com/), is a spatial decision support system for SWMM which is capable of reading all GIS data formats. PCSWMM is based on SWMM5 engine for urban drainage modeling. The SWMM model is developed by USEPA (Environmental Protection Agency (EPA)) and stands for “Storm Water Management Model”. This computer program is used for the simulation of runoff quantity and quality generated in rural (undeveloped) areas or urban areas. The program computes dynamic rainfall-runoff for single events or long term continuous records. Runoff quantities are calculated based on sub-catchments that receive rain and generate runoff and pollutants. Runoff is routed overland and below ground through channels, pipes, treatment and storage devices, pumps and regulators.

Model	Abbreviation	Primary Intended Use
P8-UCM	P8 Urban Catchment Model	Estimation of urban stormwater pollutant load
RUNQUAL		Preliminary planning or education
StormTac		Management of lake catchments and conceptual design of stormwater treatment
MOUSE	MOdel for Urban SEwers	Detailed simulation of urban drainage
SWMM	Storm Water Management Model	Detailed model for planning and preliminary design
PCSWMM	Personal Computer SWMM	Same as SWMM but with enhanced stormwater control measure (SCM)
UVQ	Urban Volume and Quality	Integrated water cycle and water re-use Used mainly for research
WBM	Water Balance Model	Planning-level assessment of water quantity
SLAMM	Source Loading And Management Model	Planning tool for load of contaminants
MUSIC	Model for Urban Stormwater Improvement Conceptualization	Conceptual design for drainage systems, with emphasis on treatment devices
PURRS	Probabilistic Urban Rainwater and wastewater Reuse Simulator	Single site water use model Originally for research but now includes commercial users, especially for rain tanks

Table 1. Different models used for stormwater management - Adapted from (Elliott and Trowsdale 2007, National Research Council 2009).

The PCSWMM model consists of different modules or blocks. The main blocks are the runoff block, transport block, and the storage and treatment block. Runoff block generates runoff and quality constituents in rainfall. The transport block is used for kinematic wave routing and for additional dry weather and quality routing, while the storage and treatment block is used for reservoir routing, simulating of treatment, and processing of storage quality. Hydraulic routing of flow is executed by the Extended Transport of Extran Block. During a simulation period, PCSWMM can trace the quantity and quality produced at each sub-catchment. In addition, it can track the quality of water, flow rate, and flow depth in pipes and channels. LID and BMPs can be modeled to reduce impervious and pervious runoff and associated pollutants transport (Rossman 2005, James, Rossman et al. 2010).

The hydrological component of PCSWMM functions on impervious and pervious subcatchments that can include depression storages. PCSWMM has the capability of accounting for different hydrologic processes that produce runoff, including (James, Rossman et al. 2010):

- Rainfall of time-varying nature
- Still surface water evaporation
- Accumulation and thawing of snow
- Rainfall capture in depression storages
- Rainfall infiltration
- Seepage of infiltration into groundwater
- Infiltration of water between groundwater and drainage network
- Nonlinear reservoir routing for overland flow
- Intercepting and retention of rainfall-runoff by different low impact measures

In addition, the hydrologic component of PCSWMM calculates pollutant load buildup and washoff of subcatchments. PCSWMM's abilities are (James, Rossman et al. 2010):

- Buildup of dry-weather pollutants on lands
- Washoff of pollutants during storms from lands
- Rainfall contribution
- Dry-weather buildup reduction due to street cleaning
- Washoff loads reduction due to BMPs
- Input from sanitary systems and user specified input at any location during dry weather to drainage network
- Water quality elements routing
- Water quality pollutants reduction due to natural processes in channels/pipes or by treatment in storage units

PCSWMM has hydraulic modeling capabilities that route runoff and water quality constituents through open channels, closed pipes, storage-treatment basins, etc. These capabilities are (James, Rossman et al. 2010):

- Modeling networks of different sizes
- Handling different shapes of pipes and channels
- Modeling flow dividers, pumps, weirs, orifices, and storage treatment units
- Using different routing methods such as kinematic wave or full dynamic wave or steady-state
- Inputting external flows and water quality input from surface runoff, ground interflows, infiltrations, dry weather sanitary flows, and inflows defined by the user

- Handling different flow regimes like backwater, free surface, surcharging, surface ponding and flooding, and reverse flow
- Using rating curves for inlet controls
- Handling control rules for operation of pumps, openings for orifices, and levels of weir crest

Generally, various research applications have confirmed that PCSWMM is an excellent program to model surface water quantities in urban areas rather than to simulate water quality (Tsihrintzis and Hamid 1997, Deliman, Glick et al. 1999, Obropta and Kardos 2007).

When modeling urban subcatchments in PCSWMM, discretization of urban subcatchments can be of fine or coarse type based on the model aim. Fine discretization results in a higher number of subcatchments than coarse discretization. Generally, coarse discretization saves on time of model construction and computation costs and is used for planning rather than detailed design which requires more of fine discretization (Zaghloul 1981).

For calibration of SWMM models, certain parameters need to be examined to check which are more sensitive than others. Zaghloul (Zaghloul 1983) examines the most sensitive parameters in the SWMM runoff block and transport block.

In the runoff block, the basic parameters are (Zaghloul 1983):

- Percent of imperviousness
- Manning’s runoff coefficient
- Ground slope
- Detention depth
- Infiltration rate
- Width of the overland flow

On the other hand, the main components of transport block are (Zaghloul 1983):

- Number of conduits in a given length
- Conduit length
- Surcharge condition
- Conduit slope
- Conduit Manning’s roughness coefficient

The most sensitive parameters in the runoff block are: percentage of imperviousness and width of overland flow, while those for the transport block are: conduit length and Manning’s roughness coefficient (Zaghloul 1983). In another study on large urban catchments that used the optimization procedure, the most sensitive parameter was imperviousness and the least sensitive parameter was Manning’s roughness for surface flow (Barco, Wong et al. 2008).

Calibration of model parameters can be done by neural networks which substitute the trial and error process. This technique was used for impervious areas, yet it still needs some work for pervious areas (Zaghloul and Abu Kiefa 2001). In general, this method requires large amounts of flow and water quality data.

Advantages of PCSWMM over other models

PCSWMM was chosen for this research due to its special capabilities of having the GIS engine that can handle the latest GIS data formats and support of the SWMM engine from EPA. The inherited capabilities from the SWMM model that are useful for this study are its dynamic hydraulic and hydrological modeling capabilities of simulating runoff quantity and quality in urban areas. It can be used for single event or long term continuous events with time varying hyetographs, depression storage, and different infiltration methods. It can be used to model large complicated drainage networks with different conduit shapes and sizes. Moreover, it has three options for routing stormwater flows which are: steady state, kinematic wave, and dynamic wave. Also, it can model the washoff of pollutants from land surfaces and route the pollutant concentration through the drainage network. In addition to its ability to model BMPs, PCSWMM can also model the reduction of pollution concentration through treatment in storage units or by natural processes in the drainage network (Environmental Protection Agency (EPA) , Rossman 2005, Poresky 2007). Finally, the SRTC (Sensitivity-based Radio Tuning Calibration) tool facilitates calibration of the model through the use of uncertainty percentage chosen by the user for certain model parameters. When running SRTC, PCSWMM model executes two runs of the model for the extreme highest and lowest percentage of the chosen uncertainty range. The SRTC tool provides a slider for the user to fine tune the parameters that best suit observed time series.

When examining the FF phenomenon, the advantages of using a computer model over traditional methods are obvious. The PCSWMM model uses data from rainfall samples that are automatically collected during rainfall events. This is much more time- and cost-effective than regular methods relying on numerous sample collections at specified timepoints throughout the duration of a storm.

Several studies have used SWMM to model urban watersheds and calibrate model outputs with real data in terms of flows and pollutant concentrations, such as the study by Tsihrintzis *et al.* (Tsihrintzis and Hamid 1998). On the other hand, the use of SWMM to specifically examine the existence of FF phenomenon was reported in only study (Mrowiec, Kamizela et al. 2009). In this study, the authors carried out the necessary calibration with respect to flows and concentrations prior to studying the existence of FF in the SWMM model output.

This research study will approach this topic from another perspective. It will consider that in the absence of successive sampling in a storm event, a single sample from each storm can still be used to examine the existence of FF phenomenon when suitable simulation input parameters are applied.

CHAPTER III:

ST ANTHONY PARK WATERSHED STORMWATER QUALITY

Study area

The Minnesota Capitol Region watershed is a small urban watershed in the Upper Mississippi River basin with all runoff discharging to the Mississippi River. The Capitol Region Watershed District (CRWD) is a special government purpose unit that manages, protects, and improves water resources within the Capitol Region watershed. CRWD is highly urbanized with a population of 245,000 and contains portions of five cities, including Falcon Heights, Lauderdale, Maplewood, Roseville, and Saint Paul. All runoff from CRWD discharges through 42 outfall pipes along a 13-mile stretch of the Mississippi River that borders the southern boundary of the District (Capitol Region Watershed District 2014).

The St. Anthony Park watershed has a drainage area of 3,418 acres of St. Paul, Falcon Heights, and Lauderdale and is the western-most watershed in CRWD. The watershed outlets directly into the Mississippi River via a storm tunnel at Desnoyer Park in St. Paul, upstream of Ford Dam (Figure 3). The watershed is primarily comprised of industrial and residential land uses with 48% impervious surface land coverage (Capitol Region Watershed District 2014).

Rationale

Stormwater runoff is one of the most significant sources of pollution to CRWD water resources. Urban development in the watershed over time has significantly impacted the quality of the Mississippi River through polluted stormwater runoff. The Mississippi River is listed on the Minnesota Pollution Control Agency's (MPCA) 2012 303(d) list of impaired waters (MPCA, 2012a) that are not meeting the standards for their designated uses of fishing, aquatic habitat, and recreation. A total maximum daily load (TMDL) study is required for impaired waters for pollutants of concern, such as nutrients, turbidity, metals, and bacteria (Capitol Region Watershed District 2014).

Several pollutants are of concern in the St Anthony Park watershed. These include heavy metals (such as cadmium, chromium, copper, lead, nickel and zinc) which can potentially arise from auto exhaust, tire wear, brakes, and some winter de-icing agents. Another pollutant category is nutrients, which includes nitrogen and phosphorus. Phosphorus is of primary concern in CRWD. Potential sources of phosphorous include fertilizers (possibly from farms bordering the north side of the St Anthony Park watershed), leaves and grass clippings, and pet and wildlife waste. A third category is sediments (TSS), which originate from sand application to roadways and parking lots for traction in the winter as well as erosion of soil particles from construction sites, lawns, and stream banks. Finally, pathogens, which include bacteria (such as *E.coli*) also contribute to water quality degradation and may potentially be supplied by illicit sanitary connections to storm drains and animal waste (Capitol Region Watershed District 2014).

The goal of this objective is to characterize the overall St. Anthony Park watershed stormwater quality trends over time by evaluating the watershed runoff pollutant concentrations, including heavy metals (cadmium, chromium, copper, lead, nickel and zinc), nutrients (ammonia and total phosphorus), sediment (TSS), and bacteria (*E. coli*). Another goal is to assess the correlation of the pollutants with rainfall parameters (precipitation depth and previous dry days). It has been shown that parameters such as rainfall intensity and rainfall volume are important factors in influencing the export of heavy metals from an urban area (Herngren, Goonetilleke et al. 2005). This evaluation is thus necessary prior to evaluating the effectiveness of stormwater structural BMPs, which in turn would inform management decisions for continued improvement of water resources.

TSS is a pollutant of major concern due to its multiple detrimental effects. By way of settling to the bottom of streams and blocking sunlight access, TSS can prevent food access and photosynthesis, leading to the degradation of aquatic ecosystems. Moreover, TSS can act as a transport agent for other pollutants (Davis and McCuen 2005). It has been shown that most of the heavy metals in urban stormwater runoff are attached to suspended solids (Herngren, Goonetilleke et al. 2005), and the majority of *E. coli* in aquatic systems are also associated with sediments (Chen and Chang 2014). Given that TSS will be used as model pollutant for PCSWMM and that several BMPs for stormwater management are designed to target particulate fractions, an in-depth understanding of the relationships between pollutants and TSS is crucial for BMPs to be of utmost efficacy in mitigating stormwater pollution.

Figure 3. The St. Anthony Park watershed monitoring site at the main outfall on the Mississippi River – Modified from (Capitol Region Watershed District 2014).

Data used

CRWD has continuous flow data and stormwater quality and quantity data for the period 2005-2013.The annual stormwater monitoring reports (2005-2013) are available on the CRWD website (www.capitolregionwd.org). Data sets for the analyzed storms, including dates, precipitation depth, previous dry days and stormwater quality are provided in the Appendix (A1-A3).

Water quality data

Sampling

CRWD collected water quality and quantity data through a full water quality station with automated samplers and water level and velocity sensors. The site had a flow logger installed for the entire calendar year and an automatic sampler (ISCO 6712, 2150 module) installed from April to November. The full water quality station was positioned at the outlet of the St. Anthony Park watershed which drains directly to the Mississippi River (Capitol Region Watershed District 2014).

The full water quality station consists of an area-velocity sensor and an automated water sampler. Area-velocity sensors measured and recorded water depth and velocity every 10 or 15 minutes, and were secured to the base and center of the pipe. They were also connected to the automated water sampler, which was housed above ground. Samplers were programmed to capture storm events that were greater than or equal to a precipitation event of 0.5 inches. When the flow of water reached a specified depth or velocity, the sampler engaged to collect water samples. In order to collect samples over the entire hydrograph, samples were collected after a specified volume of water passed through the site. These individual samples were combined and mixed to produce a single composite sample that represented stormwater quality throughout the entirety of a storm as opposed to taking a single grab sample. To create a composite sample, individual sample bottles were first shaken until the sampled water became homogenous, then poured into a 14-Liter churn sample splitter and thoroughly mixed to create a homogenous sample. Four liters of the homogenous sample were then distributed to a sample bottle provided by the Metropolitan Council Environmental Services (MCES) Laboratory.

Bacteria grab samples for *Escherichia coli* (*E. coli*) were taken during storm events when runoff was generated, sampled directly into sterilized containers, and delivered immediately to the lab for analyses due to the short sample holding time (6 hours).

Analysis

Water quality samples were delivered to the MCES Laboratory for analysis. Samples were collected during both baseflow and stormflow periods and were analyzed to determine pollutant concentrations for a suite of water quality parameters including heavy metals (cadmium, chromium, copper, lead, nickel and zinc), nutrients (ammonia and total phosphorus), sediment (total suspended solids), and bacteria (*E. coli*). Table 2 summarizes the water quality parameters examined.

Water quality standards

Currently, there are no federal or state water quality standards for stormwater. There are water quality standards under the Clean Water Act which protects the receiving waters, however. St. Anthony Park watershed stormwater flows into the Mississippi River. As such, the stormwater data was compared to two reference standards: the MPCA standards and the NSQD standards. Exceedance was defined as a sample concentration that exceeded the MPCA or NSQD standard. Percent exceedance represents the percent of storm samples exceeding the standard.

MPCA standards: The Minnesota Pollution Control Agency (MPCA) has established surface water quality standards (Table 3). Except for TP, all the MPCA standards are from Minn. Stat. § 7050.0222 and apply to Class 2B waters in the North Central Hardwood Forest ecoregion. Class 2B waters are designated for aquatic life and recreational use. All standard concentrations apply to chronic exposure. The TP MPCA standard is from the Draft Technical Support Document released by the MPCA in 2011 providing support for proposed amendments to Minn. Stat. § 7050 & 7052 (amendments are pending).

Parameter		**Abbreviation**	**Method**	**Reporting Limit**
Heavy Metal	Cadmium	Cd	MET-ICPMSV_5	0.0002 mg/L
	Chromium	Cr		0.00008 mg/L
	Copper	Cu		0.0003 mg/L
	Lead	Pb		0.0001 mg/L
	Nickel	Ni		0.0003 mg/L
	Zinc	Zn		0.0008 mg/L
Nutrient	Ammonia	NH_3	NH3_AA_3	0.005 mg/L
	Total Phosphorus	TP	NUT_AA_3	0.02 mg/L
Sediment	Total Suspended Solids	TSS	TSSVSS_3	N/A
Pathogen	Escherichia Coli	*E. coli*	Colilert and Colilert-18 with Quanti-Tray/2000 method	N/A

Table 2. Water quality parameters examined, examination method and reporting limit - Obtained from (Capitol Region Watershed District 2014).

Parameter	Unit	NSQD Standard	MPCA Standard
Cd	mg/L	0.0009	*Depends on water hardness*
Cr		0.007	
Cu		0.016	
Pb		0.016	
Ni		0.0078	
Zn		0.095	
NH_3		0.39	0.04
TP		0.28	0.04
TSS		66	30
E. coli	MPN/100 mL	1050	≤ 1260

Table 3. MPCA and NSQD standards for water quality parameters - Obtained from (Capitol Region Watershed District 2014).

The toxicity of a metal is a function of water hardness. For the St. Anthony Park watershed, the chronic toxicity standard is used, as defined in Minnesota Rules 7050.0222 for each of the 6 metals (Cr, Cd, Cu, Pb, Ni, and Zn). Equations for the chronic standard for each metal in µg/L are listed below. To convert from micrograms (µg) to milligrams (mg), the standard was divided by 1000. The corresponding values for each year in the examined interval 2005-2013 are listed in the Appendix (A4).

$$Cadmium\ Standard\ \left({}^{\mu g}/_{L}\right) = e^{0.7852*\ln[Average\ Hardness({}^{mg}/_{L})]-3.49}$$

$$Chromium\ Standard\left({}^{\mu g}/_{L}\right) = e^{0.819*\ln[Average\ Hardness({}^{mg}/_{L})]+1.561}$$

$$Copper\ Standard\left({}^{\mu g}/_{L}\right) = e^{0.620*\ln[Average\ Hardness({}^{mg}/_{L})]-0.57}$$

$$Lead\ Standard\left({}^{\mu g}/_{L}\right) = e^{1.273*\ln[Average\ Hardness({}^{mg}/_{L})]-4.705}$$

$$Nickel\ Standard\left({}^{\mu g}/_{L}\right) = e^{0.846*\ln[Average\ Hardness({}^{mg}/_{L})]+1.1645}$$

$$Zinc\ Standard\left({}^{\mu g}/_{L}\right) = e^{0.8473*\ln[Average\ Hardness({}^{mg}/_{L})]+0.7615}$$

NSQD standards: In addition to comparing St. Anthony Park watershed results to state surface water quality standards, stormwater concentrations were also compared to other urbanized areas in the United States using data reported in the National Stormwater Quality Database (NSQD). Created by researchers from the University of Alabama and the Center for Watershed Protection, it is an extensive database of stormwater data from a representative number of National Pollutant Discharge Elimination System (NPDES) Municipal Separate Storm Sewer System (MS4) Phase I stormwater permit holders.

The NSQD, Version 1.1 contains stormwater quality data from 3,765 storm events and 65 municipalities in 17 states (including Minnesota) over nearly a ten-year period (Maestre and Pitt, 2005). Data was extensively reviewed for quality assurance and control. While it includes only a small set of data from the midwest and northeast portions of the country, which have similar climatic conditions, it still provides a useful comparison of how polluted stormwater in St. Anthony Park watershed is compared to the rest of the country.

The database includes stormwater quality data for various land use types. The predominant land uses in St. Anthony Park watershed is mixed residential and industrial with 48% of the land comprised of impervious surfaces. CRWD’s stormwater quality data was compared to the NSQD’s mixed residential land use category, which has a median impervious percentage of 45% (Table 3).

<u>Precipitation data</u>

Precipitation data recorded every 15 minutes were obtained from the Minnesota Climatology Working Group (MCWG) at the University of Minnesota-St. Paul (UMN). While a low level of variability exists for precipitation events within CRWD, previous watershed model calibration within the District has shown that the precipitation amount at the UMN site adequately represents data in the District. The detailed dataset is provided in the Appendix (A1).

Statistical analysis

GraphPad Prism software, version 6.0 (San Diego, CA) was used for statistical analysis. According to the Shapiro–Wilk test, the dataset was not normally distributed. Hence, the Spearman's rank correlation method—which makes no assumptions about the distribution of the data—was applied to investigate the correlation between precipitation depth (in), previous dry days (days), and stormwater analytes for all stormflow events in the data record (2005 – 2013). The correlation analysis was also performed for datasets exceeding MPCA standards (referred to as MPCA exceedances) and datasets exceeding NSQD standards (NSQD exceedances) for each of the analytes. The correlation analysis was not performed for analytes that exceeded the MPCA/NSQD standards less than 10% of the time.

In addition, the correlation between heavy metal (Cd, Cr, Cu, Pb, Ni and Zn), nutrient (TP and NH_3), *E. coli*, and sediment (TSS) concentrations was also investigated. All statistically significant differences were tested at $\alpha = 0.05$ level. “Previous dry days” was defined as the number of days since the last measureable rainfall, and was obtained from precipitation data collected at the University of Minnesota St. Paul Campus weather station (UMN).

Results and discussion

Water quality analysis and trends

Over the analyzed period (2005-2013), it was clear that stormwater discharges of the St. Anthony Park watershed are highly contaminated, as measured by exceedance of the MPCA standards and as compared to NSQD data (Table 4). The results of the water quality analysis conducted herein underline the threat of direct discharge of St. Anthony Park watershed stormwater runoff into the Mississippi River natural waters.

MPCA standards: The chronic toxicity standards for metals are a function of water hardness. In the St. Anthony Park watershed, the highest toxicity was seen with Pb, which exceeded the MPCA allowable concentrations in over 97% of stormwater samples, followed by Cu (over 87%) and Zn (over 54%). On the other hand, Cd, Cr and Ni were within MPCA limits in > 95% of the samples tested.

NH_3 levels exceeded MPCA standards over 56% of the time. In addition, TP and TSS were of major concern since they exceeded allowable limits in over 99 and 92% of samples, respectively. Finally, *E.coli* samples collected during storm events exceeded the MPCA surface water maximum numeric standard of 1,260 MPN/100mL in 83% of the samples collected. In some cases, bacteria results were 20-100 times greater than the standard.

NSQD standards: Compared to other urbanized areas in the country, St. Anthony Park watershed stormwater concentrations for metals exceeded NSQD median concentrations for mixed-residential areas in 49-62% of the time. Similar to the MPCA comparison, Cd levels measured were within NSQD levels in > 95% of the samples tested. Similarly, NH_3 was within NSQD limits in > 91% of the samples tested.

St. Anthony Park watershed exceeded median NSQD stormwater concentrations for TP, TSS, and *E. coli* in over 40, 78 and 86% of samples tested. These data are summarized in Table 4 and depicted in Figures 4-7.

Overall, both comparisons indicate a low level of pollution concern associated with Cd and a high level of pollution concern associated with Cu, Pb, Zn, TSS and *E.coli*. On the other hand, the two methods of comparison differed on Cr and Ni, which did not exceed MPCA standards in any of the samples but exceeded NSQD levels seen in other urbanized areas ~ 50% of the time. The two methods of comparison also differed on NH_3, which (conversely) exceeded NSQD standards in ~ 8% of the samples versus over 56% of the samples with MPCA standards, and which could be reflective of the high levels of NH_3 seen in stormwater of urbanized areas in the U.S. At the same time, it underscores the importance of mitigating NH_3 pollution in the St. Anthony Park watershed stormwater. Finally, total phosphorus (TP) was seen as a major concern with the MPCA comparison (over 99% exceedance) and of intermediate concern with the NSQD comparison (over 40% exceedance), which similarly underscores the importance of mitigating TP pollution in St. Anthony Park watershed stormwater.

Parameter	NSQD Standard Exceedance	MPCA Standard Exceedance
Cd	4.7%	4.7%
Cr	49.3%	0%
Cu	62.2%	87.2%
Pb	60.1%	97.3%
Ni	51.4%	0%
Zn	57.4%	54.7%
NH_3	8.1%	56.8%
TP	40.5%	99.3%
TSS	78.8%	92.5%
E. coli	86.1%	83%

Table 4. Percentage of stormwater samples exceeding NSQD and MPCA standards. Exceedance was defined as a sample concentration that exceeded the MPCA or NSQD standard. Percent exceedance represents the percent of storm samples exceeding the standard.

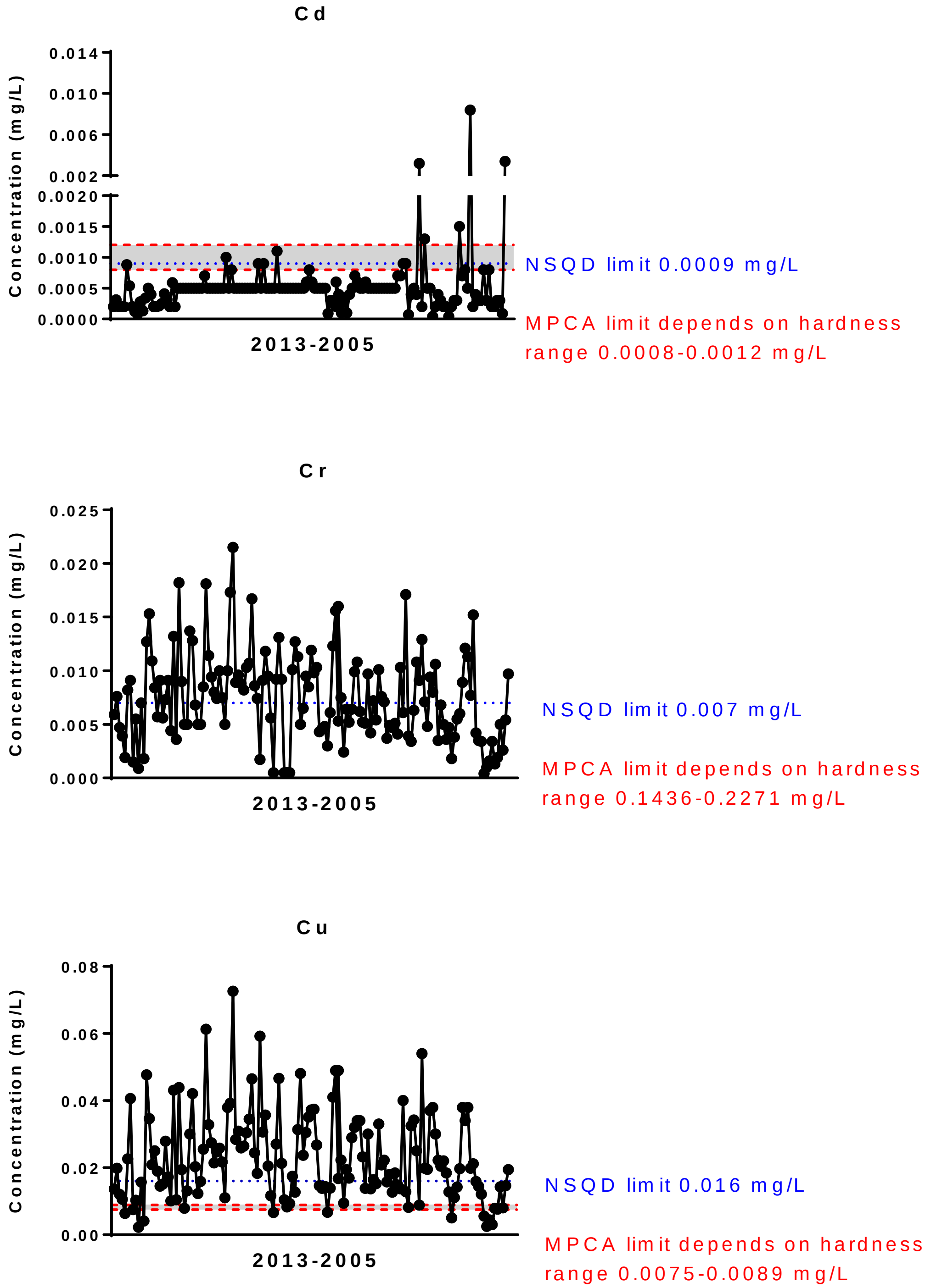

Figure 4. Stormwater concentrations of Cd, Cr and Cu for the recorded period 2005-2013.

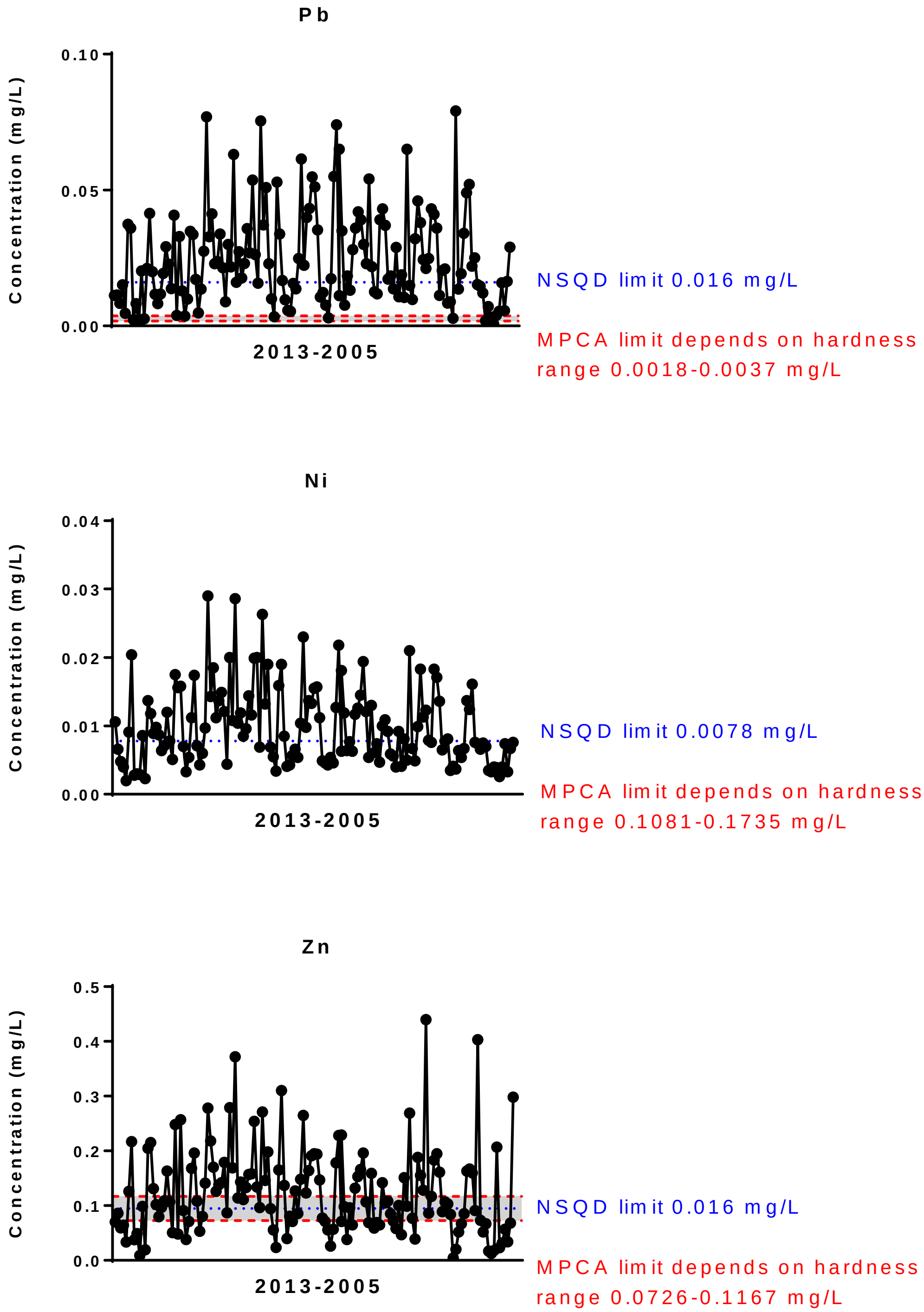

Figure 5. Stormwater concentrations of Pb, Ni and Zn for the recorded period 2005-2013.

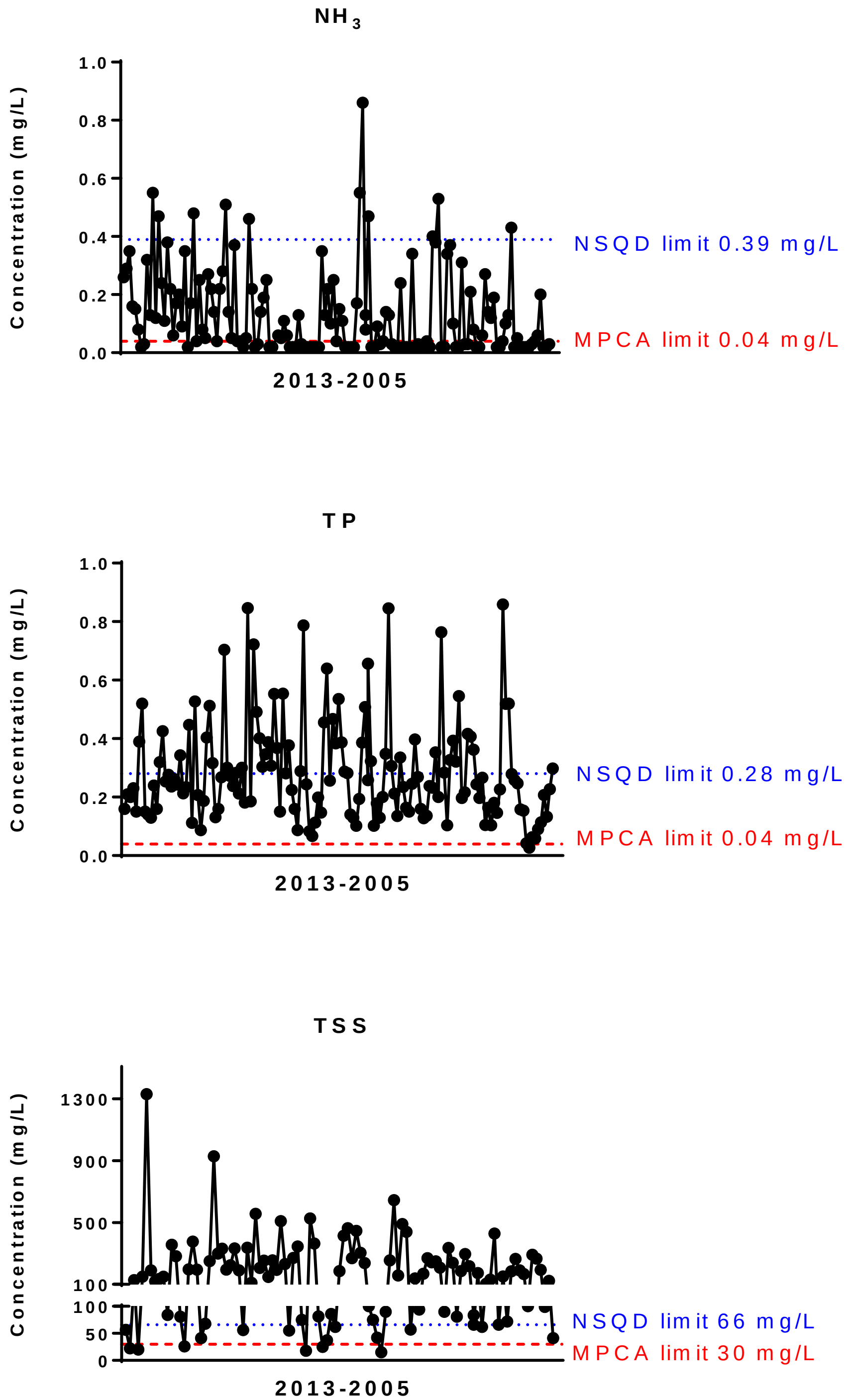

Figure 6. Stormwater concentrations of NH_3, TP and TSS for the recorded period 2005-2013.

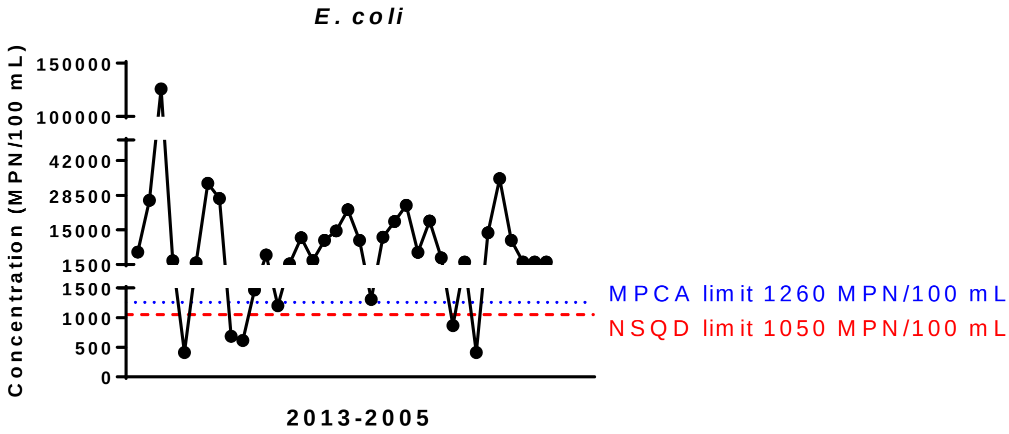

Figure 7. Stormwater concentrations of *E.coli* for the recorded period 2005-2013.

Correlation of pollutants with rainfall parameters

Using the Spearman's rank correlation method, the correlation between precipitation depth (in), previous dry days (days), and stormwater analytes for all stormflow events in the data record (2005 – 2013) was investigated.

Precipitation depth

None of the examined water quality parameters was found to be significantly correlated with precipitation depth (Table 5). A report by Gentry *et al.* (Gentry, McCarthy et al. 2006) similarly showed no statistically significant correlation between precipitation and *E. coli* in a study of Stock Creek, Tennessee. It is reasonable that the total volume of runoff from large precipitation events would dilute the pollutant concentrations but there was considerable variability. Many factors previously discussed can be playing a role, such as the degree of imperviousness, and whether there are residual pollutants or solids on the surfaces from the preceding storm runoff (Wang, Wei et al. 2011), in which case antecedent parameters (such as previous dry days) may play a stronger influence on pollutants in stormwater runoff than precipitation depth. Moreover, precipitation depth is likely to have a greater influence on pollutants that have a high fraction in the dissolved phase (Murphy, O'Sullivan et al. 2014), which suggests that pollutants in this study were mostly in the particulate phase.

Previous dry days

Most heavy metals (Cr, Cu, Ni and Zn), TP and TSS were found to be positively correlated with previous dry days (Table 5 and Figures 8-9). These data support the existence of "build-up/washoff", whereby pollutants accumulate on surfaces during long periods of dryness and are then washed off by a rain event (Novotny 1995). On the other hand, Cd, Pb, ammonia and *E. coli* were not found to be correlated with previous dry days.

Literature on pollutant build-up/washoff relationships with different rainfall characteristics is variable (Murphy, O'Sullivan et al. 2014). This may be a result of the difference in examining contaminant washoff under simulated rainfall conditions versus natural rainfall conditions, where several confounding variables of natural rainfall conditions (such as rain intensity) can have an influence. In addition, site characteristics can influence results. For example, Murphy *et al.* (Murphy, O'Sullivan et al. 2014) found that Pb had a significant correlation with previous dry days. However, the study was conducted on stormwater runoff from impermeable concrete boards in an airport in New Zealand, where atmospheric deposition from airport activity (the returning of pollutants from road traffic back to the earth's surface after being carried away by wind and spray action) is an indirect source of heavy metals in runoff that could be impacting on the results.

E. coli was not correlated to previous dry days. Similar observations were seen in an extensive study of microorganisms in urban stormwater (Olivieri, Kruse et al. 1977). Since the phase of the pollutant (dissolved versus particulate) can impact on pollutant washoff (Murphy, O'Sullivan et al. 2014), these data suggest that *E. coli* are not predominantly in a particulate phase. Further investigation into the correlation of various pollutants with TSS may help ascertain this possibility.

Parameter	**Precipitation depth**		**Previous dry days**	
	Spearman r	***p*-value**	**Spearman r**	***p*-value**
Cd	0.01375	0.8683	0.1219	0.14
Cr	0.05065	0.5409	0.1724	0.0361
Cu	-0.06131	0.4592	0.25	0.0022
Pb	0.1416	0.0861	0.1475	0.0735
Ni	0.007558	0.9274	0.3004	0.0002
Zn	0.04217	0.6108	0.2534	0.0019
NH_3	0.03399	0.6828	0.002855	0.9726
TP	-0.002896	0.9721	0.2318	0.0046
TSS	0.09848	0.237	0.2137	0.0096
E.coli	-0.07345	0.6703	-0.1878	0.2727

Table 5. Spearman's rank correlation analysis results for stormwater analyte concentrations and rainfall parameters (precipitation depth and previous dry days). Values of *p* less than 0.05 were considered statistically significant.

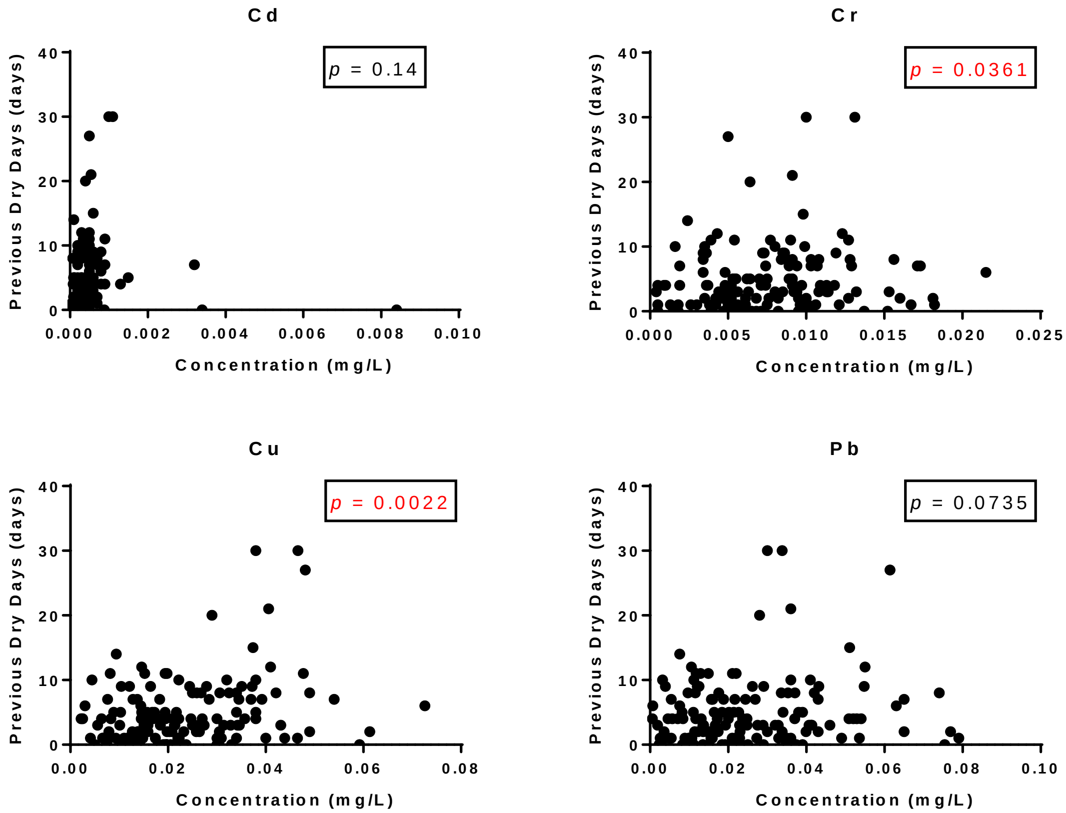

Figure 8. Correlation of Cd, Cr, Cu and Pb with previous dry days. The *p*-value for the Spearman's rank correlation is shown. Red values are significant at $\alpha = 0.05$.

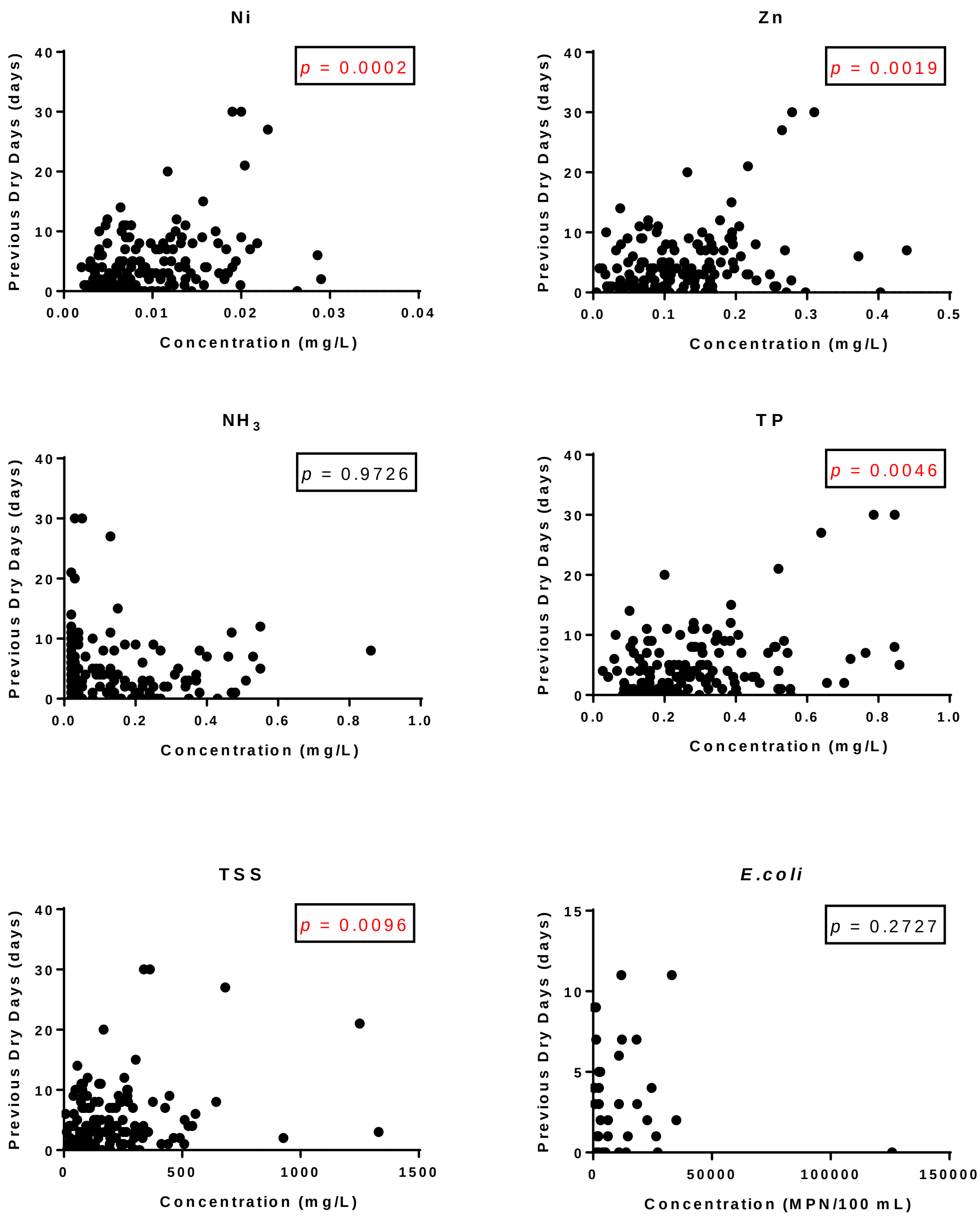

Figure 9. Correlation of Ni, Zn, NH_3, TP, TSS, and *E.coli* with previous days. The *p*-value for the Spearman's rank correlation is shown. Red values are significant at $\alpha = 0.05$.

Correlation of MPCA exceedances with rainfall parameters

To better identify which stormwaters correlated with rainfall parameters, the Spearman's rank correlation method was repeated using rainfall datasets that exceeded the MPCA standards (referred to MPCA exceedances) for each pollutant (Table 6). The rationale was to exclude from the initial analysis rainfall events where analytes were within accepted MPCA limits and focus on those with heavy pollution. This segregation might provide a better picture on how rainfall parameters influence polluted stormwaters.

The analysis was not performed for Cd, Cr and Ni due to the low level of exceedance (< 10% of data). For TP, the high level of exceedance (>99%) led to a similar result as that previously reported in Table 5. For the rest of analytes, the trends that were seen with the complete datasets (Table 5) were similarly seen with MPCA exceedances for previous dry days. Cu, Zn and TSS were significantly correlated while Pb, NH_3 and *E. coli* were not significantly correlated. These data may indicate that the influence of previous dry days on pollutant washoff in stormwater is independent of the level of accumulated pollutants on impervious surfaces.

Analysis of correlation with precipitation depth yielded similar results to those seen with the complete datasets except for Pb. High levels of Pb in stormwater that exceed MPCA standards were found to be positively correlated with precipitation depth. When all the dataset was analyzed (Table 5), Pb was the only pollutant that trended towards significance in its correlation with precipitation depth. With the exclusion of rainfall events with low Pb concentrations, the correlation became positive, which may indicate that *high* levels of Pb exist in both dissolved and particulate fractions, whereby the dissolved fraction is influenced by the precipitation depth.

Parameter	Precipitation depth		Previous dry days	
	Spearman r	*p*-value	Spearman r	*p*-value
Cd	*Not performed**			
Cr	*Not performed**			
Cu	-0.1259	0.1552	0.324	0.0002
Pb	0.1661	0.0466	0.149	0.0747
Ni	*Not performed**			
Zn	-0.0792	0.3723	0.2378	0.0067
NH_3	-0.08991	0.3109	0.1027	0.2469
TP**	-0.002896	0.9721	0.2318	0.0046
TSS	0.05915	0.4956	0.1822	0.0345
E.coli	0.09562	0.6152	0.03627	0.8491

* Test was not performed if data exceeded MPCA standards < 10% of the time (see Table 4)
* * Except for one storm, all storms recorded exceeded MPCA standards. The analysis is thus the same as in Table 5.

Table 6. Spearman's rank correlation analysis results for stormwater analytes exceeding MPCA standards (MPCA exceedances) and rainfall parameters (precipitation depth and previous dry days).

Correlation of NSQD exceedances with rainfall parameters

The Spearman's rank correlation analysis was also performed using rainfall datasets that exceeded the NSQD standards (referred to NSQD exceedances) for each pollutant (Table 7). The analysis was not performed for Cd and ammonia due to the low level of exceedance (< 10% of data).

The trends that were seen with the complete datasets (Table 5) were similarly seen with NSQD exceedances for precipitation depth, where none of the examined analytes were positively correlated. The NSQD exceedance analysis should give a clearer idea on how the St. Anthony Park watershed stormwater pollution compares to other stormwaters nationwide. The discrepancy in Pb exceedance seen with MPCA and NSQD standards may stem from the major difference in Pb levels allowed for surface water (MPCA) versus levels measured in stormwater (NSQD). The NSQD standard for Pb is over 4-fold to 8-fold higher than the range of MPCA standards calculated based on water hardness.

For previous dry days, Cr, Cu, Zn and TP were significantly correlated while *E. coli* was not. These results agree with the analysis of the complete dataset (Table 5), which may indicate that the influence of previous dry days on pollutant washoff in stormwater is independent of the level of accumulated pollutants on impervious surfaces.

On the other hand, Pb exceedances correlated positively with previous dry days while Ni and TSS did not, contrary to what was seen with the complete dataset. For Ni, the low levels detected in stormwater may limit a meaningful interpretation of how “high levels” are not affected by previous dry days. For Pb, the positive correlation of high levels of Pb with previous dry days is in agreement with the “buildup/washoff” phenomenon observed for other metals. Using Pb levels that exceeded NSQD levels excludes from the analysis Pb levels that are normally seen in other stormwaters. This may have allowed detecting the correlation of high levels of Pb with previous dry days using the NSQD exceedance but not the MPCA exceedance.

Parameter	Precipitation depth		Previous dry days	
	Spearman r	***p*-value**	**Spearman r**	***p*-value**
Cd	*Not performed**			
Cr	-0.03256	0.7142	-0.1766	0.0452
Cu	-0.1371	0.1214	0.2951	0.0007
Pb	0.0405	0.6486	0.2061	0.0191
Ni	0.1041	0.2404	0.03112	0.7263
Zn	-0.09045	0.308	0.2475	0.0047
NH_3	*Not performed**			
TP	-0.08057	0.3641	0.245	0.0051
TSS	0.04405	0.6402	0.09814	0.2967
E.coli	-0.04345	0.8165	0.1079	0.5636

* Test was not performed if data exceeded NSQD standards < 10% of the time (see Table 4).

Table 7. Spearman's rank correlation analysis results for stormwater analytes exceeding NSQD standards (NSQD exceedances) and rainfall parameters (precipitation depth and previous dry days).

Correlation of water quality parameters with TSS

Except for *E.coli*, all pollutants were significantly correlated with TSS in stormwater runoff, which illustrates that TSS is statistically associated with these other pollutants and may be an important carrier of organic matter and heavy metals (Table 8 and Figures 10-11). Similar results were reported for Cu, Pb and Zn (Li, Liu et al. 2014).

These results are also in agreement with how rainfall parameters influenced pollutant concentrations in this study, where it was observed that previous dry days (which have a strong impact on pollutants in the particulate phase) but not precipitation depth had a stronger impact on stormwater pollutant concentrations. Furthermore, they agree with published literature citing the association of most heavy metals with TSS (Maniquiz-Redillas and Kim 2014).

Parameter	Correlation with TSS	
	Spearman r	***p*-value**
Cd	0.4499	< 0.0001
Cr	0.78	< 0.0001
Cu	0.7987	< 0.0001
Pb	0.8684	< 0.0001
Ni	0.84	< 0.0001
Zn	0.802	< 0.0001
NH_3	0.2404	0.0036
TP	0.8731	< 0.0001
TSS	*N/A*	
E.coli	0.04619	0.8265

Table 8. Spearman's rank correlation analysis results for stormwater analytes and TSS.

Literature on the correlation of *E.coli* with TSS is variable. Some studies have found a positive correlation between *E.coli* and TSS in highly urbanized watersheds such as the Fanno Creek watershed in Oregon and the Little River watershed in Tennessee (Anderson, Rounds et al. 2003, Hamilton and Luffman 2009, Chen and Chang 2014), which suggested that *E.coli* were bound/adsorbed to particulate matter (Chen and Chang 2014). On the other hand, some studies showed only a weak correlation (Kay and McDonald 1983). Given the large variation of the correlation between *E. coli* and TSS, watershed landscape differences may have important impacts on the *E. coli* –TSS relationship (Chen and Chang 2014).

The implications of these correlation analyses are important and lay the ground for the rest of the study. First, most pollutants correlated positively with TSS, which provides a strong rationale for using TSS as a representative pollutant in the subsequent design of the PCSWMM model and the examination of structural BMP efficiency. Second, structural BMPs that are designed to target the particulate fraction in stormwaters are expected to be the most efficient in reducing stormwater pollution in the St. Anthony Park watershed.

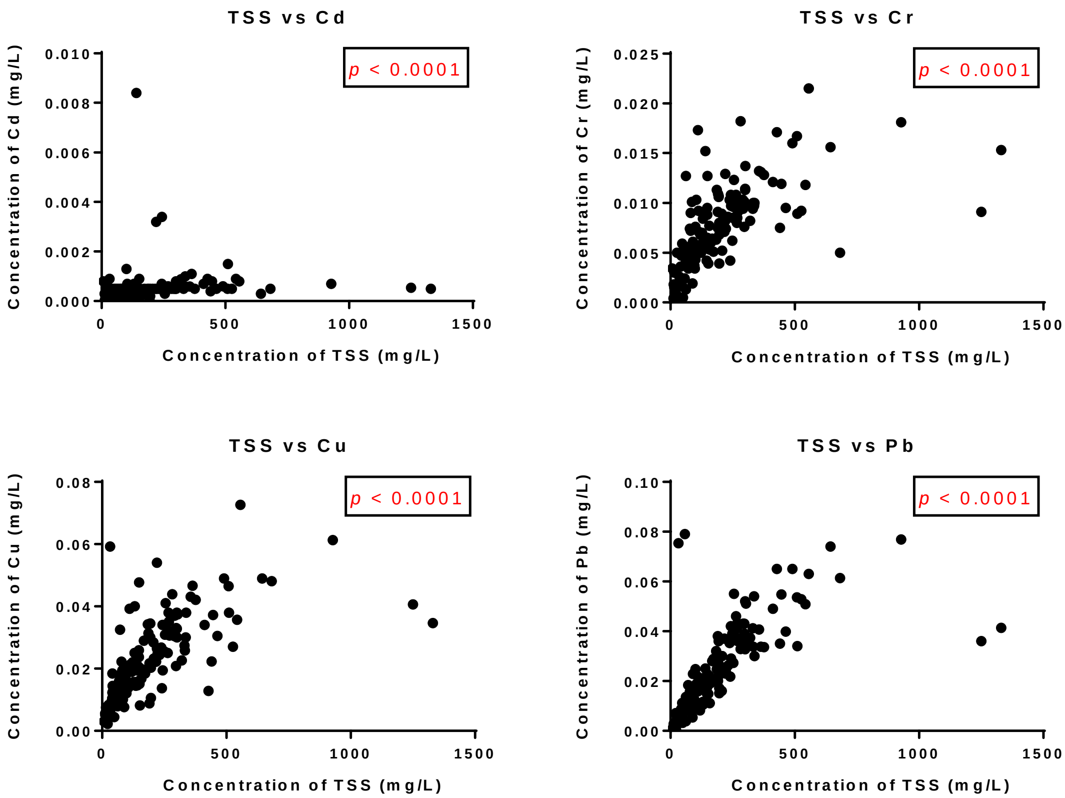

Figure 10. Correlation of Cd, Cr, Cu and Pb with TSS. The p-value for the Spearman's rank correlation is shown. Red values are significant at $\alpha = 0.05$.

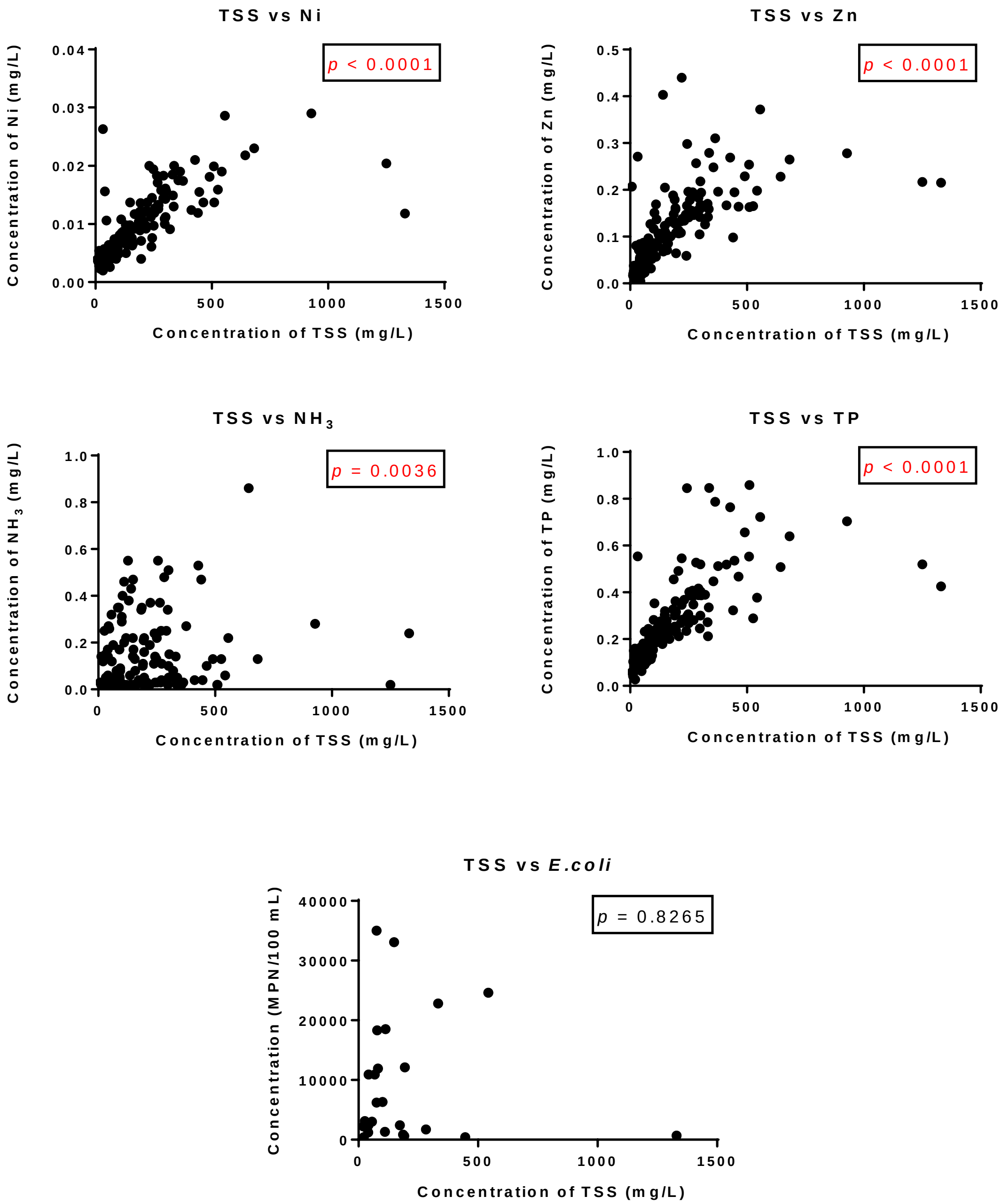

Figure 11. Correlation of Ni, Zn, NH3, TP and E.coli with TSS. The p-value for the Spearman's rank correlation is shown. Red values are significant at α = 0.05.

CHAPTER IV:

PCSWMM MODEL CALIBRATION AND VALIDATION FOR ST ANTHONY PARK WATERSHED

Data used

The St. Anthony Park watershed is located in the city of St. Paul with a total area of 3,418 acres (Figure 12) and drains directly into the Mississippi River at Desnoyer Park. In this watershed, all typical urban land usages exist (Figure 13). On average, 48 % of this watershed is impervious (Capitol Region Watershed District 2014). The various soil types and their geographic distribution within the watershed are provided in Figure 14 and Table 9.

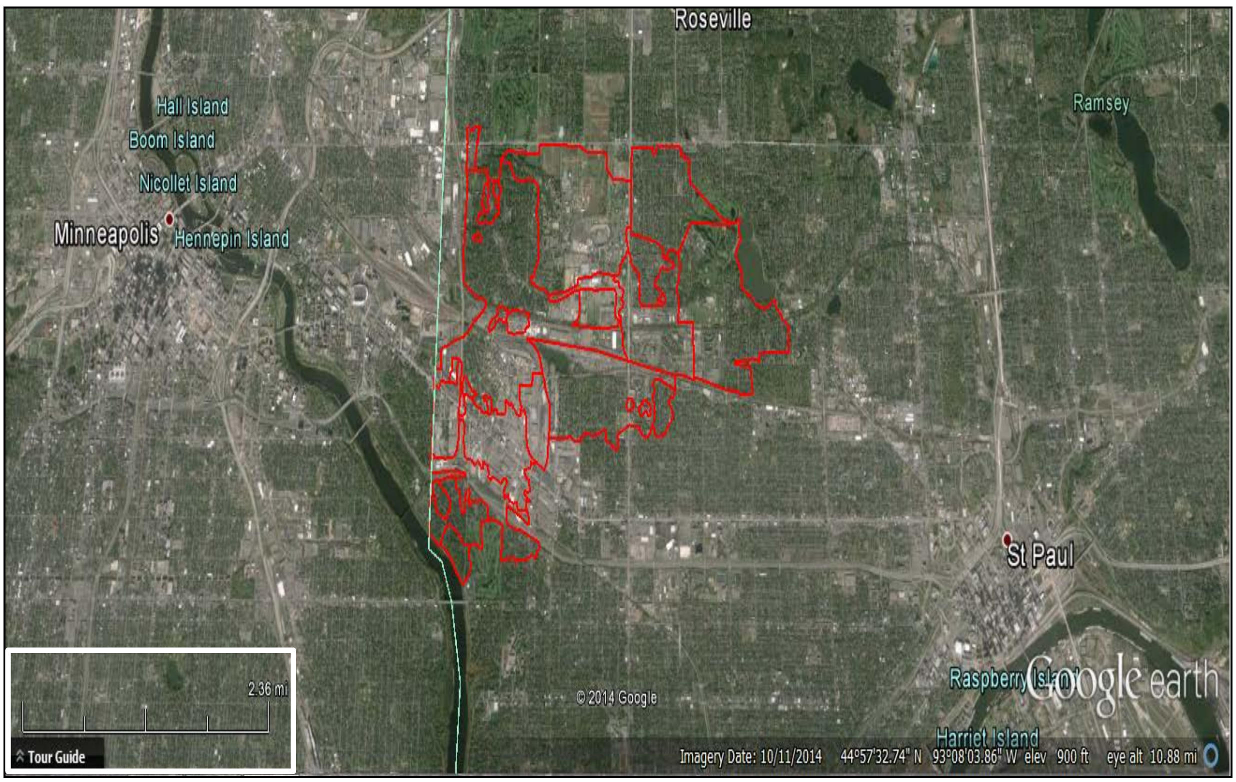

Figure 12. The St. Anthony Park watershed as seen with Google Earth. Subwatersheds are outlined by red boundaries. The total watershed area is 3,418 acres. The scale on the lower left corner (in white box) represents 2.36 miles.

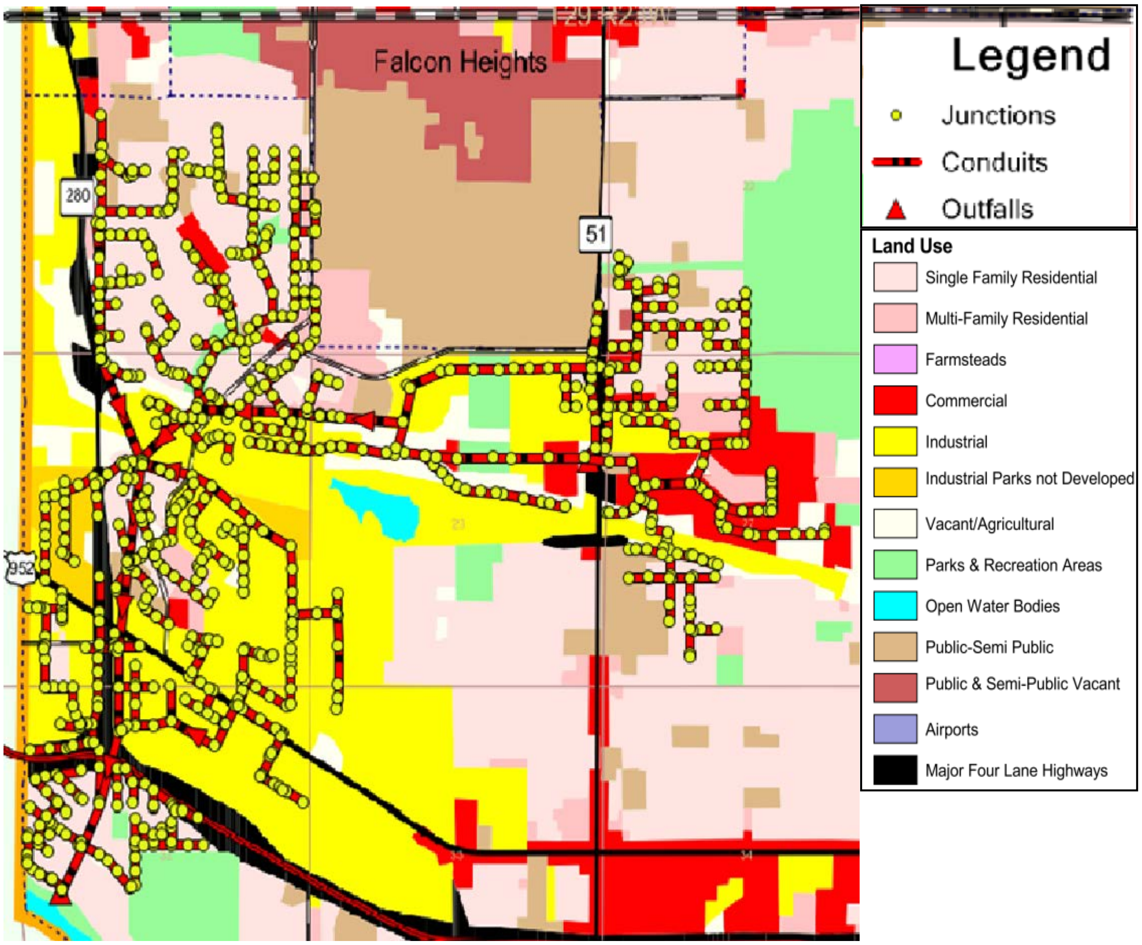

Figure 13. Land use for the St. Anthony Park watershed. The various colors denote specific land uses that are outlined in the legend. The red lines (conduits), yellow circles (junctions), and red triangles (outfalls) are for the stormwater drainage system. Modified from http://www.mngeo.state.mn.us/maps/LandUse/lu_rams.pdf.

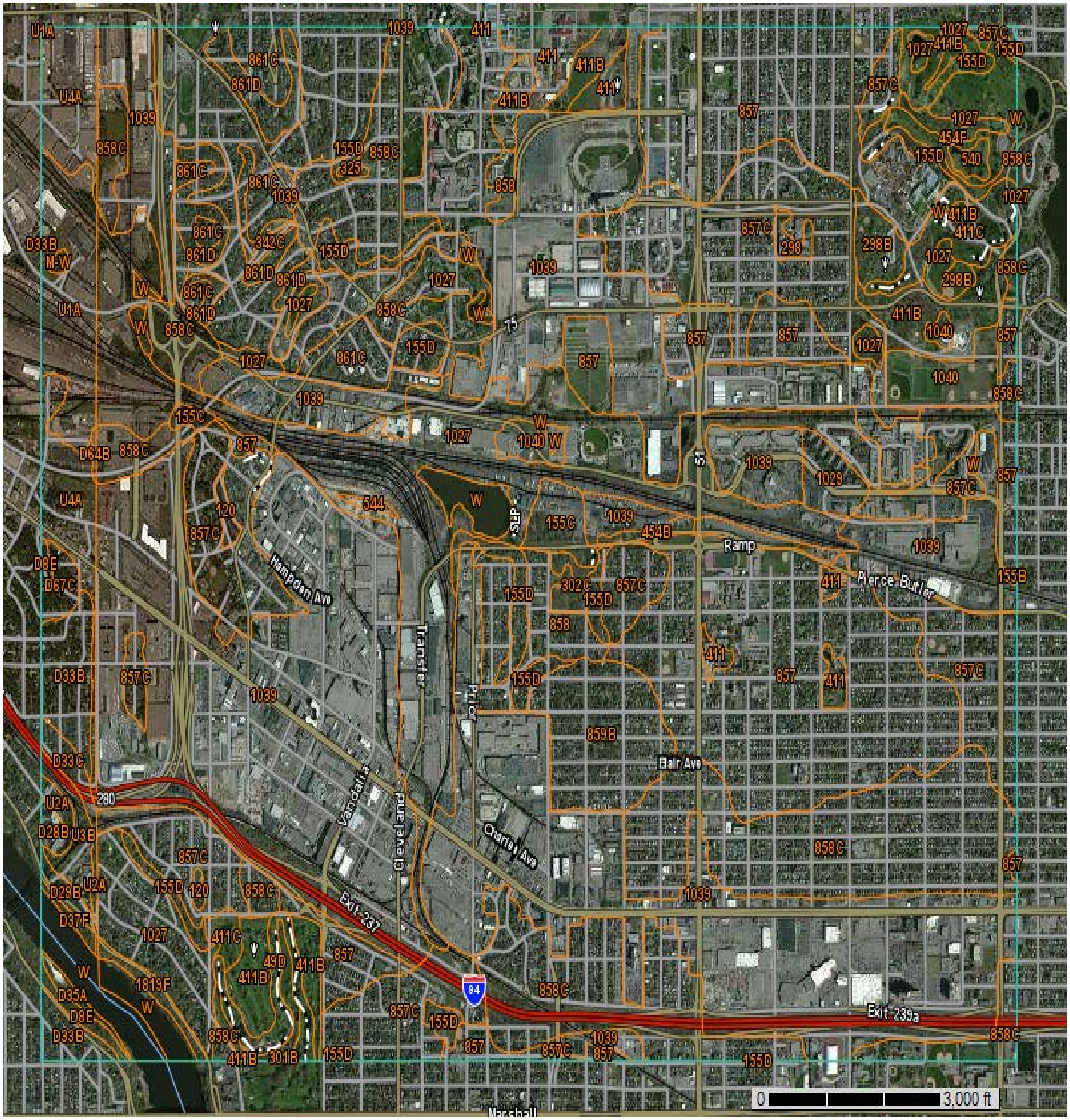

Figure 14. Soil types and their geographic distribution in the area of study (http://websoilsurvey.nrcs.usda.gov/app/). The legend is detailed in Table 9.

Map Symbol	Map Unit Name	Map Symbol	Map Unit Name
49D	Antigo silt loam, 12 to 18 percent slopes	**454F**	Mahtomedi loamy sand, 25 to 40 percent slopes
120	Brill silt loam	**540**	Seelyeville muck
155B	Chetek sandy loam, 0 to 6 percent slopes	**544**	Cathro muck
155C	Chetek sandy loam, 6 to 12 percent slopes	**857**	Urban land-Waukegan complex, 0 to 3 percent slopes
155D	Chetek sandy loam, 12 to 25 percent slopes	**857C**	Urban land-Waukegan complex, 3 to 15 percent slopes
298	Richwood silt loam, 0 to 2 percent slopes	**858**	Urban land-Chetek complex, 0 to 3 percent slopes
298B	Richwood silt loam, 2 to 6 percent slopes	**858C**	Urban land-Chetek complex, 3 to 15 percent slopes
301B	Lindstrom silt loam, 2 to 4 percent slopes	**859B**	Urban land-Zimmerman complex, 1 to 8 percent slopes
302C	Rosholt sandy loam, 6 to 15 percent slopes	**861C**	Urban land-Kingsley complex, 3 to 15 percent slopes
325	Prebish loam	**861D**	Urban land-Kingsley complex, 15 to 25 percent slopes
342C	Kingsley sandy loam, 6 to 12 percent slopes	**1027**	Udorthents, wet substratum
411	Waukegan silt loam, 0 to 2 percent slopes	**1029**	Pits, gravel
411B	Waukegan silt loam, 2 to 6 percent slopes	**1039**	Urban land
411C	Waukegan silt loam, 6 to 12 percent slopes	**1040**	Udorthents
454B	Mahtomedi loamy sand, 0 to 6 percent slopes	**1819F**	Dorerton-Rock outcrop complex, 25 to 65 percent slopes

Table 9. Legend for Figure 14. The table details map symbols and their corresponding soil types.

The St Anthony Park area has a stormwater drainage system that includes inlet structures on the streets, manholes, pipes, and a deep tunnel to carry runoff outside the area and dispose it in the Mississippi River through an outfall (Figure 15).

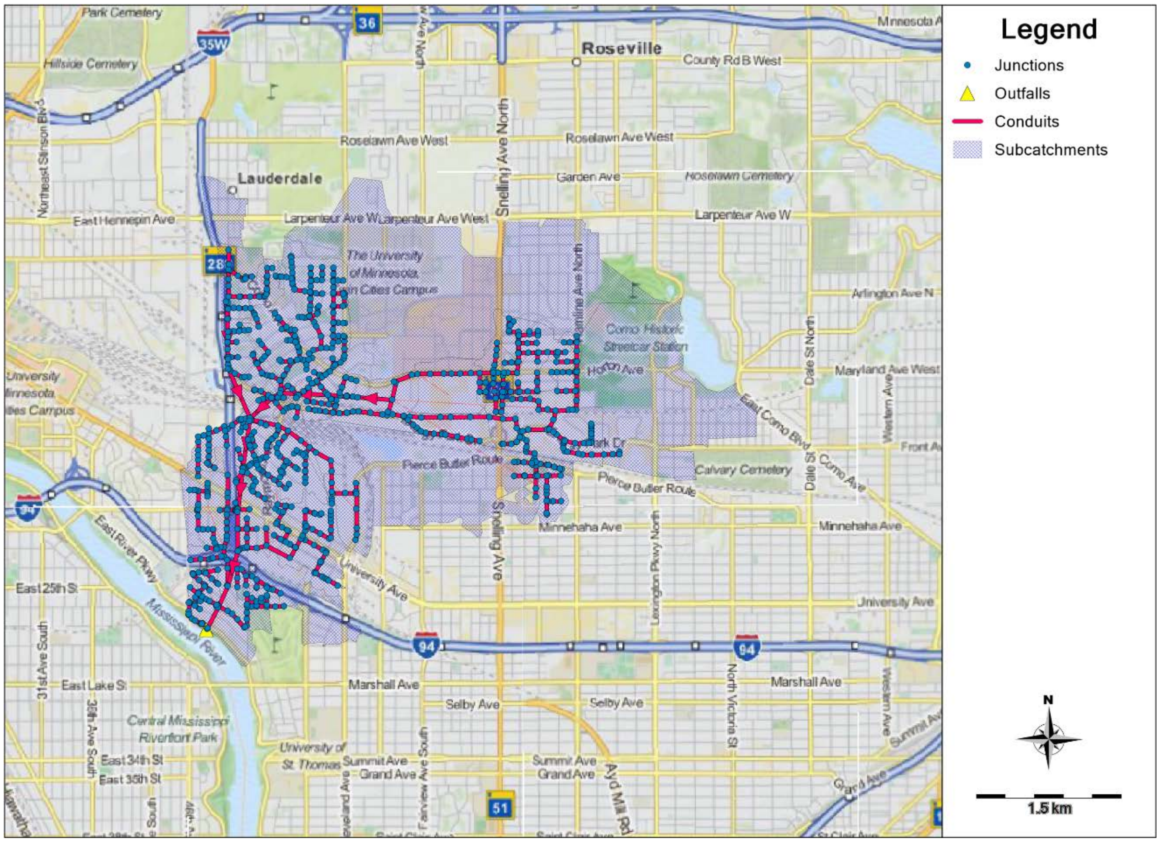

Figure 15. St Anthony Park watershed stormwater drainage system in PCSWMM. Blue circles represent junctions (manholes), yellow triangles represent outfalls while red lines represent conduits. The discretized subcatchments (blue background) are in GIS shapefile format imported into PCSWMM model.

For the purpose of building a PCSWMM model to simulate runoff generation in St. Anthony Park watershed, data regarding the hydrologic characteristics of the watershed and hydraulic properties of the drainage system was needed. CRWD provided the hydrologic data for the watershed. Discretized subcatchments in GIS shapefile format were provided by CRWD as shown in Figure 15.

The shapefiles of discretized subcatchments provide data regarding curve numbers (CN), areas, widths, slopes, percentage imperviousness , depth of storage in impervious and pervious areas, and Manning’s N (friction factor) for impervious and pervious areas. Topographic maps were also employed to ascertain the delineation of subcatchments by checking that the subcatchment boundaries follow ridge lines (Appendix A5). Detailed subcatchment parameters used in the model are provided in the Appendix (A6-A7).

Data on drainage structures was acquired from St. Paul Public Works Portal (http://pwportal.ci.stpaul.mn.us/). Plans and profiles of the drainage system were acquired from the public works site. An example of a plan and a profile are shown in Figure 16.

The plans and profiles provide information on ground level and invert level at each manhole (node), and types, sizes, slopes of pipes. Detailed drainage system parameters used in the model are provided in the Appendix (A8).

GIS shapefiles of subwatersheds were added to PCSWMM model as a first step for constructing the model. After that, manholes (generic names are nodes) and pipes (generic names are conduits) of the drainage system were located and added to the model based on plans and profiles from St. Paul Public works portal. Finally, subwatersheds were linked to specific nodes on the drainage system to outflow their runoff into them.

The main element of the drainage system in the area is a deep tunnel that receives water from shallower pipes through deep shafts (deep manholes) and conveys stormwater to an outfall on the Mississippi River (Figure 17). The deep manholes have different depths ranging from 150.5 ft at the upstream node of the deep tunnel to 26.4 ft at the downstream edge near the outfall. The deep tunnel as well as the deep shafts are not designed for stormwater storage but act as gravity conduits that transport collected stormwater directly to the outfall. The profile of the deep tunnel tunnel plotted from PCSWMM is shown in Figure 18 with nodes from L15 (upstream) to the outfall (OFmain).

Precipitation data for the area of St. Anthony Park were acquired from Minnesota Climatology Research Group at the University of Minnesota and compared and adjusted with precipitation data collected by CRWD.

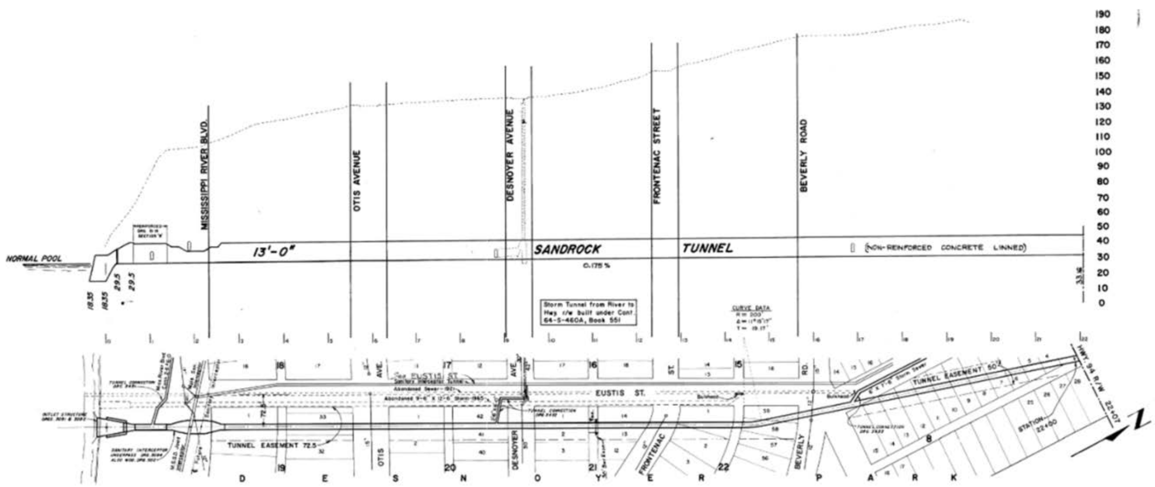

Figure 16. An example of available profiles (above) and plans (below) of drainage systems in St. Anthony Pak watershed (http://pwportal.ci.stpaul.mn.us/). The profile show the size of the tunnel (13 feet) and the invert level and ground levels of manholes and outfall (scale on the right side), which are translated as junctions in the PCSWMM model. The plan depicts the geographic location of a tunnel with respect to roads.

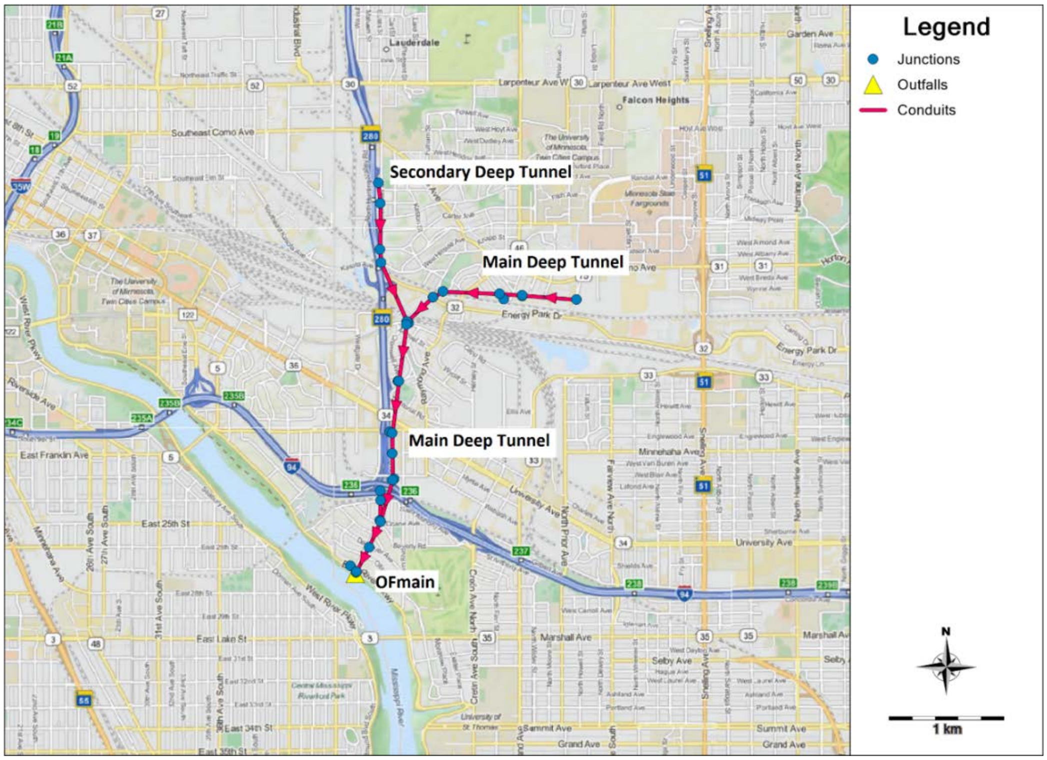

Figure 17. The deep drainage tunnels of St. Anthony Park watershed and the outfall of the main deep tunnel (OFmain) on the Mississippi River. The network is the same as in Figure 18, where blue circles represent junctions (deep manholes), yellow triangles represent outfalls while red lines represent conduits. The deep manholes have different depths ranging from 150.5 ft at the upstream node of the deep tunnel to 26.4 ft at the downstream edge near the outfall.

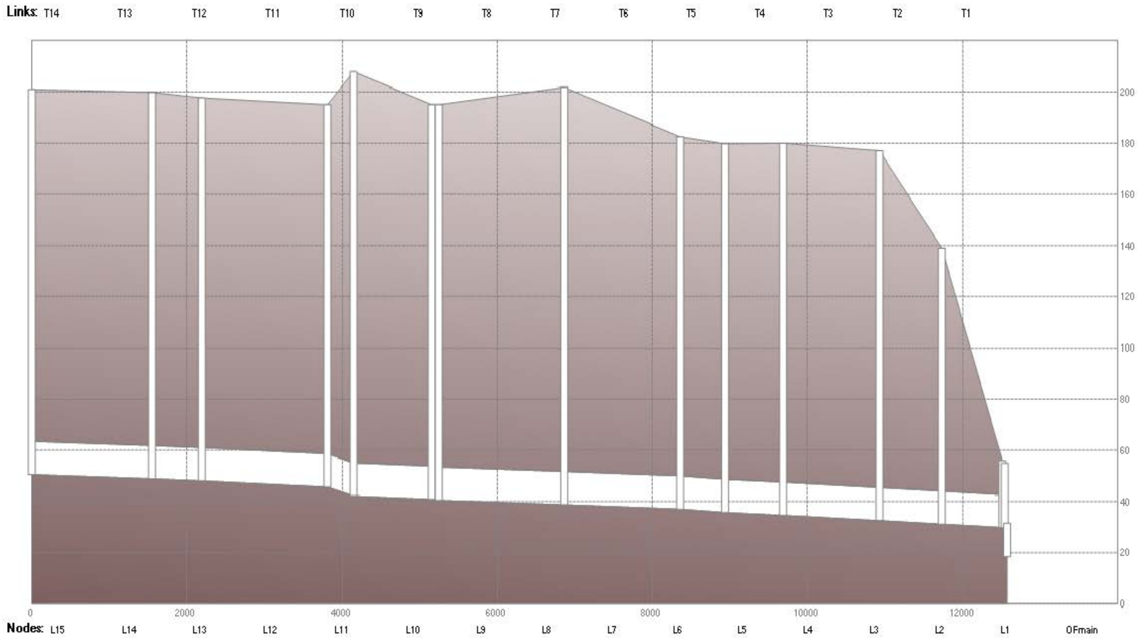

Figure 18. The main deep drainage tunnel profile of St. Anthony Park watershed as drawn by PCSWMM, with manhole numbers (Nodes; bottom) and conduits between manholes (Links, above). The elevation scale (feet above sea level) is on the right side.

Calibration of the PCSWMM model

For this model to be of practical use, calibration was performed so that the model closely matches the behavior of the real system (Gupta, Sorooshian et al. 1998). The calibration was performed over the runoff quantities (hydrographs) at the outfall of the drainage system between real flow data and simulation flow data. One storm was chosen for calibration (Figure 19). The calibration storm occurred on April 26, 2011, and had a total depth of 1.59 inch and a duration of 12.5 hr. This storm represented a typical storm event for the area and fell into the fourth quartile for depth for all storms recorded during 2005-2013.

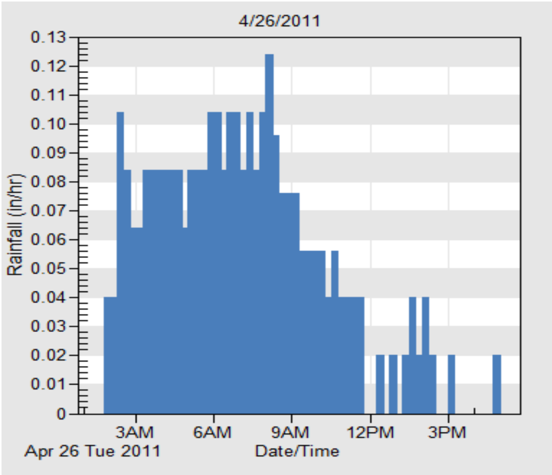

Figure 19. Precipitation hyetographs for the calibration storm recorded every 15 minutes. Data was obtained from the University of Minnesota (UMN). This storm occurred on April 26 2011 and fell into the fourth quartile for depth for all storms recorded during 2005-2013. It had a total precipitation depth of 1.59 inch and a duration of 12.5 hr.

The Sensitivity-based Radio Tuning Calibration (SRTC) tool in PCSWMM was used for calibration of the model. This method aids in calibrating the model by using a known uncertainty percentage defined by the user. The SRTC tool consists of sliders for parameters that need to be changed by a certain percentage and immediately monitor their effect on the simulation hydrographs and their conformity with the real hydrograph. The following model parameters were adjusted in a trial and error calibration process until differences between simulated and observed stream flows were minimal (as deduced from visually comparing plots of simulated and observed flow timeseries): roughness of pipes, curve numbers, Manning's N for pervious and impervious surfaces, percentage imperviousness of subcatchments, and widths and slopes of subcatchments. The calibration values of these parameters are summarized in Table 10.

Parameters		Values after Calibration	Reference Calibration Interval
Average Width		221.08 ft	-
Average Slope		0.21%	-
Surface Storage	**Impermeable Area**	0.024 inch	0.012-0.098 (inch)
	Permeable Area	0.172 inch	0.098-0.2 (inch)
Manning's Roughness Coefficient	**Permeable Area**	0.03	-
	Impermeable Area	0.011	-
Pipes		0.075	-
Drying Days		4.3 days	2-14 (days)

Table 10. Values obtained after calibration for model parameters adjusted during calibration. Reference calibration intervals (where applicable) are from (Dongquan, Jining et al. 2009).

Evaluation of the model's performance was carried out at two levels. The first level was the graphical technique, whereby the simulated hydrographs at the outfall of the watershed were plotted and compared to real observed data from the storm chosen for calibration (Figure 20).

Graphical techniques are essential for appropriate model evaluation (Legates and McCabe 1999). As seen in Figure 20, the model was able to closely reproduce the hydrograph of the calibration period, which reflects adequate calibration (Moriasi, Arnold et al. 2007). The largest difference between the simulated flow and observed flow is that the model was unable to fully reproduce a drop in the flow occurring between 6 and 9 a.m.

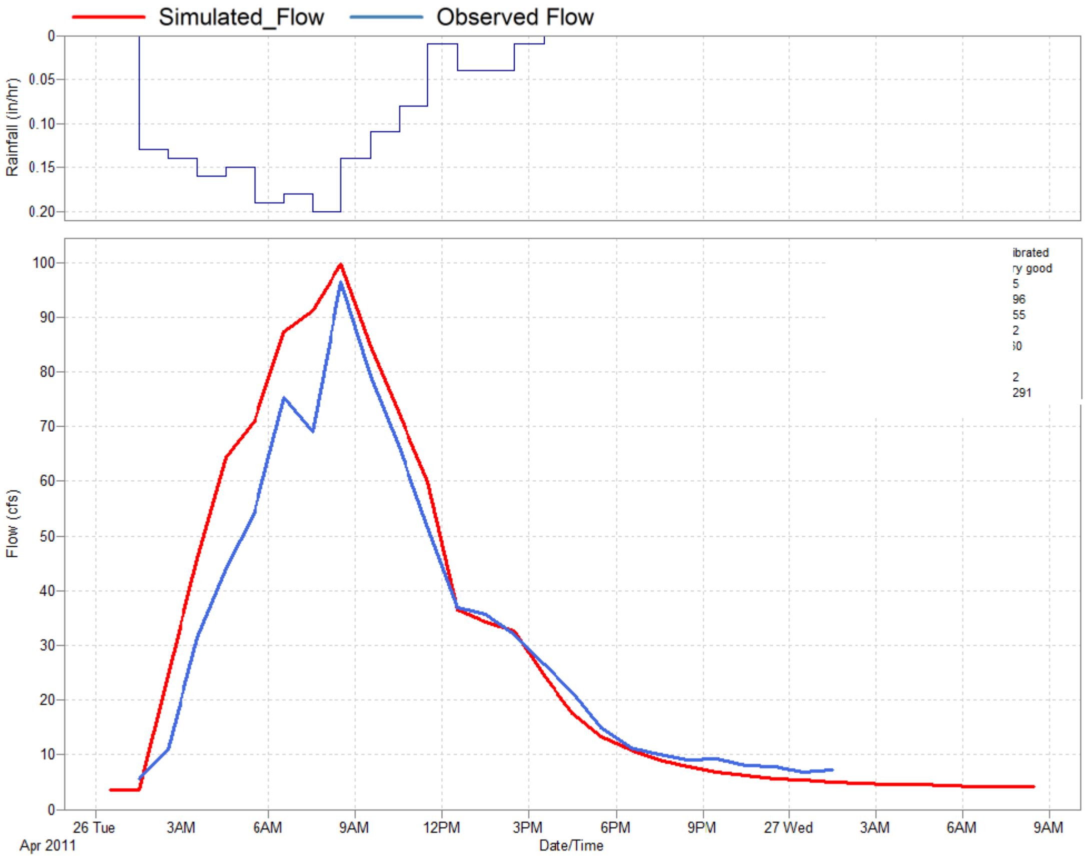

Figure 20. Hydrographs for the PCSWMM simulated flow (red) at the outfall of the subwatershed (OFmain) as compared to the observed flow (blue) for storm 1 (April 26, 2011).

After visually matching simulated flows to observed flows, the second level for evaluating model performance was quantitative statistics. A goal was set for attaining a performance level of at least “very good” in order for the model to successfully pass the calibration process. There are several quantitative statistical tests that are performed by PCSWMM for calibration as well as validation (Moriasi, Arnold et al. 2007). Out of these, three statistical tests were chosen: the coefficient of determination (R^2), the Nash-Sutcliffe efficiency coefficient (NSE), and the integrated square error (ISE). The three tests and their reference ranges are provided in Table 11.

Statistic	Definition	Range	Accepted Range	Result
R^2	Coefficient of determination	0 - 1	0.5-1	0.955
NSE	Nash-Sutcliffe efficiency coefficient	-∞ - 1	0-1	0.896
ISE	Integrated Square Error	0 - 100	0-25	5.25

Table 11. Quantitative statistics used in evaluating model calibration. The table describes the statistic, the range of values for that statistic, the range accepted for calibration, and the result obtained for the hydrograph calibration (Figure 23) – Reference ranges were obtained from (James 1997, Moriasi, Arnold et al. 2007).

The coefficient of determination (R^2) describes the proportion of the variance in measured data explained by the model. R^2 is given by:

$$R^2 = \left[\frac{\sum_{i=1}^{n} (O_i - \overline{O})(S_i - \overline{S})}{\sqrt{\sum_{i=1}^{n} (O_i - \overline{O})^2} \sqrt{\sum_{i=1}^{n} (S_i - \overline{S})^2}} \right]^2$$

Where n is the number of observations in the calibration period,

O_i is the i-th observed value,

$\overline{O}$ is the mean observed value,

S_i is the i-th model-simulated value and,

$\overline{S}$ is the mean model-simulated value.

R^2 ranges from 0 to 1. Higher values indicate less error variance. Accepted values of R^2 are typically greater than 0.5 (Dongquan, Jining et al. 2009, Santhi, Arnold et al. 2001, Van Liew, Arnold et al. 2003). R^2 is widely used for model calibration (Moriasi, Arnold et al. 2007). Typical reference range ratings are “excellent” for $R^2 > 0.85$ and “very good” for R^2 ranging 0.65-0.85 (Bharati, Lacombe et al. 2011). R^2 for PCSWMM calibration was 0.955, which is interpreted as an excellent representation of the observed flow time series.

The Nash-Sutcliffe efficiency (NSE), as defined by Nash and Sutcliffe (Nash and Sutcliffe 1970), is a normalized statistic that determines the relative magnitude of the residual variance (noise) compared to the measured data variance. NSE is given by:

$$NSE = \frac{\sum_{i=1}^{n}\left(O_i - \overline{O}\right)^2 - \sum_{i=1}^{n}(S_i - O_i)^2}{\sum_{i=1}^{n}\left(O_i - \overline{O}\right)^2}$$

NSE ranges from -∞ to 1, and reflects how well the plot of observed versus simulated data fits the 1:1 line. A value of 1 represents a perfect fit, while negative values indicate that simulated data are worse than observed data. NSE is very commonly used and was found to be the best objective function for reflecting the overall fit of a hydrograph (Sevat and Dezetter 1991). Similar to R^2, typical reference range ratings are “excellent” for NSE > 0.85 and “very good” for NSE ranging 0.65-0.85 (Bharati, Lacombe et al. 2011). NSE for PCSWMM calibration was 0.896, which represents an excellent fit.

The integral square error (ISE) describes the agreement between the time distribution of the observed and simulated values. ISE is given by:

$$ISE = \frac{\left[\sum_{i=1}^{n}(O_i - S_i)^2\right]^{1/2}}{\sum_{i=1}^{n}(O_i)} \text{ X } 100$$

Smaller ISE values indicate better agreement. As recommended by Sarma, Delleur and Rao (Sarma, Delleur et al. 1969), the calibration is considered excellent if $0 < ISE \leq 3$, very good if $3 < ISE \leq 6$, good if $6 < ISE \leq 10$, fair if $10 < ISE \leq 25$ and poor if $ISE > 25$. ISE is a useful tool for model calibration and verification (Marsalek, Dick et al. 1975, Singhofen 2001). ISE for PCSWMM calibration was 5.25, which rates the calibration as very good.

Overall, the model performed well simulating the flows in the St Anthony Park watershed, as deduced from graphical techniques and three quantitative statistic tests. Validation of the model is discussed in the following section.

Validation of the PCSWMM model

After calibration, validation of the model was performed. For the model to be valid, it should carry accuracy and predictive capability within predefined acceptable limits (Quintana Segu, Martin et al. 2009). A set consisting of several consecutive storms was chosen for validation of the model (Figure 21). This set of storms had a total depth of approximately 3.88 inch. The series of storm events occurred over a period of three days starting May 18 2013 and ending May 21 2013. Since the duration in between the storms was over 6 hours, the storms were considered individual storms rather than one long storm. As such, six individual storms were compared to storms recorded for this area by the University of Minnesota (UMN) for the period 2005-2013. The total depth of each storm was the following: 0.81 inch (third quartile) for the first storm, 0.24 inch (second quartile) for the second storm, 1.77 inch (fourth quartile) for the third storm, 0.09 inch (first quartile) for the fourth storm, 0.6 inch (fourth quartile) for the fifth storm and 0.37 inch (third quartile) for the sixth storm. Validation was performed on the OFmain hydrographs. The simulated and observed flows are shown in Figure 22.

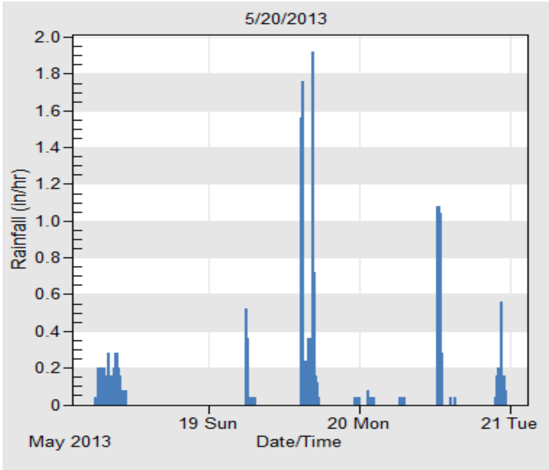

Figure 21. Rain hyetographs for the six validation storms recorded every 15 minutes. Data was obtained from University of Minnesota (UMN). The series of storm events occurred over a period of three days that started on 18th of May 2013 and ended on May 21st 2013. The total depth of each storm was: 0.81 inch (3rd quartile) for the first storm, 0.24 inch (2nd quartile) for the second storm, 1.77 inch (4th quartile) for the third storm, 0.09 inch (1st quartile) for the fourth storm, 0.6 inch (4th quartile) for the fifth storm, and 0.37 inch (3rd quartile) for the sixth storm.

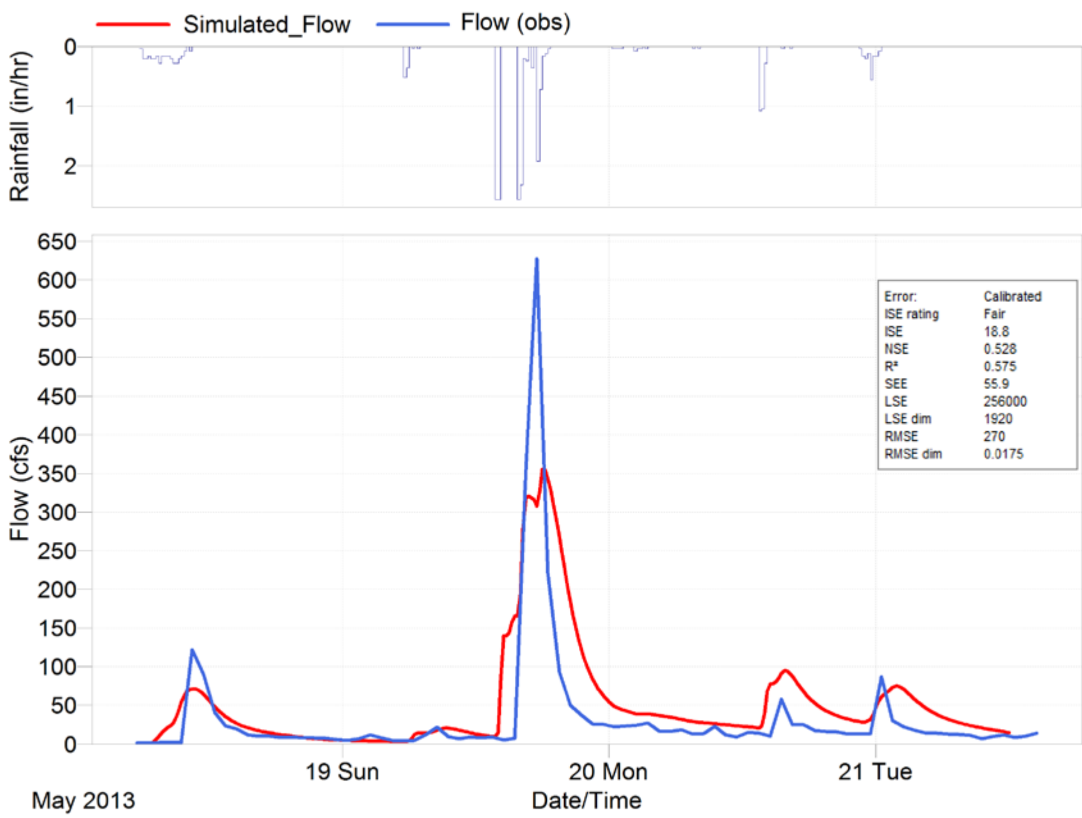

Figure 22. Hydrographs for the PCSWMM simulated flow (red) at the outfall of the subwatershed (OFmain) as compared to the observed flow (blue) for storm 2 (May 18-21, 2013).

Similarly to calibration, validation of model performance was carried out via graphical examination of the hydrographs and calculation of three quantitative statistics (R^2, NSE and ISE). Examining the hydrograph (Figure 22), it was noted that the model was able to replicate the main features of the observed flow at OFmain (drainage system outlet). It was noticed that the simulated peak flow was 44% lower than the observed peak flow in the third storm. However, this observed peak flow value was very high (> 600 cfs) and exceeded all recorded flow data values used in the model for the period 2005-2013. Subsequently, this data point was determined to be an outlier.

The three statistical tests can be used for both calibration and validation at the same intervals depicted in Table 11. A goal was set for attaining a performance level of at least “fair” in order for the model to successfully pass the validation process. In the presence of the outlier, the model performed fairly (ISE = 18.8), and produced an NSE of 0.528 (within the acceptable range of 0.5-1) and an R^2 of 0.575 (within the acceptable range of 0.5-1) (Dongquan, Jining et al. 2009) (Table 12).

Statistic	Definition	Range	Accepted Range	Result
R^2	Coefficient of determination	0 - 1	0.5-1	0.575
NSE	Nash-Sutcliffe efficiency coefficient	$-\infty$ - 1	0-1	0.528
ISE	Integrated Square Error	0 - 100	0-25	18.8

Table 12. Quantitative statistics used in validating the model. The table describes the statistic, the range of values for that statistic, the range accepted for validation, and the result obtained for the hydrograph validation (Figure 25) – Reference ranges were obtained from (James 1997, Moriasi, Arnold et al. 2007).

When performing model calibration and validation, it is common practice to set stringent statistical targets for model calibration outputs since calibration involves fine-tuning of parameters and thus manipulation of input data. On the other hand, validation statistical targets are usually less stringent as they do not involve manipulation of input data. Consequently, a target statistical performance rating of at least “very good” for calibration and at east “fair” for validation was set. The model was able to achieve both levels per the three quantitative statistical tests performed. Overall, it was concluded from the calibration and validation tests performed that the PCSWMM model acceptably simulated flow at the St Anthony Park watershed. Subsequently, the model was used for numerical examination of the first flush (FF) phenomenon in Chapter V and for structural BMP implementation in Chapter VI.

CHAPTER V:

FIRST FLUSH PHENOMENON ASSESSMENT USING PCSWMM MODEL

Rationale

The first flush phenomenon (FF) describes the high discharges of pollutants which build up on exposed surfaces and are washed off during early stages of the runoff hydrograph (Bliss, Neufeld et al. 2009). Understanding and studying the existence of FF in urban drainage systems is important for good management of treatment works during wet weather flows (Deletic 1998, Lee, Lau et al. 2004). Intervention to divert FF is becoming increasingly acknowledged as important to reduce suspended solids and dissolved contaminant loads in rainwater systems (Martinson and Thomas 2009). The need to show the existence of FF in a certain watershed is thus imperative prior to deciding on the need for most efficient BMP structures to divert pollutants during the first stages of the storm.

A lot of research has been done to study the existence of FF, with variable outcomes. For example, in a study by Deletic and Maksimovic (Deletic and Maksimovic 1998) on storm runoff into a single road inlet, the FF was depicted in a limited number of events. In another study of an urban catchment in Częstochowa, Poland (Mrowiec, Kamizela et al. 2009), FF was rare (as defined by 80% of the pollutant mass being transported in 30% of the total runoff volume or the 30/80 FF). On the other hand, Hossain *et al.* (Hossain, Imteaz et al. 2010) developed a model that continuously simulates the accumulation and wash-off of water quality pollutants. They validated the existence of the FF phenomenon using pollutant washoff data from road and roof surfaces in the Gold Coast, Australia during simulated rainfall. Lee *et al.* (Lee, Bang et al. 2002) showed that the magnitude of FF varied among different pollutants.

The standard method to check the existence of FF is to collect discrete samples during the storm, measure the concentrations of various pollutants (typically TSS), and analyze the change in pollutant concentrations over the period of the storm. While this is an accurate method to understand the pattern of change in concentrations, it is time-, effort-, and cost demanding. An alternative method would be to simulate the existence of FF using a computer model such as PCSWMM. In addition to being easier and cheaper, modeling FF would allow the incorporation of FF into subsequent model applications, such as studying how structural BMP implementation by PCSWMM can reduce or eliminate FF.

The Capital Region Watershed District (CRWD) employed ISCO samplers to collect discrete samples during storm events. However, to save the costs of analysis for so many samples, they mixed the successively-collected samples into one composite sample that represented the entire storm and calculated Event Mean Concentrations (EMCs) for sample pollutants. EMC is defined as a flow-weighted average concentration that gives an approximation of total pollutant washed off by a storm event to the total volume of the storm (Butcher 2003). EMC is mathematically represented by (Novotny 1995):

$$\text{EMC} = \frac{\text{mass of pollutant contained in the runoff event}}{\text{total volume of flow in the event}}$$

EMC is the net input from pervious and impervious areas resulting from buildup and washoff processes, and can thus change between different storms and between different sites. However, this variation could be defined by a lognormal frequency distribution (Butcher 2003). In the PCSWMM model, EMC is used as input for the pollutant washoff function. The drawback of using EMC in computer modeling is that it does not provide a clear picture on how pollutant concentrations change over the duration of the storm.

PCSWMM supports different options for buildup and washoff of pollutants on different land surfaces. Besides EMC, PCSWMM is capable of modeling the washoff of pollutants using rating curves, or exponential function. While buildup and washoff functions generate more realistic results, they are less frequently used than EMC due to the difficulty in measuring associated rates and limited data in literature (Butcher 2003)**.**

The EMC data reported by CRWD was for samples collected at the outlet of the watershed on the Mississippi river (OFmain). Since the reported EMC data for each storm represented the entire storm, examining the existence of FF from directly analyzing the EMC data is not feasible. Therefore, the objective of this chapter is to investigate numerically the existence of FF at the main outfall of St. Anthony Park watershed using the PCSWMM model by simulating pollutant generation and washoff from watershed surfaces and routing through the drainage system to the outfall on the Mississippi River (OFmain). EMC data available at OFmain can aid in building a hypothetical case related to the built PCSWMM model, where pollutants are generated with a predetermined EMC and routed over land and into the drainage system to OFmain.

For this model, and for the purpose of studying FF, TSS was used as a model pollutant in simulations since most pollutants were found to be positively correlated with TSS (Chapter III). As for TSS generation in the model, two options were considered. The first option was the EMC function, whereby the storm runoff had a mean concentration for TSS, while the second option was the exponential function for buildup and washoff of TSS.

Methods

<u>Exponential buildup and washoff and EMC washoff</u>

PCSWMM models the buildup of pollutants using power functions, exponential functions, saturation function, or external time series. While pollutant buildup is best fitted by power and hyperbolic functions, the exponential equation for buildup is typically used for water quality simulations because it is simple and is the result of a first order process (Lee, Lau et al. 2004, Kim, Zoh et al. 2006).

The exponential functions for buildup and washoff are (James, Rossman et al. 2010):

$$\text{Buildup: } B = C.\ (1-e^{-Z\,T})$$

Where B is pollutant buildup (mass/unit area), C is maximum buildup possible (mass/unit area), Z is buildup rate constant (1/day), and T is the number of previous dry days.

$$\text{Washoff: } W = E_1.q^{E_2}.K$$

Where W is rate of pollutant load washed off at time t, E_1 is the washoff coefficient, E_2 is the washoff exponent, q is the runoff rate per unit area at time t (in/hr), and K is pollutant buildup remaining on surface at time t.

The following values were adopted for the parameters of the exponential buildup and washoff equations:

Buildup: C = 0.0421 kg/m^2 (Tobio, Maniquiz-Redillas et al. 2014)

Z = 0.5 (1/day) (Kim, Zoh et al. 2006)

Washoff: E_1 = 40 [(in/hr)$^{-2.2}$ sec^{-1}] (James, Rossman et al. 2010)

E_2 = 2.2 (James, Rossman et al. 2010)

As for EMC used in this model, a value equal to 184 mg/L was adopted. This value was taken from a study of stormwater runoff in the twin cities (Minneapolis and St Paul) in

Minnesota that was based on stormwater data collected from 15 studies (Brezonik and Stadelmann 2001, Lin, Engineer Research and Development Center et al. 2004).

Routing methods: dynamic, kinematic and steady state

Simulation of water quality at OFmain of the drainage system was done using three different routing methods: dynamic wave routing, kinematic wave routing, and the steady state flow method. Dynamic wave routing generates accurate results by solving the complete one-dimensional Saint Venant flow equations for continuity and momentum for conduits and volume continuity equations at nodes (manholes in this model).

The Saint Venant Equations are (Rossman, Lewis 2006):

Continuity equation: $$\frac{\partial A}{\partial t}+\frac{\partial Q}{\partial x}=0$$

Momentum equation: $$\frac{\partial Q}{\partial t}+\frac{\partial Q^2/A}{\partial x}+gA\frac{\partial H}{\partial x}+gAS_f+gAh_L=0$$

Where:

x: distance along the conduit

t: time

A: cross sectional Area

Q: flow rate

H: hydraulic head of water in the conduit

S_f: friction slope

h_L: local energy loss per unit length of conduit

g: gravitational acceleration

Kinematic wave routing uses the normal flow assumption for routing stormwater through the drainage system. Slopes of hydraulic grade line and conduits slope are the same. This method is mostly used when flow has no restriction which may cause significant backwater or surcharging. Kinematic wave routing uses a simplified momentum equation and the following continuity equation:

$$\text{Continuity equation: } A_1V_1 = A_2V_2$$

Where A: cross sectional area

V: average velocity in pipes

In steady flow routing, it is assumed that at each computational time step, flow is uniform and steady and the normal-flow equation is used to relate flow rate to flow area. This method does not take into account backwater effects, channel storage, losses at entrances and exits, flow reversal or pressurized flow and is thus more suitable for a preliminary study than the dynamic and kinematic routing methods (James, Rossman et al. 2010).

<u>Simulation storm</u>

The temporal distribution of rainfall varies considerably during a storm as well as between different geographic regions. The U.S. Soil Conservation Service (SCS) developed four synthetic 24-hour rainfall distributions (I, IA, II, and III) using National Weather duration-frequency data to represent various regions of the United States. Type IA is the least intense and type II the most intense rainfall. Figure 23 shows the four distributions and their approximate geographic boundaries. While types I and IA represent the Pacific maritime climate with wet winters and dry summers, type III represents the Gulf of Mexico and Atlantic coastal areas with tropical storms, and type II represents the rest of the country (U.S. Soil Conservation Service June 1986). Minnesota has Type II storms. Accordingly, a type II storm was used to check the capability of detecting the presence of FF at OFmain and at nodes (deep manholes of the tunnel).

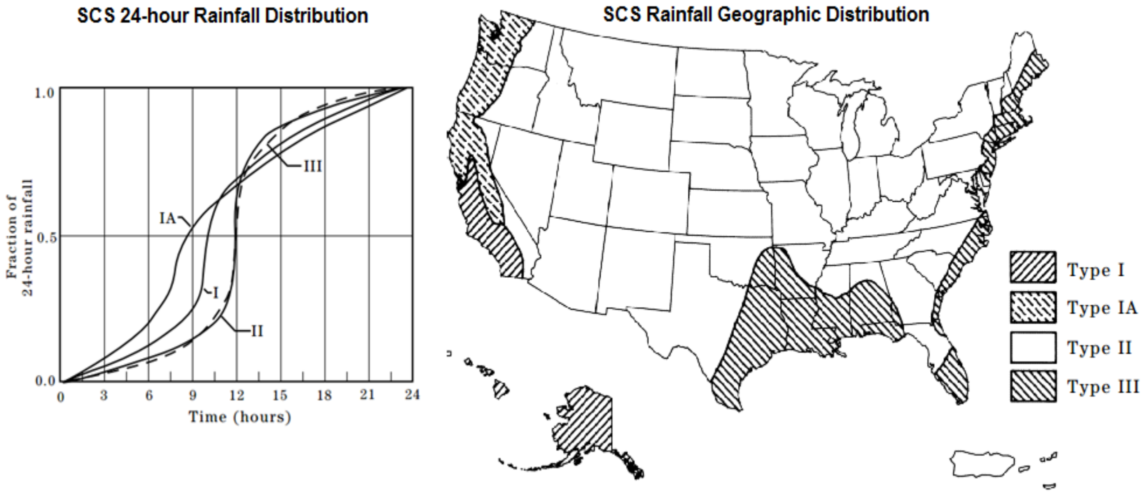

Figure 23. SCS's synthetic rainfall types I, IA, II, and III (left) and their geographic distribution in the US (right). Minnesota has Type II rainfalls which are the most intense among the four types - Modified from (U.S. Soil Conservation Service June 1986).

The rainfall hyetograph of the storm that was used for the simulations is shown in Figure 24. The storm depth was 1.25 inch, which fell into the fourth quartile of storms recorded by CRWD during 2005-2013.The same rainfall hyetograph was used for the three methods for flow routing: steady state, kinematic wave, and dynamic wave. This storm had a 0.3-year return frequency which is considered to remove 90% of suspended soilds in urban areas of the Upper Midwest (Minnesota Pollution Control Agency 2000). Storm depth does not affect the amount of pollutants washed off from urban surfaces when the washoff function is EMC; however, it is important when using exponential buildup and washoff functions since precipitation is the driving factor to wash the pollutants (James, Rossman et al. 2010).

In addition to the intensity, previous dry days are important when using the exponenial buildup and washoff functions since they represent the period when pollutants accumulate on surfaces. EMC has weak correlation with previous dry days (Kim, Zoh et al. 2006) and can therefore be used independently of previous dry days. Previous dry days have no correlation with the FF phenomenon (Lee, Bang et al. 2002) and are thus not expected to impose errors on the study of FF existence in the simulations. In this model, fifteen dry days were used as previous dry days for accumlation of pollutants. Based on analysis of the 2005-2013 record, the number of previous dry days chosen represents the longest dry period during which pollutants could accumulate on the surfaces of St. Anthony Park watershed. These pollutants are eventually washed off by the 1.25 inch storm.

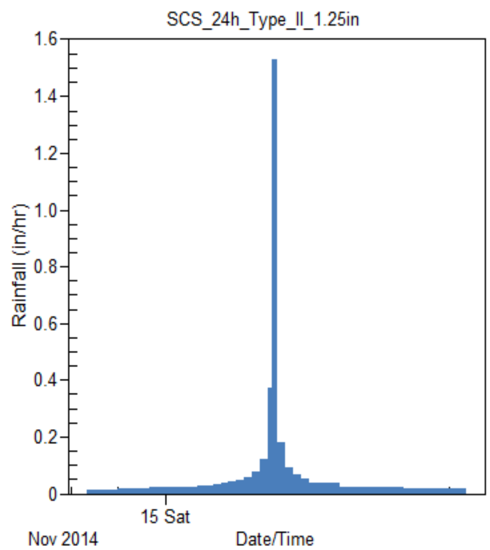

Figure 24. Hyetograph of the storm used in PCSWMM model to simulate the generation of pollutants in St. Anthony watershed. The storm was type II, had a depth of 1.25 inch and a 0.3-year return frequency. The simulation period was 53 hours.

Results and discussion

Hydrographs

The model was run under three routing methods: dynamic wave, kinematic wave, and steady state. The resultant hydrographs at the outfall (OFmain) and at the deep manholes manholes are plotted in Figures 25-27. The simulation period was 53 hours to assure that the hydrograph flow at OFmain approached zero, which would indicate that water outflew from the system.

In the dynamic wave and kinematic wave routing (Figures 25 and 26), hydrographs peaked when the storm intensity was the highest, albeit with a short lag time. In addition, node hydrographs peaked with a little time lag between them due to their location in the tunnel system either at the upstream nodes or at downstream nodes of the tunnel. Time to peak (tp) of the hydrographs differed due to the difference in timing for water to flow from one node to another and eventually to the outfall.

In addition, peak values differed among different nodes, where the highest values were observed at downstream nodes (manholes) and at OFmain. One main difference in hydrographs at OFmain between dynamic wave simulation and kinematic wave simulation is that the latter recorded higher values for flow-peaks, but both graphs had the same shape. On the other hand, when steady state routing was used, hydrographs at nodes and at OFmain peaked at the time of the highest intensity of the storm. As such, tp was the same for all node hydrographs, which is unrealistic since there should be some time lag of the hydrograph peaks with respect to the moment of highest precipitation intensity. Moreover, there should be some time lag for peaks among the nodes. When precipitation intensity increases, it should not be reflected immediately with high flows at the nodes of the system. In addition, peak values of steady state hydrographs were higher than those obtained when using dynamic wave and kinematic wave method.

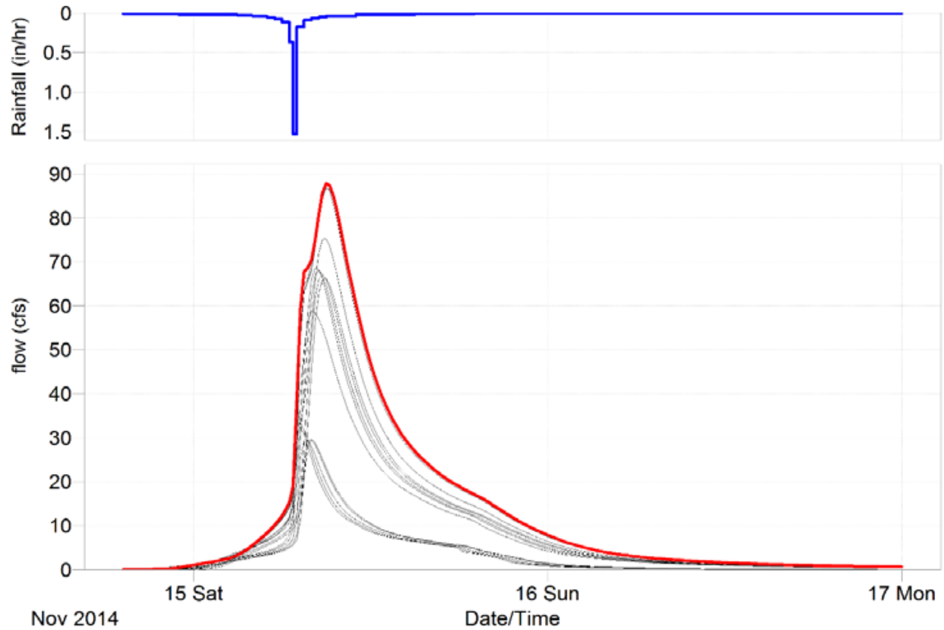

Figure 25. Top: Hyetograph. Bottom: Hydrograph at OFmain (red) and nodes (deep manholes; black) of the deep tunnel using the dynamic wave routing method.

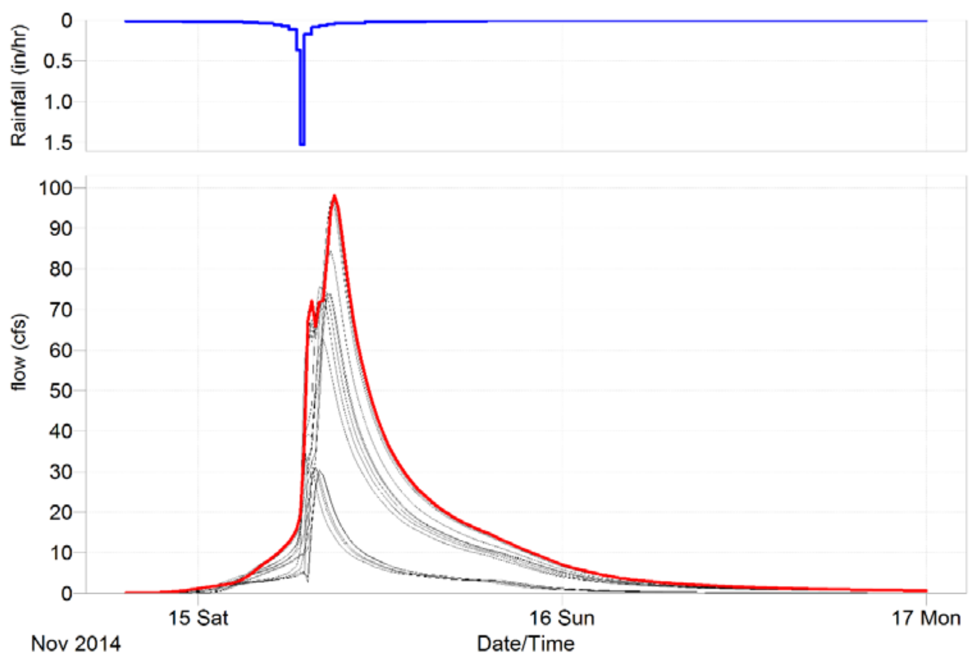

Figure 26. Top: Hyetograph. Bottom: Hydrograph at OFmain (red) and nodes (deep manholes; black) of the deep tunnel using the kinematic wave routing method.

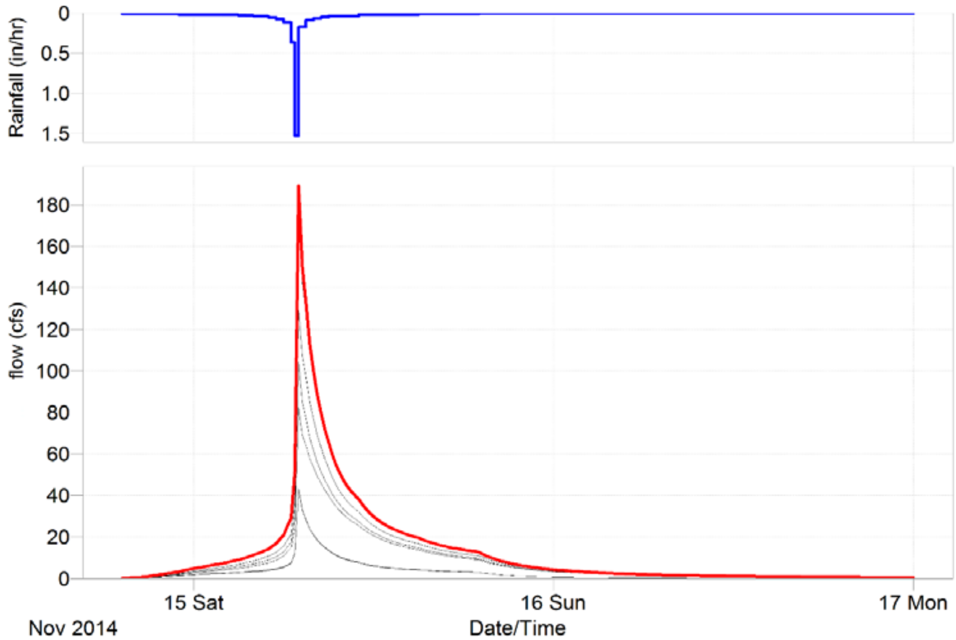

Figure 27. Top: Hyetograph. Bottom: Hydrograph at OFmain (red) and nodes (deep manholes; black) of the deep tunnel using the steady state flow routing method.

Pollutographs

Using the three routing methods, pollutographs were plotted at OFmain and at manholes of the deep tunnel for the exponential buildup and washoff functions (Figures 28-30) and for the EMC washoff function (Figures 31-33).

Figures 28-30 show the pollutographs with exponential buildup and washoff functions at the end of simulation period (53 hours) for the outfall (OFmain) and the other nodes (deep manholes) of the deep tunnel. In the dynamic and kinematic wave routing simulations (Figures 28 and 29), the pollutographs had the same shape. It was noticed that at some nodes the peaks were higher than the peak at the outfall (OFmain), which implied that the pollutants were diluted in the deep tunnel due to the fact that this tunnel received polluted runoff with different concentrations at different nodes. Figure 30 shows the pollutograph when using steady state routing. Peaks for all nodes and for OFmain occurred when precipitation intensity was highest. It was not expected to have simultaneous peaking in the system between input (precipitation) and responses of the system (flows and washing off pollutants), which suggested that the steady state routing was not producing valid, realistic results.

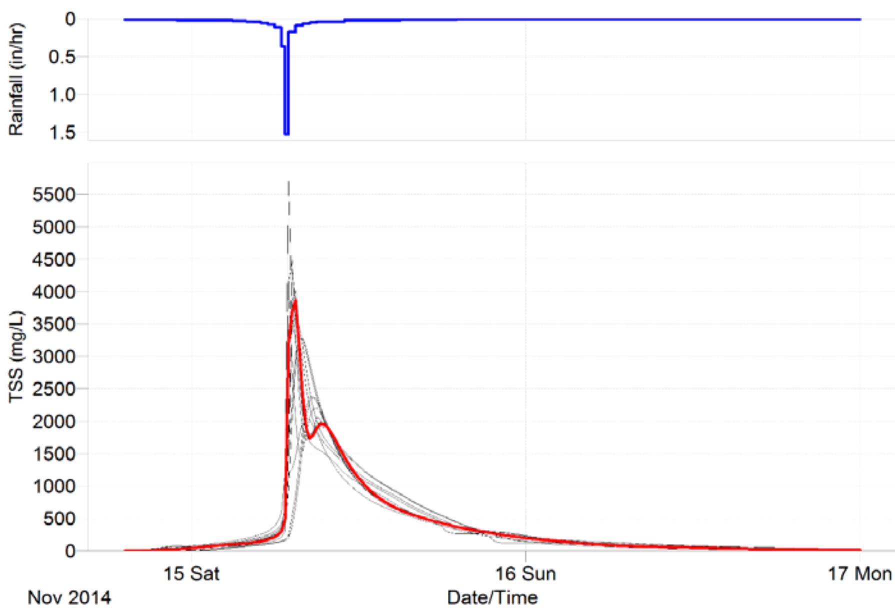

Figure 28. Top: Hyetograph. Bottom: Pollutograph at OFmain (red) and nodes (deep manholes; black) of the deep tunnel using the dynamic wave routing method with exponential functions for buildup and washoff.

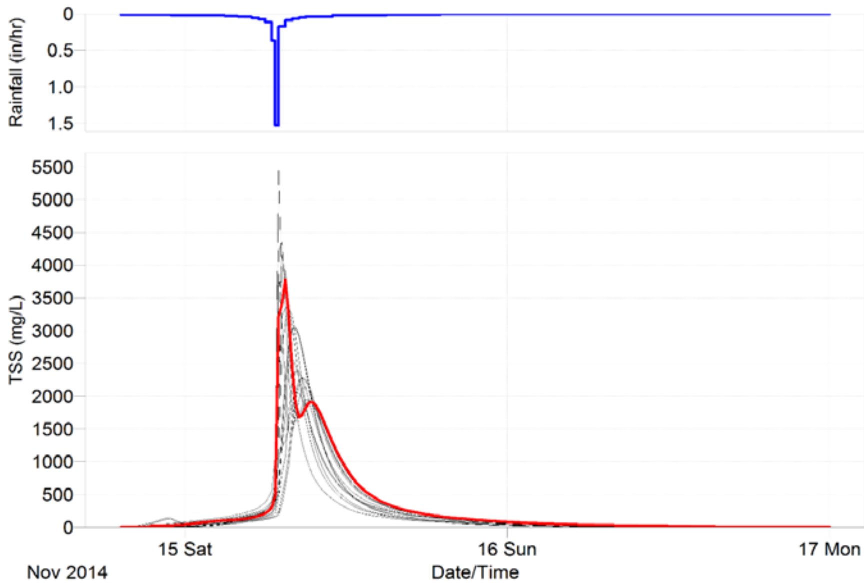

Figure 29. Top: Hyetograph. Bottom: Pollutograph at OFmain (red) and nodes (deep manholes; black) of the deep tunnel using the kinematic wave routing method with exponential functions for buildup and washoff.

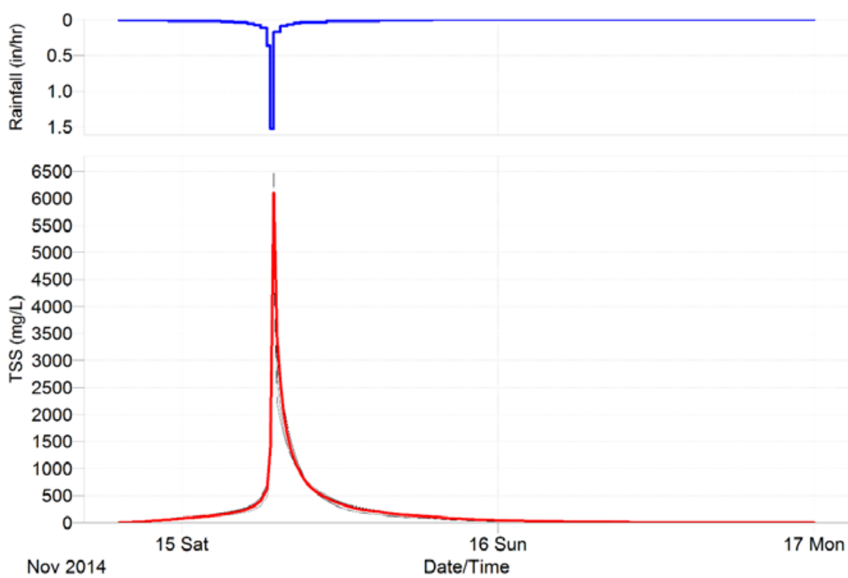

Figure 30. Top: Hyetograph. Bottom: Pollutograph at OFmain (red) and nodes (deep manholes; black) of the deep tunnel using the steady state flow routing method with exponential functions for buildup and washoff.

Figure 31-33 shows the pollutographs with EMC washoff functions at the end of simulation period (53 hours) for the outfall (OFmain) and the other nodes (deep manholes) of the deep tunnel. In the three cases of dynamic, kinematic, and steady state routing, the pollutographs showed a fixed value for TSS concentration at OFmain and other nodes of the deep tunnel. This value was 184 mg/L, which was the input to the PCSWMM system as EMC. As a result, the pollutographs had unrealistic shapes that differed significantly from the shape of a typical pollutograph produced by real data (Figure 34). The pollutographs produced using the exponential buildup and washoff functions (Figures 27-30) were more realistic since they resembled the pollutograph in Figure 34.

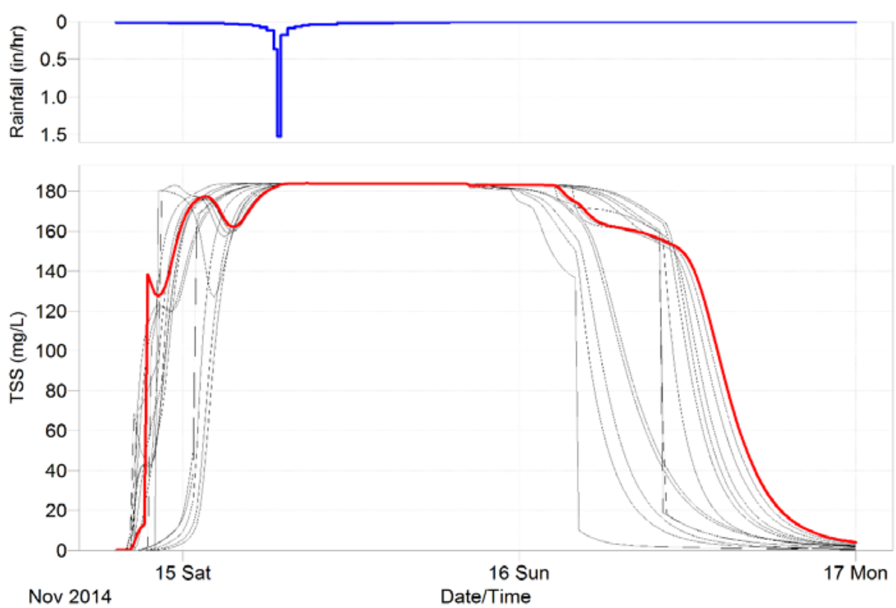

Figure 31. Top: Hyetograph. Bottom: Pollutograph at OFmain (red) and nodes (deep manholes; black) of the deep tunnel using the dynamic wave routing method with EMC washoff.

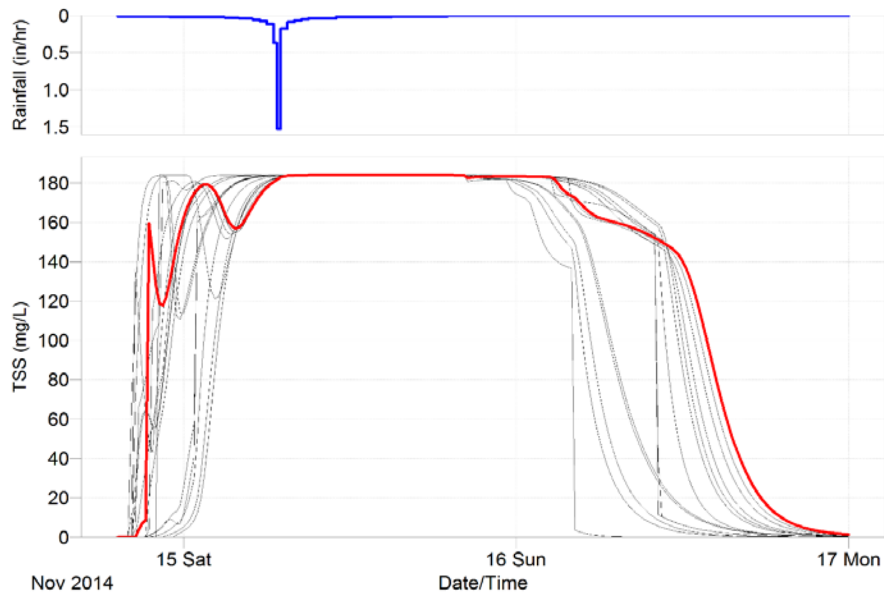

Figure 32. Top: Hyetograph. Bottom: Pollutograph at OFmain (red) and nodes (deep manholes; black) of the deep tunnel using the kinematic wave routing method with EMC washoff.

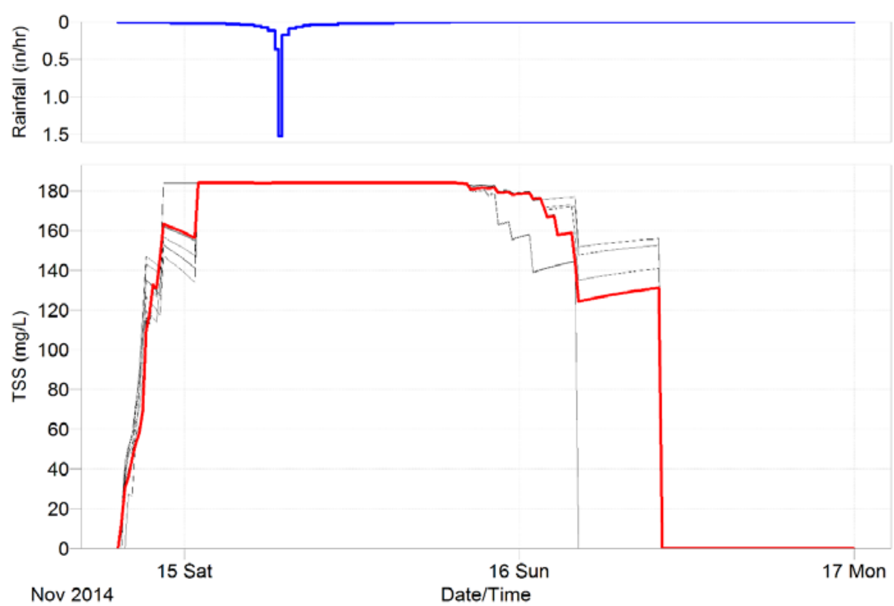

Figure 33. Top: Hyetograph. Bottom: Pollutograph at OFmain (red) and nodes (deep manholes; black) of the deep tunnel using the steady state flow routing method with EMC washoff.

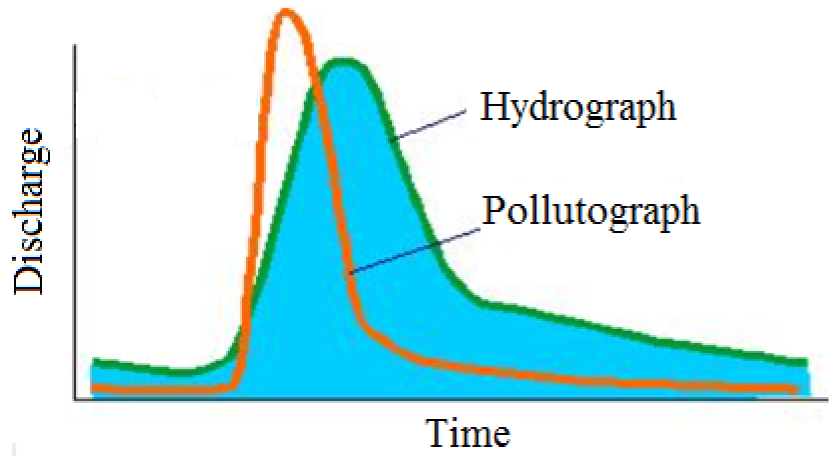

Figure 34. A typical hydrograph and pollutograph constructed from real data - Modified from (http://nrcca.cals.cornell.edu/soil/CA6/CA0658.php).

Cumulative flow versus cumulative load

To check FF existence, the plots for cumulative flow % versus cumulative load % were constructed for the three routing methods using the two washoff functions: EMC and exponential buildup and washoff functions. The results are shown in Figures 35-37.

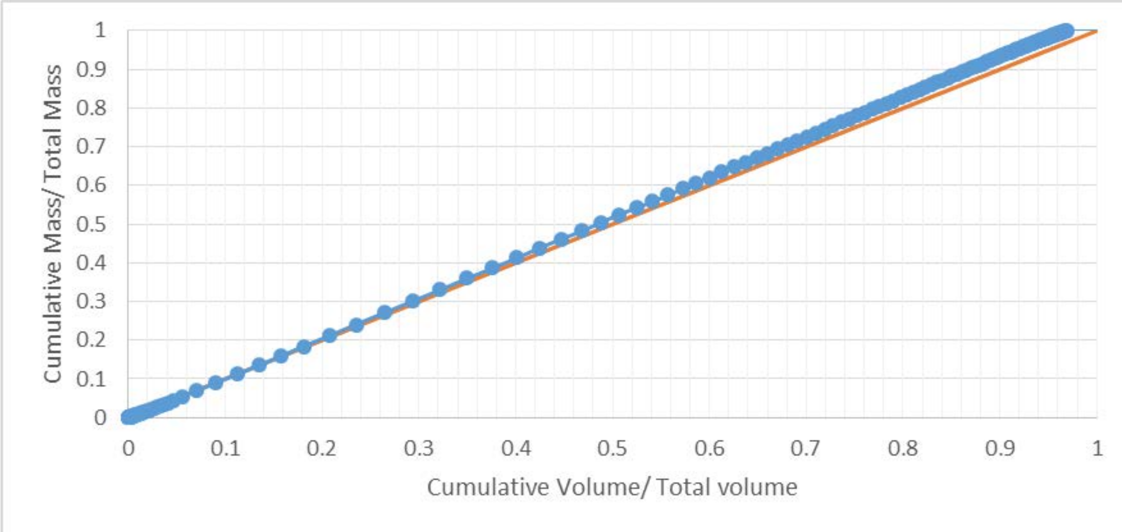

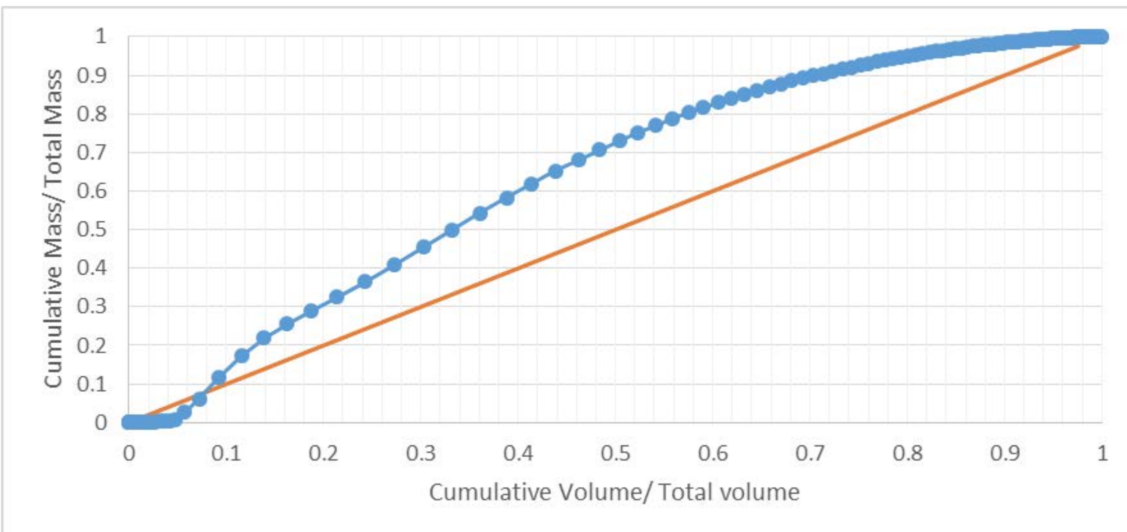

Figure 35. Cumulative volume/pollutant load for TSS at OFmain using dynamic wave routing simulation with EMC function (top) and exponential buildup/washoff function (bottom). The red line represents the 45° line.

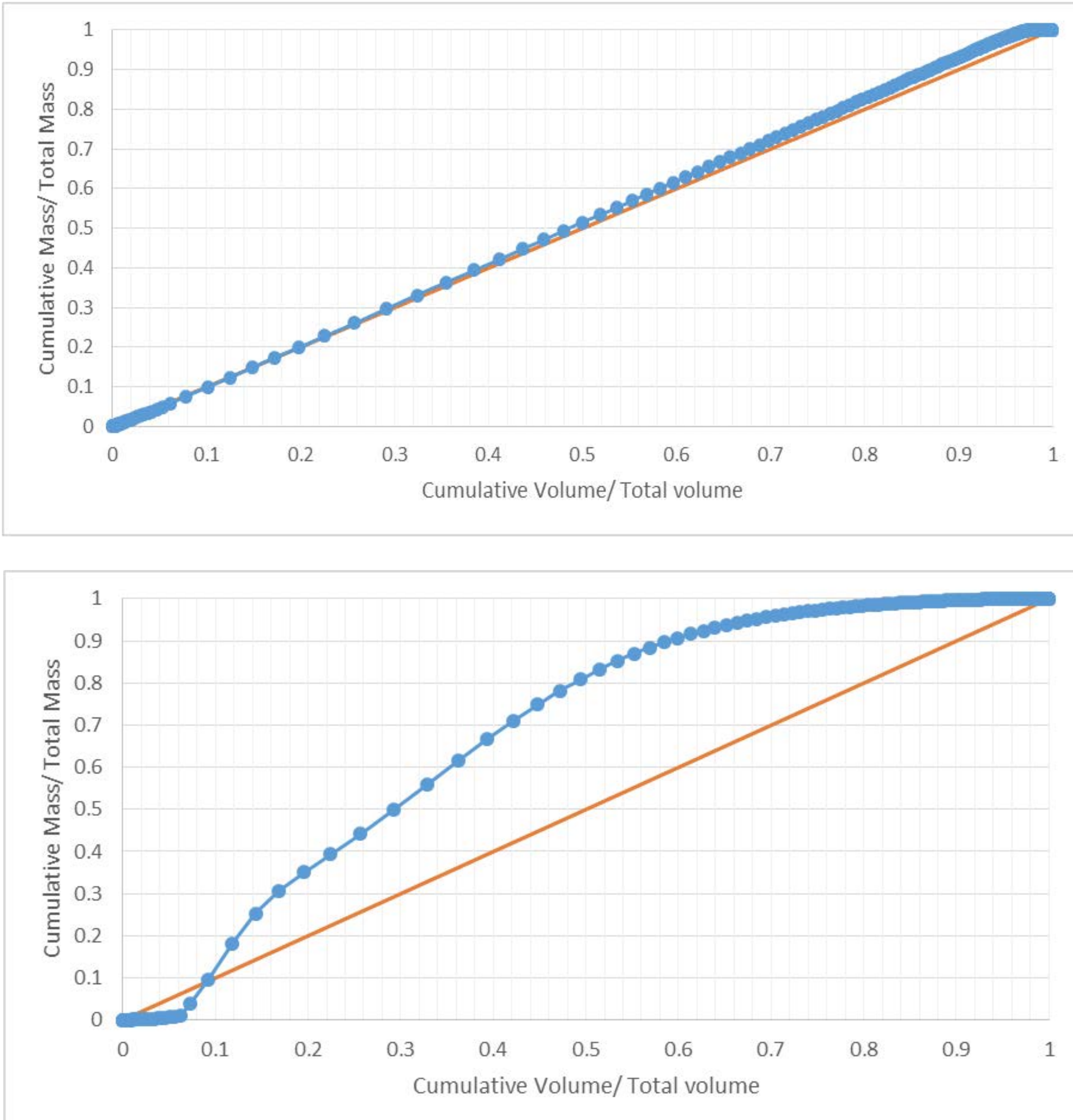

Figure 36. Cumulative volume/pollutant load for TSS at OFmain using kinematic wave routing simulation with EMC function (top) and exponential buildup/washoff function (bottom). The red line represents the 45° line.

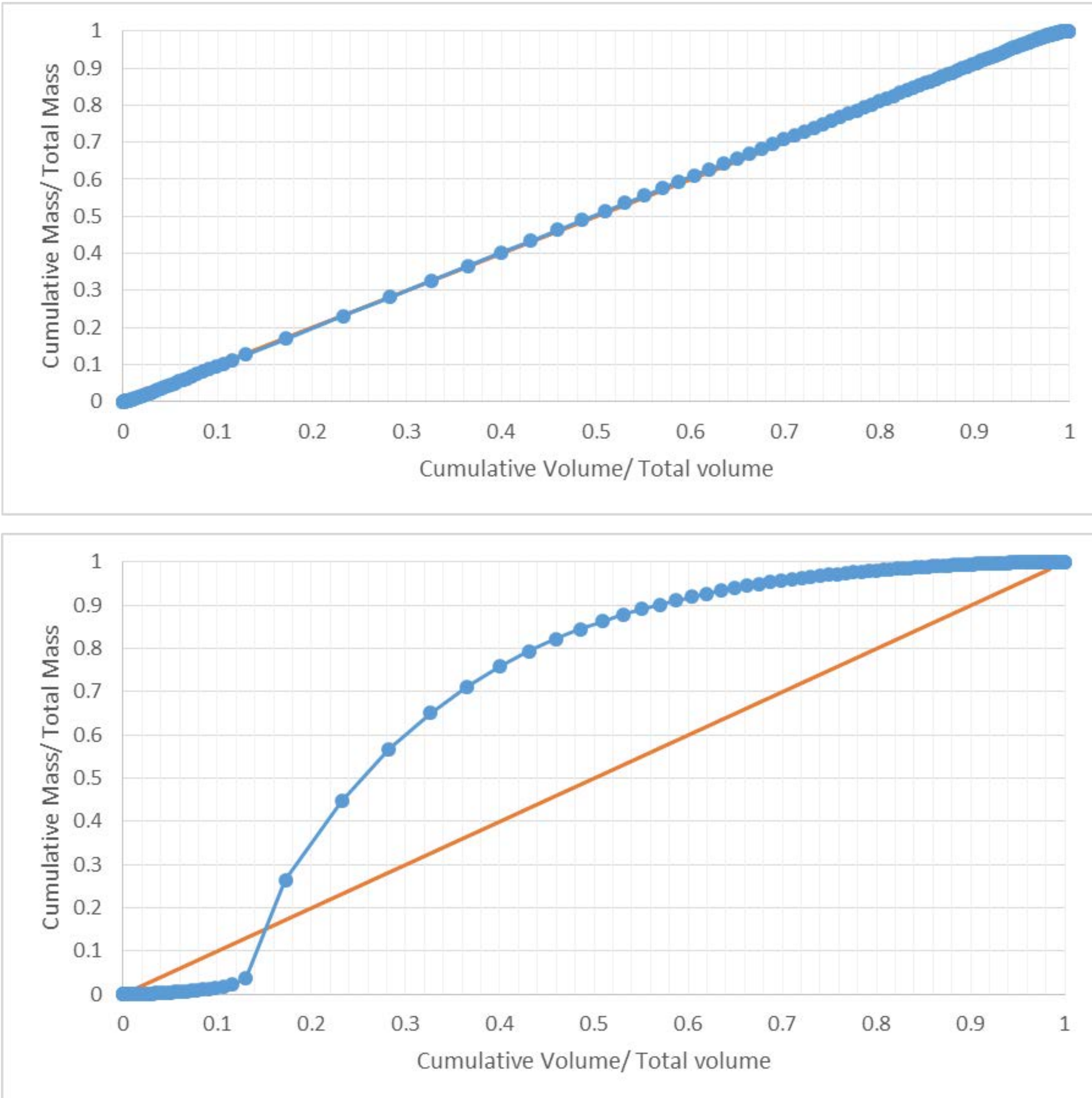

Figure 37. Cumulative volume/pollutant load for TSS at OFmain using steady state routing simulation with EMC function (top) and exponential buildup/washoff function (bottom). The red line represents the 45° line.

As shown in Figures 35 (top), 36 (top), and 37 (top) plots, when EMC function was used, there was an almost perfect overlap between the line constructed by data points and the 45^0 line. This result is numerically valid based on the fact that the pollutant concentration was fixed in the flow. However, and due to the issues seen with pollutographs at nodes and at OFmain, the EMC washoff function was not included in FF analysis.

Figures 35 (bottom), 36 (bottom), and 37 (bottom) show the cumulative flow % versus cumulative load % plots when using exponential buildup and washoff functions. These graphs were more realistic since they were based on the fact that pollutant concentration in runoff is not constant. Consequently, the FF tests were carried out on these graphs in the following section.

First flush tests

To analyze the existence of the FF phenomenon, results were compared to different definitions of FF in the literature. FF has been in some cases defined numerically, such as the definition by Saget *et al.* where 80% of the pollutant load should be transported in 30 % of runoff volume (Saget, Chebbo et al. 1995). Other stricter definitions state that FF exists when 80% of the pollutant load is transported in only 25% of runoff volume (Vorreiter and Hickey 1994). Using these two definitions, no FF was numerically depicted at the outfall of the drainage system.

A third definition holds that FF occurs when the data plot is above the 45º no-flush line, since this signifies that for a given fraction of the total flow, a greater fraction of the total load has been generated (Whipple, Grigg et al. 1983) . A fourth FF definition by Lee et al. (Lee, Bang et al. 2002) states that a certain FF coefficient (b) is calculated and if it is less than 1, then FF exists.

$$\text{FF coefficient } b = Ln(L)/Ln(F)$$

Where $L = m(t)/M$

And $F = v(t)/V$

A fifth test for FF is by calculating Δ = L – F, and if it is greater than 0.2 then FF exists (Lee, Bang et al. 2002).

Using the third definition (above the 45º no-flush line), fourth definition (FF coefficient b < 1), and fifth definition (Δ > 0.2), FF was numerically depicted in all three routing methods (Figures 38-40).

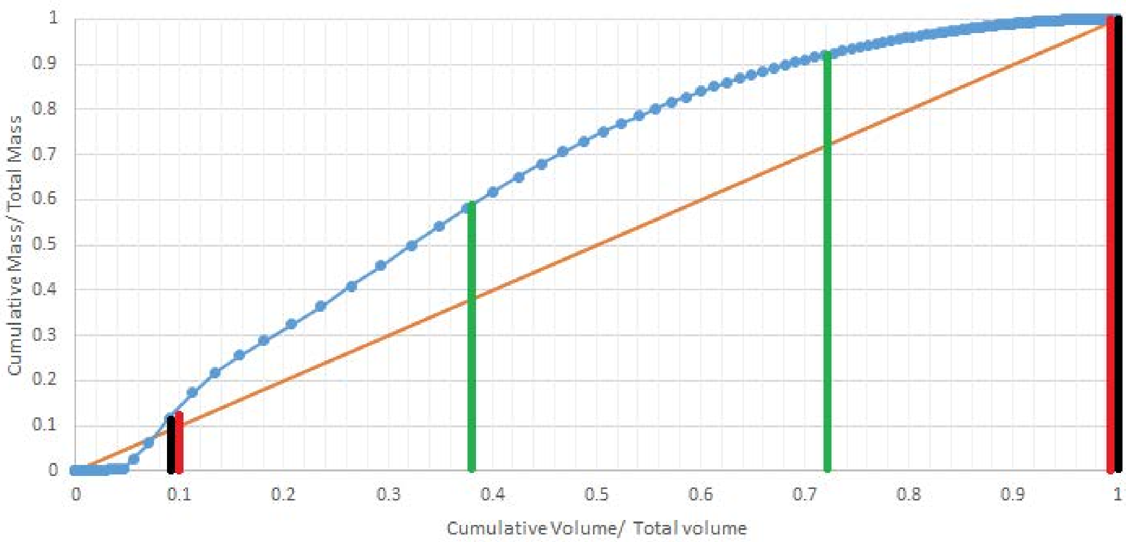

Figure 38. Cumulative volume/pollutant load for TSS at OFmain using the dynamic wave routing simulation with exponential buildup and washoff function. The orange line represents the 45° line. Black lines border the region where FF exists per the third definition (above the 45º no-flush line). Red lines border the region where FF exists per the fourth definition (FF coefficient b < 1). Green lines border the region where FF exists per the fifth definition (Δ > 0.2).

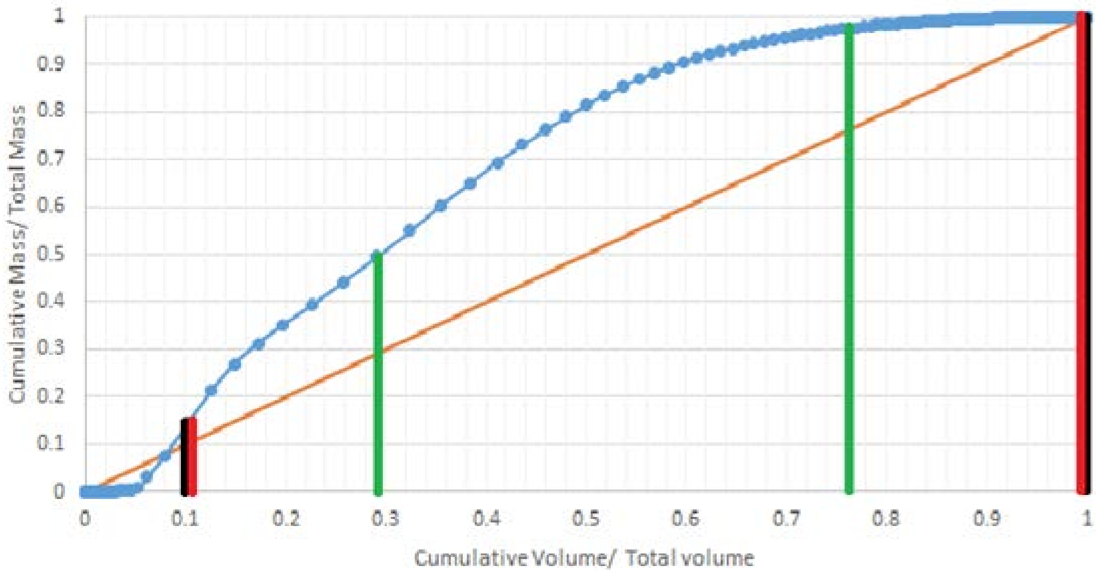

Figure 39. Cumulative volume/pollutant load for TSS at OFmain using the kinematic wave routing simulation with exponential buildup and washoff function. The orange line represents the 45° line. Black lines border the region where FF exists per the third definition (above the 45º no-flush line). Red lines border the region where FF exists per the fourth definition (FF coefficient b < 1). Green lines border the region where FF exists per the fifth definition (Δ > 0.2).

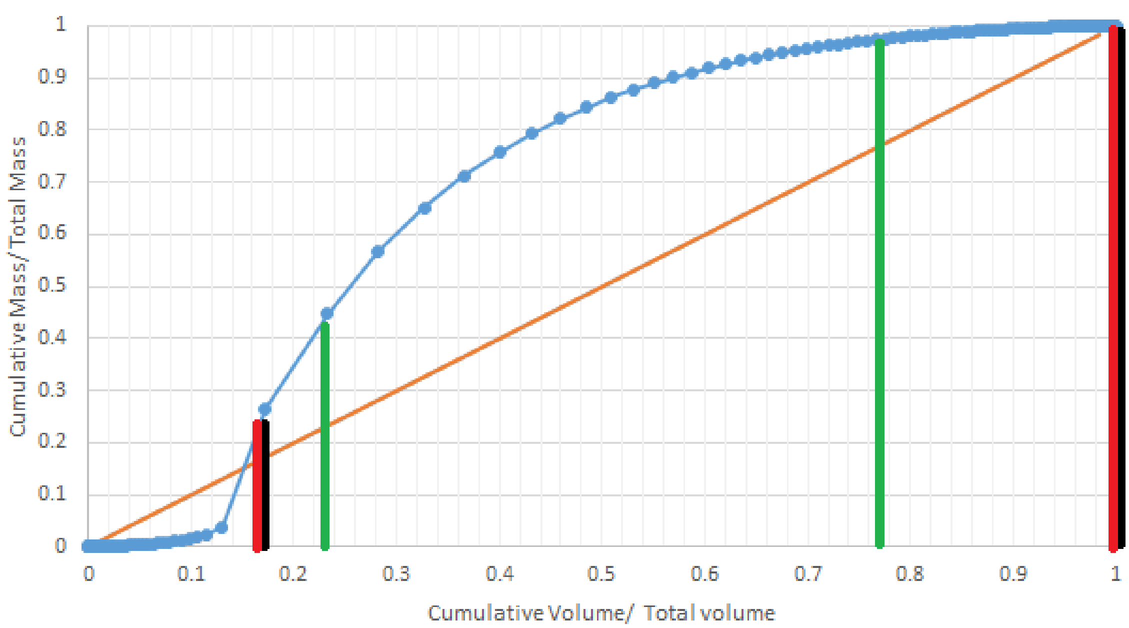

Figure 40. Cumulative volume/pollutant load for TSS at OFmain using the steady state flow routing simulation with exponential buildup/washoff. The orange line represents the 45° line. Black lines border the region where FF exists per the third definition (above the 45º no-flush line). Red lines border the region where FF exists per the fourth definition (FF coefficient b < 1). Green lines border the region where FF exists per the fifth definition (Δ > 0.2).

Collectively from these graphs, it was concluded that as runoff volume increases, pollutant concentrations increase due to the fact that the higher volume of runoff transports more pollutants. To specifically validate the existence of FF, five different definitions were utilized, and FF was found to numerically exist under three of the five definitions. In addition, FF was found to exist regardless of the routing method used. These conclusions were based on results produced using the exponential build up and washoff functions. On the other hand, The EMC washoff functions produced a line that was almost superimposed on the 45º line. Given that the pollutant concentration was fixed, these results were not surprising and might indicate that EMC functions oversimplified the washoff process and were thus less suitable for analyzing FF from real observed data than exponential build up and washoff functions.

It was also noted that the flush of pollutants at certain periods of the storm occurred simultaneously with the highest storm intensity as shown in Figures 27-30. This was only seen with the exponential build up and washoff functions but not with EMC functions (Figures 31-33). Again, this could be reflective of the oversimplified nature of EMC washoff functions which use a fixed value for pollutant concentration in runoff regardless of rainfall intensity.

A drawback to these results is that they could not be validated with real data. However, this can be easily achieved in the St Anthony Park watershed given that OFmain already harbors ISCO samplers. Rather than combining discrete samples during a storm to obtain a composite sample, the samples could be separately tested for water quality, and the results compared with the model output for FF. Taking into consideration that the model was initially calibrated for simulated flows at point of interest, calibration for water quality should in this case be performed by modifying the buildup and washoff equations parameters to match real data collected from ISCO samplers.

Overall, several conclusions can be drawn from the above outcomes. First, FF existence can be numerically depicted using PCSWMM model simulations in absence of rigorous data collection at several timepoints during storm events. Second, the exponential build up and washoff functions are better suited for analyzing FF phenomenon than EMC washoff functions due to their sophisticated nature that accounts for important variables such as rainfall intensity. Third, the definition of FF that is used in analysis greatly impacts on the result and may partially explain the discrepancy in published data (discussed in the rationale section of this Chapter). Finally, and given that FF existence was numerically observed in three out of five definitions, the existence of FF was taken into consideration in subsequent BMP studies for stormwater management at St. Anthony Park watershed.

CHAPTER VI:

STRUCTURAL BMP SCENARIO ASSESSMENT USING PCSWMM MODEL

Introduction

Understanding dominant processes influencing pollutant responses to storm events aids in the development of effective structural Best Management Practices (BMPs) that can control pollution in surface water so that it is suitable for water supply, recreation, and aquatic habitat. For the St. Anthony Park watershed, this research study identified that its stormwaters are polluted and that most pollutants examined were correlated with TSS. Additionally, First Flush (FF) was numerically detected using the PCSWMM model. The correlation of pollutants with TSS as well as the existence of FF were taken into consideration for the most efficient structural BMP choice. No single structural BMP option can be applied to all stormwater management sites. While any structural BMP has its unique water quality and quantity control capabilities, its inherent limitations, as well as the site limitations and watershed location, influence the selection of the most efficient structural BMP. Consequently, the selection of the most appropriate structural BMP to manage stormwater was based on careful evaluation of the following criteria (Debo and Reese 2002):

Criterion One- Stormwater treatment suitability

Criterion Two- Water-quality performance

Criterion Three- Site applicability

Criterion Four- Implementation considerations

An evaluation of the different structural BMP options per these four criteria is provided in the Appendix (A8). For the St. Anthony Park watershed, the choice of the most efficient structural BMP that addresses Criterion One depends on the ability of the structural BMP control option to provide water quality treatment (TSS removal) and not just water quantity treatment.

For Criterion Two, a target of at least 60% TSS removal was set. In addition to removing TSS, the BMP was expected to reduce other pollutants as well given the correlation depicted in Chapter III. Since *E. coli* did not correlate with TSS as seen in Chapter III, another target of at least 75% bacteria removal was set for the structural BMP control option.

Several location-specific factors are taken into consideration when assessing the ability of the BMP of choice to meet Criterion Three. These include the drainage area, space required (consumed), slope restrictions, minimum elevation difference (to allow for gravity operation), and the minimum depth to the seasonally high water table. For the St. Anthony Park watershed, all assessed structural BMPs meet Criterion Three. For Criterion Four, the suitability of the structural BMP for typical residential subdivision development was evaluated. In addition, a target of low construction and maintenance costs was set so that the structural BMP was economical for implementation.

Following the detailed assessment of the various structural BMP options, extended dry detention ponds (EDDPs) were chosen. EDDPs can efficiently control both water quantity (by diverting initial volumes of stormwater, thus addressing FF) and quality (by reducing suspending pollutants, thus addressing TSS). They also meet the set levels for pollutant removal. TSS removal efficiency is at least 61% (Debo and Reese 2002) but can reach 80-90% with vegetated surfaces (Chin 2006). Their reported bacteria removal efficiency is 78% (Debo and Reese 2002). Moreover, they are the least-expensive stormwater treatment practice on a cost per treated unit area, and their maintenance is estimated to be 3-5% of the construction cost annually (Debo and Reese 2002). Naturalized NDDPs are less costly than ponds that rely on highly structural design features (such as rip-rap for erosion control). In addition to enhancing water quality treatment, implementing natural vegetated systems enhance installation cost savings, which are further magnified by the additional environmental benefits provided. It is recommended that EDDP bottoms be vegetated with a variety of native species, including trees, woody shrubs and herbaceous plants rather than turf lawn (Pennsylvania Department of Environmental Protection 2005). Native vegetation cuts long-term maintenance costs due to its ability to adapt to local weather conditions, which reduces the need for maintenance, such as mowing and fertilization (Pennsylvania Department of Environmental Protection 2005). Overall, EDDPs met all set criteria as compared to other structural BMP options.

An important variable in implementing EDDPs as a structural BMP measure is their location. Two location-based designs were examined. The first was a central pond at the main outfall (OFmain), while the second was a set of smaller ponds within the vicinity of deeper manholes of the deep tunnel. The two BMP scenarios were examined using the PCSWMM model with TSS as the model pollutant using three routing methods (dynamic, kinematic and steady state).

Extended dry detention pond scenario constructs

Location of extended dry detention ponds

The aim of enhancing the quality of stormwater that is disposed into the Mississippi River at OFmain with respect to loadings of TSS during storm events demanded defining the optimal location of EDDPs in the watershed. Two options were considered: either to locate several EDDPs in the vicinity of deep manholes (shafts of the main deep tunnel) that received drainage water from the shallow dendritic network to the deep tunnel (Figure 41), or to have one big EDDP that was right before the outfall OFmain (Figure 42). The exact location of the EDDPs needed to be modified to become suitable due to site constraints. In urban areas, detention ponds should be located in open spaces like parking lots or railway tracks. In this study, emphasis was on comparing the efficacy of distributed detention ponds versus one central detention pond rather than on the suitability of the chosen detention pond locations. Nonetheless, each EDDP was placed in a feasible location for future implementation.

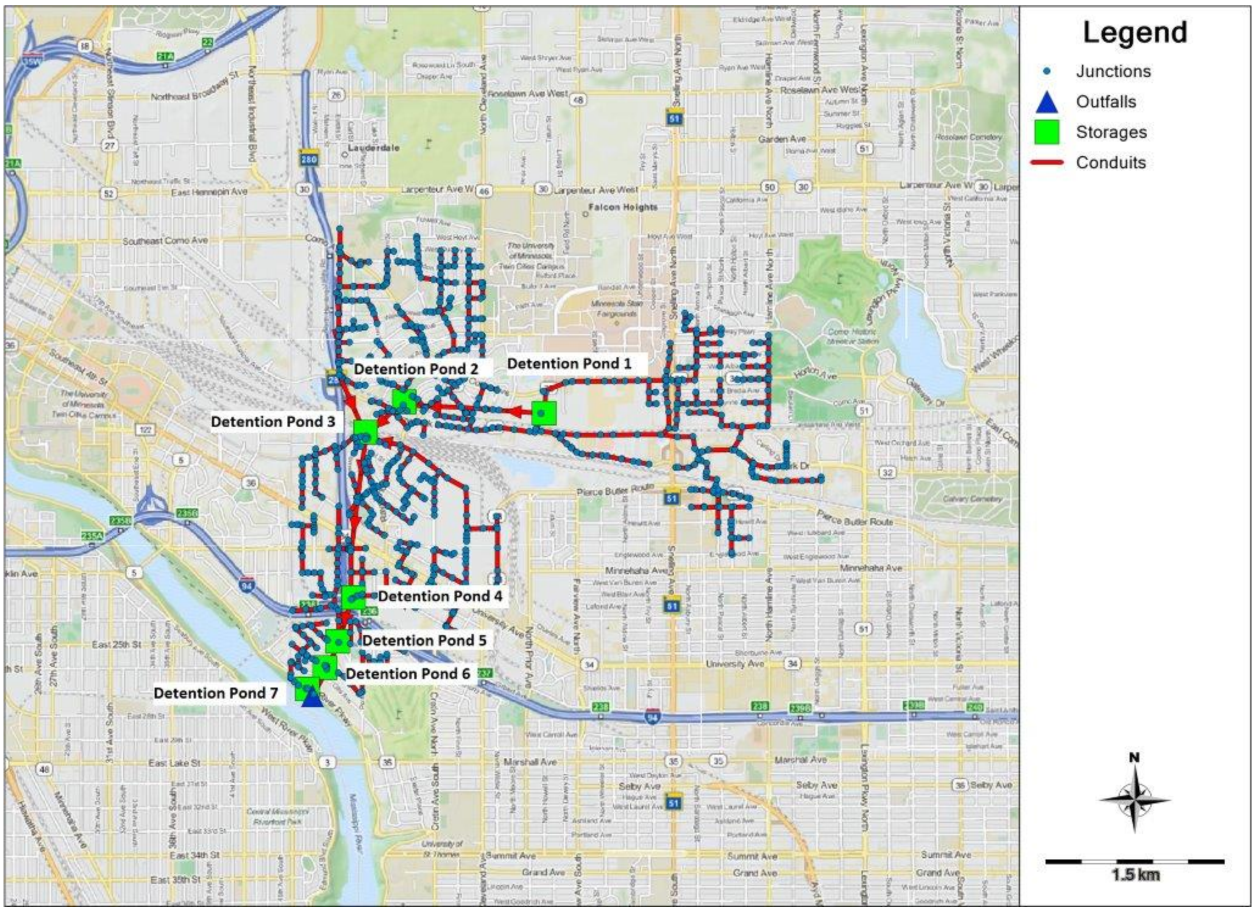

Figure 41. Option 1 for EDDP location: seven EDDPs distributed near deep manholes (shafts) of the main deep tunnel. The EDDPs in PCSWMM are named (storages) and are shown as green squares. Blue circles represent junctions (manholes), blue triangles represent outfalls while red lines represent conduits.

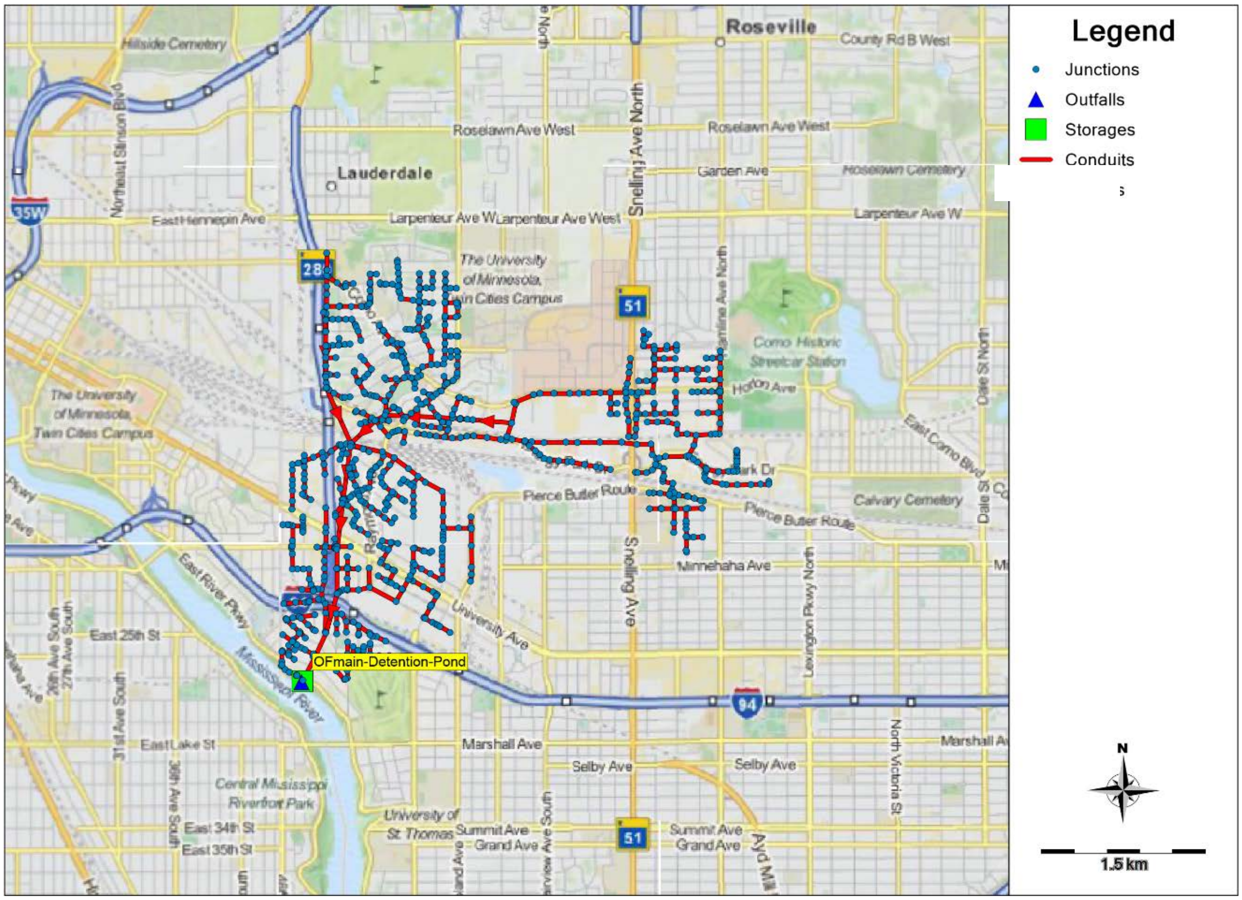

Figure 42. Option 2 for EDDP location: one EDDP located right before the outfall on the Mississippi River (OFmain). EDDPs in PCSWMM are named (storages) and are shown as green squares. Blue circles represent junctions (manholes), blue triangles represent outfalls while red lines represent conduits.

For Option 1, EDDPs had different sizes due to the different subwatersheds disposing their water in these ponds. The general layout for these ponds is shown in Figure 43. Drainage pipes would pour their stormwater in these ponds. The treated effluent from the detention ponds outflowed into the deep shafts. For Option 2, the central EDDP schematic is shown in Figure 44. In the study area, the ground surface slopes down to the location of OFmain, which implies that the deep tunnel over the watershed becomes less deep at the outfall location.

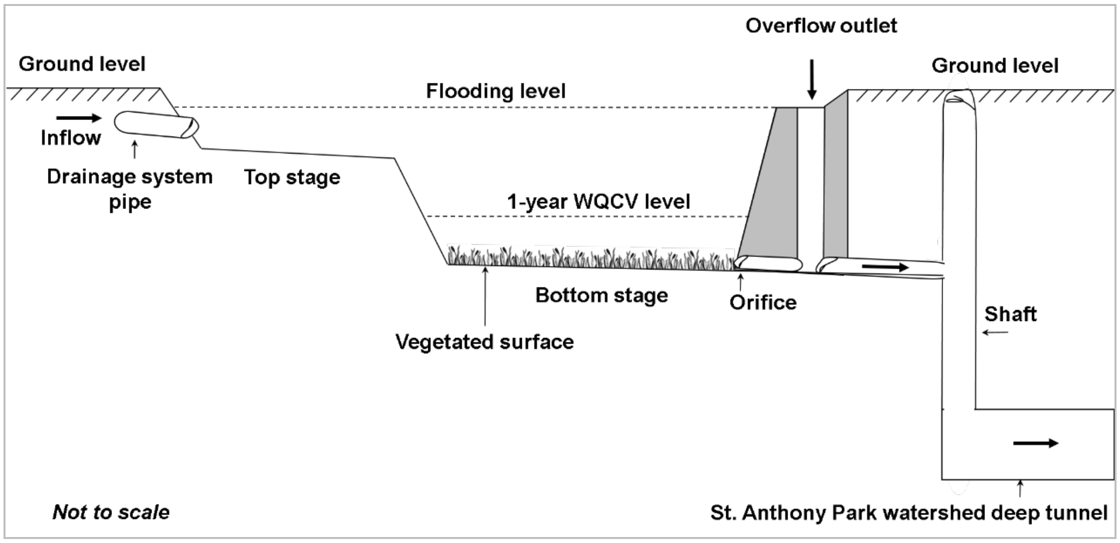

Figure 43. A schematic for extended dry detention ponds – option 1 for EDDP location. Stormwater in drainage pipes flows into the bottom stage of the extended dry detention basin and is retained long enough to achieve the targeted level of pollutant removal. The treated effluent exits through an orifice into shafts that eventually connect to the deep tunnel. The top stage remains dry except during large storms. Ponds were designed with a natural vegetated surface to enhance their pollutant removal efficacy. *WQCV*: Water quality control volume.

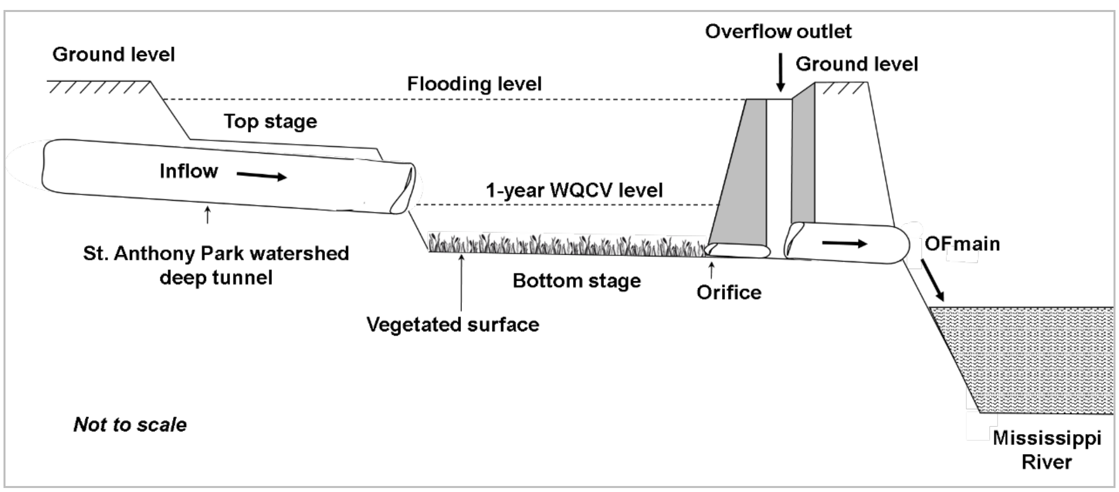

Figure 44. A schematic for extended dry detention ponds – option 2 for EDDP location. Stormwater in the deep tunnel flows into the bottom stage of the extended dry detention basin and is retained long enough to achieve the targeted level of pollutant removal. The treated effluent exits through an orifice into OFmain that drains directly into the Mississippi River. The top stage remains dry except during large storms. Ponds were designed with a natural vegetated surface to enhance their pollutant removal efficacy. WQCV: Water quality control volume.

Ground water considerations

The surficial aquifer in St. Anthony Park watershed is made of bedrock. While groundwater monitoring wells do not exist in the area, nearby wells can give an estimate on depths to groundwater. Three such observation wells (OBwells) are shown in Figure 45. Records at Minnesota Department of Natural Resources (DNR) showed that depths to groundwater level averaged 136 ft at OBwell Number 27016, 107 ft at OBwell Number 27017, and 241 ft at OBwell Number 62043(Minnesota Pollution Control Agency 2000). Debo and Reese (2002) state that there should be a minimum of 2-4 ft depth to the water table from the bottom or floor of a structural BMP control. Consequently, both EDDP location options could be implemented. Groundwater infiltration concerns may arise for option 2 (one EDDP at OFmain) given its distance from the three observation wells. While unlikely, such concerns could be easily addressed by lining the bottom and side edges of the EDDP with a 6 inch lining of concrete instead of using vegetation.

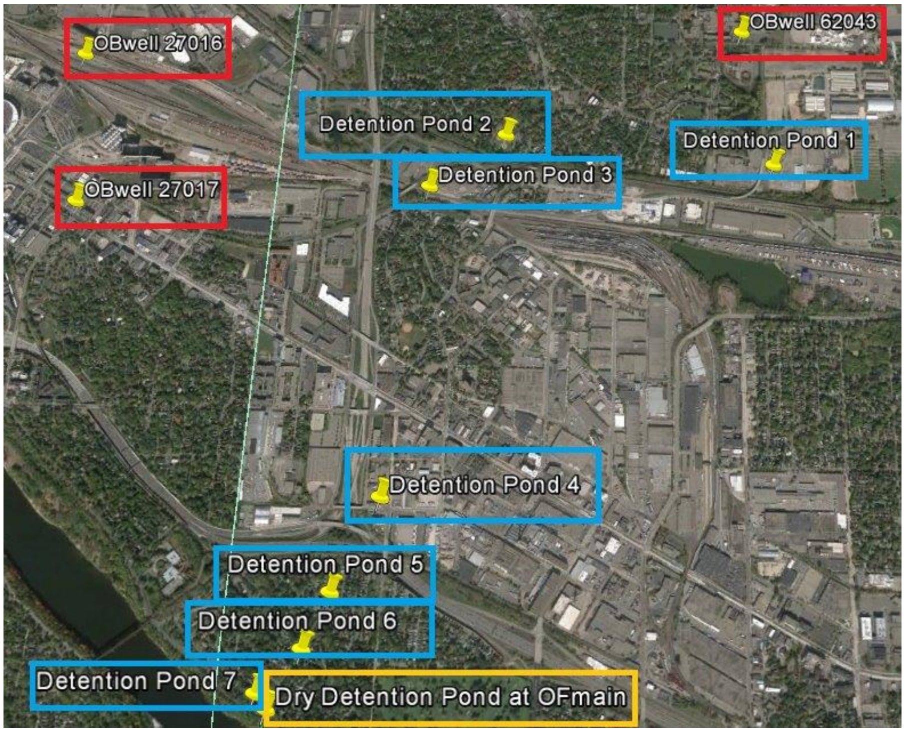

Figure 45. The location of the observation wells (OBwell Number 27016, 27017 and 62043; red boxes) with respect to the designed EDDP options 1 (distributed EDDPs, blue boxes) and option 2 (one EDDP at OFmain; yellow box) as seen from Google Earth -The OBwell locations were obtained from http://climate.umn.edu/ground_water_level/.

Sizing of extended dry detention ponds

Modeling of EDDPs in PCSWMM is possible. The ponds were modeled as storage units. The modeling process steps in PCSWMM are fundamentally similar to those in SWMM. The main steps that were used to design EDDPs in this study were (Gironás, Roesner et al. 2010):

- Calculating the water quality capture volume (WQCV)
- Determining the storage volume and outlet size to control release rates of WQCV

For the design of stormwater quality improvement structures, WQCV needed to be determined since it captures the critical runoff volume. The Urban Drainage and Flood Control District (UDFCD) had proposed a methodology to determine WQCV (Urban Drainage and Flood

Control District (UDFCD) 2007 revision). The main steps of the procedure that were applied to the design of extended dry detention ponds in this research model were:

- Calculating subcatchment's average impervious percentage
- Determining WQCV (in watershed inches) using Figure 46 and choosing a drain time of 40 hr. 40 hr lies within the range of 24-48 hr needed for EDDPs to achieve efficient TSS removal through settling. 40 hr would also allow the use of the value of 1 for the a constant (Figure 46)
- Correcting the WQCV for the St. Paul City area by multiplying it by d_6 to get $WQCV_o$ since the acquired value from Figure 49 was applicable to Colorado's high plains near foothills (Gironás, Roesner et al. 2010)

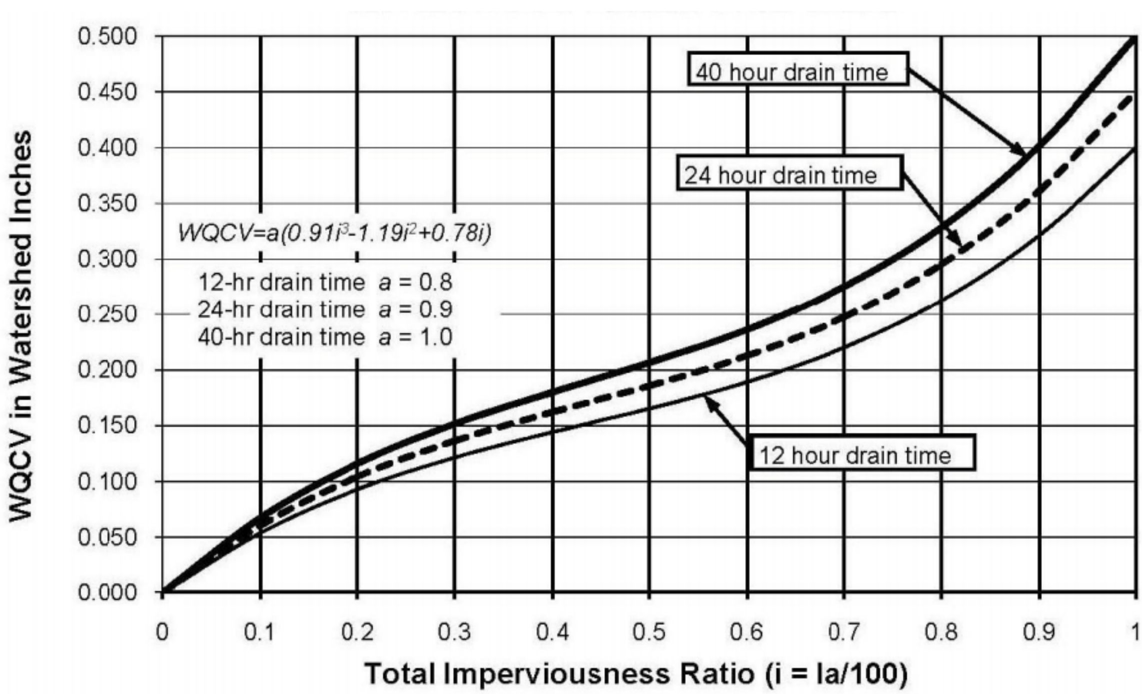

Figure 46. Water Quality Capture Volume (WQCV) based on the total imperviousness ratio (i) and the BMP drain time – Obtained from (Urban Drainage and Flood Control District (UDFCD) 2011).

The average % imperviousness in the area of study was considered uniform over all the subcatchments and equal to the St. Anthony Park average impervious percentage of 48% reported by CRWD (Capitol Region Watershed District 2014). In addition, a drain time of 40 hr was chosen as the time to drain detention ponds, thus, the corresponding value of WQCV was 0.2 in subwatershed inches. To get the WQCV in units of ac-ft, the WQCV in subwatershed inches needed to be multiplied by corresponding subwatershed areas. The same procedure was subsequently used whether the detention pond served a subcatchment as in option 1 (mentioned above) or whether it served the whole watershed (option 2). Since the study area was in rural Colorado, WQCV was corrected to be applicable for St. Paul City by using the equation (Gironás, Roesner et al. 2010):

$$WQCV_0 = d_6 \frac{\mathrm{WQCV}}{0.43}$$

Where d_6 = 0.5 inches according to Figure 47.

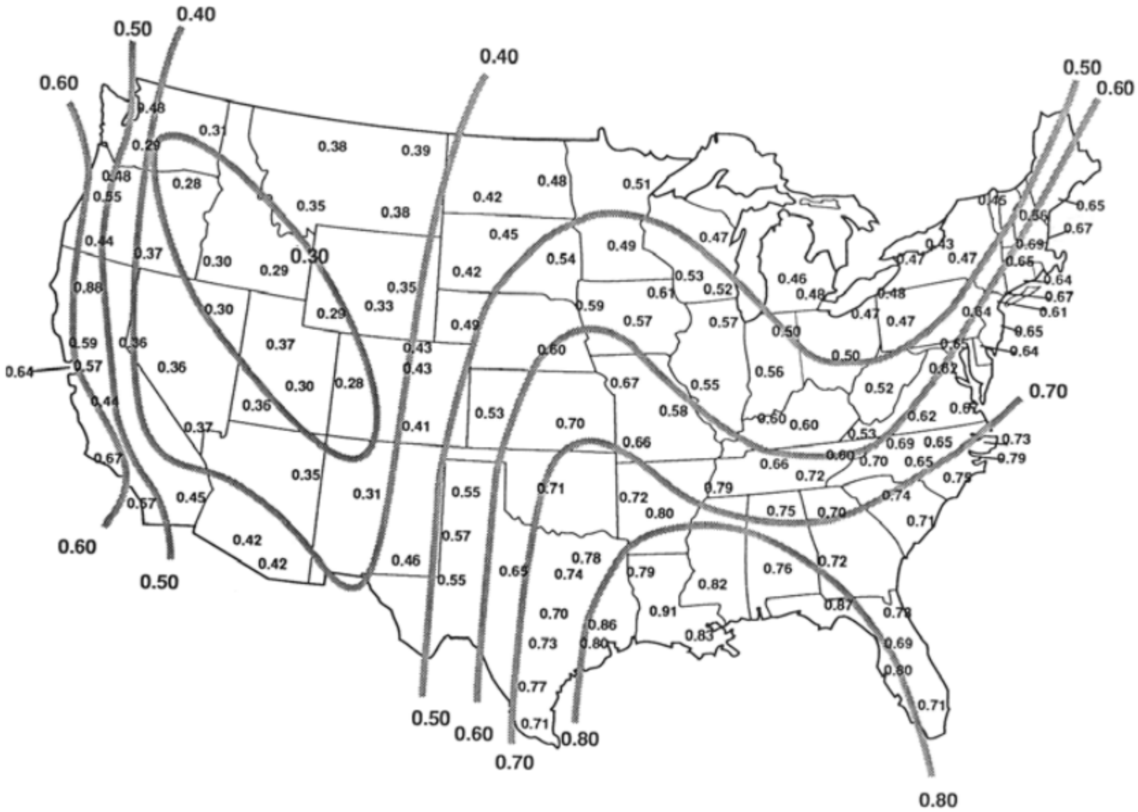

Figure 47. Map of the average runoff-producing storm's precipitation depth (d) in the United States, measured in inches. In Minnesota, d = 0.5 inches – Obtained from (Driscoll, Palhegyi et al. 1989).

The shape of the detention pond was chosen to be trapezoidal prism with a design depth of 4.3 feet as shown in Figure 48. A summary of the bottom and top areas and of the final volume for the WQCV of EDDPs is provided in the Appendix (A10). The detention ponds had an orifice that regulate the outflow of stormwater from the detention ponds. The size of the orifice was calibrated to control the outflow of the detention pond so it drained in 40 hr.

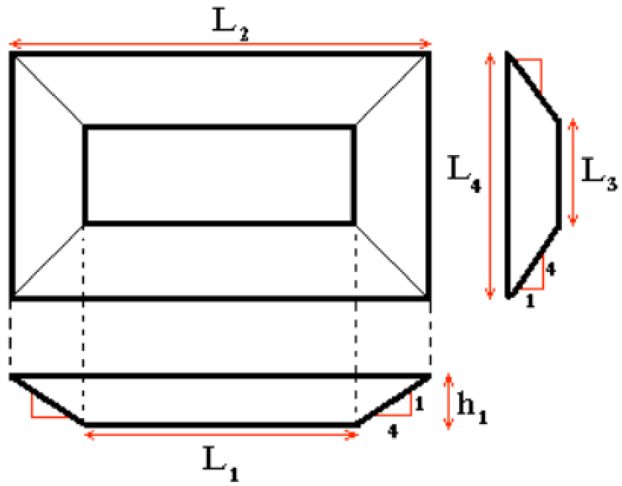

Figure 48. Geometry of the extended dry pond's bottom stage (WQCV). The lengths (L) and height (h) were used in area and volume calculations - Modified from (Gironás, Roesner et al. 2010).

Maintenance of extended dry detention ponds

Similar to other detention facilities, EDDPs need regular periodic maintenance for different problems that include (Debo and Reese 2002):

- Sedimentation accumulation
- Vegetation overgrowth
- Leakages and failures

Maintenance is necessary to ensure proper functionality of the EDDPs. Maintenance plans are implemented periodically on an annual basis and include the following measures (Debo and Reese 2002, Environmental Protection Agency (EPA) 2001, Pennsylvania Department of Environmental Protection 2005):

Sediment removal: Removal of accumulated sediments is crucial to keep the BMP operating efficiently and to reduce risks of reduced storage capacity, re-suspension of settled particles and short circuiting. Inspection should be done quarterly at minimum and more frequently in wet weather, especially after major individual storms when intense precipitation occurs. Sediment removal should be conducted when the basin is completely dry. Following sediment removal, disturbed areas need to be immediately stabilized and re-vegetated.

Soil compaction prevention: Care shall be taken to prevent compaction of soils in the bottom of the EDDP so that infiltration is encouraged through healthy plant growth.

Debris removal: Floatable material should be removed because they could close outlet structure and affect BMP hydraulics. All basin structures susceptible to entrapment of debris (such as orifices) must be inspected for clogging and excessive debris accumulation at least four times per year, as well as after every storm greater than 1 inch.

Vegetation care: In addition to removing debris and sediment, mowing and/or trimming of vegetation should be performed as necessary to sustain the system. Vegetated areas should be inspected annually for erosion and for unwanted growth of exotic/invasive species. The vegetative cover should be maintained at a minimum of 95% and reductions should be re-established.

Rainstorm information

Chapter 5 of "Protecting Water Quality in Urban Areas: Best Management Practices for Dealing with Storm Water Runoff from Urban, Suburban and Developing Areas of Minnesota" (Minnesota Pollution Control Agency 2000) mentions that a lot of variables enter into the design of ponds that make ponds not perform as designed. Consequently, the best performance that should be expected is that the EDDPs would meet design criteria on an average annual basis.

One of the variables is storm events that WQCV should be designed for. Chapter 5 (Minnesota Pollution Control Agency 2000) mentions that a WQCV designed based on a 1.25-inch event storm Type II could remove 90% of TSS in urban areas. Therefore, for the purpose of simulating the effect of adding extended dry detention ponds for the area based on options 1 and

2 (mentioned above), a rain storm of 1.25 inches with a distribution of Type II was used in the PCSWMM model. Characteristics of this storm were described in Chapter V (FF simulation storm). The hyetograph of the storm event is shown in Figure 49.

Since FF is the initial pollutant-carrying discharge that is relatively low in flow rate, small storms are expected to transport the highest pollutant load. As such, one-year storms are typically targeted to manage pollution (Gribbin 2006).

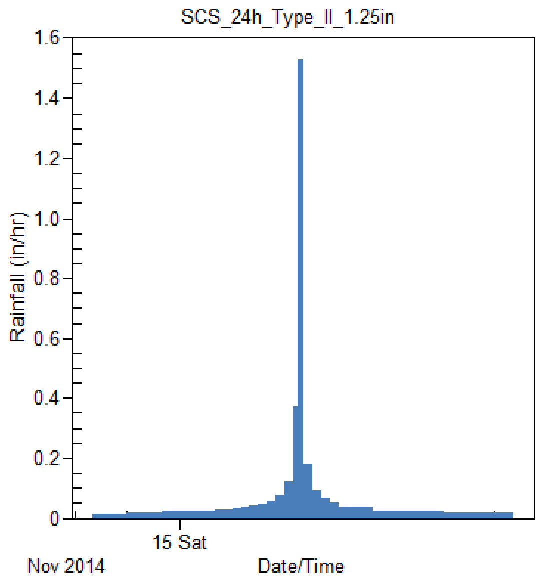

Figure 49. Hyetograph of the storm used for studying BMP scenarios in PCSWMM. The storm had a depth of 1.25 inches and a Type II distribution and lasted for 24 hr.

<u>Simulating TSS removal using PCSWMM</u>

EDDPs were modeled as storage units in PCSWMM, and the removal of TSS was simulated using a (treatment function) represented by the following exponential equation (Gironás, Roesner et al. 2010):

$$C_{t+\Delta t} = C^* + (C_t - C^*)e^{-(k/d)\Delta t}$$

Where $C_{t+\Delta t}$ is the pond's TSS concentration at time $t+\Delta t$

C^* is the residual TSS concentration of TSS that do not settle

C_t is the pond's TSS concentration at time t

k is the TSS sedimentation rate removal constant (ft/hr)

d is the water depth in the pond (ft)

k assumed a value of 0.03 ft/hr for a pond for a target TSS reduction of 95% over a 40-hr period (Gironás, Roesner et al. 2010). This value is reflective of a very small particle size and is within the 20th percentile of settling velocity distributions measured by the US EPA's Nationwide Urban Runoff Program (NURP) (EPA 1986) (Table 13). Another value of k is 0.2 ft/hr which is achieved with a larger particle size distribution (EPA 1986). Given that the actual TSS particle size distribution for the St. Antony Park watershed stormwater is unknown, both values of k were assessed.

Percent of Mass in Urban Runoff	**Average Settling Velocity (ft/hr)**
0-20	0.03
20-40	0.33
40-60	1.5
60-80	7
80-100	70

Table 13. Percent of particle mass in urban stormwater runoff as related to average setting velocity – Obtained from (EPA 1986).

Assuming that the minimum residual TSS concentration was 20 mg/L, the treatment function becomes:

For k = 0.03 ft/hr: C = 20 + (TSS-20)*EXP(-0.03/3600/DEPTH*DT)

For k = 0.2 ft/hr: C = 20 + (TSS-20)*EXP(-0.2/3600/DEPTH*DT)

Where TSS represents the concentration of TSS, 0.02/3600 or 0.3/3600 represents k (ft/s), DEPTH represents water depth d (ft), and DT represents routing time t (s).

Finally, the three routing methods (dynamic, kinematic and steady state) were employed. Table 14 summarizes the various analysis options in PCSWMM used for all simulation runs:

Flow routing method	Dynamic, kinematic and steady state
Washoff	Exponential
Wet weather time step	1 minute
Flow routing time step	15 sec
Reporting time step	1 minute
Total duration	40 hr

Table 14. Summary of analysis options in PCSWMM applied for simulation runs.

While the EMC washoff was more practical, especially since it was supported by published data in the Twin Cities in Minnesota (Lin, Engineer Research and Development Center et al. 2004), the exponential buildup and washoff was more realistic as seen in Chapter V. Consequently, focus was placed on the exponential buildup and washoff results obtained while examining EDDPs. Nonetheless, the same analysis was performed for the EMC washoff function using only the dynamic wave routing method and is provided for reference purposes in the Appendix (A11-A14).

Results

Effect of EDDP implementation on stormwater peak flow

The hydrograph outputs of the PCSWMM model after running it with the two examined EDDP scenarios (seven distributed EDDPs or one EDDP at OFmain) using the three routing methods (dynamic, kinematic, and steady state) are shown in Figure 50.

Examining the shape of the hydrographs, the following results were observed:

- Different routing methods generated different hydrograph shapes when no EDDP was used; however, areas under these hydrographs (i.e. total volume) were equal. Dynamic wave and kinematic wave routing methods generated approximately the same hydrograph shape but with different peak values. This was true regardless of BMP implementation and of the EDDP employed. On the other hand, the steady flow generated hydrographs with different shapes in comparison to the two previous methods. When BMPs were not implemented, the hydrograph peaked at a higher value as compared to the (No BMP) hydrograph of the other two methods. However, BMP implementation (regardless of their location) resulted in hydrograph peaks that were approximately equal to the corresponding peaks when using the other two routing methods.
- When structural EDDPs were used under the two location options, the hydrograph peaks at OFmain were reduced considerably regardless of the routing method, indicating that EDDPs were efficient at reducing flow peaks.
- EDDP implementation increased the time to peak (tp) for OFmain hydrographs for both options of EDDP locations using dynamic wave and kinematic wave routings. However, when using steady state routing, tp remained the same as that of (No BMP).

- After EDDP implementation, hydrograph peaks were approximately matched regardless of the EDDP location options and of the routing method.

Both EDDP locations were equally efficient at reducing peak flows as seen in Figure 50. When examining the ability of EDDPs to reduce peak flows, the seven distributed EDDPs were more efficient than a single EDDP at OFmain only for the dynamic wave routing method, reducing peak flows by 61% versus 44%. On the other hand, peak flow reduction efficiency of the distributed EDDPs was 52% for the kinematic wave and 74% for the steady state routing method, which were very similar to those achieved with the single EDDP at OFmain. These results are summarized in Table 15.

Parameter (examined at OFmain outflow)		**No BMP**	**EDDP at OFmain**	**Distributed EDDPs**
Dynamic Wave Routing Method				
Peak Stormwater flow (cfs)	Measured	101	56	40
	% Efficiency	-	44%	61%
Kinematic Wave Routing Method				
Peak Stormwater flow (cfs)	Measured	122	57	59
	% Efficiency	-	53%	52%
Steady State Routing Method				
Peak Stormwater flow (cfs)	Measured	242	60	62
	% Efficiency	-	75%	74%

Table 15. Stormwater peak flow reduction performance summary for the two BMP scenarios (EDDP at OFmain and distributed EDDPs) for the three routing methods. The simulation was run for 40 hours.

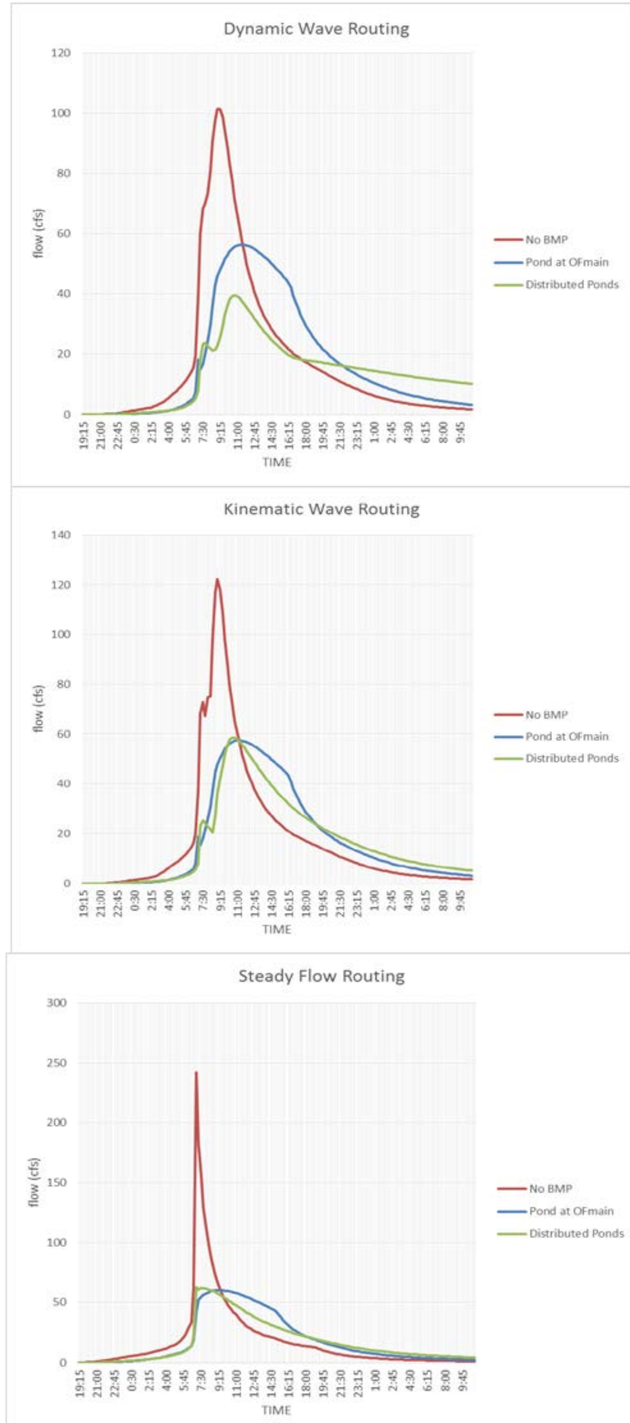

Figure 50. Hydrographs at OFmain outflow for the three routing scenarios: No BMP (red), with one EDDP at OFmain (blue), and with distributed EDDPs (green). The simulation was run for 40 hours. The flow is shown in cubic feet per second (cfs). Notice the difference in flow scales.

From these results, the following conclusions were drawn. First, both EDDP designs were able to achieve the target peak flow reduction of at least 40% regardless of the routing method employed. Second, the two locations of EDDPs were equally efficient at reducing peak stormwater flows, except for the dynamic wave routing method which showed that distributed EDDPs were superior to one EDDP at OFmain. Given that the steady state method is not very accurate as shown in previous sections, its use in computer modeling should be limited to the planning or the initial design phases for stormwater drainage system management. For thorough analysis of the behavior of the system, the dynamic wave and kinematic wave routing methods are more accurate and are preferred. The dynamic wave method has an advantage over the kinematic wave method in that it solves for backwater flows and surcharging when occurring in the system. The kinematic wave method does not solve for backwater and surcharging but gives acceptable results for routing of flows in drainage systems that were initially designed to take these volumes. Therefore, for studying effect of EDDPs on the stormwater system, both routing methods should be used and the more conservative result should be adopted.

Effect of EDDP implementation on stormwater TSS load peaks

One way to evaluate TSS removal efficiency is to compare TSS loads (kg/hr) released by the ponds (Gironás, Roesner et al. 2010). The pollutograph outputs of the PCSWMM model after running it with the two examined EDDP scenarios (distributed EDDPs or one EDDP at OFmain) were plotted for the three routing methods. For each routing method, two different values for the TSS removal constant k were examined: 0.03 ft/hr for small particles (Figure 51) and 0.2 ft/hr for large particles (Figure 52). Figure 53 allows comparison between different k values for each routing method.

Examining the shape of the pollutographs, the following conclusions were made:

- After implementing BMPs, the peaks of pollutographs decreased. The highest decrease was seen when using distributed EDDPs with k=0.2 ft/hr.
- The time to peak (tp) in pollutographs increased when dynamic and kinematic wave routing methods with EDDP at OFmain, indicating that modeled EDDP delayed pollutant accumulation in runoff. No significant change in tp was observed when distributed EDDPs were implemented. On the other hand, tp remained constant when steady state method was used for both EDDP designs.
- The shapes of pollutographs in the dynamic and kinematic wave methods were similar regardless of the k value. However, for steady state routing the shape of pollutograph was different, which may be attributed to the simplistic approach of the steady state method to modeling flow rates.
- While two peaks appeared for pollutographs when not using any BMP or when using distributed EDDPs, only one peak was observed for one EDDP at OFmain. This could be due to the different pattern of outflow of the distributed EDDPs, which were individually smaller in size than the one big EDDP at OFmain.
- Not a big difference in hydrograph shapes and peaks was observed for different k values, suggesting that EDDPs were equally efficient at removing both particle sizes. This could be due to the proximity of size distributions examined (0-20% versus 20-40%; see Table 13).
- The EDDP at OFmain was more efficient at reducing the first peak but less efficient at reducing the second peak than distributed EDDPs for all routing methods. The specific percent shaving of the two peaks are depicted in Table 16.

- Pollutographs suggest that FF could be reduced in magnitude given the reduction in both volume and TSS load. This was further examined in a following section.

Table 16 summarizes the stormwater peak TSS load reduction performance (peak shaving) for the two BMP scenarios (EDDP at OFmain and distributed EDDPs) examined at k-values of 0.02 and 0.3 ft/hr for the three routing methods. At k-values of 0.02 ft/hr, it was noted that the steady state routing method showed no difference in peak shaving between the two EDDP locations. On the other hand, and regardless of particle size, it was noted that, similar to the conclusions reached from pollutograph shapes, EDDP implemented at OFmain was less efficient at reducing the first peak than distributed EDDPs (49-56% efficiency versus ~ 69%) and also less efficient at reducing the second peak (50-58% efficiency versus 74-75%).

Table 16 and Figure 53 show that a slight enhancement of peak shaving efficacy was seen at higher k values (i.e. for larger particles) only for the EDDP at OFmain, which again could be due to the release pattern of pollutants between the big EDDP at OFmain and the smaller distributed EDDPs. Overall, small differences were seen in peak shaving efficacy when different values of the TSS removal constant k, suggesting that at initial stages of the storm when TSS loads peaked, particle size was not an influencing factor on TSS removal by the EDDPs. This is also suggested by the closeness of the pollutographs of the two k values, as seen in Figure 53.

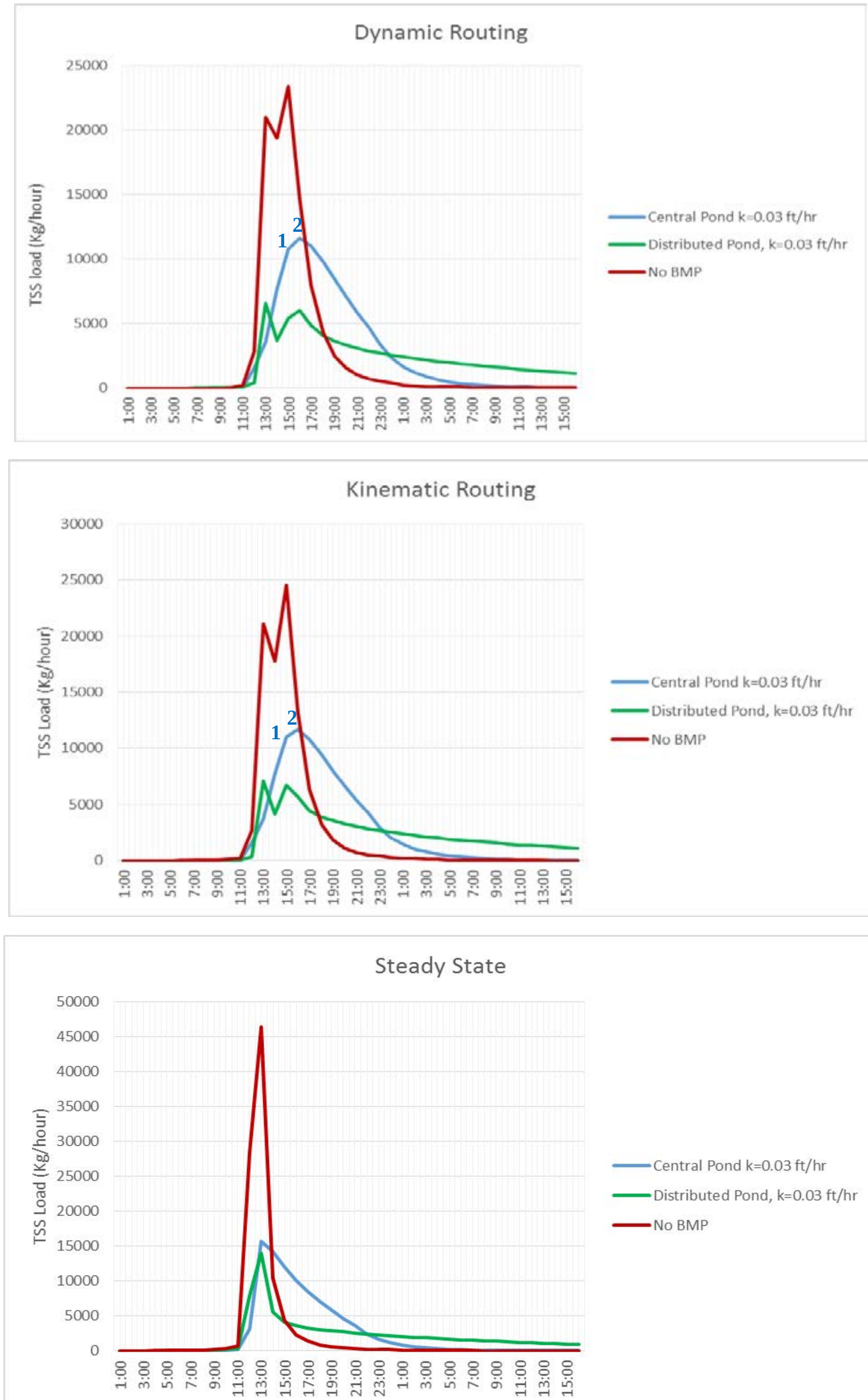

Figure 51. TSS loads (kg/hr) at OFmain outflow for the two EDDP scenarios at k = 0.03 ft/hr: No BMP (red), with distributed EDDPs (green), and with EDDP at OFmain (blue). The top, middle, and bottom panel show pollutographs for dynamic wave, kinematic wave, and steady state routing methods. Numbers 1 and 2 point to peaks on the central pond scenario. The simulation was run for 40 hours. Notice the difference in the TSS load scales.

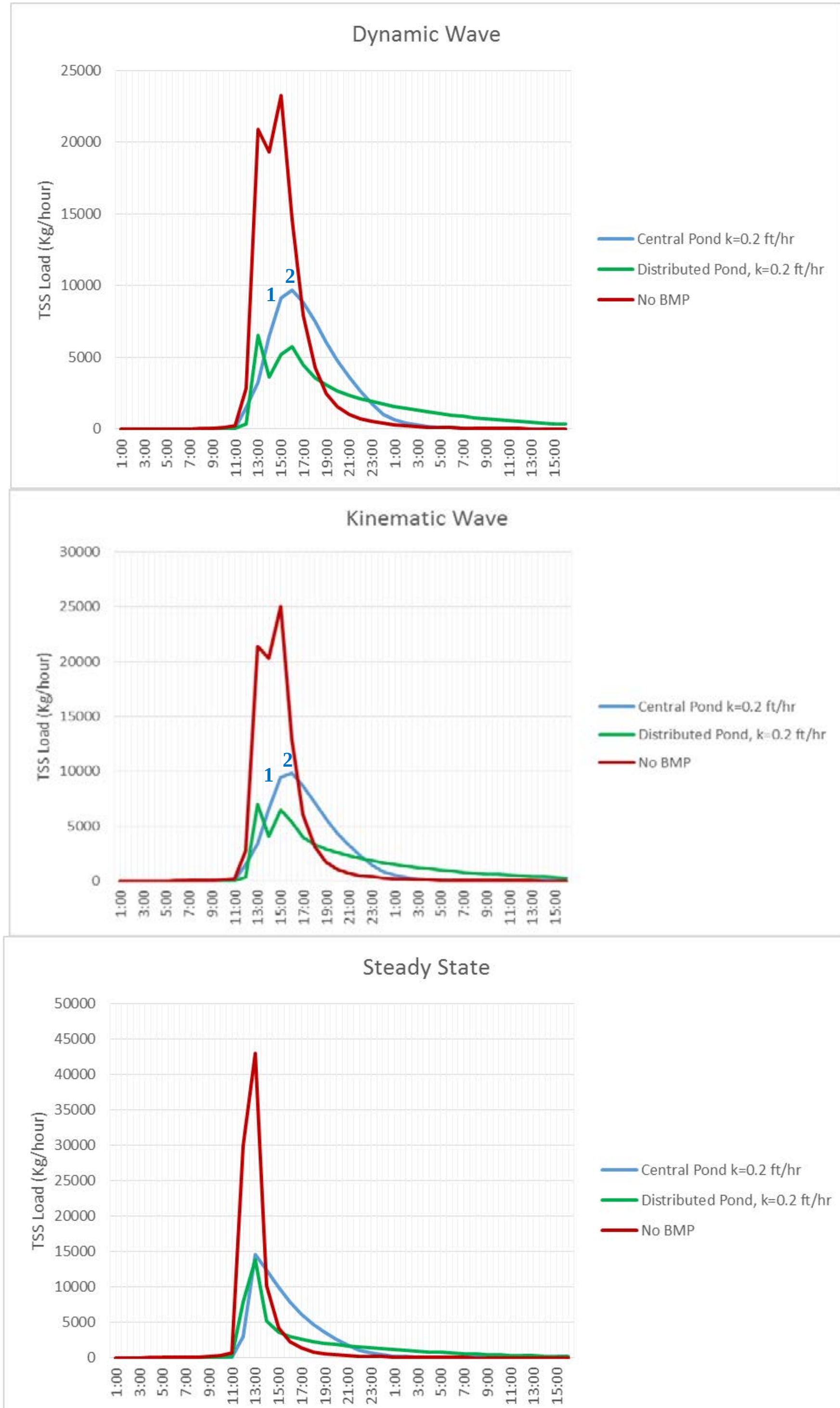

Figure 52. TSS loads (kg/hr) at OFmain outflow for the two EDDP scenarios at k = 0.2 ft/hr: No BMP (red), with distributed EDDPs (green), and with EDDP at OFmain (blue). The top, middle, and bottom panel show pollutographs for dynamic wave, kinematic wave, and steady state routing methods. Numbers 1 and 2 point to peaks on the central pond scenario. The simulation was run for 40 hours. Notice the difference in the TSS load scales.

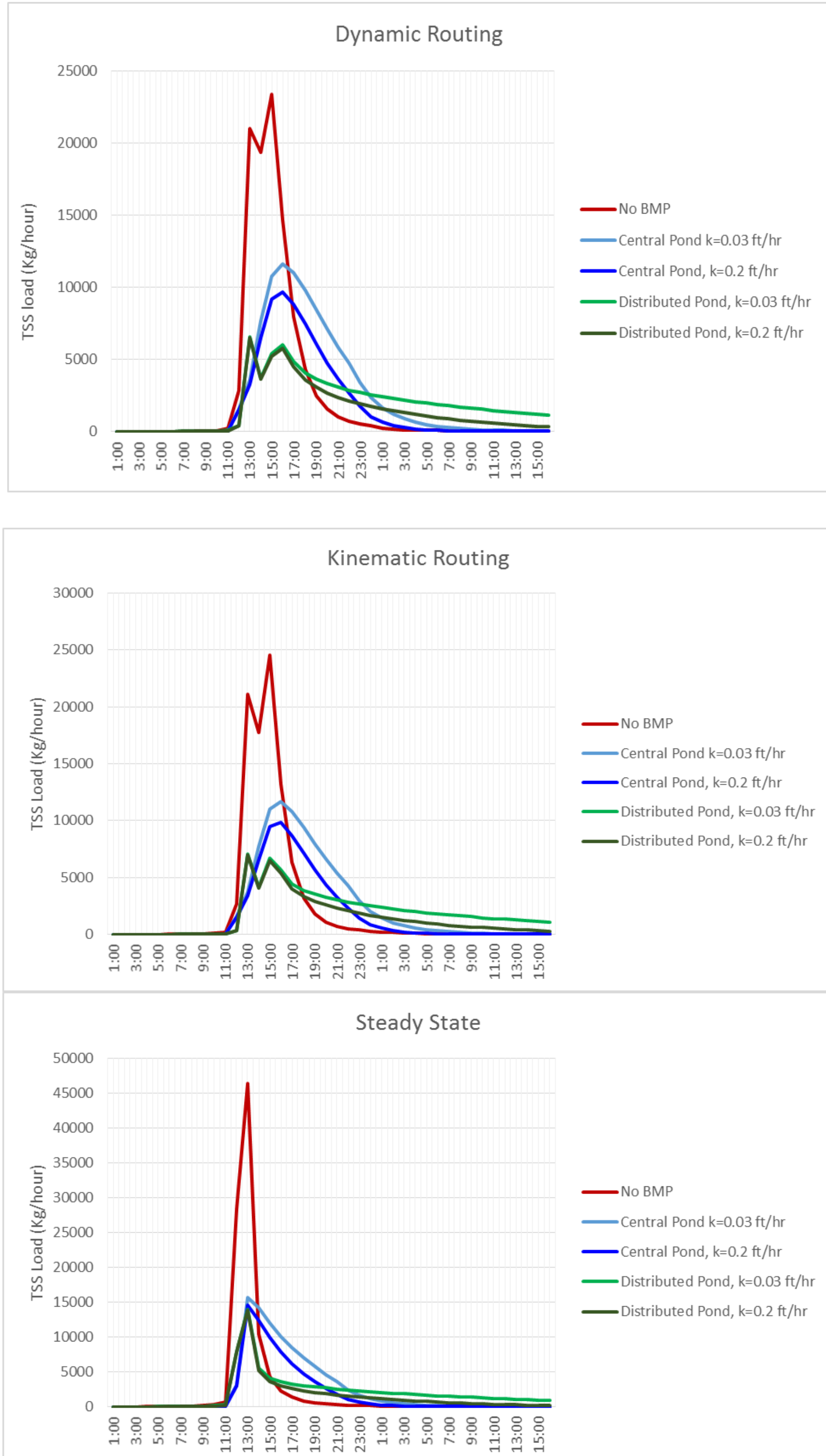

Figure 53. TSS loads (kg/hr) at OFmain outflow for the two EDDP scenarios at k = 0.03 ft/hr and k = 0.2 ft/hr: No BMP (red), distributed EDDP-k=0.03 (light green), distributed EDDP-k=0.2 (dark green), EDDP at OFmain-k=0.03 (light blue), and EDDP at OFmain-k=0.2 (dark blue). The simulation was run for 40 hours. Notice the difference in the TSS load scales.

k value	Parameter (examined at OFmain outflow)		No BMP	EDDP at OFmain	Distributed EDDPs
Dynamic Wave Routing Method					
0.03 ft/hr	Peak 1 TSS Load (kg/hr)	Measured/modeled	20995	10784	6557
		% Removal Efficiency	-	**49%**	**69%**
	Peak 2 TSS Load (kg/hr)	Measured/modeled	23351	11598	6000
		% Removal Efficiency	-	**50%**	**74%**
0.2 ft/hr	Peak 1 TSS Load (kg/hr)	Measured/modeled	20871	9146	6524
		% Removal Efficiency	-	**56%**	**69%**
	Peak 2 TSS Load (kg/hr)	Measured/modeled	23241	9684	5755
		% Removal Efficiency	-	**58%**	**75%**
Kinematic Wave Routing Method					
0.03 ft/hr	Peak 1 TSS Load (kg/hr)	Measured/modeled	21135	10986	7043
		% Removal Efficiency	-	**48%**	**67%**
	Peak 2 TSS Load (kg/hr)	Measured/modeled	24569	11698	6688
		% Removal Efficiency	-	**52%**	**73%**
0.2 ft/hr	Peak 1 TSS Load (kg/hr)	Measured/modeled	21419	9442	7007
		% Removal Efficiency	-	**56%**	**67%**
	Peak 2 TSS Load (kg/hr)	Measured/modeled	25068	9845	6478
		% Removal Efficiency	-	**61%**	**74%**
Steady State Routing Method					
0.03 ft/hr	Peak TSS Load (kg/hr)	Measured/modeled	46350	15674	14023
		% Removal Efficiency	-	**66%**	**70%**
0.2 ft/hr	Peak TSS Load (kg/hr)	Measured/modeled	42970	14628	13803
		% Removal Efficiency	-	**66%**	**68%**

Table 16. Stormwater peak TSS load reduction performance summary (peak shaving) for the two BMP scenarios (EDDP at OFmain and distributed EDDPs) examined at k-values of 0.02 and 0.3 ft/hr for the three routing methods. The simulation was run for 40 hours. Two peak TSS loads were examined at 13:00 and at 15:00 hr for the (15 Sat). For the steady state routing method, only one peak was seen at 13:00 (see Figure 52).

Effect of EDDP implementation on stormwater total TSS loads

Given the difference in peak shaving between the two EDDP locations, another measure of TSS removal efficiency besides peak shaving is to examine the reduction in the total TSS load (Table 17). The difference between the two scenarios was exemplified in the total TSS load. The seven distributed EDDPs reduced total TSS weights by 25% versus only 7% for the OFmain EDDP at k = 0.03 ft/hr, indicating that it was a more efficient structural BMP design. At a larger particle size (k = 0.2 ft/hr), % removal efficiency was still higher for the distributed design and reached 45%. These numbers were obtained for the dynamic wave routing method and were similar to those obtained with the other two routing methods. These results are summarized in Table 17.

Based on the peak shaving efficiency and total TSS load removal efficiency data presented in this section, the overall conclusion was that the distributed design was more efficient than the central EDDP design at water quality and quantity treatment. In addition, the dynamic and kinematic routing methods could be used interchangeably given the overall similar results produced with either method. As such, and for FF analysis in the following section, only the kinematic routing method was used.

k value	Parameter (examined at OFmain outflow)		No BMP	EDDP at OFmain	Distributed EDDPs
Dynamic Wave Routing Method					
0.03 ft/hr	Total TSS Weight (Tons)	Measured/modeled	101	94	76
		% Removal Efficiency	-	7%	25%
0.2 ft/hr	Total TSS Weight (Tons)	Measured/modeled	101	68	56
		% Removal Efficiency	-	33%	45%
Kinematic Wave Routing Method					
0.03 ft/hr	Total TSS Weight (Tons)	Measured/modeled	95	90	76
		% Removal Efficiency	-	5%	20%
0.2 ft/hr	Total TSS Weight (Tons)	Measured/modeled	95	66	56
		% Removal Efficiency	-	33%	43%
Steady State Routing Method					
0.03 ft/hr	Total TSS Weight (Tons)	Measured/modeled	97	92	79
		% Removal Efficiency	-	6%	19%
0.2 ft/hr	Total TSS Weight (Tons)	Measured/modeled	97	69	57
		% Removal Efficiency	-	28%	41%

Table 17. Stormwater total TSS load reduction performance summary for the two BMP scenarios (EDDP at OFmain and distributed EDDPs) examined at k-values of 0.02 and 0.3 ft/hr for the three routing methods. The simulation was run for 40 hours.

Effect of distributed EDDP implementation on FF

The distributed pond structural BMP scenario so far was superior to the OFmain detention pond scenario. Subsequently, the ability of the two EDDP designs to reduce the effect of the FF phenomenon was examined at the two values of the TSS sedimentation rate removal constant k using the kinematic wave routing method.

Figure 54 shows the cumulative volume/pollutant load for TSS at OFmain using kinematic wave routing simulation with exponential buildup/washoff function at k = 0.03 ft/hr (top) and k = 0.2 ft/hr (bottom) for the two EDDP designs. FF was detected without BMP implementation, in agreement with results seen in Chapter V. The distributed EEDP design was able to reduce the magnitude of FF better than the single EDDP at OFmain. This was observed for low particle sizes (k=0.03 ft/hr) but was lost for larger particles (k = 0.2 ft/hr), whereby both designs failed to reduce FF.

The cumulative volume/pollutant load graph was examined for the existence of FF using three FF tests as shown in Figure 55 (k=0.03 ft/hr) and Figure 56 (k=0.2 ft/hr).

As shown in Figure 55 for the distributed EDDP design, two FF tests (above the 45º no-flush line in black lines and coefficient b < 1 in red lines) numerically detected FF. However, the more stringent FF test (Δ>0.2 in green lines) did not detect FF existence. On the other hand, all three tests detected FF for the one EDDP design. These results indicate that, at least per the fifth definition of FF (Δ>0.2), the distributed EDDP design was more efficient at reducing FF.

For larger particles (k=0.2 ft/hr), Figure 54 shows that there was little improvement in the magnitude of FF following BMP implementation. In agreement, Figure 56 shows that all FF tests could detect FF in both EDDP designs, albeit to a lesser magnitude per the fifth definition (Δ>0.2) with the distributed EDDP design.

Despite the decrease in FF magnitude, FF was not completely eliminated. In addition, smaller particles were more efficiently reduced in FF than larger particles. This was a strange observation, since it was expected that larger particles would be more efficiently reduced as seen in the previous section. This observation requires validation by analyzing particle size from real data obtained from successive stormwater samples.

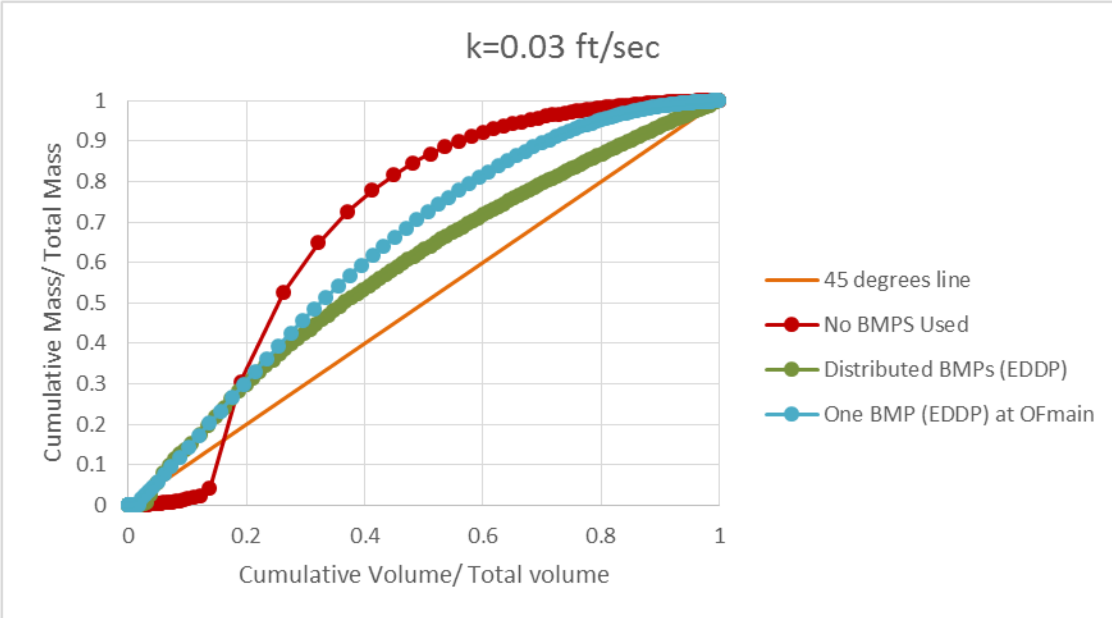

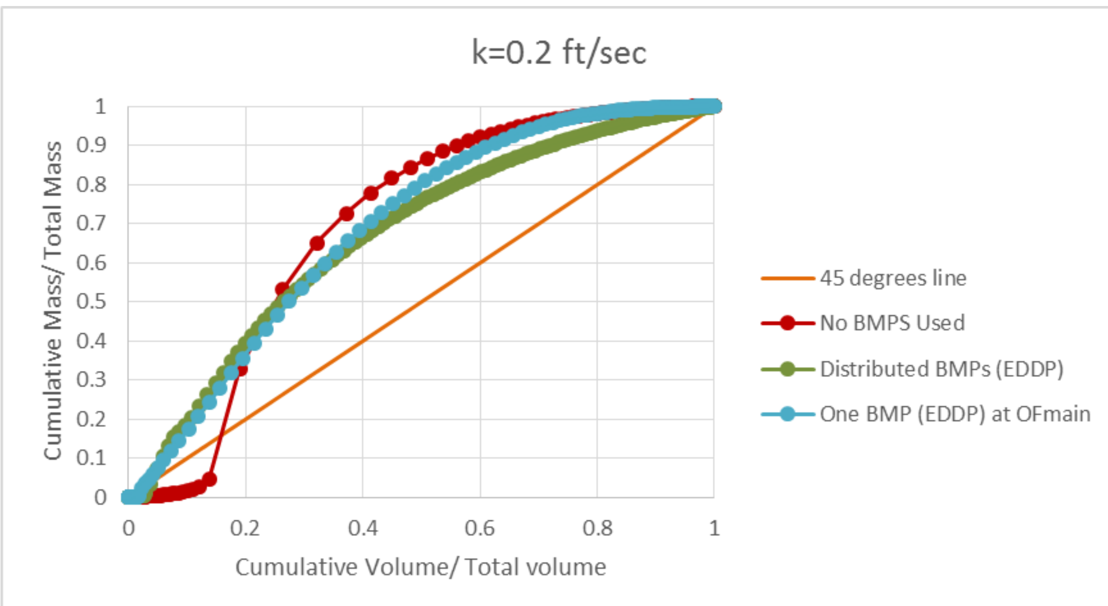

Figure 54. Cumulative volume/pollutant load for TSS at OFmain using kinematic wave routing simulation with exponential buildup/washoff function at k = 0.03 ft/hr (top) and k = 0.2 ft/hr (bottom). The orange line represents the 45° line, the red curve is for no BMP implementation the green curve is for the distributed EDDP design while the blue curve is for the one EDDP at OFmain design.

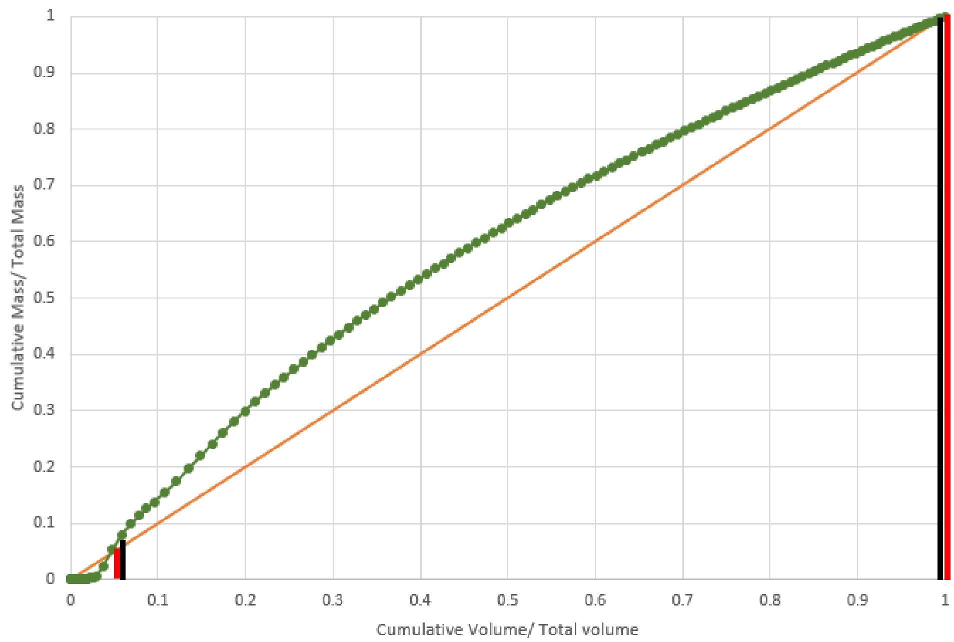

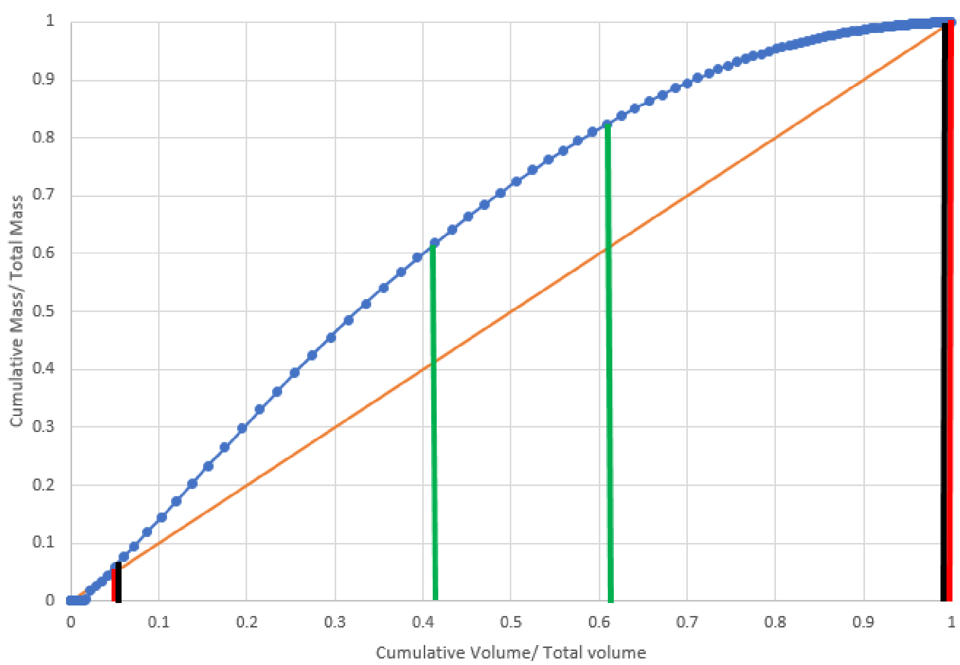

Figure 55. Cumulative volume/pollutant load for TSS at OFmain using kinematic wave routing simulation with exponential buildup/washoff function at k = 0.03 ft/hr for the distributed EDDP design (top) and the one EDDP at OFmain design (bottom). The orange line represents the 45° line. Black vertical lines border the region where FF exists per the third definition (above the 45º no-flush line). Red vertical lines border the region where FF exists per the fourth definition (FF coefficient b < 1). Green vertical lines border the region where FF exists per the fifth definition (Δ > 0.2).

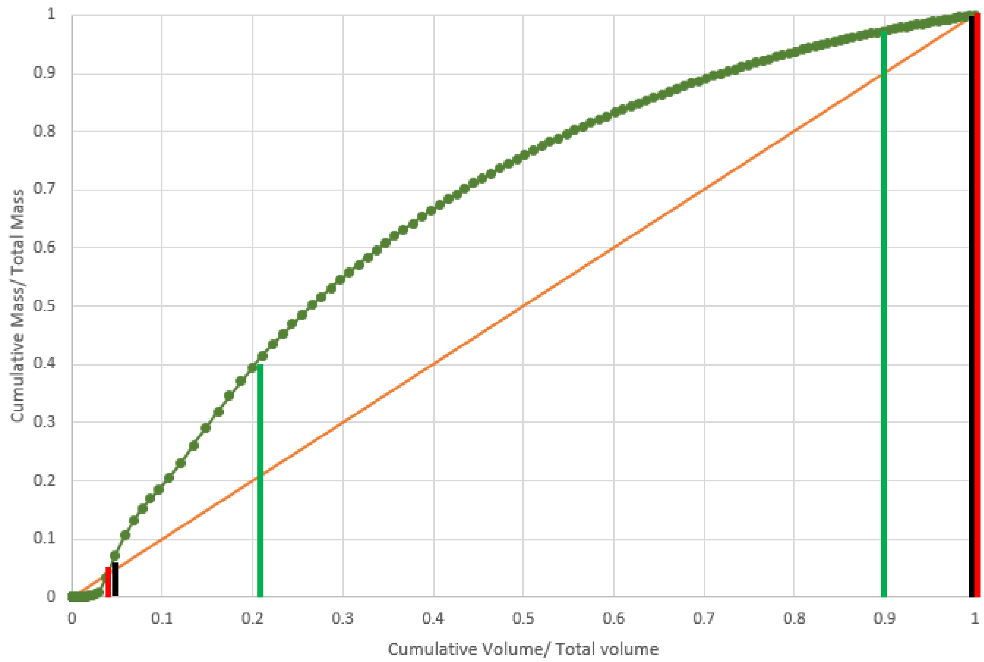

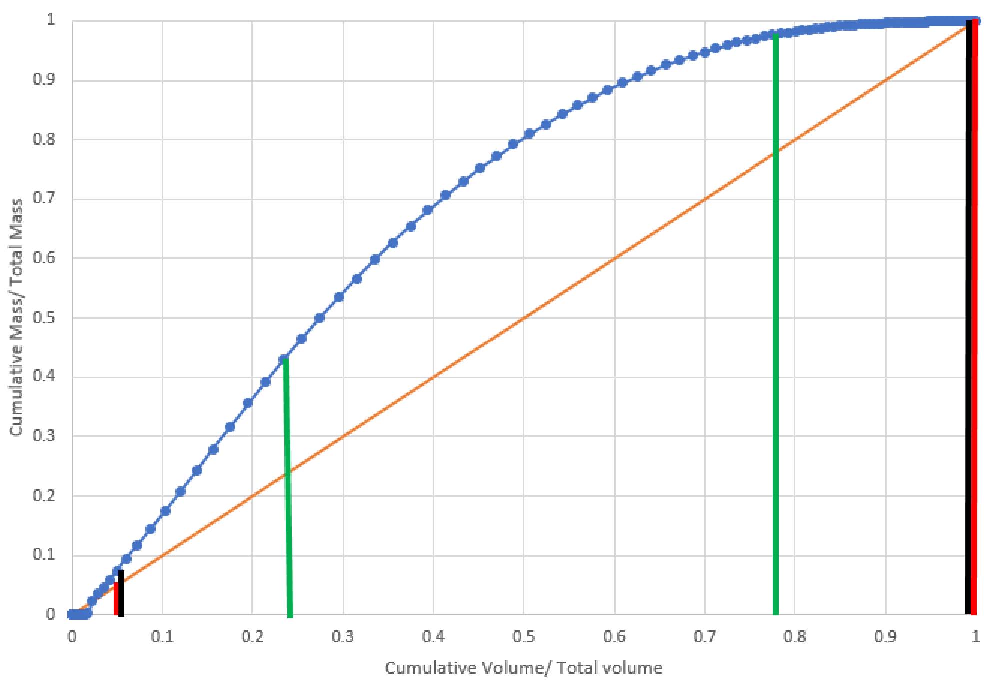

Figure 56. Cumulative volume/pollutant load for TSS at OFmain using kinematic wave routing simulation with exponential buildup/washoff function at k = 0.2 ft/hr for the distributed EDDP design (top) and the one EDDP at OFmain design (bottom). The orange line represents the 45° line. Black vertical lines border the region where FF exists per the third definition (above the 45º no-flush line). Red vertical lines border the region where FF exists per the fourth definition (FF coefficient b < 1). Green vertical lines border the region where FF exists per the fifth definition (Δ > 0.2).

Discussion

In comparing the two structural BMP designs, several factors were considered. The goal was to select an efficient structural BMP design for St. Anthony Park watershed that would reduce TSS and FF while being easy and cheap to implement and maintain. Another goal was to compare the results obtained using different routing methods in PCSWMM in order to gauge the suitability of each to address the question in hand. While the two designs were equally efficient at reducing peak stormwater flows, the distributed EDDP design was superior to the OFmain EDDP design at reducing peak and total TSS loads, suggesting that it would be the better location for implementation. Given the correlation found in Chapter III between TSS and most pollutants in this watershed, it is expected that the distributed EDDP design would also reduce these pollutants in stormwater.

The distributed EDDP design was superior to the EDDP at OFmain design in reducing stormwater peak and total TSS loads. Two possible explanations exist. The first is that the total volume of the seven distributed EDDPs exceeded that of the one EDDP at OFmain, thus allowing the distributed design a larger volume for efficiently reducing and treating stormwater. However, the sum of volumes of the seven distributed EDDPs was 154526 ft^3, which was 4% lower than the volume of 161644 ft^3 of the OFmain EDDP. As such, the other possibility is that the enhanced efficacy is primarily due to location, whereby the seven distributed EDDPs that were located at manholes receiving a lower volume (and possibly lower pollution) of stormwater could more efficiently control both water quality and quantity.

Given that larger particles settle faster and thus require less time for their removal, it was expected that the performance of EDDPs would be significantly better at higher k values than lower ones. However, the results for the two k values when examining TSS loads and TSS peaks were somewhat similar, suggesting that the small differences in particle size distribution had a negligible effect on the final removal outcome.

The distributed EDDP design achieved a TSS peak reduction of 69-75% (for both peaks), surpassing the reported efficiency of 61% for TSS removal but not reaching the target removal of 95%. In addition, the reduction in TSS total loads was only 45%. The discrepancy in the literature in how % removal efficiency is specified complicates the interpretation of these results. Nonetheless, it should be noted that the infiltration process of the vegetated surface of EDDPs was not taken into consideration by PCSWMM. Consequently, the EDDP may in reality have a higher TSS removal efficiency due to multiple TSS removal processes that may enhance its efficacy.

As previously stated, the dynamic and kinematic routing methods produced very similar results. Given that the kinematic wave routing method is ineffective in cases of flow restriction that cause significant backwater or surcharging, this suggested that surcharging was negligible in the watershed, and that either routing method is suitable for modeling purposes.

In the final examined parameter (FF), the distributed EDDP design was superior to the one OFmain EDDP design at reducing the magnitude of the FF phenomenon per the fifth definition. However, this was true for small values of k, and BMP implementation overall failed to completely eliminate FF. EDDPs require extended times to remove pollutants from stormwater via settling. Consequently, their TSS removal activity is not apparent during initial stages of the storm (when FF occurs) but rather after at least 40 hr. As such, the fact that EDDPs failed to completely eliminate FF was not surprising.

A caveat of using a numerical model for natural process examination is that the only way to validate simulated observations is via real data collection during storms post BMP implementation. Nonetheless, the high efficiencies seen with the distributed EDDP design suggest that it would be still successful at reducing stormwater pollution and the magnitude of FF and should be considered for implementation.

CHAPTER VII:

CONCLUSIONS AND RECOMMENDATIONS

This research is concerned with the study of a framework for designing structural best management practices (BMPs) for stormwater management for a large watershed that is based on comprehensive analysis of pollutants of concern, rainfall parameters of influence, and the existence of first flush (FF) (Figure 57). The framework was examined using the PCSWMM computer model in the St Anthony Park watershed, an urban watershed in Minnesota with a large drainage area of 3,418 acres that outlets directly into the Mississippi River via a storm tunnel. A comprehensive study was undertaken to characterize the overall St. Anthony Park watershed stormwater quality trends over time by evaluating the watershed runoff pollutant concentrations, assessing the correlation of the pollutants with rainfall parameters (precipitation depth and previous dry days) and with TSS, and examining the existence of FF. This evaluation was necessary prior to evaluating the effectiveness of stormwater structural BMPs, which in turn would inform management decisions for continued improvement of water resources.

In the first step, the St. Anthony Park watershed stormwater quality trends were characterized over the period of record 2005-2013 by evaluating the watershed runoff pollutant concentrations, including heavy metals (Cd, Cr, Cu, Pb, Ni, and Zn), nutrients (ammonia and total phosphorus (TP)), sediment (TSS), and bacteria (*E. coli*). It was found that stormwater discharges of the St. Anthony Park watershed were highly contaminated since the concentrations of the examined pollutants in stormwaters exceeded surface water quality standards set by the Minnesota Pollution Control Agency (MPCA) and median pollutant concentrations measured in stormwaters of other urbanized areas in the U.S.

In the second step, the correlation between precipitation depth, previous dry days, and stormwater analytes for all stormflow events in the data record was investigated using Spearman's rank correlation method. In addition, the correlation of studied analytes with TSS was similarly examined. It was found that none of the examined water quality parameters were significantly correlated with precipitation depth, while most heavy metals (Cr, Cu, Ni and Zn), TP and TSS were positively correlated with previous dry days. In addition, all pollutants were significantly correlated with TSS in stormwater runoff except for *E.coli*. These results provided a strong rationale for using TSS as a representative pollutant in the subsequent design of the PCSWMM model and the examination of structural BMP efficiency. They also indicated that structural BMPs designed to target the particulate fraction in stormwaters were expected to be the most efficient in reducing stormwater pollution.

In the third step, the PCSWMM model was built, calibrated and validated based on real storm data. Calibration and validation of model performance were carried out via graphical examination of the hydrographs and via calculation of three quantitative statistics (R^2, NSE and ISE). The model was able to achieve the target statistical performance rating of “very good” for calibration (R^2 = 0.995, NSE = 0.856, ISE = 5.25) and a rating of “fair” for validation (R^2 = 0.575, NSE = 0.528, ISE = 18.8), indicating that it acceptably simulated flow at the St Anthony Park watershed. Subsequently, the model was used for numerical examination of the first flush (FF) phenomenon and for structural BMP implementation.

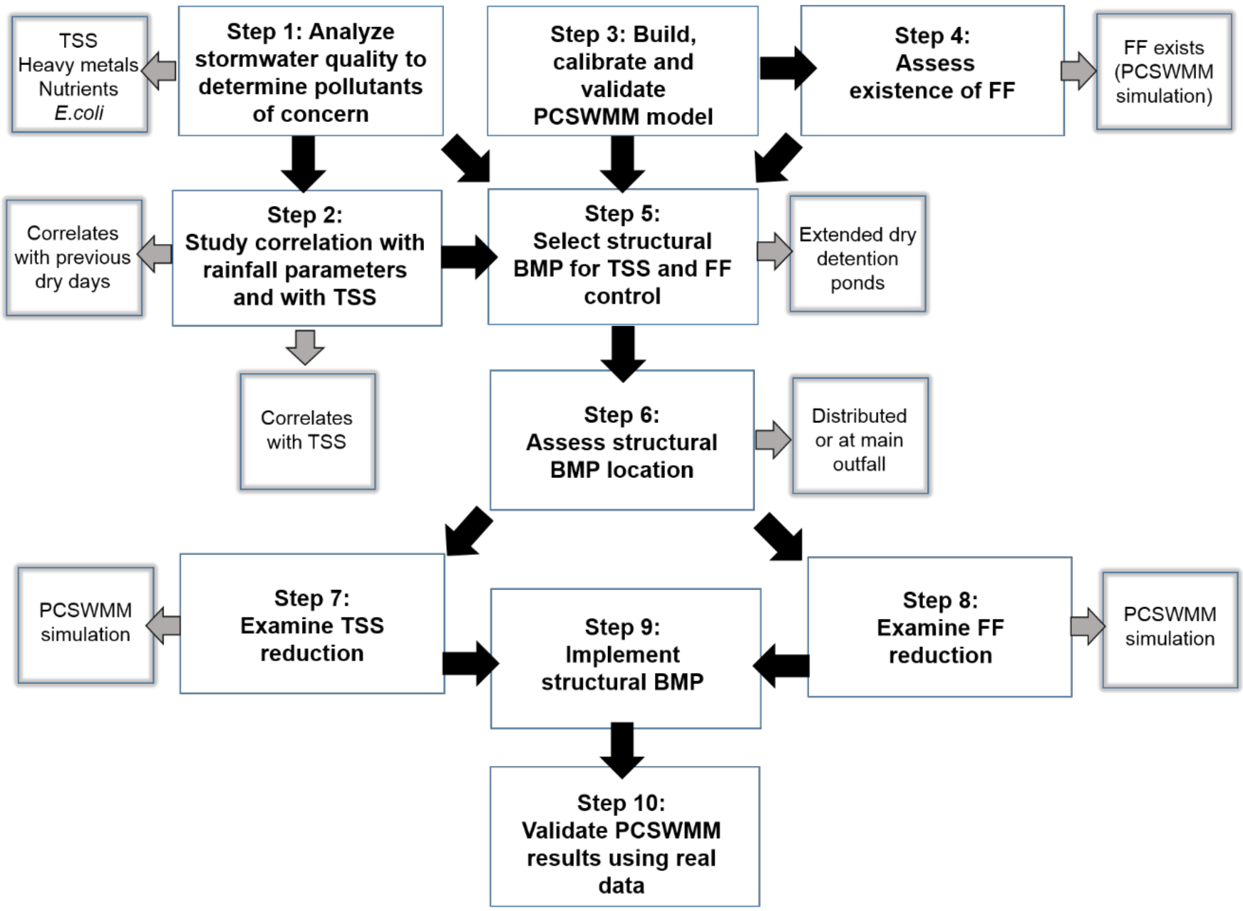

Figure 57. Proposed framework for efficient structural BMP design for large watersheds using PCSWMM model.

In the fourth step, the existence of FF was numerically examined using PCSWMM model with composited water quality samples at several timepoints during storm events. The model was run under three routing methods: dynamic wave, kinematic wave, and steady state. The resultant hydrographs suggested that the steady state routing method was not producing valid, realistic results. Pollutographs suggested that the EMC washoff function was not producing valid, realistic results, and that the exponential build up and washoff functions were better suited for analyzing FF phenomenon due to their sophisticated nature. Using five different definitions of the FF phenomenon, FF could be numerically simulated with the PCSWMM model per three definitions, namely the third definition (above the 45º no-flush line), fourth definition (FF coefficient b < 1), and fifth definition ($\Delta > 0.2$). FF could not be numerically detected using the first definition (80/30) and second definition (80/25). The existence of FF was taken into consideration in subsequent structural BMP studies.

In the fifth step, several structural BMP options were compared based on stormwater treatment suitability, water-quality performance, site applicability, and implementation considerations. Subsequently, extended dry detention ponds (EDDPs) were chosen based on their ability to control both water quantity and quality and on their low construction and maintenance costs. In the sixth step, the PCSWMM model was employed to investigate EDDPs at two different locations, either as seven distributed EDDPs located at manholes, or as one large EDDP located at the main outfall (OFmain). The seventh step was achieved by examining the ability of the two designs to achieve a target of at least 40% stormwater peak flow reduction, at least 30% total TSS load reduction, and at least 60% peak TSS load reduction. It was found that the distributed EDDP design was similar to the one EDDP at OFmain design in reducing stormwater peak flow (52-61%) but superior in reducing total TSS loads (20-25% for small particles and 43-45% for larger particles based on the particle sedimentation rate removal constant k) and in reducing peak TSS loads (67-75%). These efficiencies were obtained using the dynamic and kinematic wave routing methods, indicating that they could be used interchangeably for this watershed. The steady state routing method produced unrealistic results and was subsequently excluded from FF analysis.

In the eighth step, the ability of EDDPs to reduce FF was examined. It was found that the distributed EDDP design was superior to the one OFmain EDDP design, eliminating FF per the stringent fifth definition ($\Delta > 0.2$). This was true for small values of the sedimentation rate removal constant k. However, larger values of k, and other FF tests (above the 45º no-flush line and FF coefficient $b < 1$) showed that BMP implementation overall failed to completely eliminate FF. This suggested that the extended time required by EDDPs to efficiently remove pollutants from stormwater via settling would compromise their ability to completely eliminate FF.

Several recommendations can be made in order to build upon and further improve the conclusions of this research study. First, PCSWMM was able to show FF numerically, but a full validation of this result requires successive sampling during one or more storm events. This is easily achieved given that the watershed already harbors ISCO samplers. Rather than combining the samples collected successively into one composite sample, the samples could be separately examined for their pollutant concentrations, and the resultant field data used for PCSWMM validation for the FF phenomenon. Second, examining the TSS particle size would also be useful, as it would clarify the sedimentation rate removal constant k to be used in BMP design. Moreover, it would help understand how pollutants (such as heavy metals) may correlate with different particle sizes, which has major implications for urban water quality management (Herngren et al. 2005). Third, other pollutants beside TSS could be examined using the built PCSWMM model, which would potentially provide more direct evidence on their removal by the implemented BMP. Fourth, the vegetated surface of EDDPs could potentially enhance the results obtained in this study for TSS and other pollutants given that filtration by vegetation was not included as a pollutant removal mechanism in the model. For example, as seen in Chapter III, *E.coli* levels were in exceedance of water quality standards but did not correlate with TSS. While *E. coli* was not specifically examined with PCSWMM, extended dry detention ponds can reduce 78% of stormwater bacteria, and are thus expected to contribute significantly to reducing *E.coli* contamination in the St. Anthony Park watershed stormwater (Debo and Reese 2002). The vegetated surface may thus contribute to reducing *E.coli* loads in addition to TSS loads. Finally, other BMP options (such as infiltration systems) have been shown to have higher removal efficiencies for TSS as well as other dissolved pollutants (Minnesota Pollution Control Agency 2000). These systems, while attractive in their removal efficiency characteristics, suffer from the drawbacks of being expensive to implement and maintain. Moreover, they were difficult to couple to the study area drainage system given that it consisted of underground drainage pipes connected to deep tunnels. Nonetheless, expanding the study to these systems could better inform legislators and decision makers on the various options available for optimal stormwater management at the St. Anthony Park watershed.

Overall, the implemented framework is expected to significantly help in designing structural BMPs for stormwater management in large watersheds using the PCSWMM model by taking into consideration several influencing factors so as to enhance the efficiency of the implemented BMP design.

APPENDIX:

St. Anthony Park watershed data

Year	Date	PD	PPD	Cd	Cr	Cu	Pb	Ni
2013	9-Apr	0.32	0	0.0002	0.0059	0.0136	0.0112	0.0106
	1-May	0.35	2	0.00031	0.0076	0.0198	0.0114	0.0066
	18-May	0.81	0	0.0002	0.0047	0.012	0.0083	0.0048
	30-May	0.17	0	0.0002	0.0039	0.0106	0.0151	0.004
	21-Jun	1.23	4	0.0002	0.0019	0.0064	0.0046	0.002
	21-Jun	1.59	0	0.00088	0.0082	0.0226	0.0374	0.0091
	29-Aug	0.67	21	0.00054	0.0091	0.0406	0.036	0.0204
	15-Sep	0.15	0	0.0002	0.0015	0.0075	0.0023	0.0028
2012	24-May	2.86	5	0.00012	0.0055	0.0103	0.0082	0.003
	14-Jun	0.76	4	0.00008	0.00089	0.0022	0.0006	0.0029
	18-Jul	1.26	5	0.00028	0.007	0.0157	0.0202	0.0086
	24-Jul	0.2	1	0.00013	0.0018	0.0041	0.0026	0.0023
	15-Aug	0.52	11	0.00034	0.0127	0.0477	0.0211	0.0137
2011	22-Mar	0.81	3	0.0005	0.0153	0.0346	0.0414	0.0118
	26-Apr	1.26	4	0.0004	0.0109	0.0209	0.02	0.0089
	20-May	0.23	8	0.0002	0.0084	0.025	0.0116	0.0098
	21-May	0.36	0	0.0002	0.0057	0.019	0.0082	0.0087
	14-Jun	1.22	4	0.00021	0.0091	0.0145	0.0117	0.0064
	21-Jun	0.7	3	0.00025	0.0056	0.0151	0.0193	0.0071
	10-Jul	0.71	9	0.00041	0.0073	0.0279	0.0291	0.012
	15-Jul	1.51	5	0.00031	0.0091	0.0172	0.0227	0.0078
	19-Jul	1.64	3	0.0002	0.0044	0.0101	0.0137	0.0051
	12-Oct	0.43	3	0.00059	0.0132	0.0431	0.0407	0.0175
	14-Dec	0.39	9	0.0002	0.0036	0.0104	0.0039	0.0156
2010	10-Mar	0.12	1	0.0005	0.0182	0.0439	0.0329	0.0158
	7-May	0.48	11	0.0005	0.009	0.0194	0.0129	0.007
	11-May	0.5	2	0.0005	0.005	0.0079	0.0036	0.0033
	13-May	0.29	1	0.0005	0.005	0.0131	0.0099	0.0054
	13-May	0.38	0	0.0005	0.0137	0.03	0.0348	0.0112
	2-Jun	0.32	8	0.0005	0.0128	0.0421	0.0336	0.0174
	4-Jun	0.49	2	0.0005	0.0068	0.0203	0.0171	0.0071
	5-Jun	0.31	1	0.0005	0.005	0.0123	0.0048	0.0043
	8-Jun	0.48	3	0.0005	0.005	0.0159	0.0135	0.006
	11-Jun	0.8	3	0.0005	0.0085	0.0255	0.0275	0.0097
	25-Jun	2	2	0.0007	0.0181	0.0613	0.0769	0.029
	14-Jul	0.12	3	0.0005	0.0114	0.0328	0.0328	0.0143
	17-Jul	1.5	3	0.0005	0.0094	0.0274	0.0412	0.0185
	27-Jul	0.54	3	0.0005	0.008	0.0214	0.0229	0.0112
	8-Aug	0.62	4	0.0005	0.0074	0.0247	0.0237	0.0137
	10-Aug	0.32	2	0.0005	0.01	0.0258	0.0338	0.0149
	15-Sep	0.48	5	0.0005	0.0075	0.0217	0.0214	0.0121
	22-Sep	0.92	1	0.0005	0.005	0.011	0.0089	0.0044
	24-Oct	0.39	30	0.001	0.01	0.038	0.03	0.02

Year	Date	PD	PPD	Cd	Cr	Cu	Pb	Ni
2009	31-Mar	0.26	7	0.0005	0.0173	0.0392	0.0217	0.0108
	26-Apr	0.58	6	0.0008	0.0215	0.0726	0.063	0.0286
	6-Jun	0.48	7	0.0005	0.0089	0.0284	0.016	0.0104
	7-Jun	0.15	1	0.0005	0.0096	0.0309	0.0273	0.0119
	16-Jun	0.43	8	0.0005	0.0088	0.0259	0.0176	0.0085
	27-Jun	0.32	2	0.0005	0.0082	0.0264	0.023	0.0096
	27-Jun	0.22	0	0.0005	0.0103	0.0304	0.0358	0.0144
	21-Jul	0.57	7	0.0005	0.0107	0.0345	0.0269	0.0116
	22-Jul	0.69	1	0.0005	0.0167	0.0465	0.0536	0.0199
	31-Jul	0.6	9	0.0005	0.0086	0.0244	0.0262	0.02
	7-Aug	0.75	7	0.0005	0.0074	0.0183	0.0157	0.0069
	7-Aug	0.46	0	0.0009	0.00171	0.0592	0.0754	0.0263
	15-Aug	0.79	8	0.0005	0.0091	0.0306	0.0371	0.0132
	19-Aug	0.31	4	0.0009	0.0118	0.0357	0.0509	0.019
	19-Aug	1.18	0	0.0005	0.0095	0.0205	0.0229	0.0069
	20-Aug	0.39	1	0.0005	0.0056	0.0116	0.01	0.0055
	21-Aug	0.22	1	0.0005	0.0005	0.0066	0.0034	0.0034
	25-Aug	0.61	4	0.0005	0.0092	0.027	0.0529	0.0159
	25-Sep	0.33	30	0.0011	0.0131	0.0466	0.0338	0.019
	1-Oct	0.24	3	0.0005	0.0092	0.0213	0.0167	0.0085
	1-Oct	1.38	0	0.0005	0.0005	0.0104	0.0096	0.0041
	5-Oct	1.81	4	0.0005	0.0005	0.0083	0.0057	0.0043
	15-Oct	0.24	1	0.0005	0.0005	0.0093	0.0054	0.0057
	21-Oct	0.55	1	0.0005	0.0101	0.0174	0.0156	0.0066
	23-Oct	0.44	2	0.0005	0.0127	0.0127	0.0136	0.0054
2008	24-Apr	0.29	3	0.0005	0.0113	0.0314	0.0248	0.0104
	11-Jul	0.54	27	0.0005	0.005	0.0481	0.0614	0.023
	11-Jul	0.31	0	0.0005	0.0065	0.0237	0.0223	0.0098
	19-Jul	0.56	2	0.0005	0.0095	0.0305	0.0399	0.0137
	3-Aug	0.32	9	0.0006	0.0085	0.0351	0.0432	0.0133
	12-Aug	0.7	9	0.0008	0.0119	0.0372	0.0548	0.0155
	27-Aug	1.13	15	0.0006	0.0098	0.0374	0.0511	0.0157
	23-Sep	0.58	8	0.0005	0.0103	0.0268	0.0353	0.0112
	5-Oct	0.28	12	0.0005	0.0043	0.0146	0.0106	0.0049
	7-Oct	1.14	2	0.0005	0.0046	0.0138	0.0123	0.0046
	13-Oct	0.49	6	0.0005	0.0048	0.0144	0.0076	0.0043
	7-Nov	0.21	1	0.0005	0.003	0.0067	0.003	0.0054
2007	30-Mar	1.09	2	0.00009	0.0061	0.0139	0.0174	0.0046
	22-Apr	0.48	12	0.0003	0.0123	0.041	0.055	0.0127
	30-Apr	0.32	8	0.0003	0.0156	0.049	0.074	0.0218
	5-May	0.16	5	0.0002	0.0053	0.0168	0.0111	0.0063
	7-May	0.26	2	0.0006	0.016	0.049	0.065	0.0181
	8-May	0.73	1	0.0004	0.0075	0.0223	0.035	0.0119
	22-May	0.74	14	0.0001	0.0024	0.0094	0.0076	0.0064
	29-May	0.27	5	0.0003	0.0064	0.0194	0.0184	0.0077
	2-Jun	0.51	4	0.0001	0.0052	0.0169	0.0131	0.0063
	8-Jul	0.65	20	0.0004	0.0064	0.029	0.028	0.0117
	18-Jul	1.24	10	0.0005	0.0099	0.032	0.036	0.0126

Year	Date	PD	PPD	Cd	Cr	Cu	Pb	Ni
2007	26-Jul	0.07	8	0.0007	0.0108	0.034	0.042	0.0145
	10-Aug	0.63	5	0.0006	0.0062	0.034	0.039	0.0194
	13-Aug	0.82	2	0.0005	0.0052	0.0232	0.03	0.0121
	19-Aug	0.66	1	0.0005	0.0051	0.0138	0.0229	0.0054
	27-Aug	0.85	4	0.0006	0.0097	0.03	0.054	0.013
	28-Aug	1.32	1	0.0005	0.0042	0.0137	0.0218	0.0061
	6-Sep	0.85	9	0.0005	0.0072	0.0164	0.0125	0.0074
	18-Sep	0.93	11	0.0005	0.0054	0.0152	0.0118	0.0047
	18-Sep	0.3	0	0.0005	0.0101	0.033	0.039	0.01
	20-Sep	1.8	2	0.0005	0.0076	0.0208	0.043	0.0109
	24-Sep	0.77	4	0.0005	0.0071	0.0222	0.037	0.0092
	30-Sep	0.17	4	0.0005	0.0037	0.0158	0.0172	0.0059
	30-Sep	0.4	0	0.0005	0.0049	0.018	0.0184	0.0056
	2-Oct	0.57	2	0.0005	0.0047	0.0127	0.0136	0.004
	5-Oct	0.58	3	0.0005	0.0051	0.0184	0.0289	0.0092
	18-Oct	0.56	1	0.0005	0.0041	0.0148	0.0107	0.0041
2006	28-Apr	0.34	7	0.0007	0.0103	0.013725	0.0188	0.0081
	29-Apr	0.33	1	0.0007	0.0061	0.04	0.0105	0.005
	8-May	0.63	7	0.0009	0.0171	0.012802	0.065	0.021
	5-Jun	0.61	11	0.0009	0.0039	0.008136	0.0149	0.0067
	24-Jun	0.65	8	0.00007	0.0034	0.0325	0.0097	0.0049
	16-Jul	0.27	3	0.0004	0.0063	0.034259	0.032	0.0099
	19-Jul	0.6	3	0.0005	0.0108	0.025	0.046	0.0183
	24-Jul	0.8	5	0.0004	0.0091	0.008861	0.038	0.0113
	1-Aug	0.29	7	0.0032	0.0129	0.054	0.0244	0.0123
	1-Aug	0.51	0	0.0002	0.0071	0.0198	0.0211	0.0079
	6-Aug	0.34	4	0.0013	0.0048	0.0195	0.0248	0.0076
	13-Aug	0.57	7	0.0005	0.0094	0.037	0.043	0.0183
	23-Aug	0.51	10	0.0005	0.008	0.038	0.041	0.0171
	24-Aug	1.6	1	0.00004	0.0106	0.03	0.036	0.0136
	3-Sep	0.2	10	0.0002	0.0035	0.0222	0.0112	0.0065
	3-Sep	0.08	0	0.0004	0.0068	0.0204	0.0204	0.0078
	17-Sep	0.22	1	0.0003	0.005	0.022	0.021	0.0081
	22-Sep	0.83	4	0.0002	0.0036	0.0184	0.0084	0.0035
2005	19-Apr	0.27	0	0.0002	0.0047	0.0128	0.0089	0.0041
	13-May	0.3	0	0.00004	0.0018	0.005	0.0028	0.0037
	16-May	0.39	1	0.0002	0.0038	0.0111	0.079	0.0064
	18-May	0.51	0	0.0003	0.0055	0.0142	0.0135	0.0054
	8-Jun	0.7	0	0.0003	0.006	0.0197	0.0192	0.0067
	4-Jun	0.21	5	0.0015	0.0089	0.038	0.034	0.0137
	13-Jun	0.87	1	0.0007	0.0121	0.034	0.049	0.0124
	20-Jun	0.8	4	0.0008	0.0113	0.038	0.052	0.0161
	27-Jun	0.74	11	0.0005	0.0077	0.0198	0.022	0.0076
	27-Jun	1.11	0	0.0084	0.0152	0.0212	0.025	0.0074
	20-Jul	0.62	2	0.0002	0.0042	0.0159	0.0152	0.0066
	23-Jul	0.78	2	0.0004	0.0035	0.0144	0.0146	0.0075
	4-Aug	0.25	9	0.0003	0.0034	0.0121	0.0121	0.007
	8-Aug	0.49	3	0.0003	0.0004	0.0056	0.0019	0.0035

Year	Date	PD	PPD	Cd	Cr	Cu	Pb	Ni
2005	16-Aug	0.28	4	0.0008	0.001	0.0025	0.0071	0.0033
	17-Aug	0.19	10	0.0003	0.0016	0.0044	0.0032	0.004
	26-Aug	2.6	6	0.0008	0.0034	0.003	0.0007	0.0039
	5-Sep	0.59	1	0.0002	0.0013	0.0079	0.0039	0.0026
	3-Sep	0.45	7	0.0002	0.0019	0.0076	0.0054	0.004
	21-Sep	1.85	1	0.0003	0.005	0.0143	0.0159	0.0074
	24-Sep	0.2	1	0.0003	0.0026	0.008	0.0056	0.0033
	4-Oct	0.89	5	0.00009	0.0054	0.0146	0.0164	0.0067
	4-Oct	4.4	0	0.0034	0.0097	0.0194	0.029	0.0076

A1. Stormwater data used in this study for the record period (2005-2013). It includes data for storms, precipitation depth (PD; measured in inches), previous dry days (PPD; measured in days) and concentrations (mg/L) for Cd, Cr, Cu, Pb and Ni.

Year	Date	PD	PPD	Zn	NH_3	TP	TSS
2013	9-Apr	0.32	0	0.0704	0.26	0.16	47
	1-May	0.35	2	0.0861	0.29	0.21	100
	18-May	0.81	0	0.0593	0.35	0.2	88
	30-May	0.17	0	0.0645	0.16	0.23	196
	21-Jun	1.23	4	0.0335	0.15	0.15	32
	21-Jun	1.59	0	0.126	0.08	0.39	320
	29-Aug	0.67	21	0.217	0.02	0.52	1250
	15-Sep	0.15	0	0.0376	0.03	0.15	15
2012	24-May	2.86	5	0.0491	0.32	0.14	56.6
	14-Jun	0.76	4	0.0088	0.13	0.13	22.2
	18-Jul	1.26	5	0.0984	0.55	0.24	127
	24-Jul	0.2	1	0.0194	0.12	0.16	20.1
	15-Aug	0.52	11	0.205	0.47	0.32	149
2011	22-Mar	0.81	3	0.215	0.24	0.425	1330
	26-Apr	1.26	4	0.131	0.11	0.254	191
	20-May	0.23	8	0.102	0.38	0.276	130
	21-May	0.36	0	0.08	0.22	0.236	119
	14-Jun	1.22	4	0.0967	0.06	0.261	135
	21-Jun	0.7	3	0.109	0.17	0.243	150
	10-Jul	0.71	9	0.163	0.2	0.343	84
	15-Jul	1.51	5	0.107	0.09	0.213	356
	19-Jul	1.64	3	0.0506	0.35	0.234	40
	12-Oct	0.43	3	0.248	0.02	0.447	282
	14-Dec	0.39	9	0.0481	0.17	0.112	81
2010	10-Mar	0.12	1	0.257	0.48	0.527	26
	7-May	0.48	11	0.0909	0.04	0.207	94
	11-May	0.5	2	0.0383	0.25	0.087	301
	13-May	0.29	1	0.0709	0.08	0.187	376
	13-May	0.38	0	0.168	0.05	0.404	196
	2-Jun	0.32	8	0.196	0.27	0.512	41
	4-Jun	0.49	2	0.108	0.22	0.316	68
	5-Jun	0.31	1	0.0531	0.14	0.131	250
	8-Jun	0.48	3	0.0804	0.04	0.16	928
	11-Jun	0.8	3	0.141	0.22	0.268	300
	25-Jun	2	2	0.278	0.28	0.704	331
	14-Jul	0.12	3	0.218	0.51	0.3	196
	17-Jul	1.5	3	0.17	0.14	0.272	223
	27-Jul	0.54	3	0.126	0.05	0.238	333
	8-Aug	0.62	4	0.138	0.37	0.283	190
	10-Aug	0.32	2	0.142	0.04	0.212	56

Year	Date	PD	PPD	Zn	NH_3	TP	TSS
2010	15-Sep	0.48	5	0.179	0.04	0.3	338
	22-Sep	0.92	1	0.0869	0.02	0.181	110
	24-Oct	0.39	30	0.279	0.05	0.846	556
2009	31-Mar	0.26	7	0.169	0.46	0.185	206
	26-Apr	0.58	6	0.372	0.22	0.722	253
	6-Jun	0.48	7	0.114	0.02	0.491	148
	7-Jun	0.15	1	0.143	0.03	0.401	220
	16-Jun	0.43	8	0.111	0.14	0.304	291
	27-Jun	0.32	2	0.133	0.19	0.346	194
	27-Jun	0.22	0	0.157	0.25	0.388	509
	21-Jul	0.57	7	0.158	0.02	0.307	231
	22-Jul	0.69	1	0.254	0.02	0.553	78
	31-Jul	0.6	9	0.134	3.89	0.368	32
	7-Aug	0.75	7	0.0964	0.06	0.15	271
	7-Aug	0.46	0	0.271	0.05	0.554	543
	15-Aug	0.79	8	0.146	0.11	0.281	148
	19-Aug	0.31	4	0.198	0.06	0.377	75
	19-Aug	1.18	0	0.0944	0.02	0.225	18
	20-Aug	0.39	1	0.0557	0.02	0.16	526
	21-Aug	0.22	1	0.0235	0.02	0.087	364
	25-Aug	0.61	4	0.165	0.13	0.289	113
	25-Sep	0.33	30	0.31	0.03	0.787	50
	1-Oct	0.24	3	0.137	0.02	0.244	25
	1-Oct	1.38	0	0.0398	0.02	0.083	37
	5-Oct	1.81	4	0.0807	0.02	0.067	86
	15-Oct	0.24	1	0.0712	0.02	0.113	62
	21-Oct	0.55	1	0.127	0.02	0.199	186
	23-Oct	0.44	2	0.0856	0.02	0.147	682
2008	24-Apr	0.29	3	0.148	0.35	0.455	148
	11-Jul	0.54	27	0.265	0.13	0.64	464
	11-Jul	0.31	0	0.123	0.22	0.256	269
	19-Jul	0.56	2	0.164	0.1	0.467	446
	3-Aug	0.32	9	0.191	0.25	0.384	304
	12-Aug	0.7	9	0.195	0.04	0.535	238
	27-Aug	1.13	15	0.194	0.15	0.387	100
	23-Sep	0.58	8	0.147	0.11	0.287	75
	5-Oct	0.28	12	0.0771	0.02	0.282	42
	7-Oct	1.14	2	0.0711	0.02	0.14	15
	13-Oct	0.49	6	0.0557	0.02	0.13	90
	7-Nov	0.21	1	0.0262	0.02	0.102	255

Year	Date	PD	PPD	Zn	NH_3	TP	TSS
2007	30-Mar	1.09	2	0.057	0.17	0.194	644
	22-Apr	0.48	12	0.178	0.55	0.386	158
	30-Apr	0.32	8	0.228	0.86	0.508	490
	5-May	0.16	5	0.071	0.08	0.258	440
	7-May	0.26	2	0.229	0.13	0.656	57
	8-May	0.73	1	0.098	0.47	0.323	138
	22-May	0.74	14	0.038	0.02	0.102	94
	29-May	0.27	5	0.096	0.02	0.179	168
	2-Jun	0.51	4	0.065	0.09	0.13	270
	8-Jul	0.65	20	0.132	0.03	0.2	243
	18-Jul	1.24	10	0.153	0.04	0.348	249
	26-Jul	0.07	8	0.166	0.14	0.845	208
	10-Aug	0.63	5	0.196	0.13	0.306	90
	13-Aug	0.82	2	0.107	0.03	0.212	336
	19-Aug	0.66	1	0.069	0.02	0.135	240
	27-Aug	0.85	4	0.159	0.02	0.335	81
	28-Aug	1.32	1	0.059	0.24	0.235	74
	6-Sep	0.85	9	0.069	0.02	0.164	298
	18-Sep	0.93	11	0.065	0.02	0.15	297
	18-Sep	0.3	0	0.142	0.02	0.245	217
	20-Sep	1.8	2	0.105	0.34	0.397	96
	24-Sep	0.77	4	0.108	0.02	0.269	71
	30-Sep	0.17	4	0.085	0.03	0.16	66
	30-Sep	0.4	0	0.072	0.02	0.128	173
	2-Oct	0.57	2	0.058	0.03	0.136	62
	5-Oct	0.58	3	0.1	0.04	0.238	104
	18-Oct	0.56	1	0.047	0.02	0.232	131
2006	28-Apr	0.34	7	0.151	0.4	0.353	428
	29-Apr	0.33	1	0.099	0.38	0.2	152
	8-May	0.63	7	0.269	0.53	0.764	72
	5-Jun	0.61	11	0.077	0.02	0.284	184
	24-Jun	0.65	8	0.039	0.02	0.104	264
	16-Jul	0.27	3	0.188	0.34	0.327	190
	19-Jul	0.6	3	0.155	0.37	0.393	220
	24-Jul	0.8	5	0.128	0.1	0.321	114
	1-Aug	0.29	7	0.44	0.02	0.545	100
	1-Aug	0.51	0	0.086	0.02	0.197	292
	6-Aug	0.34	4	0.117	0.31	0.216	267
	13-Aug	0.57	7	0.183	0.03	0.416	194
	23-Aug	0.51	10	0.195	0.03	0.407	78

Year	Date	PD	PPD	Zn	NH_3	TP	TSS
2006	24-Aug	1.6	1	0.161	0.21	0.362	120
	3-Sep	0.2	10	0.089	0.08	0.244	123
	3-Sep	0.08	0	0.107	0.02	0.197	41
	17-Sep	0.22	1	0.103	0.02	0.266	44
	22-Sep	0.83	4	0.084	0.06	0.105	13
2005	19-Apr	0.27	0	0.0045	0.27	0.164	58
	13-May	0.3	0	0.0204	0.14	0.104	64
	16-May	0.39	1	0.052	0.12	0.18	162
	18-May	0.51	0	0.067	0.19	0.146	510
	8-Jun	0.7	0	0.085	0.02	0.226	412
	4-Jun	0.21	5	0.163	0.02	0.859	300
	13-Jun	0.87	1	0.167	0.04	0.519	156
	20-Jun	0.8	4	0.16	0.1	0.52	140
	27-Jun	0.74	11	0.091	0.13	0.279	145
	27-Jun	1.11	0	0.403	0.43	0.258	92
	20-Jul	0.62	2	0.073	0.02	0.247	98
	23-Jul	0.78	2	0.052	0.05	0.158	12
	4-Aug	0.25	9	0.067	0.02	0.154	21
	8-Aug	0.49	3	0.017	0.02	0.042	49
	16-Aug	0.28	4	0.0127	0.02	0.027	7
	17-Aug	0.19	10	0.0183	0.02	0.063	62
	26-Aug	2.6	6	0.207	0.03	0.059	89
	5-Sep	0.59	1	0.023	0.04	0.09	110
	3-Sep	0.45	7	0.032	0.06	0.114	35
	21-Sep	1.85	1	0.057	0.2	0.207	142
	24-Sep	0.2	1	0.034	0.02	0.133	244
	4-Oct	0.89	5	0.068	0.02	0.227	47
	4-Oct	4.4	0	0.298	0.03	0.298	100

A2. Stormwater data used in this study for the record period (2005-2013). It includes date for concentrations (mg/L) for Zn, NH_3, TP and TSS. Storms shown are the same as those in A1 and therefore have the same PD and PPD.

Year	Date	PD	PDD	*E.coli*
2013	1-May	0.35	2	6300
	9-Jul	0.78	1	26500
	18-Sep	0.13	0	125900
2012	24-May	2.86	5	3000
	14-Jun	0.76	4	411
	24-Jul	0.2	1	2203
	15-Aug	0.52	11	33100
	25-Oct	0.79	0	27200
2011	22-Mar	0.81	3	687
	26-Apr	1.26	4	614
	9-May	0.35	0	1468
	15-Jun	0.64	0	5200
	14-Dec	0.39	9	1203
2010	10-Mar	0.12	1	1733
	7-May	0.48	11	11900
	11-May	0.5	2	3100
	8-Jun	0.48	3	10900
	14-Jun	0.25	1	14600
	10-Aug	0.32	2	22800
	23-Sep	1.42	0	10900
2009	31-Mar	0.26	7	1308
	21-Jul	0.57	7	12100
	7-Aug	0.75	7	18300
	19-Aug	0.31	4	24600
	20-Aug	0.39	1	6200
	1-Oct	0.24	3	18500
	6-Oct	1.47	0	4100
2008	24-Apr	0.29	3	866
	31-Jul	0.07	5	2420
	12-Aug	0.7	9	411
	11-Sep	0.17	0	13900
	7-Oct	1.14	2	35000
	13-Oct	0.49	6	10900
2007	24-May	0.58	0	2420
	5-Oct	0.58	3	2420
2006	22-Sep	0.83	4	2420

A3. Stormwater data used in this study for the record period (2005-2013). It includes data for storms, precipitation depth (PD; measured in inches), previous dry days (PPD; measured in days) and concentrations (MPN/100 mL) for *E.coli*.

MPCA metal standards

Parameter	05*	06	07	08	09	10	11	12	13
Hardness (storm)	--	97	84	92	91	75	112	86	64
Cd	0.0011		0.0009	0.0010	0.0011	0.0009	0.0012	0.001	0.0008
Cr	0.2018		0.1794	0.1933	0.1916	0.1631	0.2271	0.1822	0.1436
Cu	0.0096		0.0088	0.0093	0.0093	0.0082	0.0105	0.0089	0.0075
Pb	0.0031		0.0025	0.0029	0.0028	0.0022	0.0037	0.0026	0.0018
Ni	0.1537		0.1360	0.1469	0.1456	0.1232	0.1735	0.1382	0.1081
Zn	0.1033		0.0914	0.0988	0.0979	0.0828	0.1167	0.0929	0.0726

* Hardness was not provided. Data for 2006 were used to set standard levels for 2005.

A4. MPCA standard levels for heavy metals for each year of the record period 2005-2013. Average stormwater hardness concentrations for each year were used in the calculations.

Topographic map for the delineation of subcatchments in

PCSWMM model

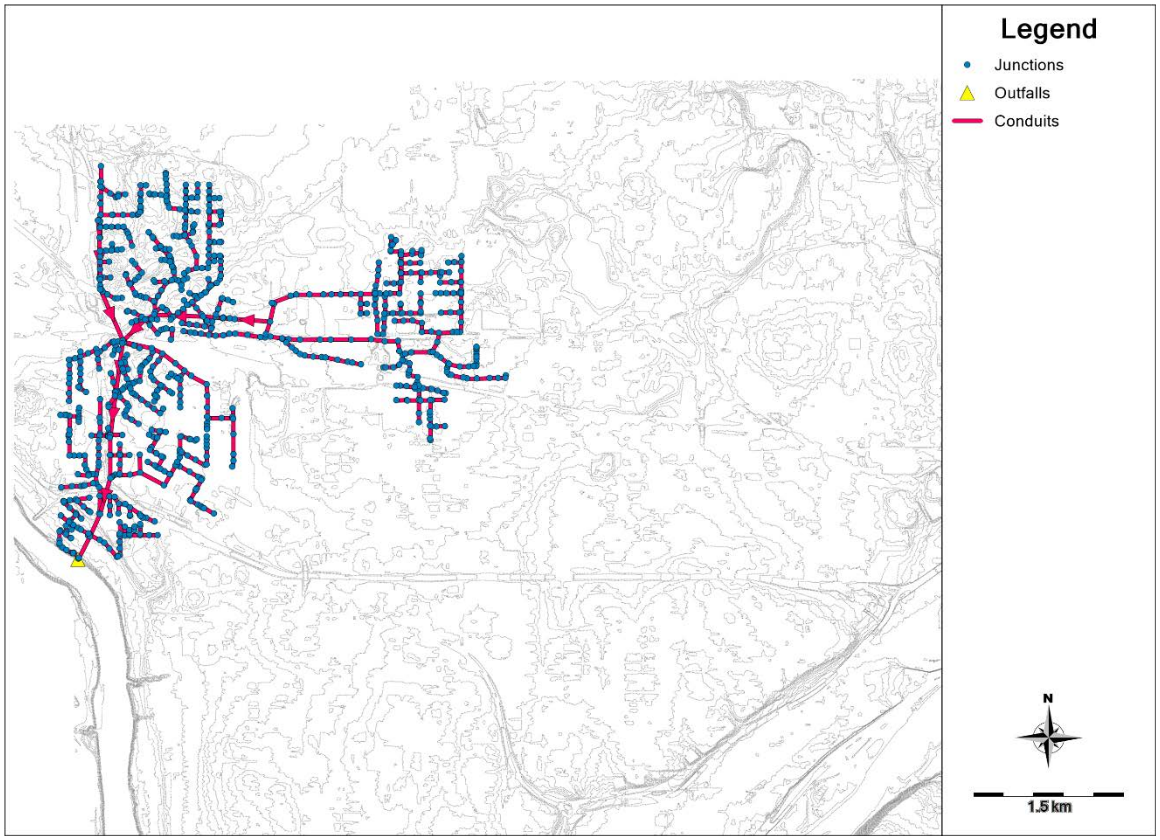

A5. St Anthony Park watershed stormwater topographic map. Grey lines represent 10-feet contour lines. The network is the same as in Figure 15, where blue circles represent junctions (manholes), yellow triangles represent outfalls while red lines represent conduits.

Subcatchment parameters used in PCSWMM model

SUBWS	Curve Number	Total Area (ac)	COMMERCIAL	HIGH WAY_AC	HIGH_ DENSITY	INSTITUTION
COMO7	75.69	298.2	2.39	76.48	1.75	12.47
SAP18	73.26	579.22	0.9	6.91	242.36	254.46
SAP24	74.34	19.73	0	4.97	2.81	5.67
SAP25	74.78	5.92	0	1.65	0.03	0.02
SAP23	75.21	6.3	0	1.26	0.36	2.3
COMO3	74.91	515.83	33.93	101.3	20.08	2.92
SAP1	76.69	84.64	0.38	29.07	12.14	3.87
SAP26	75.6	2.05	0	0.59	0	0
SAP5	75.14	40.91	1.78	10.1	21.89	0.04
SAP2	78.26	1.83	0	0.63	0	0
SAP13	82.85	8.48	2.26	2.55	0.02	0
SAP7	82.15	19.22	1.96	2.11	0.13	0
SAP10	69.16	6.59	0.08	0.75	0	0
SAP16	76.15	83.22	22.58	21.92	0.34	0.68
SAP15	71.74	6.47	0	2.82	0	0
SAP3	75.18	37.67	0	10.62	1.78	0.7
SAP9	72.26	3.63	0.07	1.21	2.35	0
SAP14	72.97	150.54	0.15	74.05	2.98	0
SAP11	77.42	86.18	0.16	26.74	0	0
SAP12	82.54	17	1.68	5.11	0	0
MRB16	82.56	35.68	0	13.51	0.95	0
SAP17	75.89	193.08	18.13	47.86	1.71	0.21
SAP29	76.25	383.13	60.38	90.29	6.43	44.26
SAP28	74.53	63.18	10.97	1.73	0	0
SAP4	76.26	826.06	31.28	189.24	39.25	45.17
SAP27	76.85	264.57	44.8	66.5	46.03	0.04
SAP30	75.24	20.74	0	5.38	5.47	3.32
SAP34	80.53	81.98	1.07	8.93	0	0

A6. Subcatchment parameters (curve number, total area, commercial, highway_AC, high_density and institution) used in the PCSWMM model.

SUBWS	INDUSTRIAL	LOW_DENSIT	PARK_OPEN_	WATER_AC	UNDEVELOPE
COMO7	0.77	151.46	49.65	0	3.22
SAP18	0.01	12.51	0	0	62.09
SAP24	0	6.11	0	0	0.18
SAP25	0	3.68	0	0	0.54
SAP23	0	2.35	0	0	0.03
COMO3	16.45	97.58	221.69	0.67	21.88
SAP1	0	38	0	0	1.18
SAP26	0	1.46	0	0	0
SAP5	3.77	0.94	0	0	2.39
SAP2	0	1.2	0	0	0
SAP13	2.4	0.16	0	0	1.11
SAP7	14.03	0.03	0	0	0.97
SAP10	5.77	0	0	0	0
SAP16	30.28	4.05	0	0	3.36
SAP15	0	0.39	3.27	0	0
SAP3	0	22.04	0	0	2.52
SAP9	0	0	0	0	0
SAP14	32.38	26.05	3.59	0	11.33
SAP11	0	39.84	14.19	0.1	5.25
SAP12	0	7.71	0	0	2.5
MRB16	0	16.34	2.32	0.27	2.56
SAP17	102.35	0	0.03	0	22.79
SAP29	35.13	103.14	0	0	43.51
SAP28	17.98	0	0	0	32.5
SAP4	190.82	222.45	20.38	0	87.47
SAP27	50.75	28.84	6.76	0	20.85
SAP30	0	6.54	0	0	0.04
SAP34	70.07	0	0	0	1.91

A7. Subcatchment parameters (industrial, low-density, park_open, water-AC, and undeveloped) used in the PCSWMM model.

Drainage system parameters used in PCSWMM model

Name	Inlet Node	Outlet Node	Length (ft)	Inlet Offset (ft)	Outlet Offset (ft)	Cross-Section	Geom1 (ft)	Geom2 (ft)	Barrels	Slope (ft/ft)
C1	223396	223378	179.25	0	0	CIRCULAR	1	0	1	0.04904
C10	187574	187576	100	0	0	CIRCULAR	2.25	0	1	0.0143
C100	223502	241898	25.8	0	0	CIRCULAR	2	0	1	0.04812
C101	241918	223502	27.01	0	0	CIRCULAR	2	0	1	0.01185
C102	241898	270740	374.11	0	0	CIRCULAR	2	0	1	0.03708
C103	223488	223490	56	0	1.8	CIRCULAR	1.25	0	1	0.02483
C104	223490	223492	276.02	0	0.25	CIRCULAR	1.25	0	1	0.02453
C105	223492	241916	59.94	0	0	CIRCULAR	1.25	0	1	0.00834
C106	241916	223464	314.59	0	1.03	CIRCULAR	1.25	0	1	0.04136
C107	270740	223472	16.91	0	0	CIRCULAR	2	0	1	0.03663
C108	223472	223464	20.74	0	0	CIRCULAR	3	0	1	0.00386
C109	223464	223482	24.11	0	0	CIRCULAR	3	0	1	0.00581
C11	187576	187556	31	0	0	CIRCULAR	2.5	0	1	0.02259
C110	223482	223480	208.23	0	0	CIRCULAR	3	0	1	0.006
C111	223480	241912	339.52	0	0.5	CIRCULAR	3	0	1	0.00592
C112	270204	215044	178.62	0	0	CIRCULAR	3.5	0	1	0.01792
C113	223486	270738	56	0	0	CIRCULAR	1.25	0	1	0.01
C114	270738	1490282	173.42	0	0	CIRCULAR	1.25	0	1	0.01003
C115	215022	215004	182.6	0	0	CIRCULAR	4	0	1	0.02301
C116	1490282	223498	129.52	0	0	CIRCULAR	1.25	0	1	0.03036
C117	223498	241912	37.07	0	0.13	CIRCULAR	1.25	0	1	0.01052
C118	241912	215024	221.51	0	0	CIRCULAR	3.5	0	1	0.00501
C119	215024	215668	216.54	0	0	CIRCULAR	3.5	0	1	0.0049
C12	187556	187558	149	0	0	CIRCULAR	2.5	0	1	0.00584
C120	215668	270204	238.3	0	0	CIRCULAR	3.5	0	1	0.00504
C121	215004	215090	116.95	0	0	CIRCULAR	4	0	1	0.06392
C122	215018	215070	197.74	0	0	CIRCULAR	4.5	0	1	0.01599
C123	215044	215054	189.19	0	0	CIRCULAR	3.5	0	1	0.00603
C124	215054	215012	183.48	0	18.53	CIRCULAR	3.5	0	1	0.0054
C125	215012	215048	271.87	0	0	CIRCULAR	5	0	1	0.00592

Name	Inlet Node	Outlet Node	Length (ft)	Inlet Offset (ft)	Outlet Offset (ft)	Cross-Section	Geom1 (ft)	Geom2 (ft)	Barrels	Slope (ft/ft)
C126	215048	215022	184.77	0	0	CIRCULAR	4	0	1	0.02073
C127	215070	215020	223.48	0	0	CIRCULAR	6	0	1	0.00787
C128	L13	L12	1611.22	0	0	CIRCULAR	13	0	1	0.00151
C129	214794	214832	173.01	0	0	CIRCULAR	1.25	0	1	0.04258
C13	187558	187560	146	0	0	CIRCULAR	2.5	0	1	0.00945
C130	214832	217906	38.89	0	0.31	CIRCULAR	1.25	0	1	0.0144
C131	217908	217880	147.37	0	0	CIRCULAR	1.25	0	1	0.03905
C132	270036	243320	256.23	0	0	CIRCULAR	4.5	0	1	0.00265
C133	215090	215018	193.25	0	0	CIRCULAR	4.5	0	1	0.01035
C134	215056	215088	150.38	0	0	CIRCULAR	1.25	0	1	0.00771
C135	215088	215018	197.8	0	0	CIRCULAR	1.25	0	1	0.01365
C136	223401	224588	501.41	0	0	CIRCULAR	2	0	1	0.03103
C137	243616	243618	235.01	0	0	CIRCULAR	3	0	1	0.0074
C138	243618	242878	124.01	0	0	CIRCULAR	1	0	1	0.00758
C139	242878	220782	285.7	0	12.76	CIRCULAR	3	0	1	0.00784
C14	187560	215376	223	0	0	CIRCULAR	3	0	1	0.00404
C140	220782	1522347	313.56	0	1	CIRCULAR	4.5	0	1	0.01113
C141	242766	268362	601.75	0	0	CIRCULAR	1.25	0	1	0.034
C142	242978	227240	253	0	0	CIRCULAR	1.25	0	1	0.0509
C143	227196	227240	63.64	0	0	CIRCULAR	2.25	0	1	0.02169
C144	240698	193402	31.65	0	0	CIRCULAR	3	0	1	0.02307
C145	240676	240662	458.02	0	0	CIRCULAR	1.5	0	1	0.0129
C146	240670	240668	58.02	0	0	CIRCULAR	1	0	1	0.00569
C147	240668	240666	218.01	0	0	CIRCULAR	1.25	0	1	0.01697
C148	240666	240664	280.17	0	0	CIRCULAR	1.25	0	1	0.02399
C149	240664	240662	70.01	0	0	CIRCULAR	1.5	0	1	0.024
C15	220400	240338	185.98	0	0	CIRCULAR	1.25	0	1	0.00721
C150	240662	240678	198.03	0	0	CIRCULAR	1.5	0	1	0.03481
C151	240678	243666	200.09	0	0	CIRCULAR	1.5	0	1	0.04904
C152	233548	243666	22.13	0	0	CIRCULAR	2.75	0	1	0.01672
C153	243666	240694	42.13	0	0	CIRCULAR	2.75	0	1	0.01638
C154	240694	243674	249.22	0	0	CIRCULAR	3	0	1	0.0069
C155	243674	240698	249.57	0	0	CIRCULAR	3	0	1	0.00793

Name	Inlet Node	Outlet Node	Length (ft)	Inlet Offset (ft)	Outlet Offset (ft)	Cross-Section	Geom1 (ft)	Geom2 (ft)	Barrels	Slope (ft/ft)
C156	1521418	1521413	219	0	0	CIRCULAR	1.75	0	1	0.00607
C157	1521413	193402	13.01	0	0	CIRCULAR	1.75	0	1	0.06857
C158	193402	248004	30.53	0	0	CIRCULAR	3	0	1	0.02031
C159	248004	240686	257.81	0	0	CIRCULAR	3	0	1	0.01462
C16	240338	243688	106.64	0	0	CIRCULAR	1.25	0	1	0.01895
C160	240686	240690	53.42	0	0	CIRCULAR	1	0	1	0.02153
C161	240690	240692	139.19	0	0	CIRCULAR	3.5	0	1	0.00754
C162	240692	233542	177.62	0	0	CIRCULAR	3.5	0	1	0.00394
C163	233542	238214	122.13	0	0	CIRCULAR	3.5	0	1	0.01302
C164	243690	243672	121.12	0	0	CIRCULAR	1.25	0	1	0.00388
C165	243672	243670	167.6	0	0	CIRCULAR	1.25	0	1	0.0043
C166	243670	243668	120.99	0	0	CIRCULAR	1.75	0	1	0.00802
C167	243668	240652	47.99	0	0	CIRCULAR	1.75	0	1	0.0319
C168	243694	243692	63.02	0	0	CIRCULAR	1.25	0	1	0.00841
C169	243692	273768	256.97	0	0	CIRCULAR	1.5	0	1	0.00623
C17	240336	243688	342.51	0	0	CIRCULAR	1.5	0	1	0.00491
C170	273768	240654	51	0	0	CIRCULAR	1.5	0	1	0.01824
C171	240660	219720	288.98	0	0	CIRCULAR	1.25	0	1	0.02312
C172	243680	243678	355.71	0	0	CIRCULAR	1.5	0	1	0.00405
C173	243678	240354	70.27	0	0	CIRCULAR	1.5	0	1	0.0732
C174	240658	240656	290.03	0	0	CIRCULAR	1.25	0	1	0.00517
C175	240656	240654	287.99	0	0	CIRCULAR	1.25	0	1	0.01066
C176	240654	240652	348	0	0	CIRCULAR	1.75	0	1	0.01923
C177	240652	219720	157.03	0	0	CIRCULAR	2.5	0	1	0.00904
C178	219720	240354	163	0	0	CIRCULAR	2.5	0	1	0.00724
C179	240354	267390	209.36	0	0	CIRCULAR	2.5	0	1	0.01696
C18	243688	240340	158.92	0	0	CIRCULAR	1.5	0	1	0.02064
C180	267390	187570	215.85	0	0	CIRCULAR	2.5	0	1	0.04392
C181	187570	187568	230.09	0	0	CIRCULAR	2.5	0	1	0.05891
C182	187568	267392	65.78	0	0	CIRCULAR	2.5	0	1	0.02555
C183	267392	187594	42.54	0	0	CIRCULAR	2.5	0	1	0.13424
C184	187594	187584	358.21	0	0	CIRCULAR	2.75	0	1	0.00771
C185	187584	267394	259.86	0	0	CIRCULAR	3	0	1	0.00596

Name	Inlet Node	Outlet Node	Length (ft)	Inlet Offset (ft)	Outlet Offset (ft)	Cross-Section	Geom1 (ft)	Geom2 (ft)	Barrels	Slope (ft/ft)
C186	267394	187586	186.83	0	0	CIRCULAR	3	0	1	0.00578
C187	217880	217906	191.06	0	0.25	CIRCULAR	1.25	0	1	0.03142
C188	268356	242990	104.99	0	0	CIRCULAR	1.5	0	1	0.01781
C189	242990	242974	163	0	0	CIRCULAR	1.5	0	1	0.01055
C19	240340	240342	230.02	0	0	CIRCULAR	1.5	0	1	0.03319
C190	242988	242986	60	0	0	CIRCULAR	1.5	0	1	0.00317
C191	242986	242984	62	0	0	CIRCULAR	1.5	0	1	0.00194
C192	242984	242974	66.99	0	0	CIRCULAR	1.5	0	1	0.00642
C193	242974	220812	313.99	0	0	CIRCULAR	2.25	0	1	0.02144
C194	242650	242648	139.99	0	0	CIRCULAR	1.25	0	1	0.00679
C195	242648	242646	61.02	0	0	CIRCULAR	2	0	1	0.00688
C196	242646	220812	99.99	0	0	CIRCULAR	2.25	0	1	0.03002
C197	220812	220314	454.01	0	0	CIRCULAR	3.5	0	1	0.00322
C198	220314	220312	148	0	0	CIRCULAR	3.5	0	1	0.00203
C199	220312	220310	35.01	0	0	CIRCULAR	3.5	0	1	0.00486
C2	231884	230956	106.27	0	0	CIRCULAR	3	0	1	0.00649
C20	240342	240344	60.68	0	0	CIRCULAR	1.5	0	1	0.05513
C200	220310	220308	50.02	0	0	CIRCULAR	3.5	0	1	0.0054
C201	220308	220814	186.98	0	0	CIRCULAR	3.5	0	1	0.00599
C202	220814	220788	448.52	0	0	CIRCULAR	3.5	0	1	0.00484
C203	220788	220786	153.25	0	0	CIRCULAR	3.5	0	1	0.00607
C204	220786	220784	180	0	0	CIRCULAR	3.5	0	1	0.00911
C205	220784	273180	172.03	0	0	CIRCULAR	3.5	0	1	0.00657
C206	273180	242438	304.99	0	0	CIRCULAR	3.5	0	1	0.00626
C207	242438	242436	164.02	0	0	CIRCULAR	3.5	0	1	0.00847
C208	242436	220302	187	0	0	CIRCULAR	3.5	0	1	0.00797
C209	220302	220808	83.01	0	0	CIRCULAR	3.5	0	1	0.01108
C21	223378	225032	262.56	0	0	CIRCULAR	1.25	0	1	0.01566
C210	220808	220782	109.99	0	17.56	CIRCULAR	3.5	0	1	0.01837
C211	243614	243612	347.99	0	0	CIRCULAR	1.5	0	1	0.00661
C212	243612	243610	42.01	0	0	CIRCULAR	1.5	0	1	0.01262
C213	243610	220302	44.01	0	0	CIRCULAR	2.25	0	1	0.04731
C214	232186	232182	359.2	0	0	CIRCULAR	4	0	1	0.00345

Name	Inlet Node	Outlet Node	Length (ft)	Inlet Offset (ft)	Outlet Offset (ft)	Cross-Section	Geom1 (ft)	Geom2 (ft)	Barrels	Slope (ft/ft)
C215	218552	217886	330.37	0	0	CIRCULAR	1	0	1	0.09836
C216	217886	214808	35.5	0	0	CIRCULAR	1.25	0	1	0.05388
C217	217872	217902	273.81	0	0	CIRCULAR	1.25	0	1	0.04094
C218	217902	268050	141.78	0	0	CIRCULAR	1.5	0	1	0.05333
C219	268050	217900	67.95	0	0	CIRCULAR	1.5	0	1	0.05601
C22	225032	224584	46.5	0	0	CIRCULAR	1.25	0	1	0.01269
C220	217900	217918	207.88	0	0	CIRCULAR	1.5	0	1	0.05879
C221	217918	214800	175.61	0	0	CIRCULAR	1.75	0	1	0.04189
C222	214800	217898	212.3	0	0	CIRCULAR	1.75	0	1	0.03559
C223	217898	214796	187.81	0	0	CIRCULAR	2	0	1	0.02157
C224	214796	214808	191.46	0	0	CIRCULAR	2.25	0	1	0.01854
C225	214808	217896	172.68	0	0	CIRCULAR	3	0	1	0.00492
C226	217896	219594	80	0	132.8	CIRCULAR	3	0	1	0.0015
C227	219598	219594	198.51	0	0	CIRCULAR	5	0	1	0.79454
C228	J1	J14	394.82	0	0	CIRCULAR	2	0	1	0.02663
C229	J14	227210	45.4	0	0	CIRCULAR	2	0	1	0.07399
C23	224584	225030	189.78	0	0	CIRCULAR	1.25	0	1	0.01302
C230	224588	220914	9.42	0	0	CIRCULAR	3	0	1	0.13061
C231	220914	220920	161.99	0	0	CIRCULAR	3.5	0	1	0.0121
C232	227240	227210	313.64	0	0	CIRCULAR	7.25	0	1	0.00064
C233	233544	240680	299.45	0	0	CIRCULAR	1.75	0	1	0.00427
C234	240680	238216	311.23	0	0	CIRCULAR	1.75	0	1	0.00604
C235	240332	243696	89.02	0	0	CIRCULAR	1.25	0	1	0.00753
C236	243696	240682	60.99	0	0	CIRCULAR	1.25	0	1	0.06672
C237	233546	238218	300.28	0	0	CIRCULAR	2.25	0	1	0.00323
C238	238218	240682	241.29	0	0	CIRCULAR	2.25	0	1	0.0029
C239	240682	274226	398.44	0	0	CIRCULAR	2.25	0	1	0.00304
C24	225030	214806	208.28	0	0	CIRCULAR	1.25	0	1	0.02305
C240	238226	272654	36.93	0	0	CIRCULAR	1.25	0	1	0.00298
C241	272654	274226	250.41	0	0	CIRCULAR	1.5	0	1	0.00367
C242	274226	238224	177.49	0	0	CIRCULAR	2.5	0	1	0.00287
C243	238224	238212	222.08	0	0	CIRCULAR	2.5	0	1	0.00414
C244	238212	238222	264.14	0	0	CIRCULAR	2.5	0	1	0.00322

Name	Inlet Node	Outlet Node	Length (ft)	Inlet Offset (ft)	Outlet Offset (ft)	Cross-Section	Geom1 (ft)	Geom2 (ft)	Barrels	Slope (ft/ft)
C245	240696	238212	321.09	0	0	CIRCULAR	1	0	1	0.02748
C246	238222	238216	156.38	0	0	CIRCULAR	2.5	0	1	0.01375
C247	241370	241348	358.67	0	0	CIRCULAR	2	0	1	0.01843
C248	241348	241364	287.47	0	0	CIRCULAR	2.5	0	1	0.01155
C249	241364	241366	88.21	0	0	CIRCULAR	4	0	1	0.00363
C25	214806	217884	46.06	0	0	CIRCULAR	1.25	0	1	0.01933
C250	241366	241374	47.16	0	0	CIRCULAR	4	0	1	0.00424
C251	241374	241354	281.61	0	0	CIRCULAR	4	0	1	0.00678
C252	241354	1522347	102.94	0	0	CIRCULAR	4	0	1	0.031
C253	242416	273176	196.88	0	0	CIRCULAR	1	0	1	0.00411
C254	273176	242404	220.14	0	0	CIRCULAR	1	0	1	0.00731
C255	242404	242870	647.27	0	0	CIRCULAR	1	0	1	0.00317
C256	242870	265290	512.55	0	0	CIRCULAR	1	0	1	0.00193
C257	265290	241458	36.74	0	0	CIRCULAR	1	0	1	0.00299
C258	241466	242876	285.35	0	0	CIRCULAR	1	0	1	0.05229
C259	242876	241458	49.46	0	0	CIRCULAR	1	0	1	0.16833
C26	217884	217878	102.7	0	0	CIRCULAR	1.25	0	1	0.02055
C260	241458	241460	352.09	0	0	ARCH	7.33	4.5	1	0.00204
C261	241460	265286	437.2	0	0	ARCH	7.33	4.5	1	0.00204
C262	265286	272868	61.29	0	0	ARCH	7.33	4.5	1	0.00147
C263	242868	242866	92	0	0	CIRCULAR	1.25	0	1	0.00489
C264	242866	242580	105.99	0	0	CIRCULAR	1.25	0	1	0.00547
C265	242580	272868	211.48	0	0	CIRCULAR	1.25	0	1	0.03246
C266	272868	242874	307.85	0	0	CIRCULAR	6.5	0	1	0.00201
C267	242874	242832	382.35	0	0	CIRCULAR	6.5	0	1	0.00199
C268	242832	241648	371.3	0	0	CIRCULAR	6.5	0	1	0.00207
C269	241648	242762	572.99	0	0	CIRCULAR	6.5	0	1	0.00208
C27	217878	218556	39.72	0	0	CIRCULAR	1.25	0	1	0.35415
C270	J11	220796	578.67	0	8.5	CIRCULAR	1	0	1	0.00453
C271	242764	243056	64.78	0	0	CIRCULAR	2.25	0	1	0.01019
C272	242872	241464	170.81	0	0	CIRCULAR	2.25	0	1	0.00457
C273	241464	241668	222.15	0	0	CIRCULAR	2.5	0	1	0.00608
C274	241668	242742	226.82	0	0	CIRCULAR	2.5	0	1	0.00595

Name	Inlet Node	Outlet Node	Length (ft)	Inlet Offset (ft)	Outlet Offset (ft)	Cross-Section	Geom1 (ft)	Geom2 (ft)	Barrels	Slope (ft/ft)
C275	242742	242770	269.38	0	0	CIRCULAR	2.5	0	1	0.0098
C276	191832	242748	174.8	0	0	CIRCULAR	1	0	1	0.02627
C277	242748	243076	82.5	0	0	CIRCULAR	1.5	0	1	0.02049
C278	243076	243068	47.76	0	0	CIRCULAR	2	0	1	0.00335
C279	243068	242854	147.44	0	0	CIRCULAR	2	0	1	0.0095
C28	218556	217868	65.67	0	0	CIRCULAR	1.25	0	1	0.19276
C280	242854	242840	124.87	0	0	CIRCULAR	2	0	1	0.00833
C281	242840	241650	51.56	0	0	CIRCULAR	2	0	1	0.0394
C282	241650	242856	52.59	0	0	CIRCULAR	2	0	1	0.00761
C283	242752	273446	101.45	0	0	CIRCULAR	1.5	0	1	0.00444
C284	273446	242744	281.97	0	0	CIRCULAR	1.5	0	1	0.00387
C285	242744	242856	82.32	0	0	CIRCULAR	1.5	0	1	0.01604
C286	242856	242846	283	0	0	CIRCULAR	3.5	0	1	0.00799
C287	242846	273444	134.73	0	0	CIRCULAR	3.5	0	1	0.00772
C288	273444	242154	176.66	0	0	CIRCULAR	3.5	0	1	0.00425
C289	242154	243326	178.14	0	0	CIRCULAR	1	0	1	0.00258
C29	217868	215002	56.02	0	0	CIRCULAR	1.5	0	1	0.01893
C290	243326	270036	274.97	0	0	CIRCULAR	4.5	0	1	0.00178
C291	242732	243070	168.08	0	0	CIRCULAR	2.5	0	1	0.01178
C292	L12	L11	335.41	0	0	CIRCULAR	13	0	1	0.01026
C293	243646	243320	539.81	0	0	CIRCULAR	8	0	1	0.00198
C294	242762	243066	276.07	0	0	CIRCULAR	5	0	1	0.00181
C295	243066	243646	380.05	0	0	CIRCULAR	5	0	1	0.00203
C296	243160	243178	193.45	0	0	CIRCULAR	1.5	0	1	0.01008
C297	243178	273734	344.2	0	0	CIRCULAR	1.5	0	1	0.01441
C298	217008	217220	19.24	0	0	CIRCULAR	3	0	1	0.66916
C299	218114	271244	282.01	0	0	CIRCULAR	1.25	0	1	0.01294
C3	230956	230978	172.98	0	0.63	CIRCULAR	3	0	1	0.00659
C30	215002	214802	153.98	0	0	CIRCULAR	1.5	0	1	0.06436
C300	271244	216812	154.07	0	0	CIRCULAR	1.5	0	1	0.01214
C301	216812	218116	345.52	0	0.27	CIRCULAR	1.5	0	1	0.01357
C302	218116	267764	396.37	0	0	CIRCULAR	1.75	0	1	0.00606
C303	267764	217218	126.2	0	0	CIRCULAR	2	0	1	0.00721

Name	Inlet Node	Outlet Node	Length (ft)	Inlet Offset (ft)	Outlet Offset (ft)	Cross-Section	Geom1 (ft)	Geom2 (ft)	Barrels	Slope (ft/ft)
C304	217218	217006	270.93	0	0	CIRCULAR	2	0	1	0.00495
C305	217006	216112	282.89	0	0	CIRCULAR	2	0	1	0.00771
C306	216112	217222	169.01	0	0	CIRCULAR	2.25	0	1	0.00846
C307	217222	216106	184.11	0	0	CIRCULAR	3	0	1	0.00255
C308	216106	217004	166.84	0	0	CIRCULAR	3	0	1	0.00252
C309	217004	217212	230.22	0	0	CIRCULAR	3	0	1	0.00239
C31	214802	217916	301.87	0	0	CIRCULAR	1.5	0	1	0.08314
C310	217212	217008	192.91	0	0	CIRCULAR	3	0	1	0.0027
C311	231888	232174	132.93	0	0	CIRCULAR	2.5	0	1	0.0173
C312	232174	273408	48.72	0	0	CIRCULAR	2.5	0	1	0.099
C313	273408	231884	69.28	0	0	CIRCULAR	3	0	1	0.0065
C314	230676	230822	55.25	0	0	CIRCULAR	2	0	1	0.01484
C315	230822	231864	418.79	0	0	CIRCULAR	2	0	1	0.00401
C316	230818	230950	275.31	0	0	CIRCULAR	1.25	0	1	0.01406
C317	230950	231592	153.39	0	0	CIRCULAR	1.5	0	1	0.00567
C318	231592	231864	65.87	0	0	CIRCULAR	1.5	0	1	0.01837
C319	231864	230662	226.8	0	0	CIRCULAR	2.5	0	1	0.00307
C32	217916	218554	337.84	0	0	CIRCULAR	1.75	0	1	0.03077
C320	230662	230952	134.67	0	0	CIRCULAR	2.5	0	1	0.00597
C321	230952	273378	103.79	0	0	CIRCULAR	3	0	1	0.00279
C322	273378	230948	373.2	0	0	CIRCULAR	3	0	1	0.00413
C323	243654	243176	178.37	0	7.4	CIRCULAR	5	0	1	0.029
C324	243352	243654	143.37	0	0.5	CIRCULAR	4.5	0	1	0.003
C325	247988	L4	33.9	0	0	ARCH	6.92	7.5	1	0.13635
C326	248014	L3	60	0	80.43	RECT_CLOSED	6	2.5	1	0.11077
C327	241564	242768	250.46	0	0.71	CIRCULAR	1.25	0	1	0.0236
C328	242768	242732	316.97	0	0	CIRCULAR	1.75	0	1	0.00836
C329	220790	190064	377.37	0	0	CIRCULAR	3	0	1	0.00397
C33	218554	219596	27.56	0	0	CIRCULAR	1.75	0	1	0.09881
C330	242760	243066	241.97	0	0	CIRCULAR	3.5	0	1	0.00839
C331	215378	1521368	13	0	49	CIRCULAR	3	0	1	0.07715
C332	243070	242756	152.73	0	0.21	CIRCULAR	2.5	0	1	0.01198
C333	242756	243350	291.74	0	0	CIRCULAR	2.75	0	1	0.00792

Name	Inlet Node	Outlet Node	Length (ft)	Inlet Offset (ft)	Outlet Offset (ft)	Cross-Section	Geom1 (ft)	Geom2 (ft)	Barrels	Slope (ft/ft)
C334	243350	243648	176.55	0	0	CIRCULAR	3	0	1	0.00714
C335	243648	243334	191.77	0	0	CIRCULAR	3.5	0	1	0.00261
C336	243334	243322	197.04	0	0	CIRCULAR	3.5	0	1	0.00609
C337	242746	242738	76.55	0	0	CIRCULAR	1.25	0	1	0.01921
C338	242834	242738	227.27	0	0	CIRCULAR	2	0	1	0.00466
C339	242738	242852	249.33	0	0	CIRCULAR	2	0	1	0.00746
C34	219596	219598	373.58	0	0	CIRCULAR	3	0	1	0.0215
C340	242852	243342	227.15	0	0	CIRCULAR	2	0	1	0.00748
C341	243342	243336	175.45	0	0	CIRCULAR	2	0	1	0.01134
C342	243336	243166	219.06	0	0	CIRCULAR	2.5	0	1	0.00803
C343	243166	243322	184.01	0	0	CIRCULAR	2.5	0	1	0.02229
C344	243344	243322	157.65	0	0	CIRCULAR	1.25	0	1	0.00381
C345	242864	242146	299.36	0	0	CIRCULAR	1.25	0	1	0.02205
C346	242146	273152	204.69	0	0	CIRCULAR	1.5	0	1	0.0258
C347	273152	242152	95.25	0	2.97	CIRCULAR	2	0	1	0.0313
C348	242148	243354	296.48	0	0	CIRCULAR	4	0	1	0.00206
C349	243354	242152	134.88	0	0	CIRCULAR	4	0	1	0.00237
C35	270730	223386	30.02	0	0	CIRCULAR	1.5	0	1	0.06811
C350	243650	243164	183.23	0	0	CIRCULAR	1.5	0	1	0.01026
C351	243164	243180	108.7	0	0	CIRCULAR	1.5	0	1	0.01168
C352	243180	243352	40.88	0	8.2	CIRCULAR	1.5	0	1	0.02569
C353	242862	242860	179.14	0	0	CIRCULAR	1	0	1	0.02932
C354	242860	243164	156.88	0	0	CIRCULAR	1	0	1	0.03668
C355	216032	220796	897.77	0	0	CIRCULAR	7.5	0	1	0.0015
C356	220796	1521212	345	0	0	CIRCULAR	7.5	0	1	0.00475
C357	1521212	220792	334.09	0	0	CIRCULAR	7.5	0	1	0.00362
C358	220792	220798	141.49	0	0	CIRCULAR	7.5	0	1	0.00558
C359	220798	269270	109.28	0	0	CIRCULAR	7.5	0	1	0.08329
C36	223390	223388	221.49	0	0	CIRCULAR	1.25	0	1	0.09442
C360	269270	J13	32.59	0	120.097	CIRCULAR	1	0	1	0.10303
C361	J13	L5	54.69	0	0	CIRCULAR	13	0	1	0.08761
C362	218038	215092	54.88	0	140.14	CIRCULAR	1.75	0	1	0.00911
C363	215508	216542	144.27	0	0	CIRCULAR	1.5	0	1	0.00659

Name	Inlet Node	Outlet Node	Length (ft)	Inlet Offset (ft)	Outlet Offset (ft)	Cross-Section	Geom1 (ft)	Geom2 (ft)	Barrels	Slope (ft/ft)
C364	216542	215538	83.34	0	0	CIRCULAR	1.75	0	1	0.00636
C365	215538	217726	281.17	0	0	CIRCULAR	1.75	0	1	0.00598
C366	217726	215674	182.65	0	0	CIRCULAR	1.75	0	1	0.05395
C367	215674	216248	76.54	0	0	CIRCULAR	1.75	0	1	0.02182
C368	216248	216246	133.18	0	0	CIRCULAR	1.75	0	1	0.02125
C369	216246	218038	194.02	0	0	CIRCULAR	1.75	0	1	0.03481
C37	223388	223386	56.05	0	0	CIRCULAR	1.5	0	1	0.03463
C370	219724	248014	58.76	0	0	RECT_CLOSED	6	2.5	1	0.08134
C371	238214	233538	274.27	0	0	CIRCULAR	3.5	0	1	0.00263
C372	233538	219724	23.02	0	0	CIRCULAR	3.5	0	1	0.21645
C373	187586	243686	357.48	0	0	CIRCULAR	3	0	1	0.00607
C374	243686	243684	29.99	0	0	CIRCULAR	3	0	1	0.16839
C375	243684	219724	14.99	0	0	CIRCULAR	3	0	1	0.23361
C376	1521368	L2	235.45	0	2.7	RECT_CLOSED	6	2.5	1	0.02422
C377	238216	273764	325.98	0	113.2	CIRCULAR	2.5	0	1	0.04822
C378	242152	243338	212.51	0	0	CIRCULAR	3.5	0	1	0.00221
C379	243338	243174	300.67	0	0	CIRCULAR	3.5	0	1	0.00419
C38	223386	223384	67.99	0	0	CIRCULAR	2	0	1	0.00662
C380	243174	243352	79.09	0	0.5	CIRCULAR	4	0	1	0.00253
C381	273734	243176	28.8	0	0	CIRCULAR	1.5	0	1	0.86973
C382	243176	219712	6.02	0	125.14	CIRCULAR	5	0	1	0.01661
C383	219712	L9	76.28	0	3.26	RECT_CLOSED	7	10	1	0.00131
C384	243320	243330	395.54	0	0	CIRCULAR	8	0	1	0.00185
C385	243330	219712	925.79	0	136.14	CIRCULAR	8	0	1	0.00624
C386	215552	209664	271.98	0	0	CIRCULAR	3	0	1	0.005
C387	269340	215556	233.64	0	0	CIRCULAR	3	0	1	0.00492
C388	215556	215552	272.11	0	5.7	CIRCULAR	3	0	1	0.00518
C389	221202	L13	190.16	0	0	ARCH	2.5	6	1	0.00263
C39	223384	J2	225.8	0	0	CIRCULAR	2	0	1	0.02773
C390	215544	216198	168	0	0	CIRCULAR	1.5	0	1	0.00667
C391	209664	221202	14.75	0	137.66	CIRCULAR	3	0	1	0.00542
C392	216198	221202	12.74	0	138.07	CIRCULAR	1.5	0	1	0.00863
C393	240924	240940	200.67	0	0	CIRCULAR	1.25	0	1	0.00488

Name	Inlet Node	Outlet Node	Length (ft)	Inlet Offset (ft)	Outlet Offset (ft)	Cross-Section	Geom1 (ft)	Geom2 (ft)	Barrels	Slope (ft/ft)
C394	241186	241264	196.59	0	0.15	CIRCULAR	1.5	0	1	0.00392
C395	241264	240940	231.68	0	0.2	CIRCULAR	1.5	0	1	0.00393
C396	240940	241262	296.11	0	0.15	CIRCULAR	1.5	0	1	0.00496
C397	241262	241284	355.33	0	0.75	CIRCULAR	1.5	0	1	0.01368
C398	241284	232332	285.05	0	0.61	CIRCULAR	1.75	0	1	0.01098
C399	232332	270948	70.12	0	0.3	CIRCULAR	2.5	0	1	0.00285
C4	230978	231870	299.67	0	0	CIRCULAR	3	0	1	0.00517
C40	J2	201862	337.16	0	0	CIRCULAR	2	0	1	0.01605
C400	270948	232338	42.45	0	0.2	CIRCULAR	2.75	0	1	0.00353
C401	232338	232342	266.3	0	0.75	CIRCULAR	2.75	0	1	0.00293
C402	232342	230976	320.37	0	0	CIRCULAR	3.5	0	1	0.00365
C403	231982	230976	53.01	0	3.02	CIRCULAR	1.25	0	1	0.01472
C404	230976	232316	331.12	0	0.15	CIRCULAR	3.5	0	1	0.00293
C405	232316	232318	322.22	0	4.48	CIRCULAR	3.5	0	1	0.00264
C406	241272	240922	371.31	0	0.15	CIRCULAR	1.25	0	1	0.01002
C407	240922	240926	284.62	0	0.8	CIRCULAR	1.25	0	1	0.01061
C408	240926	241284	37.09	0	2.91	CIRCULAR	1.5	0	1	0.0178
C409	232324	216268	166.13	0	0.15	CIRCULAR	1.25	0	1	0.02589
C41	201862	220920	51.52	0	0	CIRCULAR	2	0	1	0.11964
C410	216268	232334	204.27	0	0.6	CIRCULAR	1.25	0	1	0.02546
C411	232334	217190	216.28	0	0	CIRCULAR	1.75	0	1	0.01003
C412	217190	232340	217	0	0	CIRCULAR	1.75	0	1	0.00949
C413	232340	270948	39.85	0	2.94	CIRCULAR	2	0	1	0.00954
C414	231984	273656	300.05	0	0	CIRCULAR	1.25	0	1	0.02691
C415	273656	231982	301.01	0	0	CIRCULAR	1.25	0	1	0.01837
C416	232318	232326	115.6	0	4.49	CIRCULAR	3.5	0	1	0.02077
C417	232326	216280	125.72	0	3.9	CIRCULAR	3.5	0	1	0.01933
C418	216280	220538	453.24	0	0.05	CIRCULAR	3.5	0	1	0.00481
C419	216272	216300	300	0	0	CIRCULAR	3.5	0	1	0.003
C42	242980	242982	244.01	0	0	CIRCULAR	3	0	1	0.00627
C420	216300	220538	282	0	0	CIRCULAR	4	0	1	0.00301
C421	216302	232322	297.33	0	1	CIRCULAR	1.25	0	1	0.00504
C422	232322	231986	299.86	0	0	CIRCULAR	2.25	0	1	0.003

Name	Inlet Node	Outlet Node	Length (ft)	Inlet Offset (ft)	Outlet Offset (ft)	Cross-Section	Geom1 (ft)	Geom2 (ft)	Barrels	Slope (ft/ft)
C423	231986	232344	306.23	0	0	CIRCULAR	2.75	0	1	0.0031
C424	232344	216272	288.39	0	0	CIRCULAR	3.5	0	1	0.00312
C425	272672	240824	47	0	3.19	CIRCULAR	1	0	1	0.00617
C426	240824	240822	32	0	0	CIRCULAR	2.25	0	1	0.01969
C427	240822	240820	82.98	0	0	CIRCULAR	2.25	0	1	0.00928
C428	240820	240818	91.02	0	0	CIRCULAR	2.25	0	1	0.0111
C429	240818	272670	75.99	0	0	CIRCULAR	2.25	0	1	0.00816
C43	242982	243616	234.98	0	0	CIRCULAR	3	0	1	0.0057
C430	272670	240816	81.01	0	0	CIRCULAR	2.25	0	1	0.01062
C431	240816	240814	126.01	0	0	CIRCULAR	2.25	0	1	0.01032
C432	240814	240832	101.21	0	0	CIRCULAR	2.25	0	1	0.01502
C433	240832	241150	87.41	0	0	CIRCULAR	2.5	0	1	0.02621
C434	241150	240834	159.93	0	0	CIRCULAR	2.5	0	1	0.02602
C435	240834	232186	299.77	0	0	CIRCULAR	2.5	0	1	0.04796
C436	243662	243658	83.27	0	0	CIRCULAR	1.25	0	1	0.00781
C44	225002	223516	34.91	0	0	CIRCULAR	1.25	0	1	0.02436
C440	239648	240918	86.76	0	0.1	CIRCULAR	1.75	0	1	0.00357
C441	240918	239666	240.07	0	0	CIRCULAR	1.75	0	1	0.0055
C442	239666	239678	285.27	0	0	CIRCULAR	2.25	0	1	0.00554
C443	239678	239656	413.09	0	0	CIRCULAR	2.5	0	1	0.00557
C444	239656	231872	329.42	0	0	CIRCULAR	2.5	0	1	0.00677
C445	231872	273406	126.26	0	0	CIRCULAR	2.5	0	1	0.00824
C446	273406	232166	393.84	0	0	CIRCULAR	2.5	0	1	0.01498
C447	232166	231874	79.13	0	0	CIRCULAR	3	0	1	0.01036
C448	231874	231876	108.92	0	0	CIRCULAR	3	0	1	0.00982
C449	231876	230856	124.2	0	0	CIRCULAR	3	0	1	0.01015
C45	223516	225024	128.75	0	0	CIRCULAR	1.25	0	1	0.00986
C450	230856	230858	94.74	0	0	CIRCULAR	3	0	1	0.01034
C451	230858	232182	49.18	0	0.56	CIRCULAR	3	0	1	0.01118
C452	232182	232180	42.26	0	0	CIRCULAR	4	0	1	0.01018
C453	232180	230866	302.43	0	0	CIRCULAR	4.5	0	1	0.00298
C454	230866	232496	149.36	0	0	CIRCULAR	4.5	0	1	0.00301
C455	232496	232306	160.35	0	0	CIRCULAR	4.5	0	1	0.00318

Name	Inlet Node	Outlet Node	Length (ft)	Inlet Offset (ft)	Outlet Offset (ft)	Cross-Section	Geom1 (ft)	Geom2 (ft)	Barrels	Slope (ft/ft)
C456	230682	230664	417.95	0	0	CIRCULAR	1.5	0	1	0.00605
C457	230664	230948	63.66	0	0	CIRCULAR	1.5	0	1	0.09435
C458	230948	260142	309.7	0	0	CIRCULAR	3.5	0	1	0.00559
C459	260142	230644	59.56	0	0	CIRCULAR	4	0	1	0.0042
C46	225024	224692	43.66	0	0	CIRCULAR	1.25	0	1	0.01008
C460	230644	232216	434.94	0	0	CIRCULAR	3.5	0	1	0.00294
C461	230654	230660	342.04	0	0.25	CIRCULAR	1.5	0	1	0.00292
C462	230660	230944	21.86	0	0	CIRCULAR	1.75	0	1	0.00457
C463	230944	230946	375.73	0	0	CIRCULAR	1.75	0	1	0.01065
C464	215376	215378	30	0	0	CIRCULAR	3	0	1	0.03669
C465	231586	230652	286.22	0	0	CIRCULAR	1.75	0	1	0.00472
C466	230652	230946	430.27	0	0	CIRCULAR	2.5	0	1	0.00174
C467	230946	231888	341.6	0	0	CIRCULAR	2.5	0	1	0.00615
C468	232068	232504	70.7	0	0	CIRCULAR	1.25	0	1	0.09448
C469	232504	232190	258.91	0	0	CIRCULAR	1.25	0	1	0.0112
C47	224692	225018	183.41	0	0	CIRCULAR	1.25	0	1	0.07188
C470	232190	232184	199.45	0	0	CIRCULAR	1.25	0	1	0.05493
C471	232184	273672	188.89	0	1.82	CIRCULAR	1.25	0	1	0.02886
C472	231870	231880	86.07	0	0	CIRCULAR	3	0	1	0.01359
C473	231880	231882	71.72	0	0	CIRCULAR	3	0	1	0.24383
C474	1544766	1544594	123.91	0	0	CIRCULAR	1.25	0	1	0.00799
C475	1544594	1544599	207.72	0	0.2	CIRCULAR	1.25	0	1	0.0053
C476	1544599	273408	271.66	0	0	CIRCULAR	1.5	0	1	0.01329
C477	231886	232164	82.37	0	0.5	CIRCULAR	1.25	0	1	0.00607
C478	232164	232212	199.61	0	0	CIRCULAR	1.75	0	1	0.00311
C479	232212	232204	202.63	0	0.25	CIRCULAR	1.75	0	1	0.00188
C48	225018	225016	164.72	0	1.9	CIRCULAR	1.25	0	1	0.07635
C480	232204	231868	50.31	0	0	CIRCULAR	1.75	0	1	0.00994
C481	231868	231892	234.13	0	0.04	CIRCULAR	2	0	1	0.00513
C482	231892	273408	284.83	0	0	CIRCULAR	1.75	0	1	0.032
C483	231882	230882	226.94	0	0	CIRCULAR	3.5	0	1	0.00401
C485	230882	230958	170.57	0	0	CIRCULAR	3.5	0	1	0.00405
C486	230958	273672	93.1	0	0	CIRCULAR	3.5	0	1	0.00473

Name	Inlet Node	Outlet Node	Length (ft)	Inlet Offset (ft)	Outlet Offset (ft)	Cross-Section	Geom1 (ft)	Geom2 (ft)	Barrels	Slope (ft/ft)
C487	272830	240932	248.87	0	0.25	CIRCULAR	1.25	0	1	0.00462
C488	240932	240930	45.16	0	0	CIRCULAR	1.5	0	1	0.01063
C489	240930	241288	317.64	0	0.25	CIRCULAR	1.75	0	1	0.00296
C49	225016	225006	58.05	0	1.54	CIRCULAR	1.25	0	1	0.00775
C490	241288	241246	283.06	0	0	CIRCULAR	2	0	1	0.00403
C491	241246	240934	48.68	0	0	CIRCULAR	2	0	1	0.00411
C492	240934	241252	320.28	0	0	CIRCULAR	2	0	1	0.00699
C493	192644	240930	113.34	0	0	CIRCULAR	1.25	0	1	0.00529
C494	241192	240934	303.69	0	0	CIRCULAR	1.25	0	1	0.0136
C495	241252	240928	311.8	0	0	CIRCULAR	2	0	1	0.0547
C496	242124	241274	247.54	0	0	CIRCULAR	1.25	0	1	0.00299
C497	241274	241268	170.82	0	0	CIRCULAR	1.25	0	1	0.00691
C498	241268	241250	46.88	0	0	CIRCULAR	1.75	0	1	0.00256
C499	242106	272856	172.9	0	0	CIRCULAR	1.25	0	1	0.00289
C5	232216	231884	113.6	0	0	CIRCULAR	3.5	0	1	0.00546
C50	187806	223508	60.5	0	1	CIRCULAR	1.5	0	1	0.05519
C500	272856	193106	9	0	0	CIRCULAR	1.25	0	1	0.01111
C501	193106	241274	47.42	0	0	CIRCULAR	1.25	0	1	0.01012
C502	216110	L15	437.06	0	128.64	CIRCULAR	10	0	1	0.00364
C503	217922	217914	182.34	0	0.25	CIRCULAR	1.5	0	1	0.04634
C506	217906	217866	186.01	0	0	CIRCULAR	1.5	0	1	0.03497
C507	L11	L10	1010.8	0	0	CIRCULAR	13	0	1	0.00125
C508	220864	217226	66.74	0	0	CIRCULAR	1	0	1	0.03448
C509	L15	L14	1551.64	0	0	CIRCULAR	13	0	1	0.00109
C51	223508	225014	142.36	0	0	CIRCULAR	1.5	0	1	0.05586
C510	216102	216098	185.75	0	0	CIRCULAR	1.25	0	1	0.02159
C511	216098	215516	186.6	0	0.25	CIRCULAR	1.25	0	1	0.01796
C512	215516	215514	34.13	0	0.25	CIRCULAR	1.5	0	1	0.01143
C513	215514	209666	344.78	0	0.75	CIRCULAR	1.75	0	1	0.00638
C514	215570	215512	85.7	0	0	CIRCULAR	2.5	0	1	0.00385
C515	209666	215570	194.39	0	0	CIRCULAR	2.5	0	1	0.00345
C516	217228	187488	160.92	0	0	CIRCULAR	1	0	1	0.00746
C517	187488	187490	209.48	0	0	CIRCULAR	1	0	1	0.0074

Name	Inlet Node	Outlet Node	Length (ft)	Inlet Offset (ft)	Outlet Offset (ft)	Cross-Section	Geom1 (ft)	Geom2 (ft)	Barrels	Slope (ft/ft)
C518	215512	220882	226.74	0	0	CIRCULAR	2.5	0	1	0.7894
C519	187490	220882	30.24	0	141.77	CIRCULAR	1.25	0	1	0.00562
C52	225014	225012	177.18	0	0.25	CIRCULAR	1.5	0	1	0.06396
C520	220882	L14	13.82	0	0	ARCH	2.5	6	1	0.0362
C521	L14	L13	643.72	0	0	CIRCULAR	13	0	1	0.00126
C522	193462	215028	193.06	0	0	CIRCULAR	1	0	1	0.00368
C523	215028	270210	173.98	0	0.25	CIRCULAR	1	0	1	0.01144
C524	270210	215036	38.1	0	0	CIRCULAR	1.25	0	1	0.01969
C525	215036	215034	155.2	0	0	CIRCULAR	1.25	0	1	0.04147
C526	215034	215064	251.15	0	0	CIRCULAR	1.25	0	1	0.04332
C527	215064	215032	230.98	0	0	CIRCULAR	1.5	0	1	0.04477
C528	215032	215030	113.81	0	0	CIRCULAR	1.5	0	1	0.04547
C529	215030	270208	159.52	0	0	CIRCULAR	2.5	0	1	0.00702
C53	225012	224694	189.03	0	0	CIRCULAR	1.75	0	1	0.05298
C530	270208	215042	183.97	0	0	CIRCULAR	2.5	0	1	0.00859
C531	215042	215080	29.71	0	0	CIRCULAR	2.5	0	1	0.0033
C532	215080	215062	76.93	0	0	CIRCULAR	2.5	0	1	0.00458
C533	215062	215672	205.62	0	0	CIRCULAR	2.75	0	1	0.00404
C534	215672	215084	41.58	0	0	CIRCULAR	2.75	0	1	0.01275
C535	215084	270686	134.54	0	0	CIRCULAR	2.75	0	1	0.00632
C536	270686	230330	141.37	0	0	CIRCULAR	2.75	0	1	0.00552
C537	215014	215504	204.95	0	0	CIRCULAR	1	0	1	0.02084
C538	215504	209648	52.82	0	0	CIRCULAR	1	0	1	0.06622
C539	209648	230330	68.92	0	0	CIRCULAR	1	0	1	0.03513
C54	224694	224682	178.55	0	1.24	CIRCULAR	1.75	0	1	0.04176
C540	230330	269340	241.86	0	1.59	CIRCULAR	2.75	0	1	0.01079
C541	216200	270974	175.47	0	0	CIRCULAR	1	0	1	0.06826
C542	270974	230322	60.59	0	0	CIRCULAR	1.25	0	1	0.00363
C543	230322	269340	127.99	0	1.75	CIRCULAR	1.25	0	1	0.00406
C544	J8	215062	272.68	0	2.55	CIRCULAR	1.25	0	1	0.01981
C545	217882	217904	198.87	0	0.7	CIRCULAR	2	0	1	0.00613
C546	217904	217894	59.97	0	0.37	CIRCULAR	2	0	1	0.01101
C547	217876	217864	229.3	0	0.05	CIRCULAR	1.5	0	1	0.0205

Name	Inlet Node	Outlet Node	Length (ft)	Inlet Offset (ft)	Outlet Offset (ft)	Cross-Section	Geom1 (ft)	Geom2 (ft)	Barrels	Slope (ft/ft)
C548	268048	217874	122.26	0	0	CIRCULAR	1.25	0	1	0.01963
C549	217874	214804	62.16	0	0.3	CIRCULAR	1.25	0	1	0.02349
C55	224682	225006	52.63	0	0	CIRCULAR	2	0	1	0.03041
C550	214804	214818	18.8	0	0	CIRCULAR	2	0	1	0.01596
C551	214818	217920	259.02	0	0	CIRCULAR	2	0	1	0.01058
C552	215052	215046	70.87	0	0.73	CIRCULAR	1.5	0	1	0.01623
C553	217920	215026	107.75	0	0	CIRCULAR	2	0	1	0.00984
C554	215026	215060	286.2	0	1.5	CIRCULAR	2	0	1	0.01013
C555	215046	215058	307.03	0	1.19	CIRCULAR	1.5	0	1	0.03889
C556	217894	217912	346.65	0	0.44	CIRCULAR	2	0	1	0.01878
C557	217912	217864	118.11	0	1	CIRCULAR	2	0	1	0.00508
C558	217864	215040	329.45	0	0	CIRCULAR	3.5	0	1	0.0031
C559	215058	215020	66.83	0	0	CIRCULAR	1.5	0	1	0.17281
C56	225006	225010	113.77	0	0	CIRCULAR	2.5	0	1	0.01099
C560	215040	215066	189.63	0	0	CIRCULAR	3.5	0	1	0.0029
C561	215066	215086	136.97	0	0	CIRCULAR	3.5	0	1	0.00307
C562	215086	215060	35.35	0	0	CIRCULAR	3.5	0	1	0.21589
C563	215010	215068	118.73	0	0	CIRCULAR	1	0	1	0.05085
C564	215068	270202	163.19	0	0	CIRCULAR	1	0	1	0.04656
C565	270202	215066	45.34	0	5.04	CIRCULAR	1	0	1	0.0331
C566	215038	215070	92.23	0	0	CIRCULAR	3	0	1	0.05006
C567	215060	215006	47.12	0	0	CIRCULAR	3	0	1	0.02548
C568	215006	215050	110.68	0	0	CIRCULAR	3	0	1	0.01807
C569	215050	215038	236.19	0	0	CIRCULAR	3	0	1	0.09832
C57	225010	224690	69.09	0	0	CIRCULAR	2.5	0	1	0.02461
C570	217866	217870	155.63	0	0	CIRCULAR	1.5	0	1	0.04593
C571	217870	217922	43.26	0	0.6	CIRCULAR	1.5	0	1	0.03145
C572	217914	216260	180.3	0	0.75	CIRCULAR	1.75	0	1	0.02891
C573	268030	268064	140.81	0	0	CIRCULAR	1.25	0	1	0.00845
C574	268064	218048	353.72	0	0.25	CIRCULAR	1.25	0	1	0.00905
C575	218048	218046	181.74	0	0	CIRCULAR	1.5	0	1	0.03397
C576	218046	218042	144.4	0	0	CIRCULAR	1.5	0	1	0.05006
C577	218042	218044	182.81	0	0	CIRCULAR	1.5	0	1	0.05616

Name	Inlet Node	Outlet Node	Length (ft)	Inlet Offset (ft)	Outlet Offset (ft)	Cross-Section	Geom1 (ft)	Geom2 (ft)	Barrels	Slope (ft/ft)
C578	218044	268066	46.05	0	0	CIRCULAR	1.5	0	1	0.01086
C579	216252	216256	49.05	0	0	CIRCULAR	1.25	0	1	0.02917
C58	224690	241926	170.82	0	0	CIRCULAR	2.5	0	1	0.02876
C580	216256	216264	283.83	0	0	CIRCULAR	1.25	0	1	0.04825
C581	216264	268066	47.16	0	0	CIRCULAR	1.25	0	1	0.06182
C582	268066	217728	335	0	0	CIRCULAR	2	0	1	0.02257
C583	217728	216258	53.98	0	1.15	CIRCULAR	2	0	1	0.00926
C584	216258	215506	170.17	0	0	CIRCULAR	2.5	0	1	0.01328
C585	215506	215536	114.53	0	1.77	CIRCULAR	2.5	0	1	0.01249
C586	215536	215542	70.01	0	0	CIRCULAR	2.25	0	1	0.03473
C587	215542	215554	278.07	0	0	CIRCULAR	2.25	0	1	0.03649
C588	215554	209652	36.05	0	0	CIRCULAR	2.25	0	1	0.1633
C589	215020	270206	268.39	0	0	CIRCULAR	6	0	1	0.00503
C59	241926	223504	348.34	0	0	CIRCULAR	3.5	0	1	0.00301
C590	270206	215548	226.9	0	0	CIRCULAR	6	0	1	0.00494
C591	215548	209652	223.43	0	0	CIRCULAR	6	0	1	0.00515
C592	209652	221200	325.92	0	0	CIRCULAR	6	0	1	0.48136
C593	241290	1626294	72.2	0	0	CIRCULAR	1.5	0	1	0.00762
C595	221200	L12	92.36	0	0	CIRCULAR	1	0	1	0.00076
C596	241194	1626294	89.89	0	0	CIRCULAR	1.5	0	1	0.0089
C597	1626294	240936	303.33	0	0	CIRCULAR	2	0	1	0.00508
C598	240936	241278	364.55	0	0.28	CIRCULAR	2.75	0	1	0.00296
C599	241254	240936	99.08	0	0	CIRCULAR	1.5	0	1	0.02069
C6	187572	240344	209.01	0	0	CIRCULAR	1.25	0	1	0.0314
C60	223504	241924	183.22	0	0	CIRCULAR	3.5	0	1	0.00311
C600	241250	241260	327.28	0	0	CIRCULAR	1.75	0	1	0.00302
C601	240938	241188	22.45	0	0	CIRCULAR	1.5	0	1	0.06248
C602	241260	240938	104.58	0	0	CIRCULAR	1.75	0	1	0.02458
C603	241174	241172	324.44	0	0	CIRCULAR	1.5	0	1	0.0053
C604	241172	241166	308.88	0	0	CIRCULAR	1.5	0	1	0.01068
C605	241188	241178	228.89	0	0	CIRCULAR	1.5	0	1	0.02942
C606	241178	241166	34.46	0	0	CIRCULAR	2	0	1	0.05959
C607	241278	241196	269.89	0	0.5	CIRCULAR	3	0	1	0.00333

Name	Inlet Node	Outlet Node	Length (ft)	Inlet Offset (ft)	Outlet Offset (ft)	Cross-Section	Geom1 (ft)	Geom2 (ft)	Barrels	Slope (ft/ft)
C608	241170	241182	237.5	0	0	CIRCULAR	1.75	0	1	0.00223
C609	241182	241180	199	0	0	CIRCULAR	1.75	0	1	0.00291
C61	224684	223510	226.55	0	0	CIRCULAR	1	0	1	0.06098
C610	241180	241176	29	0	11.73	CIRCULAR	1.75	0	1	0.0031
C611	241166	241168	325.8	0	0	CIRCULAR	3.5	0	1	0.00239
C612	241168	241176	311.69	0	6.1	CIRCULAR	3.5	0	1	0.00263
C613	241196	241292	332.21	0	0.4	CIRCULAR	3.5	0	1	0.00292
C614	241292	272852	285.44	0	0	CIRCULAR	4	0	1	0.00336
C615	272852	241176	20.31	0	0	CIRCULAR	4	0	1	0.00443
C616	240928	241292	14.88	0	0	CIRCULAR	2	0	1	0.14048
C617	241176	230962	364.43	0	0	CIRCULAR	5	0	1	0.00132
C618	231972	231970	271.65	0	0	CIRCULAR	1.25	0	1	0.0099
C619	231970	231974	41	0	0	CIRCULAR	1.5	0	1	0.00805
C62	223510	223518	204.78	0	0.5	CIRCULAR	1	0	1	0.06165
C620	231974	231968	270	0	0	CIRCULAR	1.5	0	1	0.00641
C621	231968	230968	48.51	0	0	CIRCULAR	1.5	0	1	0.01175
C622	230968	230970	329.99	0	0	CIRCULAR	1.75	0	1	0.01509
C623	230970	232222	270.5	0	0	CIRCULAR	1.75	0	1	0.01464
C624	232222	230756	56.67	0	1	CIRCULAR	1.75	0	1	0.01977
C625	230756	230758	250.02	0	0	CIRCULAR	2.25	0	1	0.01412
C626	230758	230760	213.98	0	0	CIRCULAR	2.25	0	1	0.01486
C627	230760	230762	64.5	0	5	CIRCULAR	2.25	0	1	0.04081
C628	273416	230776	28.52	0	0	CIRCULAR	2.25	0	1	0.00281
C629	230776	230756	285.99	0	0	CIRCULAR	2.25	0	1	0.00318
C63	223518	224700	177.77	0	0	CIRCULAR	1.5	0	1	0.01474
C630	1544728	1544733	39.44	0	0.57	CIRCULAR	1.75	0	1	0.01369
C631	1544733	1545140	288.17	0	0	CIRCULAR	2.25	0	1	0.00885
C632	1545140	230762	264.96	0	0	CIRCULAR	2.5	0	1	0.0071
C633	230762	1544674	154.23	0	0	CIRCULAR	2.5	0	1	0.00914
C634	1544674	1545194	292.17	0	0	CIRCULAR	3	0	1	0.0037
C635	1545194	1544651	234.92	0	0	CIRCULAR	3	0	1	0.00902
C636	1544651	1544654	184.07	0	0	CIRCULAR	3	0	1	0.00386
C637	216276	230770	35.62	0	7.44	CIRCULAR	1.75	0	1	0.02246

Name	Inlet Node	Outlet Node	Length (ft)	Inlet Offset (ft)	Outlet Offset (ft)	Cross-Section	Geom1 (ft)	Geom2 (ft)	Barrels	Slope (ft/ft)
C638	1544704	1544699	143.57	0	2.82	CIRCULAR	2.5	0	1	0.01003
C639	1544699	1544694	212.55	0	0.09	CIRCULAR	3	0	1	0.00588
C64	224700	223514	170.15	0	0	CIRCULAR	1.5	0	1	0.02157
C640	1544694	1545295	257.39	0	0	CIRCULAR	3.5	0	1	0.00427
C641	1544654	OF3	235.46	0	0	CIRCULAR	3.5	0	1	0.00794
C642	1545295	1545289	245.8	0	0	CIRCULAR	3.5	0	1	0.00228
C643	1545289	1544654	456.18	0	0	CIRCULAR	3.5	0	1	0.00476
C644	231980	231976	206	0	0	CIRCULAR	2.75	0	1	0.02549
C645	231976	273418	317.01	0	0	CIRCULAR	3	0	1	0.00215
C646	273418	230772	324.49	0	0	CIRCULAR	3.5	0	1	0.01341
C647	231978	273418	197.53	0	0	CIRCULAR	2	0	1	0.02101
C648	230772	220850	308.99	0	0	CIRCULAR	5.5	0	1	0.00379
C649	220850	220852	356	0	0	CIRCULAR	5.5	0	1	0.00354
C65	223514	225004	35.8	0	1	CIRCULAR	1.5	0	1	0.03522
C650	220852	220854	289.16	0	0	CIRCULAR	5.5	0	1	0.00446
C651	220854	220856	266.01	0	0	CIRCULAR	5.5	0	1	0.00425
C652	220856	220858	468.06	0	0	CIRCULAR	5.5	0	1	0.004
C653	220858	220860	428.02	0	0	CIRCULAR	5.5	0	1	0.00507
C654	220860	220862	191.88	0	0	CIRCULAR	5.5	0	1	0.00485
C655	220862	220864	647.03	0	0	CIRCULAR	5.5	0	1	0.02037
C657	230770	230772	468.32	0	0	CIRCULAR	5.5	0	1	0.00248
C658	243322	242148	277.55	0	0	CIRCULAR	4	0	1	0.00231
C659	241270	241200	235.97	0	0	CIRCULAR	1.75	0	1	0.01657
C66	223506	225022	210.4	0	0	CIRCULAR	1.25	0	1	0.0441
C660	241200	241294	201.66	0	0	CIRCULAR	1.75	0	1	0.02501
C661	241294	241296	326.76	0	0	CIRCULAR	1.75	0	1	0.02501
C662	241296	216346	177.39	0	0	CIRCULAR	1.75	0	1	0.02521
C663	216346	216276	53.38	0	0	CIRCULAR	1.75	0	1	0.04519
C664	230962	230764	311.05	0	0	CIRCULAR	5	0	1	0.0018
C665	230764	230766	129	0	0	CIRCULAR	5	0	1	0.00178
C666	230766	230768	202.99	0	0	CIRCULAR	5	0	1	0.00236
C667	230768	230770	155.68	0	0	CIRCULAR	5	0	1	0.00687
C668	217206	216110	171.27	0	0	CIRCULAR	10	0	1	0.00683

Name	Inlet Node	Outlet Node	Length (ft)	Inlet Offset (ft)	Outlet Offset (ft)	Cross-Section	Geom1 (ft)	Geom2 (ft)	Barrels	Slope (ft/ft)
C669	217226	L15	590.72	0	124.4	CIRCULAR	10	0	1	0.00728
C67	225022	225004	231.77	0	0.75	CIRCULAR	1.25	0	1	0.04492
C670	217216	267766	669.23	0	0	CIRCULAR	1	0	1	0.00197
C671	216108	216110	112.86	0	0	CIRCULAR	5	0	1	0.02366
C672	273672	220536	185.29	0	0	CIRCULAR	3.5	0	1	0.02797
C673	220536	232066	166.17	0	0	CIRCULAR	8	0	1	0.00211
C674	232066	230860	328.21	0	0	CIRCULAR	8	0	1	0.00207
C675	232306	220534	51.79	0	0	CIRCULAR	4.5	0	1	0.02801
C676	220534	230864	28.55	0	0	CIRCULAR	7	0	1	0.0007
C677	230864	232506	639.74	0	0	CIRCULAR	7	0	1	0.00227
C678	232506	232508	190.38	0	0	CIRCULAR	7	0	1	0.00231
C679	232508	220536	84.78	0	0	CIRCULAR	7	0	1	0.01156
C68	225004	223460	198.49	0	0	CIRCULAR	2	0	1	0.04155
C680	220538	232176	314.49	0	0	CIRCULAR	5	0	1	0.00362
C681	232176	220534	374.42	0	0	CIRCULAR	6	0	1	0.00657
C687	230860	232312	421.4	0	0	CIRCULAR	8	0	1	0.00202
C688	232312	232494	463.33	0	0	CIRCULAR	8	0	1	0.00395
C689	209654	230326	340.52	0	0	CIRCULAR	1.5	0	1	0.00485
C69	223460	241914	208.67	0	1.63	CIRCULAR	2	0	1	0.03827
C690	232494	217216	657.25	0	0	CIRCULAR	9	0	1	0.00204
C691	217010	217210	384.3	0	0	CIRCULAR	9	0	1	0.00393
C692	230326	230328	200.3	0	0	CIRCULAR	1.75	0	1	0.00499
C693	267766	217208	349.28	0	0	CIRCULAR	9	0	1	0.002
C694	217208	217010	649.25	0	0	CIRCULAR	9	0	1	0.00206
C695	230328	215608	69.39	0	0	CIRCULAR	1.75	0	1	0.01052
C696	215608	215518	101.61	0	0	CIRCULAR	1.75	0	1	0.00512
C697	217210	217220	207.99	0	0	CIRCULAR	10	0	1	0.00163
C698	217220	217206	385.92	0	0	CIRCULAR	10	0	1	0.00233
C699	216408	216410	238.1	0	0	CIRCULAR	3.5	0	1	0.0002
C7	240344	240346	226	0	0	CIRCULAR	2	0	1	0.0204
C70	223462	223474	217.15	0	0	CIRCULAR	1.5	0	1	0.00806
C700	216410	216412	249.8	0	0	CIRCULAR	3.5	0	1	0.0002
C701	216412	270958	258.51	0	0	CIRCULAR	3.5	0	1	0.0002

Name	Inlet Node	Outlet Node	Length (ft)	Inlet Offset (ft)	Outlet Offset (ft)	Cross-Section	Geom1 (ft)	Geom2 (ft)	Barrels	Slope (ft/ft)
C702	270958	216414	246.71	0	0	CIRCULAR	3.5	0	1	0.0002
C703	216414	216416	39.62	0	0	CIRCULAR	3.5	0	1	0.0002
C704	216416	215550	232.26	0	0	CIRCULAR	3.5	0	1	0.0002
C705	215540	215606	219.37	0	0	CIRCULAR	1.25	0	1	0.0306
C706	215606	215558	146.62	0	0	CIRCULAR	1.25	0	1	0.03699
C707	215558	209668	216.54	0	0	CIRCULAR	2.25	0	1	0.00938
C708	209668	215550	245.48	0	0	CIRCULAR	2.25	0	1	0.002
C709	215562	216194	34.27	0	0	CIRCULAR	2.25	0	1	0.01255
C71	223474	223468	170.72	0	0	CIRCULAR	1.5	0	1	0.00785
C710	215550	270674	228.03	0	0	CIRCULAR	3.5	0	1	0.00145
C711	270674	217012	256.96	0	0	CIRCULAR	3.5	0	1	0.0014
C712	217012	217224	200.78	0	0	CIRCULAR	3.5	0	1	0.00543
C713	217224	217214	197.84	0	0	CIRCULAR	3.5	0	1	0.00197
C714	217214	216100	398.79	0	0	CIRCULAR	3.5	0	1	0.00236
C715	216100	271246	423.38	0	0	CIRCULAR	4	0	1	0.00246
C716	271246	216108	152.95	0	0	CIRCULAR	4	0	1	0.00196
C717	216194	209656	214.28	0	0	CIRCULAR	2.5	0	1	0.00401
C718	215518	209662	171.46	0	0	CIRCULAR	1.75	0	1	0.02334
C719	209662	215546	372.47	0	0	CIRCULAR	2	0	1	0.00537
C72	223468	241914	24.81	0	3.4	CIRCULAR	1.5	0	1	0.02016
C720	215546	L11	238.97	0	148.83	CIRCULAR	2.25	0	1	0.00017
C721	209656	216192	298.54	0	0	CIRCULAR	2.5	0	1	0.00593
C722	216192	L11	130.77	0	152.14	CIRCULAR	2.5	0	1	0.00696
C723	215578	215576	150.29	0	0	CIRCULAR	2.5	0	1	0.006
C724	215576	215574	192.53	0	0	CIRCULAR	2.5	0	1	0.00919
C725	215574	215572	139.17	0	0	CIRCULAR	2.5	0	1	0.00125
C726	216406	215580	189.73	0	0	CIRCULAR	13	0	1	0.00125
C727	215580	215572	186.8	0	0	CIRCULAR	13	0	1	0.00125
C728	215572	L11	27.98	0	152.84	CIRCULAR	13	0	1	0.00129
C73	241924	241914	29.99	0	0	CIRCULAR	3.5	0	1	0.00433
C730	273764	247988	572.51	0	0	ARCH	6.92	6.5	1	0.01401
C731	241336	241360	250.69	0	0	CIRCULAR	1.5	0	1	0.00439
C732	241360	190064	110.36	0	0	CIRCULAR	1.5	0	1	0.01903

Name	Inlet Node	Outlet Node	Length (ft)	Inlet Offset (ft)	Outlet Offset (ft)	Cross-Section	Geom1 (ft)	Geom2 (ft)	Barrels	Slope (ft/ft)
C733	190064	190066	97.81	0	0	CIRCULAR	1.5	0	1	0.00204
C734	190066	189858	163.79	0	0	CIRCULAR	1.5	0	1	0.00366
C735	189858	189862	201.68	0	0	CIRCULAR	1.5	0	1	0.01091
C736	189862	1481538	18.67	0	0	CIRCULAR	1.5	0	1	0.20219
C737	1481538	216032	403.62	0	0	CIRCULAR	7	0	1	0.00248
C738	216260	217732	237.15	0	0.5	CIRCULAR	2.5	0	1	0.00476
C739	220576	1481538	349.64	0	0	CIRCULAR	5	0	1	0.00821
C74	241914	223466	203.12	0	0	CIRCULAR	3.5	0	1	0.01014
C740	243056	272882	137.58	0	0	CIRCULAR	2.25	0	1	0.01112
C741	272882	242734	9.39	0	0	CIRCULAR	2.25	0	1	0.06082
C742	216196	209660	209.8	0	0	CIRCULAR	1.5	0	1	0.00696
C743	209660	270684	212.73	0	0	CIRCULAR	1.5	0	1	0.007
C744	270684	209650	46.13	0	0	CIRCULAR	1.5	0	1	0.06299
C745	209670	209650	109.23	0	0	CIRCULAR	3.5	0	1	0.00302
C746	209650	230320	267.22	0	0	CIRCULAR	3.5	0	1	0.00363
C747	230320	215560	138.9	0	0	CIRCULAR	3.5	0	1	0.01159
C748	215560	230324	47.46	0	0	CIRCULAR	3.5	0	1	0.07799
C749	230324	221200	272.51	0	0	CIRCULAR	3.5	0	1	0.58294
C75	223466	223470	248.64	0	0.243	CIRCULAR	3.5	0	1	0.00843
C750	227214	268358	183.92	0	0	CIRCULAR	1	0	1	0.00571
C751	268358	227216	253.41	0	0	CIRCULAR	1.5	0	1	0.00616
C752	227216	268364	237.08	0	0	CIRCULAR	1.5	0	1	0.00844
C753	268364	243062	264.55	0	0	CIRCULAR	2	0	1	0.01074
C754	243062	242750	225.57	0	0	CIRCULAR	2.25	0	1	0.01029
C755	242750	242764	94.63	0	0	CIRCULAR	2.25	0	1	0.00951
C756	242734	243060	50.18	0	0	CIRCULAR	1	0	1	0.01176
C757	243060	242848	94.37	0	0	CIRCULAR	1	0	1	0.02311
C758	243318	243346	229.8	0	0	CIRCULAR	1.25	0	1	0.0104
C759	243346	243162	141	0	0	CIRCULAR	1.25	0	1	0.01142
C76	241904	270736	223.34	0	0	CIRCULAR	3.5	0	1	0.01899
C760	243162	243172	49.63	0	0	CIRCULAR	1.25	0	1	0.01048
C761	243172	242150	143.62	0	0	CIRCULAR	1.25	0	1	0.0078
C762	242150	243332	64.35	0	0	CIRCULAR	1.25	0	1	0.0101

Name	Inlet Node	Outlet Node	Length (ft)	Inlet Offset (ft)	Outlet Offset (ft)	Cross-Section	Geom1 (ft)	Geom2 (ft)	Barrels	Slope (ft/ft)
C763	243332	243644	66.8	0	0	CIRCULAR	1.25	0	1	0.01303
C764	243644	243170	84.49	0	0	CIRCULAR	1.25	0	1	0.00994
C765	243170	241656	313.78	0	0	CIRCULAR	1.25	0	1	0.0255
C766	241656	241566	122.25	0	0	CIRCULAR	1.25	0	1	0.02487
C767	241566	242838	121.12	0	0	CIRCULAR	2	0	1	0.01139
C768	242838	241658	58.83	0	0	CIRCULAR	2	0	1	0.01139
C769	241658	242848	89.03	0	0	CIRCULAR	2	0	1	0.02708
C77	223470	241904	125.53	0	0	CIRCULAR	3.5	0	1	0.01163
C770	243348	243168	160.11	0	0	CIRCULAR	1.25	0	1	0.00606
C771	243168	243324	117.03	0	0.25	CIRCULAR	1.5	0	1	0.00658
C772	243324	243328	244.95	0	0.25	CIRCULAR	1.75	0	1	0.00355
C773	243328	243340	149.86	0	0	CIRCULAR	2	0	1	0.00687
C774	243340	242754	259.72	0	0	CIRCULAR	2	0	1	0.00539
C775	242754	242848	186.36	0	0	CIRCULAR	2	0	1	0.01465
C778	243658	243660	123.86	0	0	CIRCULAR	1.25	0	1	0.00412
C779	243660	242858	22.99	0	0	CIRCULAR	1.25	0	1	0.0013
C78	241900	223478	81.16	0	0	CIRCULAR	1.5	0	1	0.00899
C780	242858	243340	75.8	0	0	CIRCULAR	1.5	0	1	0.01649
C781	1522347	266492	158.16	0	100.22	CIRCULAR	5.5	0	1	0.00474
C782	266492	273764	277.88	0	0	ARCH	6.92	6.5	1	0.01054
C783	220920	220918	335.01	0	0	CIRCULAR	4	0	1	0.01024
C784	220918	220916	229.99	0	0	CIRCULAR	4.5	0	1	0.00909
C785	220916	219598	366.4	0	0	CIRCULAR	5	0	1	0.0155
C786	219594	246276	580.07	0	0	CIRCULAR	8	0	1	0.00149
C787	215092	J5	373.07	0	0	CIRCULAR	8	0	1	0.00126
C788	J5	L10	1832.4	0	1	CIRCULAR	8	0	1	0.00124
C789	246276	215092	1317.62	0	0	CIRCULAR	8	0	1	0.00114
C79	223478	241906	165.23	0	0.5	CIRCULAR	1.5	0	1	0.00902
C790	268362	227212	150.27	0	0	CIRCULAR	2	0	1	0.01471
C791	227212	227196	373.07	0	0	CIRCULAR	2.25	0	1	0.00898
C792	220816	L7	86.6	0	0	CIRCULAR	6	0	1	0.0797
C793	L8	L7	1497.32	0	0	CIRCULAR	13	0	1	0.00118
C794	242558	242556	116	0	0	CIRCULAR	1.75	0	1	0.00914

Name	Inlet Node	Outlet Node	Length (ft)	Inlet Offset (ft)	Outlet Offset (ft)	Cross-Section	Geom1 (ft)	Geom2 (ft)	Barrels	Slope (ft/ft)
C795	242556	242554	129.98	0	0	CIRCULAR	1.75	0	1	0.01777
C796	242554	242552	132.02	0	0	CIRCULAR	2.75	0	1	0.0028
C797	242552	220564	273.35	0	0	CIRCULAR	2.75	0	1	0.00417
C798	220564	242386	264	0	0	CIRCULAR	2.75	0	1	0.00314
C799	242386	242384	68.99	0	0	CIRCULAR	3	0	1	0.00667
C8	240346	240350	39	0	0	CIRCULAR	2	0	1	0.00897
C80	241906	273128	42.44	0	0	CIRCULAR	2	0	1	0.00471
C800	242578	242570	71.01	0	0	CIRCULAR	1.25	0	1	0.00873
C801	242570	242568	161.99	0	0	CIRCULAR	1.5	0	1	0.03583
C802	242568	242566	42.01	0	0	CIRCULAR	2	0	1	0.00571
C803	242566	242564	269.99	0	0	CIRCULAR	2	0	1	0.00248
C804	242564	242572	45.99	0	0	CIRCULAR	2	0	1	0.02371
C805	242572	242086	428.97	0	0	CIRCULAR	3.5	0	1	0.00254
C806	242086	220776	105.03	0	0	CIRCULAR	3.5	0	1	0.01238
C807	241478	241476	263	0	0	CIRCULAR	1	0	1	0.02792
C808	242384	242092	345.79	0	0	CIRCULAR	3	0	1	0.00578
C809	242092	242090	295.21	0	0	CIRCULAR	3	0	1	0.00518
C81	273128	270736	266.39	0	0.35	CIRCULAR	2	0	1	0.00503
C810	242090	242088	238	0	0	CIRCULAR	3	0	1	0.01042
C811	242088	220776	55.01	0	0	CIRCULAR	3	0	1	0.01491
C812	220776	220578	140.99	0	0	CIRCULAR	4	0	1	0.01362
C813	220578	242084	173.49	0	0	CIRCULAR	4	0	1	0.02018
C814	242084	220576	122	0	0	CIRCULAR	5	0	1	0.01402
C82	223476	241920	113.54	0	0	CIRCULAR	1.25	0	1	0.01956
C828	188398	188448	357.46	0	0	CIRCULAR	1.25	0	1	0.00476
C829	188448	188438	69.37	0	0	CIRCULAR	1.5	0	1	0.01514
C83	241920	223500	88.68	0	0	CIRCULAR	1.25	0	1	0.02245
C830	188438	188410	70.24	0	0	CIRCULAR	2.25	0	1	0.0047
C831	188410	188400	110.68	0	0	CIRCULAR	2.25	0	1	0.00578
C832	188400	188414	250.87	0	0	CIRCULAR	2.25	0	1	0.00869
C833	188414	188392	36	0	0	CIRCULAR	2.5	0	1	0.01306
C834	188392	187598	22	0	0	ARCH	3.02	1.88	1	0.00955
C835	187598	187596	353.8	0	0	CIRCULAR	2.5	0	1	0.00743

Name	Inlet Node	Outlet Node	Length (ft)	Inlet Offset (ft)	Outlet Offset (ft)	Cross-Section	Geom1 (ft)	Geom2 (ft)	Barrels	Slope (ft/ft)
C836	187596	242398	44.31	0	0	CIRCULAR	2.5	0	1	0.01512
C837	242398	242396	35.81	0	0	CIRCULAR	3	0	1	0.0148
C838	242396	242394	303	0	0	CIRCULAR	3	0	1	0.01485
C839	242394	220778	50.95	0	0	CIRCULAR	3	0	1	0.03279
C84	223500	223496	121.77	0	0	CIRCULAR	1.25	0	1	0.02366
C840	220778	220566	52	0	0	CIRCULAR	4	0	1	0.00904
C841	220566	220568	99	0	0	CIRCULAR	4	0	1	0.00222
C842	220568	220570	322	0	0	CIRCULAR	4	0	1	0.00565
C843	220570	220572	359	0	0	CIRCULAR	4	0	1	0.00685
C844	220572	220574	112	0	0	CIRCULAR	4	0	1	0.0067
C845	220574	220576	49.22	0	0	ARCH	4.88	3	1	0.03619
C846	241476	241472	42	0	0	CIRCULAR	1.25	0	1	0.14557
C847	241474	241472	172.03	0	0	CIRCULAR	1.25	0	1	0.00169
C848	241472	272870	239.17	0	0	CIRCULAR	2	0	1	0.00472
C849	272870	241470	41	0	0	CIRCULAR	2	0	1	0.02415
C85	223496	270736	54.53	0	3.19	CIRCULAR	1.25	0	1	0.02238
C850	241470	241468	332.01	0	0	CIRCULAR	2	0	1	0.00922
C851	241468	242434	91.02	0	0	CIRCULAR	2	0	1	0.01373
C852	242434	273178	229.73	0	0	CIRCULAR	2.25	0	1	0.00993
C853	273178	242432	192.99	0	0	CIRCULAR	2.25	0	1	0.01067
C854	242432	220790	63.02	0	0	CIRCULAR	2.25	0	1	0.03922
C857	242682	242680	162	0	0	CIRCULAR	1.25	0	1	0.00525
C858	242680	241470	116.98	0	0	CIRCULAR	1.25	0	1	0.00453
C859	227194	241358	308.71	0	0	CIRCULAR	1.25	0	1	0.02268
C86	270736	241908	247.88	0	0.34	CIRCULAR	4.5	0	1	0.03112
C860	241358	241378	45.83	0	0	CIRCULAR	1.25	0	1	0.05463
C861	242548	241338	295.84	0	0.31	CIRCULAR	2.25	0	1	0.00815
C862	241338	241378	30.83	0	0	CIRCULAR	3	0	1	0.03343
C863	241340	241342	315.29	0	0	CIRCULAR	1.75	0	1	0.00688
C864	241342	241378	297.48	0	0	CIRCULAR	2.25	0	1	0.01009
C865	241378	273426	294.46	0	0	CIRCULAR	2.75	0	1	0.00849
C866	227208	227222	254.89	0	0	CIRCULAR	1.25	0	1	0.01354
C867	227222	227228	224.8	0	0	CIRCULAR	1.5	0	1	0.01157

Name	Inlet Node	Outlet Node	Length (ft)	Inlet Offset (ft)	Outlet Offset (ft)	Cross-Section	Geom1 (ft)	Geom2 (ft)	Barrels	Slope (ft/ft)
C868	227228	227204	98.56	0	0	CIRCULAR	1.75	0	1	0.01218
C869	227204	227236	124.86	0	0	CIRCULAR	1.75	0	1	0.01177
C87	241908	241910	168.9	0	0	CIRCULAR	5	0	1	0.00261
C870	227236	227234	150.92	0	0	CIRCULAR	2	0	1	0.00563
C871	227234	227232	118.88	0	0	CIRCULAR	2	0	1	0.00631
C872	227232	242736	299.73	0	0	CIRCULAR	2.25	0	1	0.004
C873	242736	243058	185.65	0	0	CIRCULAR	2.25	0	1	0.01503
C874	243652	241654	307.86	0	0	CIRCULAR	1	0	1	0.02437
C875	241654	273454	308.65	0	0	CIRCULAR	1	0	1	0.03738
C876	241574	J12	57.19	0	148.98	CIRCULAR	4	0	1	0.00699
C877	J12	L8	20.16	0	0	CIRCULAR	13	0	1	0.06262
C878	242848	241660	174.6	0	0	CIRCULAR	3.5	0	1	0.0063
C879	241660	243074	85.34	0	0	CIRCULAR	3.5	0	1	0.01348
C88	241910	215666	370.85	0	0	CIRCULAR	5	0	1	0.00315
C880	243074	242850	110.14	0	0	CIRCULAR	4	0	1	0.0039
C881	242850	243058	87.18	0	0	CIRCULAR	4	0	1	0.00379
C882	243058	241574	23.6	0	0	CIRCULAR	4	0	1	0.00466
C883	273454	J12	49.77	0	156.13	CIRCULAR	1.75	0	1	0.00683
C884	L10	L9	91.44	0	0	CIRCULAR	13	0	1	0.00405
C885	L9	L8	1619.86	0	0	CIRCULAR	13	0	1	0.00109
C886	273426	L6	23.01	0	130.18	CIRCULAR	2.75	0	1	0.32945
C887	273436	242654	65.97	0	0	CIRCULAR	2	0	1	0.00227
C888	242654	241570	359.01	0	0	CIRCULAR	2	0	1	0.00206
C889	241570	241572	109	0	0	CIRCULAR	2	0	1	0.00174
C89	215666	215012	390.82	0	0	CIRCULAR	5	0	1	0.00307
C890	241572	241574	28	0	0	CIRCULAR	2	0	1	0.06658
C891	217732	217730	269.07	0	0	CIRCULAR	3	0	1	0.00305
C892	227200	227190	174.32	0	0	CIRCULAR	1.5	0	1	0.0345
C893	227190	227210	50.39	0	0	CIRCULAR	1.75	0	1	0.03674
C894	227210	268360	43.89	0	0	CIRCULAR	2.25	0	1	0.20248
C895	268360	227226	17.99	0	0	CIRCULAR	2.25	0	1	0.08592
C896	227226	220816	16.81	0	115.33	CIRCULAR	2.25	0	1	0.35048
C897	216262	216260	296.21	0	0	CIRCULAR	1	0	1	0.09992

Name	Inlet Node	Outlet Node	Length (ft)	Inlet Offset (ft)	Outlet Offset (ft)	Cross-Section	Geom1 (ft)	Geom2 (ft)	Barrels	Slope (ft/ft)
C898	216254	215676	238	0	0.25	CIRCULAR	1	0	1	0.07712
C899	215676	217730	100	0	1.75	CIRCULAR	1.25	0	1	0.012
C9	240350	187574	300	0	0	CIRCULAR	1.75	0	1	0.04164
C90	224696	225008	216	0	0	CIRCULAR	1	0	1	0.05383
C900	217730	215092	30.34	0	136.04	CIRCULAR	3	0	1	0.13808
C901	L7	L6	579.35	0	0	CIRCULAR	13	0	1	0.00235
C902	L6	L5	750.8	0	0	CIRCULAR	13	0	1	0.00145
C903	L5	L4	1232.14	0	0	CIRCULAR	13	0	1	0.00173
C904	L4	L3	804.7	0	0	CIRCULAR	13	0	1	0.00174
C905	L3	L2	782.03	0	0	CIRCULAR	13	0	1	0.00179
C906	L2	L1	30.49	0	0	CIRCULAR	13	0	1	0.00328
C908	241662	242758	134.49	0	0	CIRCULAR	1.25	0	1	0.00491
C909	242758	241652	143.81	0	0	CIRCULAR	2	0	1	0.00299
C91	225008	223512	195	0	0.35	CIRCULAR	1	0	1	0.04708
C910	241652	272890	123.65	0	0	CIRCULAR	2	0	1	0.00307
C911	272890	242770	98.42	0	0	CIRCULAR	2	0	1	0.0366
C912	242770	241664	32.53	0	0	CIRCULAR	3.5	0	1	0.00369
C913	241664	242760	83.21	0	0	CIRCULAR	3.5	0	1	0.00841
C92	223512	224686	28	0	0	CIRCULAR	2	0	1	0.01607
C93	224686	224698	24	0	0	CIRCULAR	2	0	1	0.01625
C94	224698	241902	206	0	0	CIRCULAR	2	0	1	0.015
C95	241902	241918	195	0	0	CIRCULAR	2	0	1	0.01708
C96	224688	225020	172.65	0	0	CIRCULAR	1	0	1	0.06507
C97	225020	224686	148.06	0	0.7	CIRCULAR	1	0	1	0.07457
C98	223484	241922	52	0	1	CIRCULAR	1	0	1	0.02
C99	241922	223502	313	0	0.53	CIRCULAR	1.25	0	1	0.03805
C0	L1	OFmain	30.59	0	0	CIRCULAR	13	0	1	0.39143

A8. Drainage system parameters used in the PCSWMM model.

Criteria for structural BMP selection

		Treatment suitability	Water Quality Performance			Implementation Considerations			
Structural Control Category	Structural Control	Water Quality	TSS (≥60% removal)	Bacteria (≥75% removal)	Site Applicability	Residential Subdivision Use	Construction Cost (low)	Maintenance Cost (low)	Disadvantages to Avoid
Stormwater Ponds	Extended dry detention pond	✓	✓	✓	✓	✓	✓	✓	
	Wet pond	✓	✓	✓	✓	✓	✓	✓	Odor/safety
	Wet extended detention pond	✓	✓	✓	✓	✓	✓	X	Odor/safety
	Micropool extended detention pond	✓	✓	✓	✓	✓	✓	✓	Odor/safety
	Multiple Ponds	✓	✓	✓	✓	✓	✓	X	Odor/safety
Stormwater Wetlands	Shallow wetland	✓	✓	✓	✓	✓	X	X	
	Shallow extended detention wetland	✓	✓	✓	✓	✓	X	X	
	Pond/Wetland	✓	✓	✓	✓	✓	X	X	
	Pocket wetland	✓	✓	✓	✓	✓	X	X	Odor/mosquito
Bioretention	Bioretention Areas	✓	✓	ID	✓	✓	X	X	
Sand Filters	Surface Sand Filter	✓	✓	X	✓	X	X	X	
	Perimeter Sand Filter	✓	✓	X	✓	X	X	X	
Infiltration	Infiltration Trench	✓	✓	✓	✓	X	X	X	
Enhanced Swales	Dry Swale	✓	✓	ID	✓	✓	X	✓	
	Wet Swale	✓	✓	ID	✓	✓	X	✓	Odor/mosquito

A9. Criteria employed during evaluation of structural BMPs to be implemented for the St Anthony Park watershed. An arrow indicates that the BMP meets the examined criteria, while an X mark indicates that it does not. *ID*: insufficient data – Modified from (Debo and Reese 2002).

Areas and volumes of extended dry detention ponds

Location	Detention Pond Name	WQCV Bottom Area (m^2)	WQCV Top Area (m^2)	Volume of EDDP (ft^3)
Deep Manholes (L1-L7)	Detention Pond-7	1135	1997	1332
	Detention Pond-6	128	491	19194
	Detention Pond-5	3728	5199	15405
	Detention Pond-4	2925	4240	6939
	Detention Pond-3	14950	17786	70382
	Detention Pond-2	97	427	1128
	Detention Pond-1	8268	10405	40146
OFmain	OFmain Detention Pond	35437	39746	161644

A10. Top and bottom areas and final volume of WQCV of dry extended detention ponds (EDDPs) placed at deep manholes and at OFmain.

Extended dry detention pond examination using the EMC

washoff function

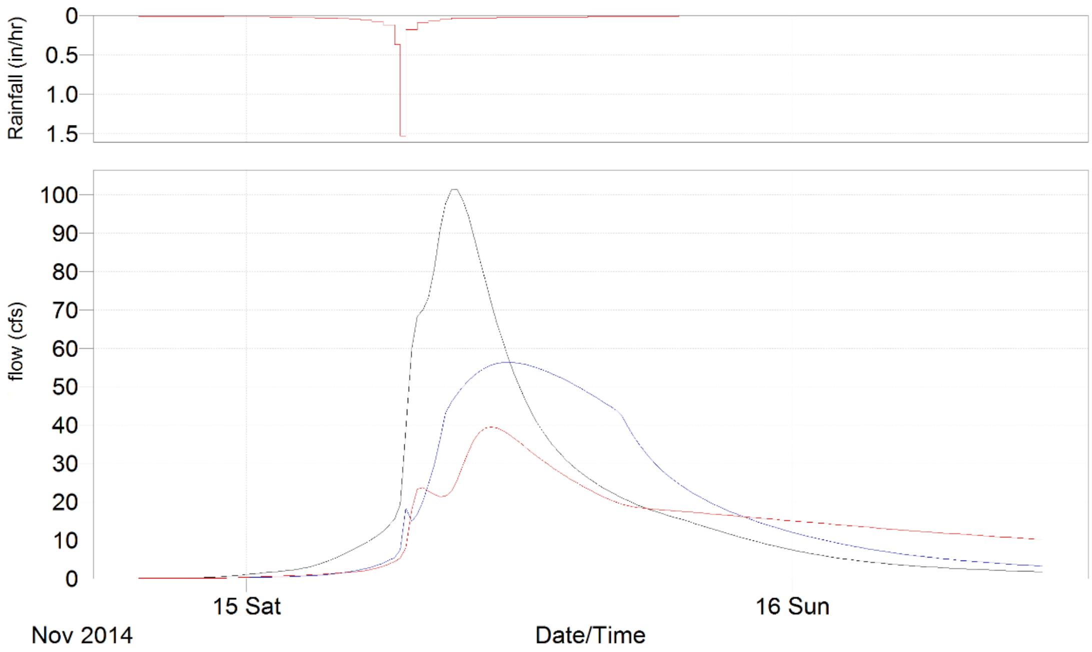

A11. Top: hyetograph. Bottom: hydrographs at OFmain outflow for the two EDDP scenarios using the dynamic wave routing method: No BMP (black), with distributed EDDPs (red), and with one EDDP at OFmain (blue). The simulation was run for 40 hours. The flow is shown in cubic feet per second (cfs).

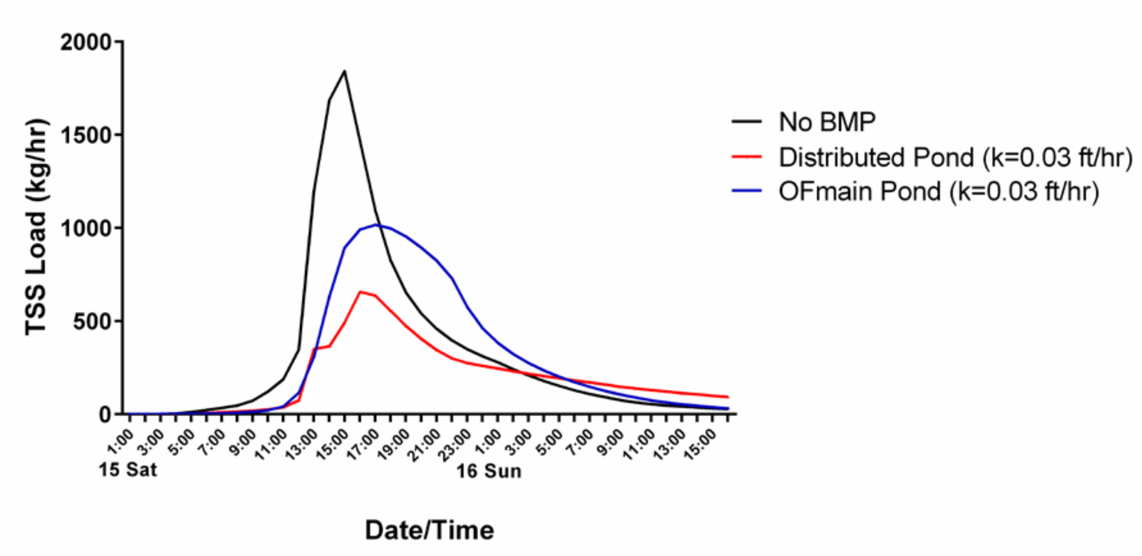

A12. TSS loads (kg/hr) at OFmain outflow for the two EDDP scenarios at k = 0.03 ft/hr: No BMP (black), with distributed EDDPs (red), and with EDDP at OFmain (blue). The simulation was run for 40 hours.

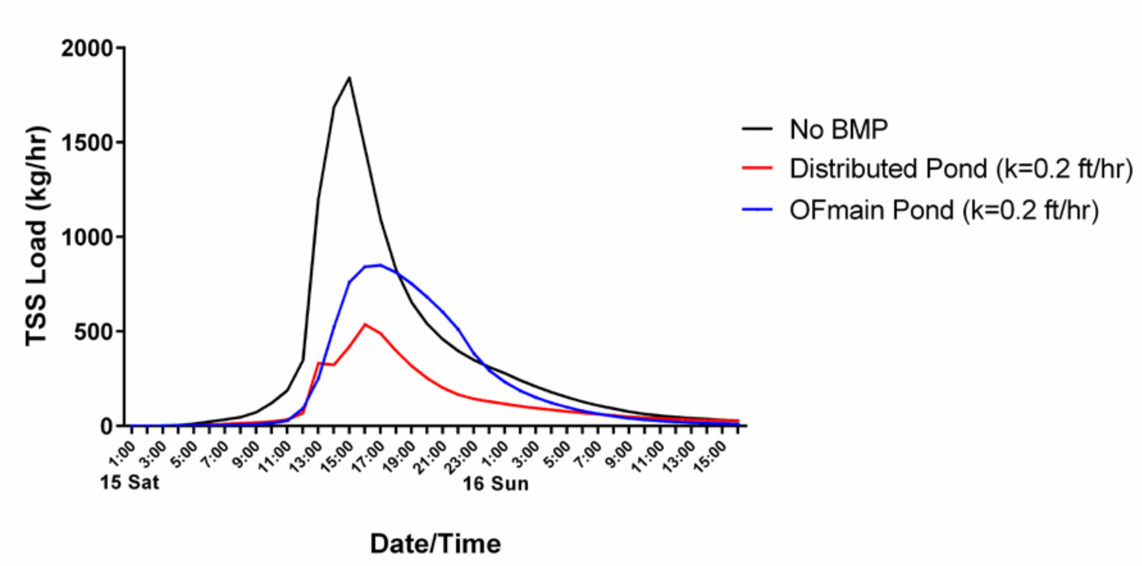

A13. TSS loads (kg/hr) at OFmain outflow for the two EDDP scenarios at k = 0.2 ft/hr: No BMP (black), with distributed EDDPs (red), and with EDDP at OFmain (blue). The simulation was run for 40 hours.

k value	Parameter (examined at OFmain outflow)		No BMP	Detention Pond at OFmain	Distributed Detention Ponds
0.03 ft/hr	Peak TSS Load (kg/hr)	Measured	1842	895	492
		% Efficiency	-	51%	73%
0.2 ft/hr	Peak TSS Load (kg/hr)	Measured	1842	761	420
		% Efficiency	-	59%	77%

A14. Stormwater TSS load reduction performance summary (peak shaving) for the two BMP scenarios (detention pond at OFmain and distributed detention ponds) examined at k-values of 0.02 and 0.3 ft/hr. The simulation was run for 40 hours. Peak TSS loads were examined at 15:00 hr (15 Sat) (see A12 and A13).

REFERENCES

Akan, A. O. and R. J. Houghtalen (2003). Urban hydrology, hydraulics, and stormwater quality: engineering applications and comput. Hoboken, N.J. :, John Wiley & Sons.

Anderson, C. W., et al. (2003). Phosphorus and E. coli and their relation to selected constituents during storm runoff conditions in Fanno Creek, Oregon, 1998-99. Portland, Ore. : Denver, CO, U.S. Dept. of the Interior, U.S. Geological Survey ; U.S. Geological Survey, Information Services [distributor].

Barco, J., et al. (2008). "Automatic Calibration of the U.S. EPA SWMM Model for a Large Urban Catchment." Journal of Hydraulic Engineering **134**(4): 466-474.

Bharati, L., et al. (2011). The impacts of water infrastructure and climate change on the hydrology of the Upper Ganges River Basin. Colombo, Sri Lanka, International Water Management Institute. **142**.

Bliss, D. J., et al. (2009). "Storm Water Runoff Mitigation Using a Green Roof." Environmental Engineering Science **26**(2): 407-418.

Brezonik, P. L. and T. H. Stadelmann (2001). "Analysis and predictive models of stormwater runoff volumes, loads, and pollutant concentrations from watersheds in the Twin Cities metropolitan area, Minnesota, USA." Water research **36**: 1743-1757.

Butcher, J. B. (2003). "Buildup, Washoff, and Event Mean Concentrations." JAWRA Journal of the American Water Resources Association **39**(6): 1521-1528.

Capitol Region Watershed District (2014). 2013 Stormwater Monitoring Report.

Center for Watershed Protection (CWP) (2003b). Impacts of Impervious Cover on Aquatic Systems. Ellicott City, MD.

Chapra, S. C. (1997). Surface water-quality modeling / Steven C. Chapra. New York :, McGraw-Hill.

Chen, H. J. and H. Chang (2014). "Response of discharge, TSS, and E. coli to rainfall events in urban, suburban, and rural watersheds." Environ Sci Process Impacts **16**(10): 2313-2324.

Chin, D. A. (2006). Water-quality engineering in natural systems. Hoboken, N.J. :, Wiley-Interscience.

Chow, V. T. (1964). Handbook of applied hydrology; a compendium of water-resources technology. New York, McGraw-Hill.

Committee on the Mississippi River and the Clean Water Act: David A. Dzombak (2007). Mississippi River Water Quality and the Clean Water Act: Progress, Challanges, and Opportunities, The National Academy of Sciences.

Davis, A. P. (2005). "Green Engineering Principles Promote Low-impact Development." Environmental Science & Technology **39**(16): 338A-344A.

Davis, A. P. and R. H. McCuen (2005). Stormwater management for smart growth / Allen P. Davis and Richard H. McCuen. New York :, Springer Science.

Davis, B. and G. Birch (2010). "Comparison of heavy metal loads in stormwater runoff from major and minor urban roads using pollutant yield rating curves." Environmental Pollution **158**(8): 2541-2545.

Debo, T. N. and A. Reese (2002). Municipal Stormwater Management Boca Raton, FL, CRC Press.

Deletic, A. (1998). "The first flush load of urban surface runoff." Water research **32**(8): 2462-2470.

Deletic, A. B. and C. T. Maksimovic (1998). "Evaluation of water quality factors in storm runoff from paved areas." Journal of Environmental Engineering-Asce **124**: 869-879.

Deliman, P. N., et al. (1999). Review of Watershed Water Quality Models. TX, USA, US Army Corps of Engineers. **W-99-1**.

Driscoll, E. D., et al. (1989). Analysis of storm events characteristics for selected rainfall gauges throughout the United States. Washington, D.C., U.S. Environmental Protection Agency (EPA).

Elliott, A. H. and S. A. Trowsdale (2007). "A review of models for low impact urban stormwater drainage." Environmental Modelling & Software **22**(3): 394-405.

Environmental Protection Agency (EPA). "Storm Water Management Model (SWMM) - Version 5.1.007 with Low Impact Development (LID) Controls." Retrieved November 10, 2014, from http://www.epa.gov/nrmrl/wswrd/wq/models/swmm/.

Environmental Protection Agency (EPA) (1999). Preliminary Data Summary of Urban Storm Water Best Management Practices. Washington D.C., Office of water.

Environmental Protection Agency (EPA) (2014). "Dry detention ponds." Retrieved November 13, 2014, from http://water.epa.gov/polwaste/npdes/swbmp/Dry-Detention-Ponds.cfm.

Fletcher, T. D., et al. (2013). "Understanding, management and modelling of urban hydrology and its consequences for receiving waters: A state of the art." Advances in Water Resources **51**(0): 261-279.

Geiger, W. (1987). Flushing effects in combined sewer systems. The 4th International Conference on Urban Drainage, Lausanne, Switzerland.

Gentry, R. W., et al. (2006). "Escherichia coli Loading at or Near Base Flow in a Mixed-Use Watershed." Journal of Environmental Quality **35**(6): 2244-2249.

Gironás, J., et al. (2010). Storm Water Management Model. Applications Manual. Cincinnati, United States Environmental Protection Agency.

Gribbin, J. E. (2006). Introduction to hydraulics and hydrology with applications for stormwater management Clifton Park, NY, Delmar Cengage Learning.

Gromaire-Mertz, M. C., et al. (1999). "Characterisation of urban runoff pollution in Paris." Innovative Technologies in Urban Storm Drainage 1998 (Novatech '98), Selected Proceedings of the 3rd NOVATECH Conference on Innovative Technologies in Urban Storm Drainage **39**(2): 1-8.

Gupta, H. V., et al. (1998). "Toward improved calibration of hydrologic models: Multiple and noncommensurable measures of information." Water Resources Research **34**(4): 751-763.

Hamilton, J. L. and I. Luffman (2009). "Precipitation, Pathogens, and Turbidity Trends in the Little River, Tennessee." Physical Geography **30**(3): 236-248.

Herngren, L., et al. (2005). "Understanding heavy metal and suspended solids relationships in urban stormwater using simulated rainfall." Journal of environmental management **76**(2): 149-158.

Hopkinson, C., Jr. and J. Day, Jr. (1980). "Modeling hydrology and eutrophication in a Louisiana swamp forest ecosystem." Environmental management **4**(4): 325-335.

Hossain, I., et al. (2010). "Development of a Catchment Water Quality Model for Continuous Simulations of Pollutants Build-up and Wash-off." International Journal of Environmental, Ecological, Geological and Mining Engineering **4**(1).

Huber, W. C. (1986). Deterministic Modeling of Urban Runoff Quality. Urban Runoff Pollution. H. C. Torno, J. Marsalek and M. Desbordes. Germany, Springer-Verlag Berlin Heidelberg**:** 167.

Huston, R., et al. (2009). "Characterisation of atmospheric deposition as a source of contaminants in urban rainwater tanks." Water research **43**(6): 1630-1640.

Hvitved-Jacobsen, T., et al. (2010). Urban and highway stormwater pollution : concepts and engineering. Boca Raton, FL CRC Press/Taylor & Francis.

James, W. (1997). Advances in Modeling the Management of Stormwater Impacts, CRC Press.

James, W., et al. (2010). User's Guide to SWMM 5. USA, Computational Hydraulics International.

Kay, D. and A. McDonald (1983). "Predicting coliform concentrations in upland impoundments: design and calibration of a multivariate model." Applied and Environmental Microbiology **46**(3): 611-618.

Kibler, D. F. and G. U. American (1982). Urban stormwater hydrology Washington, D.C.: American Geophysical Union.

Kim, L., et al. (2006). "Estimating Pollutant Mass Accumulation on Highways during Dry Periods." Journal of Environmental Engineering **132**(9): 985-993.

Lee, H., et al. (2004). "Seasonal first flush phenomenon of urban stormwater discharges." Water Res **38**(19): 4153-4163.

Lee, J. H., et al. (2002). "First flush analysis of urban storm runoff." Science of The Total Environment **293**(1-3): 163-175.

Legates, D. R. and G. J. McCabe (1999). "Evaluating the use of "goodness-of-fit" Measures in hydrologic and hydroclimatic model validation." Water Resources Research **35**(1): 233-241.

Li, C., et al. (2014). "Characterization and first flush analysis in road and roof runoff in Shenyang, China." Water Sci Technol **70**(3): 397-406.

Lin, J. P., et al. (2004). Review of published export coefficient and event mean concentration (EMC) data, U.S. Army Engineer Research and Development Center.

Linsley, R. K., et al. (1949). Applied hydrology. New York, McGraw-Hill.

Maniquiz-Redillas, M. and L.-H. Kim (2014). "Fractionation of heavy metals in runoff and discharge of a stormwater management system and its implications for treatment." Journal of Environmental Sciences **26**(6): 1214-1222.

Marsalek, J., et al. (1975). "Comparative evaluation of three urban runoff models " JAWRA Journal of the American Water Resources Association **11**: 306–328.

Martinson, D. B. and T. H. Thomas (2009). Quantifying the first-flush phenomenon: effects of first-flush on water yield and quality. 14th International Rainwater Catchment Systems Conference. Kuala Lumpur.

Maryland Department of the Environment (2000). Maryland Stormwater Design Manual Volumes I and II. Baltimore, MD.

Minnesota Pollution Control Agency (2000). Protecting Water Quality in Urban Areas: Best Management Practices for Dealing with Storm Water Runoff from Urban, Suburban and Developing Areas of Minnesota. St Paul, MN. **Chapter 5**.

Moriasi, D. N., et al. (2007). "Model evaluation guidelines for systematic quantification of accurary in watershed simulations." Transactions of the ASABE: American Society of Agricultural and Biological Engineers **50**(3): 885-900.

Mrowiec, M., et al. (2009). "Occurrence of first flush phenomenon in drainage system of Czestochowa." Environment Protection Engineering **35**(2): 73-80.

Murphy, L., et al. (2014). Influence of Meteorological Characteristics on Atmospheric Contaminant Loadings in Stormwater Runoff at an International Airport. World Environmental and Water Resources Congress 2014**:** 75-84.

Nash, J. E. and J. V. Sutcliffe (1970). "River flow forecasting through conceptual models: Part 1. A discussion of principles." J. Hydrology **10**(3): 282-290.

National Research Council (2009). Urban Stormwater Management in the United States. Washington, DC, The National Academies Press.

Novotny, V. (1995). Water Quality Management Library-Volume 9/Nonpoint Pollution And Urban Stormwater Management. Lancaster, Pennsylvania 17604 U.S.A., Technomic Publishing Company, Inc.

Novotny, V. (2003). Water quality : diffuse pollution and watershed management Hoboken, NJ :, J. Wiley.

Novotny, V. and G. Chesters (1981). Handbook of nonpoint pollution : sources and management New York: Van Nostrand Reinhold.

Obropta, C. C. and J. S. Kardos (2007). "Review of Urban Stormwater Quality Models: Deterministic, Stochastic, and Hybrid Approaches." JAWRA Journal of the American Water Resources Association **43**(6): 1508-1523.

Olivieri, V., et al. (1977). Microorganisms in urban stormwater: Cincinnati, Ohio. U. S. E. P. Agency**:** 181 p.

Pennsylvania Department of Environmental Protection (2005). Draft Pennsylvania Stormwater Management Manual. Harrisburg, PA.

Poresky, A. (2007). "SWMM simulation of watershed hydrology and hydraulics." Retrieved November 9 2014, from http://www.cwemf.org/workshops/22Jun07Wrkshp/SWMMPresentation.pdf.

Quintana Segu, P., et al. (2009). "Improvement, calibration and validation of a distributed hydrological model over France." Hydrology and Earth System Sciences (HESS) & Discussions (HESSD).

Reif, A. G., et al. (2002). Assessment of Stream Quality Using Biological Indices at Selected Sites in the Schuylkill River Basin, Chester County, Pennsylvania, 1981-97, U.S. Geological Survey.

Rossman, L. E. (2005). Storm-water management model - User's manual version 5.0, National Risk Management Research Laboratory. U. S. E. P. Agency. Cincinnati. OH.

Saget, A., et al. (1995). The first flush in sewer system. The International Conference on Sewer Solids – Characteristics, Movement, Effects and Control, Dundee, U.K.

Santhi, C., et al. (2001). " Validation of the SWAT model on a large river basin with point and nonpoint sources." J. American Water Resources Assoc. **37**(5): 1169-1188.

Sarma, P. G. S., et al. (1969). A program in urban hydrology, Part II. West Lafayette, IN, Purdue University, Water Resources research Center. **Tech. Rept. No. 99**.

Schueler, T. (1997). "Influence of Ground Water on Performance of Stormwater Ponds in Florida." Watershed Protection Techniques **2**(4): 525-528.

Sevat, E. and A. Dezetter (1991). "Selection of calibration objective functions in the context of rainfall-runoff modeling in a Sudanese savannah area." Hydrological Sci. J. **36**(4): 307-330.

Seybert, T. A. (2006). Stormwater management for land development : methods and calculations for quantity contro. Hoboken, N.J.: John Wiley.

Shepherd, J. M., et al. (2002). "Rainfall Modification by Major Urban Areas: Observations from Spaceborne Rain Radar on the TRMM Satellite." Journal of Applied Meteorology **41**(7): 689-701.

Singhofen, P. J. (2001). Florida Association of Stormwater Utilities 2001 Annual Conference.

Taebi, A. and R. L. Droste (2004). "Pollution loads in urban runoff and sanitary wastewater." Science of The Total Environment **327**(1-3): 175-184.

Thomann, R. V. and J. A. Mueller (1987). Principles of surface water quality modeling and control New York :, Harper & Row.

Tobio, J. A. S., et al. (2014). Design Optimisation of Rain Garden Treating Roof Runoff Using Stormwater Management Model. 13th International Conference on Urban Drainage. Sarawak, Malaysia.

Tong, S. T. Y. and W. Chen (2002). "Modeling the relationship between land use and surface water quality." Journal of environmental management **66**(4): 377-393.

Tsihrintzis, V. A. and R. Hamid (1997). "Modeling and Management of Urban Stormwater Runoff Quality: A Review." Water Resources Management **11**(2): 136-164.

Tsihrintzis, V. A. and R. Hamid (1998). "Runoff quality prediction from small urban catchments using SWMM." Hydrological Processes **12**(2): 311-329.

U.S. Soil Conservation Service (June 1986). Technical Release 55: Urban Hydrology for Small Watersheds. Washington, D.C., USDA (U.S. Department of Agriculture)**:** 146 pp.

Urban Drainage and Flood Control District (UDFCD) (2007 revision). Urban Storm Drainage Criteria Manual. Denver, CO.

Urban Drainage and Flood Control District (UDFCD) (2011). "Urban Storm Drainage Criteria Manual Volume 3 ".

Van Liew, M. W., et al. (2003). "Hydrologic simulation on agricultural watersheds: Choosing between two models." Trans. ASAE **46**(6): 1539-1551.

Viessman, W., et al. (1989). Introduction to hydrology. New York :, Harper & Row.

Vorreiter, L. and C. Hickey (1994). Incidence of the First Flush Phenomenon in Catchments of the Sydney Region [online]. In: Water Down Under 94: Surface Hydrology and Water Resources Papers; Preprints of Papers. , Barton, ACT: Institution of Engineers**:** 359-364.

Walsh, C. J., et al. (2005). "The urban stream syndrome: current knowledge and the search for a cure." Journal of the North American Benthological Society **24**(3): 706-723.

Wang, L., et al. (2011). "Urban nonpoint source pollution buildup and washoff models for simulating storm runoff quality in the Los Angeles County." Environmental Pollution **159**(7): 1932-1940.

Wanielista, M. P., et al. (1997). Hydrology : water quantity and quality control New York :, John Wiley & Sons.

Ward, R. C. (1975). Principles of hydrology. London ; New York :, McGraw-Hill.

Zaghloul, N. A. (1981). "SWMM model and level of discretization." Journal of the Hydraulics Division **107**(11): 1535-1545.

Zaghloul, N. A. (1983). "Sensitivity analysis of the SWMM Runoff-Transport parameters and the effects of catchment discretisation." Advances in Water Resources **6**(4): 214-223.

Zaghloul, N. A. and M. A. Abu Kiefa (2001). "Neural network solution of inverse parameters used in the sensitivity-calibration analyses of the SWMM model simulations." Advances in Engineering Software **32**(7): 587-595.

Zhao, J.-w., et al. (2007). "Pollutant loads of surface runoff in Wuhan City Zoo, an urban tourist area." Journal of Environmental Sciences **19**(4): 464-468.

Zoppou, C. (2001). "Review of urban storm water models." Environmental Modelling & Software **16**(3): 195-231.